PN ABX-488
12.061E

FINAL REPORT

Covering period: October 1992 to October 1995

Submitted to the Office of the Science Advisor
U.S. Agency for International Development

THE SPECIFIC ROLE OF GRANULOSA AND THECA CELLS IN RESUMPTION OF MEIOSIS.

Principal investigator: Dr. Josef Fulka
Institute of Animal Physiology and Genetics
277 21 Liběchov, Czech Republic

Tel number: +42 206 697 024
Fax number: +42 206 697 186

Collaborator: Prof. Richard Schultz
University of Pennsylvania, Dept. of Biology
Leidy Laboratory of Biology, Philadelphia, PA 19104-6018, USA

Tel number: 215 662 6070
Fax number: 215 349 5118

Project number: 12.061 E

A.I.D. Grant Project Officer: John Daly, Ph.D.

REC'D IN R&D/R
1995

Project duration: October 1992 to October 1995

CC:BOSTID

TABLE OF CONTENTS

Executive Summary 1

Research Objectives 3

Methods and Results 5

Impact, relevance and Technology Transfer 8

Project Activities 9

Project Productivity 10

Future Work 11

Executive Summary.

The accomplished results enriched the knowledge about maturation inhibiting activity of porcine parietal membrana granulosa. A piece of this follicular compartment arrest pig, cattle and mouse oocytes after their release from antral follicles in germinal vesicle stage. The background of the inhibition and the molecules responsible for this phenomenon arrest were not defined. It was only clearly demonstrated that gap junctions mediating cell to cell communications did not occur between parietal granulosa and cumulus oophorus. On the other hand, our experiments revealed the existence of functional communication between somatic (cumulus oophorus) and germ cells during initial phase of bovine oocytes maturation. Later, after 6 h of culture metabolic contact remained well conserved only between cells of cumulus oophorus and disappeared between them and oocyte. The interaction between cumulus cells was maintained irrespective of the deposition of hyaluronic acid in extracellular spaces leading to the expansion of cumulus complex. It was also found that synthesis and deposition of mucinous substances was accompanied with deep morphological and structural changes of cumulus cells. Additional information was obtained about participation of the oocyte in the production of cumulus expansion enabling factor. In contrast to the mouse, in the pig this factor was produced also by cumulus cells and under certain hormonal conditions also by granulosa cells.

In another group of experiments the attention was paid to the molecular events that are involved in chromatin condensation and nuclear membrane dissolution in initial phases of maturation. These studies conducted originally with various developmental categories of rabbit oocytes clearly demonstrated close relation between the level of activation of histone H1 kinase and the degree of chromatin condensation. Identical relations were observed also in bovine and porcine oocytes. Moreover, in these experiments was documented the role of protein synthesis and protein phosphorylation on the activation of histone H1 kinase.

In the laboratory of Prof. R.M. Schultz (Univ. of Pennsylvania) our colleague together with other members of the staff had developed rapid, nonradioactive method for the analysis of the modification of mouse zona pellucida induced by fertilization. Later, this method was applied in the evaluation in human zona pellucida and the authors suggested a possible exploitation for the identification of deficiencies after IVF failure. In this laboratory described also basic molecular events that occur immediately after fertilization and the participation of the $p34^{cdc2}$ cyclin B complex and myelin basic protein complex in the formation of pronucleus.

The accomplished results were published or submitted for publication in 14 papers that appeared in international journals. However, more important for the institute was the chance to train our young people in first class laboratories in USA and some European countries. Approximately half of the budget was used for this purpose. Due to this fact we have at present experienced persons who are able to communicate with world scientific community on standard level.

Research Objectives.

Already for several decades extensive studies have been addressed to the problems associated with mammalian oocytes maturation. Original morphological approach for the assessment of maturation progression has been gradually complemented by methods allowing to investigate this process on molecular level. By this way it was collected many information, however, still remain many events far from clear understanding and only a part of embryos derived from the oocytes matured in vitro possesses full developmental competence. At present only approximately 20-30 healthy looking blastocysts are harvested from 100 oocytes selected after in vitro maturation for the fertilization. It in believed that these disappointing results could be improved by the creation of more suitable conditions to which are oocytes exposed for maturation. Due to the fact that the ovaries of commercially slaughtered females represent nearly unlimited source of potential candidates for the generation of embryos, one can't be surprised by the effort for to the improvement of oocytes parameters after maturation. Unfortunately, the understanding about the control of synthetic activity in the oocytes that is realized in close interaction with adjacent somatic cells remains very low. Therefore, the production of embryos from this material for breeding and experimental purposes has still severe limitations.

The research objectives of present proposal were based on our preliminary results and focused to the studies of interaction between somatic and germ cells during maturation and to the nuclear changes that are associated with initiation and progression of this process. The significance of mutual functional relations between these two types of cells were repeatedly documented.

In context following specific objectives were selected:

1. To determine if the maturation inhibiting activity of pig membrana granulosa is not species specific and to isolate the components that are responsible for meiotic block.
2. To determine under in vitro conditions specific role of theca and granulosa cells in resumption of meiosis induced by LH and assess the role of cumulus expansion and cell to cell communication in resumption of meiosis.
3. To test developmental ability of oocytes matured under various developmental conditions.

Actually the studies concerning of mammalian oocyte maturation have in our laboratory relatively long tradition and quite a few papers about various aspects of this process were published in well recognized international journals. From this point of view we

were convinced that it will be hardly possible to make dramatic break in the strategies used for the production of competent oocytes in vitro. Our aim was rather to contribute with accomplished results to the elucidation of selected events that would help the suggestion of more suitable environment for maturation. Concomitantly we preferred to perform our studies in close contact with international scientific community. Therefore we arranged this stays of several young members of the staff in first class laboratories abroad particularly in U.S.A. The realization of this intention consumed considerable part of the budget, however we have now in the institute well trained young scientists. They are able to introduce new experimental approaches that allow to investigate problems on molecular level.

Methods and Results.

During three year studies, beside well developed cultivation system, broad spectrum of experimental methods was employed. All of them including results are in details described in published or submitted papers that are enclosed to Final Report. Papers appeared exclusively in peer-reviewed international journals.

List of publications that were supported from the budget and originated in the institute.

List of Publications:

Kalous, J.; Sutovsky, P.; Rimkevicova, Z.; Shioya, Y.; Lie, B.-L.; Motlik, J. (1993) Pig membrana granulosa cells prevent resumption of meiosis in cattle oocytes. *Mol. Reprod. Develop.* 34, 58-64

Nagyova, E.; Kalous, J.; Sutovsky, P.; Motlik, J. (1993) Is cAMP decrease essential for resumption of meiosis in mouse oocytes? *Reprod. Nutr. Develop.* 33, 419-428

Kalous, J.; Kubelka, M.; Rimkevicova, Z.; Guerrier, P.; Motlik, J. (1992) Okadaic acid accelerates germinal vesicle breakdown and overcomes cycloheximide and 6-dimethylaminopurine block in cattle and pig oocytes. *Develop. Biol.* 157, 448-451

Sutovsky, P.; Jelinkova, L.; Antalikova, L.; Motlik, J. (1993) Ultrastructural cytochemistry of the nucleus and nucleolus in growing rabbit oocytes. *Biol. Cell* 77, 173-180

Jelinkova, L.; Kubelka, M.; Motlik, J.; Guerrier, P. (1994) Chromatin condensation and histone H1 kinase activity during growth and maturation of rabbit oocytes. *Mol. Reprod. Develop.* 37, 210-215

Sutovsky, P.; Flechon, J.E.; Flechon, B.; Peynot, N.; Motlik, J.; Chesne, P.; Heyman, Y. (1993) Dynamics changes of gap junctions, cytoskeleton and extracellular matrix during in vitro culture of cattle oocyte cumulus complex.
Biol. Reprod. 49, 1277-1287

Sutovsky, P.; Flechon, J.E.; Pavlok, A. (1994) Microfilaments, microtubulles and intermediate filaments fulfil differential roles in gonadotropin induced expansion of bovine cumulus oophorus.
Reprod. Nutr. Develop. 34, 415-425

Sutovsky, P.; Flechon, J.E.; Pavlok, A. (1995) F-actin is involved in control of bovine cumulus expansion.
Mol. Reprod. Develop. 41, 521-529

Sutovsky, P.; Motlik, J. (1994) Cumulus expansion in mammals: Cumulus Granulosa Cell Cytoskeleton/Extracellular Matrix/Oocyte Secretion Interactions.
Arta 6, 304-315

Prochazka, R.; Nagyova, E.; Motlik, J. (1995) Porcine Cumulus and Mural Granulosa Cells Secrete Cumulus Expansion Enabling Factor (CEEF)
Submitted: *Biol. Reprod.*

Sutovsky, P.; Kalous, J.; Kalab, P.; Kubelka, M.; Moos, J.; Schultz, R.M.; Motlik, J. (1995) The Effect of Membrana Granulosa Cells on Histone H1 and MAP Kinase Activity in Mammalian Oocytes.
Submitted: *Dev. Biol.*

Some experiments were carried out in the collaboration with coworkers from other countries, particularly from France and U.S.A. In these instances the visitors from our Institute exploited the equipment and specific reagents as monoclonal antibodies that were not for disposal in domestic lab.

List of publications originated during the stay of Dr. Jiří Moos in The Division of Reproductive Biology, Univ. of Pennsylvania, Philadelphia - Head; Prof. R.M. Schultz.

Moos, J.; Kalab, P.; Schultz, R.M.; Kopf G.S. (1994) Rapid, nonradioactive, and quantitative method to analyze zona pellucida modifications in singel mouse eggs. *Mol. Reprod. Develop.* 38, 91-93

Moos, J.; Visconti, P.E.; Moore, G.D.; Schultz, R.M.; Kopf, G.S. (1995) Potential Role of Mitogen-Activated Protein Kinase in Pronuclear Envelope Assembly and Disassembly Following Fertilization of Mouse Eggs. *Biol. Reprod.* 53, 692-699

Moss, J.; Faundes, D.; Kopf, G.S.; Schultz, R.M. (1995) Composition of the human zona pellucida and modifications following fertilization. *Mol. Human. Reproduction* 10, 00-00

Papers that will be submitted for publication soon:

Carrera, A., Moos, A., Gerton, G.L., Tesarik, J., Kopf, G.S., Moss, S.B. (1995) Tyrosine phosphorylation of a A kinase anchor proteins in human sperm: Regulation by a calcium/calmodulin-dependent mechanism.

Moos, J., Kopf, G.S., Schultz, R.M. (1995) Cyclohexim-induced calcium-independent egg activation: Effect on cdc2/cyclin B kinase, MAP kinase, zona pellucida modification, chromatin condensation, and microtubule organization.

Dr. Jiří Moos took a chance to work with Prof. R.M. Schultz from April, 1993 to the expiration of the grant support (approximately 30 months). His stay was covered from the grant budget and as obvious he fully exploited the opportunity to learn methods used for studies of oocytes maturation and their activation after fertilization on molecular level. Research activity is clearly evident from the list of publications.

Impact: Relevance and Technology Transfer.

Most important impact represents the preparation of this project. Actually it was our first trial for the support from international sources. Due to the previous isolation we had no experience in such activity and only instructions provided kindly by Prof. R.M. Schultz increased a chance for the acceptance of our application. This help can't be appreciated enough particularly in the light of present situation when the financial support of research programs is realized according to the quality of submitted applications. Such competition has been introduced in praxis even in domestic grant agencies that were recently established also in Czech Republic.

The support from A.I.D. increased also the possibility to initiate fruitful contacts with scientific communities abroad. If necessary grant financial sources were used for the active participation on several international meetings, for the stays of young workers in foreign laboratories and particularly for the long term stay of Dr. J. Moos in U.S.A. These activities made possible to exchange the ideas with persons aged in similar topic and particularly to learn new methods. By this way our experimental approaches have been increased and maintained on good international standard. The publications clearly support these arguments and concomitantly indicate that our studies were in narrow context with the research efforts in developed countries. It is not ease to mention all positive details, however, we feel that the authority of the Institute has been increased and now quite a few scientists from developed countries call for consultation or collaboration.

Special value has accomplished results. They inform the international community about professional ability of persons working in our laboratories and also contribute to the characterization of the established scientific profile. Such progress could be achieved only due to the grant support. The available financial means were used mainly for supplying laboratory with chemicals, glass, small items and animals and of course for the training of the staff. From more expensive equipment left behind after the completion of the project only 2 stereomicroscopes and 1 computer. No finances were used for the improvement of salaries.

Project Activities.

No special meetings connected with the project realization were organized. The results accomplished were presented in parts on common French-Czech-Slovak symposium realized in Košice (Slovakia) in November 1994. The expension for participants (4 persons) was covered from the grant budget.

In March 24.-25.1994 was held in Krakow (Poland) meeting called First Integrated European Conference on Progress in Embryo Technology and Genetic Engineering in Cattle and Sheep Breeding and 4 persons obtained financial support.

In the year 1993 attended 2 persons the conference about nucleolar structure and function organized in Budapest (Hungary) with the financial contribution from the budget.

In limited instances from the budget were covered only transport expenses to persons visiting some European laboratories with the aim to conduct common experiments.

Project Productivity.

The evaluation of scientific aspects allows to admit that during studies was accomplished more results that we originally expected (See list of Publications). Also the introduction of progressive experimental methods, as well as the establishment of new contacts with scientists from developed countries represents promising contribution for future research. However, according to our opinion most profitable for the institute was the training of young colleagues in well known laboratories, particularly in USA. Without the support from A.I.D. such possibilities would hardly available. It should be also emphasized that we exploited for this purpose relatively high amount of financial sources. However, we anticipate that the skill of young members will open the way for effective international collaboration and also will enhance our chances to compete in grant application on national and international levels.

On the other hand it should be confess that the original idea, to find an approach to the regulation of the maturation of bovine oocytes by porcine granulosa cells was not completed sufficiently. The working hypothesis calculating with total inhibiton of germinal vesicle progression after addition of these particular cells was not fully confirmed. Our experiments repeatedly revealed the onset of chromatin condensation irrespective of employed culture systems. These observations prevent to suggest more effective culture environment for the production of competent bovine oocytes in vitro. Our results rather stimulate further studies that would elucidate in more details the background of inhibiting activity derived from mural granulosa.

Moreover, new situation in the agriculture strongly affected also the accomplishment of the final goal-the creation of more effective culture system. For cattle breeding were in previous years typical large farms. At that time it was easy to find animals for the realization of field experiments. The transformation of agriculture and the transfer of animals and soil to private hands resulted in dramatic reduction of cattle population and in the formation of small breeds. New owners exposed to strong economical pressure had only marginal interest for the introduction of progressive technologies, that may be associated with unknown results. Therefore, to select suitable animals for the evaluation of viability of bovine embryos was accompanied with serious problems. We believe that these difficulties are transient only and the situation will be stabilized soon again.

Future Work.

The knowledge concerning mutual interaction between germ cells and adjacent somatic compartment remains still incomplete. Only little is known about the participation of follicular cells during oocyte growth and also the mechanisms responsible for meiotic arrest of fully grown oocytes are unclear. These topics that are studied in several laboratories in developed countries will be investigated also in our institute in next years. The laboratories are relatively well equipped for these aims and also human capacity is sufficiently prepared to perform experiments on high level. Moreover, the results obtained during previous three years provide good starting points for this intention. Now we are able to detect activity of several key enzymes including histone H1 and MAP kinases and we would like to search for molecules that are responsible for their activation. We anticipate that observations obtained in oocyte model may be valuable indicators for the characterization of similarities or differences between meiotic and mitotic cell cycle.

The second line of research will be addressed to the extension of knowledge concerning the background of inhibiting activity originated in membrana granulosa cells. For these aims, as well as for the investigation of the role of the oocyte for cumulus expansion, will be employed methods allowing to study these processes on molecular level.

For the realization of suggested projects several grant applications were submitted. Two were accepted and supported from national grant agencies, the fate of others is still open.

BIOLOGY OF REPRODUCTION 49, 1277–1287 (1993)

Dynamic Changes of Gap Junctions and Cytoskeleton during In Vitro Culture of Cattle Oocyte Cumulus Complexes[1]

PETER ŠUTOVSKÝ,[2,3] JACQUES E. FLÉCHON,[4] BERNADETTE FLÉCHON,[4] JAN MOTLIK,[3] NATHALIE PEYNOT,[5] PATRICK CHESNE,[5] and YVAN HEYMAN[5]

Institute of Physiology and Genetics of Animals,[3] 277 21 Liběchov, Czech Republic
Unité de Biologie Cellulaire et de Microscopie Electronique[4] and Unité de Biologie du Développement[5]
Institut National de Recherche Agronomique, 78 350 Jouy-en-Josas, France

ABSTRACT

Changes in cell to cell contact and distribution of cytoskeletal components were investigated during in vitro culture of cattle oocyte cumulus complexes (OCC). Freeze fracture analysis (FF), microinjections of the fluorescent dye Lucifer Yellow (LY), immunofluorescence, and ultrastructural immunocytochemistry were used. The cumulus cells (CC) remained in close contact via gap junctions (GJ) constituted of connexin43 (Cx43) during the entire culture time. Whereas the GJ decreased in diameter after 24 h of culture, their number was still substantially great at that time. The Cx43 positive GJ, localized between corona radiata cell projections and oolemma, disappeared after 6 h of culture. Concomitantly, the OCC lost the ability to transfer LY from cumulus to oocyte, and connexin32 (Cx32) became detectable in the oocytes. Both the changes in corona-oocyte coupling and cumulus expansion were preceded by the redistribution of F-actin in cytoplasm of CC. These data indicate that functional GJ linked the CC until the second meiotic arrest. However, the removal of Cx43-positive GJ interconnecting cytoplasmic projections of corona radiata cells with the oocyte was temporally correlated with germinal vesicle breakdown. The present results suggest the pivotal role of the cytoskeleton (F-actin) in cumulus expansion.

INTRODUCTION

The cell populations in mammalian follicles are interconnected by an extensive network of gap junctions (GJ) [1]. These widespread structures contain transmembrane channels formed by hexamers of proteins belonging to the connexin family [2–4]. The physiological function of follicular GJ consists in the mediation of nutritional support [5], electric coupling, and transport of messenger molecules from follicle cells to the oocyte [6]. Whereas the ultrastructure and distribution of follicle cell GJ has been well described [7–14], only incomplete evidence exists about the connexins participating in their formation [3, 15]. Moreover, the explanation of the role of follicular GJ in oocyte final maturation is controversial (for review, see [16, 12]).

Numerous ultrastructural studies have shown a substantial decrease in cell to cell communication during in vivo or in vitro maturation of mammalian oocyte cumulus complex (OCC). The authors of those studies suggested that LH-induced loss of GJ could trigger the resumption of oocyte meiotic maturation by reducing the transport of meiosis-inhibitory substance(s) from the somatic to the germinal compartment of the follicle [1, 11, 14, 16, 17–19]. Whereas these findings have been supported by several physiological studies [19–21], a majority of metabolic cooperation assays have shown that passage of small radiolabeled molecules from the cumulus cells (CC) to an oocyte continues at an unchanged rate for several hours after resumption of meiosis [22–27]. These results suggest that cell-to-cell contacts are not interrupted in response to gonadotropin stimulation under in vivo or in vitro conditions.

Recent studies by Wert and Larsen [13] and Chen et al. [28] have demonstrated the influence of actin-blocking drugs on cumulus expansion and on cell-to-cell communication. However, the changes in cell coupling during cumulus expansion were not evaluated in relation to the distribution of basic cytoskeletal components in CC. The expansion of cumulus is believed to be the result of an increase in synthesis of hyaluronic acid, glycosaminoglycans, and glycoproteins [29–33]. Moreover, it is generally accepted that cells in an expanded cumulus do not communicate [29, 34].

To demonstrate the dynamics in the redistribution of GJ and cytoskeletal proteins during in vitro maturation of bovine OCC, we employed the methods of immunofluorescence, immunoelectron microscopy, microinjections of fluorescent dyes, and quantitative freeze-fracture analysis (FF). Our findings indicate that the volumetric expansion of cumulus oophorus is triggered by an assembly of F-actin in CC and that these cells at all stages of cumulus expansion are interconnected by an extensive network of functional GJ built of connexin43 (Cx43). Synthesis of another GJ protein, connexin32 (Cx32), starts in oocyte cytoplasm after 6 h of culture. The results offer a new perspective in the study of cumulus expansion and suggest caution in interpretation of the role fulfilled by follicular GJ in the resumption of oocyte meiotic maturation.

Accepted July 16, 1993
Received February 15, 1993
[1]This work was partially supported by AID grant number 12061E. The stay of P. Šutovský in INRA Jouy-en-Josas was supported by scholarship from CIES Paris, France.
[2]Correspondence.

12

MATERIALS AND METHODS

Sample Collection and Culture

Cattle ovaries were collected at a local slaughterhouse and the OCC were aspirated from 4–8-mm large antral follicles. Only compact OCC with a minimum of five layers of CCs were used for the culture. The OCC were cultured in the conditions routinely used to obtain viable bovine oocytes for in vitro fertilization and embryo transfer [35, 36]. After brief washing, OCC were placed in culture dishes (Nunc, Roskilde, Denmark) bottom-coated with a monolayer of bovine granulosa cells. The culture was carried out in M199 culture medium containing 10% fetal calf serum (FCS, Flow Laboratories, McLean, VA), 1 μg/ml of estradiol, and 10 μg/ml of FSH LH (Stimufol, Rhone-Merieux, France) at 39°C in a humid atmosphere of 5% CO_2 in air. The cultured OCC were fixed at 3-h intervals from 0 to 24 h and processed by the methods described below. For a portion of the oocytes, the CC were removed via a short incubation in M199 containing 0.5% hyaluronidase and gentle pipetting and the zona pellucida (ZP) was dissolved in 0.5% pronase solution.

Immunofluorescence

The OCC and zona-free oocytes were fixed for 20 min in 2.5% paraformaldehyde in Dulbecco's PBS, pH 7.3 (Oxoid Unipath, England), then incubated for 1 h in a solution of 50 mM ammonium chloride, washed, and conserved in 0.1 M PBS containing 0.05% sodium azide (NaN_3) and 1 mM PMSF (Serva, Heidelberg, Germany).

The following antibodies were used for indirect immunofluorescence: anti-Cx43 rabbit polyclonal antibody [37], kindly provided by Dr. D. Gros (University of Marseille, France), diluted 1/10; anti-Cx32 rat monoclonal antibody [38] (Developmental Studies Hybridoma Bank, Baltimore, MD) diluted 1:5; anti-tubulin TU-01 mouse monoclonal antibody [39] from Dr. V. Viklicky (Institute of Molecular Genetics, Praha, Czech Republic), diluted 1:30; anti-vimentin mouse monoclonal antibody [40] from Dr. I. Virtanen (University of Helsinki, Finland), diluted 1:2; TRITC-conjugated anti-rat IgG, diluted 1:300 (Jackson Immunoresearch Laboratories, West Grove, PA), FITC-conjugated anti-rabbit IgG, diluted 1:200 (Pasteur Diagnostics Sanofi, Marne la Coquette, France), and FITC-conjugated anti-mouse IgG, diluted 1:300 (Biosys, Compiegne, France). Counterstains such as Hoechst 33258 (Sigma, St. Louis, MO) and rhodamine-phalloidin (Molecular Probes, Eugene, OR) were used. Thirty-five to fifty OCC were processed with each antibody. The immunofluorescence protocol included blockage of the nonspecific reactions by preincubation in 0.1 M PBS containing 2% BSA, NaN_3 and 0.05% saponin (Sigma); incubation for 1 h with primary antibody; washing in 0.1 M PBS with 0.2% BSA, NaN_3, and saponin, and treatment by anti-species-specific secondary antibody. In several experiments, the F-actin was stained with rhodamine-phalloidin diluted (1:50) in the solution of secondary antibody. Hoechst 33258 was applied at a concentration of 5 μg/ml after the secondary antibody and served as a control for oocyte nuclear maturation. After repeated washings, the samples were mounted on slides in a mixture of Mowiol V 4–88 (Hoechst, Frankfurt, Germany) and *n*-propyl gallate (Sigma). The antibodies and fluorescent dyes were diluted in the same solution that was used for preincubation. Controls were performed using preimmune serum obtained from the donor of the primary polyclonal antibody. The OCC were examined and photographed with a Polyvar (Reichert-Jung, Wien, Austria) fluorescent microscope.

Freeze Fracture

The OCC cultured for 0, 12, and 24 h were fixed in a 1% glutaraldehyde and 0.5% paraformaldehyde mixture, then were washed in 0.1 M sodium cacodylate and impregnated with 20% cacodylate-buffered glycerol. For each time point, six OCC were frozen in nitrogen slush and fractured in a Reichert-Jung Cryofract 190 freeze-fracture apparatus; ten grids with fractured cytoplasmic membranes were obtained for each time point. The replicas were examined in Philips CM 12 and JEOL 1200 EX (Jeol Ltd., Tokyo, Japan) electron microscopes. Individual GJ plaques from both the protoplasmic (P) and the exoplasmic (E) fracture faces were photographed at a magnification of 50 000×, and their surfaces were measured manually. In addition, the total area of scanned fractional membrane was recorded, representing 20850 μm^2 at 0 h, 6300 μm^2 at 12 h, and 3150 μm^2 at 24 h. The average area of total GJ, the average area of GJ plaques per 100 μm^2 of scanned fractional membrane, and the average number of GJ plaques per 100 μm^2 of scanned fractional membrane were calculated for each time point. Both fields of fractional membrane containing GJ and fields of GJ-free membranes were measured and included in this calculation.

Electron Microscopy

The OCC were fixed in a mixture of 0.6% paraformaldehyde and 2.5% glutaraldehyde for 1 h; they were then postfixed in 1% osmium tetroxide, dehydrated by an ascending series of ethanol, and embedded in Epon 812 (Serva). The blocks were sectioned in Reichert-Jung Ultracut F, contrasted by uranyl acetate and lead citrate, and observed by electron microscopy.

Ultrastructural Immunocytochemistry

OCC and zona-free oocytes were fixed in a 2.5% paraformaldehyde and 0.1% glutaraldehyde mixture, dehydrated in an ascending series of ethanol, and embedded in LR White resin medium (TAAB, Reading, UK). Ultrathin sections were placed on nickel grids and blocked by preincubation with 0.1 M PBS containing 2% BSA for 1 h. Then the grids were incubated overnight with anti-Cx43 antibody

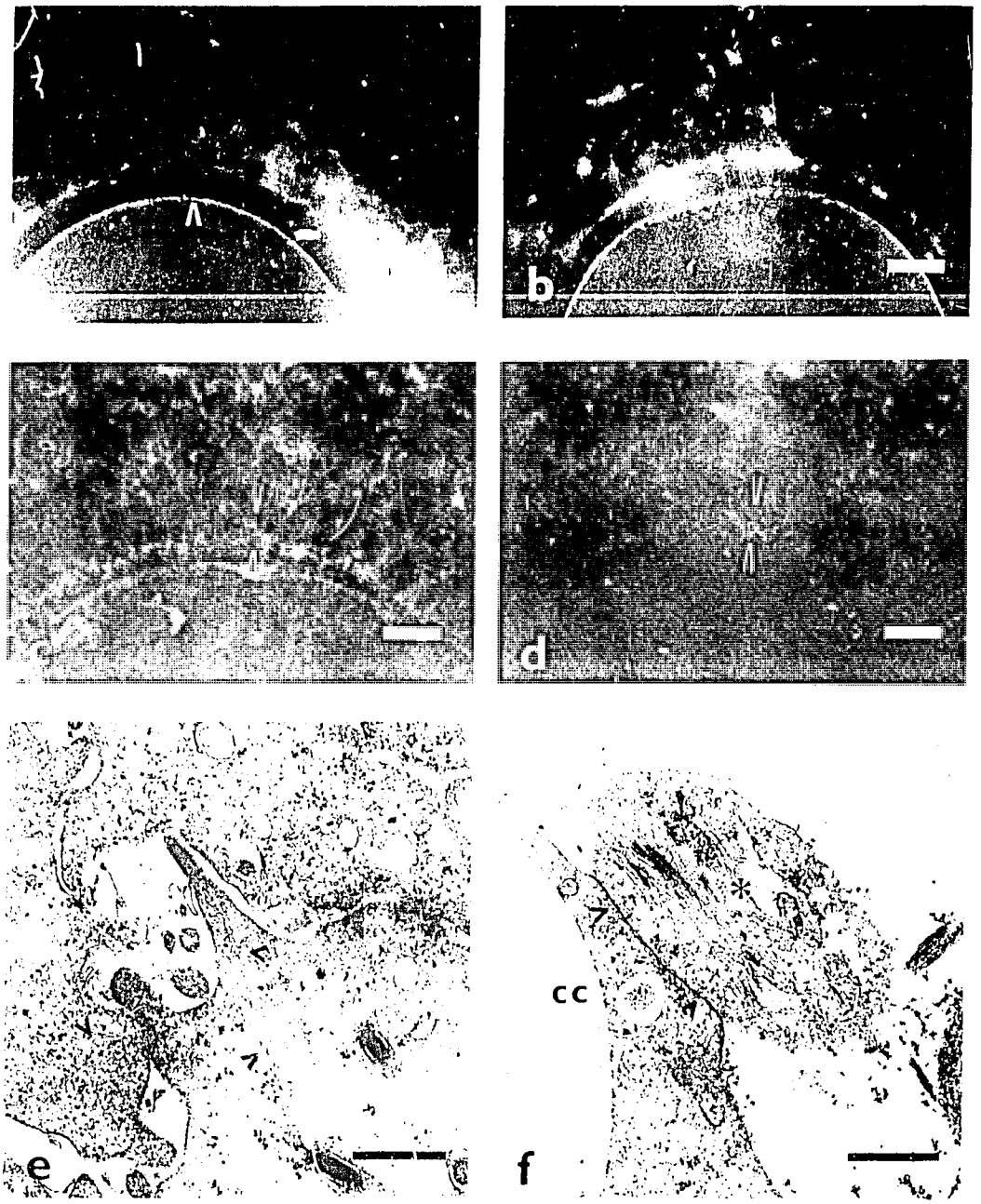

FIG. 1. Distribution of F-actin in cattle OCC, demonstrated by rhodamine-phalloidin staining and electron microscopy. a) Diffuse labeling of F-actin with rhodamine-phalloidin in a freshly isolated OCC. Note the cortical ring of actin in the oocyte (arrows). Bar = 20 μm. b) F-actin is assembled in large clusters around the zona pellucida and in CC of an OCC cultured for 6 h. Bar = 20 μm. c) An irregular bright rim of F-actin-containing corona radiata projections (arrows) surrounds the ZP of an OCC after 24 h of culture. Labeling with rhodamine-phalloidin. Bar = 15 μm. d) The same OCC as in Figure C, double-labeled for Cx43. Numerous small GJ (arrows), concentrated around ZP, coincide with corona radiata projections in Figure C. Bar = 15 μm. e) Electron micrograph of CC in an OCC cultured for 3 h shows ruffled cytoplasmic membranes at the beginning of the formation of cytoplasmic projections. Note the bundles of actin microfilaments (arrows) in ruffled membrane profiles. Bar = 500 nm. f) An ultrathin section of an OCC after 24 h of culture. A large CC projection containing longitudinally arranged microfilaments (asterisk) is interconnected with another CC through large GJ (arrows). Bar = 500 nm.

14

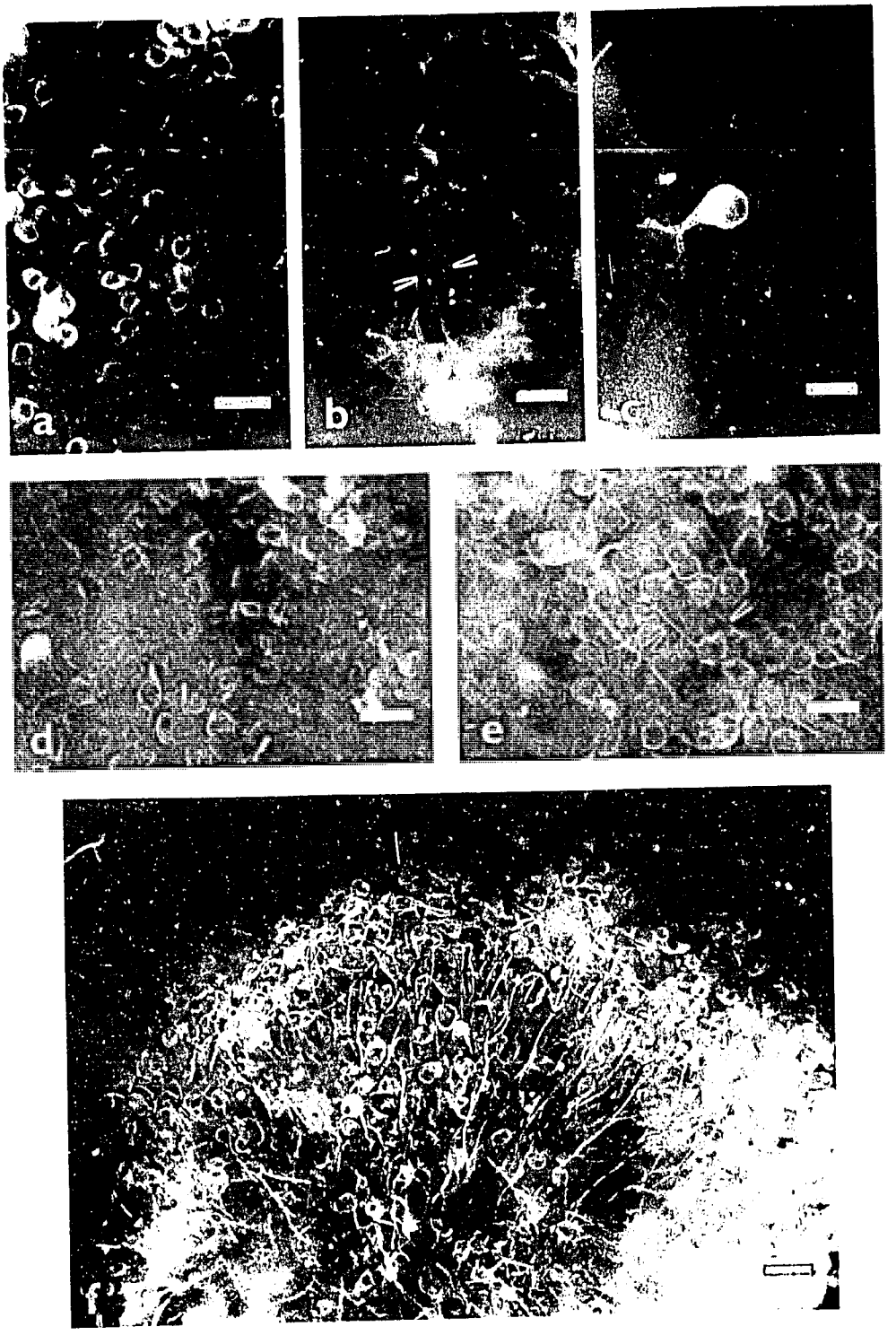

15

diluted to 1:4, in rabbit F(ab) biotinylated fragments (Bio Cell, Cardiff, UK), and in colloidal gold-conjugated streptavidin (particle size 15 nm; Amersham, Buckinghamshire, England) for 1 h. Ultrathin sections were stained with uranyl acetate and lead citrate.

Dye Coupling Assay

The fluorescent dye Lucifer Yellow (LY; Sigma) was used in 5% concentration in 5 mM lithium chloride and pressure injected into different compartments of the OCC. The injection device included an epifluorescence-equipped Olympus IMT-2 microscope with video camera, two micromanipulators (DeFonbrune; Technical Products International, St. Louis, MO), and an automatic microinjector (Eppendorf 5242, Hamburg, Germany). For the injections into oocytes, the OCC were held with a micropipette and injected horizontally. Vertical injections into CC were also performed; in this procedure the OCC were not held. A total of 34 OCC were injected at different times of in vitro culture.

Statistical Analysis

The diameters of all GJ plaques measured for each time point were expressed as mean ± SEM. The data were evaluated by analysis of variance and Duncan's Multiple Range test. Differences of $p < 0.05$ were considered statistically significant.

RESULTS

Nuclear Maturation and Cumulus Expansion

Staining with Hoechst 33258 showed highly condensed chromosomal bivalents in oocytes cultured for 6 h. The first polar body appeared between 18 and 21 h of culture. After 24 h, all oocytes used were in metaphase (M) II stage. After 9–12 h, the expansion of the cumulus became detectable under the stereomicroscope. The oocytes in M II were surrounded by fully expanded cumuli with polarized CC forming long cytoplasmic projections oriented towards the oocytes. The cells in such OCC were separated by large intercellular spaces (Fig. 3C). The rate of cumulus expansion was similar to that observed in cattle OCC in vivo [41] and in vitro [35].

FIG. 2. Indirect immunofluorescence labeling of α-tubulin and vimentin. a) Perinuclear rings of microtubules in CC at the onset of culture. Bar = 25 μm. b) The α-tubulin was also localized in cytoplasmic projections (arrows) linking CC after 12 h of culture. Bar = 20 μm. c) The anchorage of corona radiata cell at ZP of an oocyte partially denuded after 24 h of culture, as shown by TU 01 antibody. Bar = 15 μm. d) Regular arrangement of vimentin filaments in CC at the onset of culture. Bar = 20 μm. e) The cytoplasmic projections (arrows) of CC in an OCC cultured for 12 h are loaded with intermediate filaments constituted of vimentin. Bar = 20 μm. f) The expanded cumulus of an OCC cultured for 24 h, shown by indirect immunofluorescence with anti-vimentin antibody. Bar = 25 μm.

Microfilaments

Microfilaments containing F-actin were homogenously distributed in the cytoplasm of CC at the onset of in vitro culture (Fig. 1A). The corona radiata cells penetrated across the ZP via numerous cytoplasmic projections filled with F-actin. This type of cellular projection and a regular ring of F-actin in cortical ooplasm remained visible during the entire culture period. The F-actin cytoskeleton underwent substantial changes within the first 3 h of incubation when large bundles of F-actin and ruffled membranes appeared in CC (Fig. 1B). After 6–9 h of culture, F-actin redistribution continued concomitantly with the formation of an anastomosing network of cytoplasmic projections between CC resulting in extension of intercellular spaces. During further culture, the F-actin ring of corona radiata projections increased in thickness around the ZP. Double immunofluorescent labeling with anti-Cx43 antibody and rhodamine-phalloidin revealed that this ring of F-actin corresponded with the rim of small GJ interconnecting the CC projections over the ZP (Fig. 1, C and D). Ultrastructural observations demonstrated the association of the microfilament bundles with ruffled regions of cytoplasmic membranes in the cumuli undergoing expansion (Fig. 1E). However, such an association was never observed between microfilaments and GJ membranes, even when they occurred in close vicinity (Fig. 1F).

Microtubules and Intermediate Filaments

Both the α-tubulin-containing microtubules and intermediate filaments built of vimentin formed regular rings around the nuclei of CC at the onset of culture (Fig. 2, A and D). After 9–12 h of culture, these two cytoskeletal components filled the cytoplasmic projections interconnecting the CC (Fig. 2, B and E). In the OCC cultured for 24 h, the anchorage of corona radiata cells to the ZP was visualized by use of antibodies against these proteins (Fig. 2, C and F). Vimentin and α-tubulin labeling was not found in the projections penetrating across the ZP.

Cumulus-to-Cumulus Cell Gap Junctions

Indirect immunofluorescence showed that CC in freshly isolated OCC were coupled by large GJ constituted of Cx43 (Fig. 3A). No changes in GJ labeling pattern were observed up to 6–9 h of culture. After 9–12 h of culture, the immunofluorescent labeling became punctate. After 24 h of culture, a large population of CC communicated through small Cx43-positive GJ (Fig. 3B). Ultrastructural immunocytochemistry demonstrated that corona radiata cells in expanded OCC were attached to ZP by branched cytoplasmic projections (Fig. 3C) and that they contained numerous small GJ (Figs. 1D and 3D).

Freeze-fracture analysis revealed that the range of GJ sizes was similar at all time points (0.003–0.503 μm^2 at 0 h, 0.003–0.625 μm^2 at 12 h, 0.003–0.550 μm^2 at 24 h). However, the

16

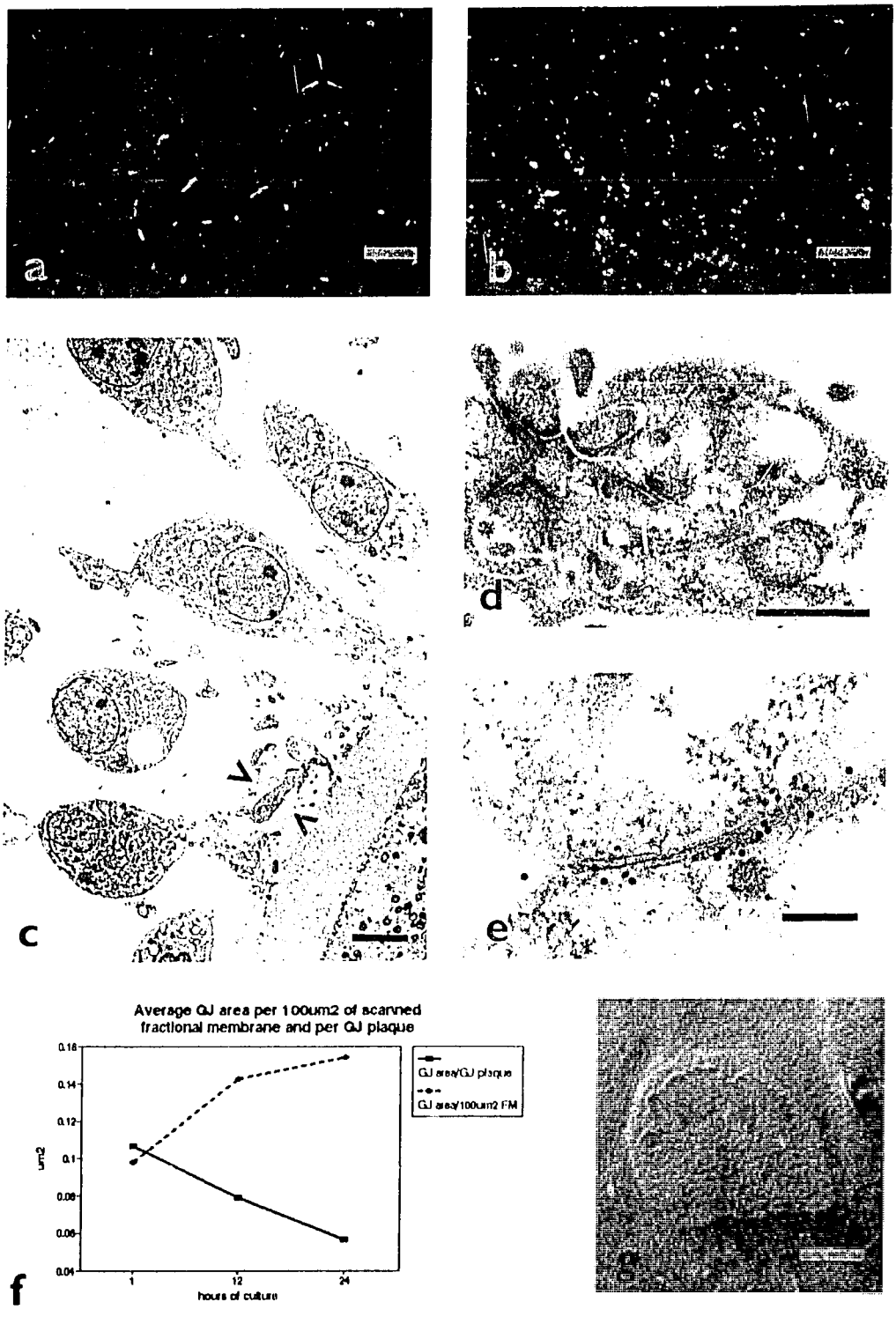
a
b
c
d
e
Average GJ area per 100um2 of scanned fractional membrane and per GJ plaque
GJ area/GJ plaque
GJ area/100um2 FM
um2
0.18
0.14
0.12
0.1
0.08
0.06
0.04
1
12
24
hours of culture
f
g

17

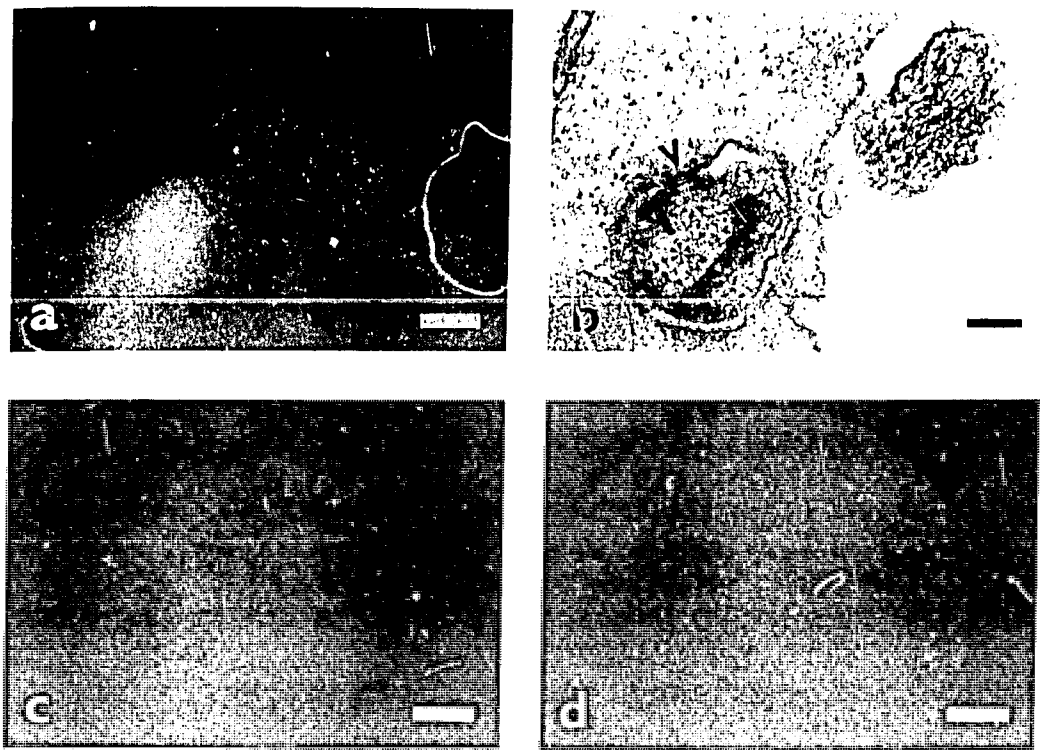

FIG. 4. Cumulus-to-oocyte GJ and expression of Cx32 in bovine oocytes. (A) Small GJ on the oolemma of an oocyte from freshly isolated OCC, demonstrated via immunofluorescence with anti-Cx43 antibody. Bar = 15 μm. B) Electron micrograph of an oocyte cultured for 3 h. Bulbous ending of CC projection (asterisk) is coupled with oolemma by small GJ (arrow). Bar = 100 nm. C) No labeling of Cx32 was found in cattle oocytes up to 6 h of culture. Bar = 25 μm. D) An oocyte isolated from the OCC after 6 h of culture. The Cx32-positive structures were visualized via anti-Cx32 followed by Texas red-conjugated secondary antibody. Bar = 25 μm.

mean diameter of individual GJ plaques dropped substantially after 12 and 24 h of culture (Fig. 3F). This decrease was compensated by an increase in number of GJ plaques per 100 μm^2 of fractional membrane area, represented by 0.92 plaques at 0 h, 1.81 plaques at 12 h, and 2.70 plaques at 24 h. Such a redistribution of GJ plaques caused considerable elevation of the average area of GJ plaques per 100 μm^2 of scanned fractional membrane after 24 h of culture (Fig. 3F).

FIG. 3. Cumulus-to-cumulus cell GJ in cattle OCC. A) Cumulus cells in a freshly isolated OCC are interconnected by large GJ positive for Cx43. Bar = 10 μm. B) Punctate pattern of immunofluorescent labeling with anti-Cx43 in an OCC after 24 h of culture. Bar = 10 μm. C) Ultrathin section of an OCC cultured for 24 h. Corona radiata cells form a ring of crossed cytoplasmic projections around ZP (arrows). Bar = 5 μm. D) Clump of such projections, interconnected by small GJ, labeled via the anti-Cx43 colloidal gold method. Bar = 500 nm. E) A large GJ linking two CC expresses strong positivity to anti-Cx43 antibody. Bar = 500 nm. F) Average area of total GJ plaques measured in FF replicates and average area of GJ per 100 μm^2 of scanned fractional membrane. The mean diameters of GJ plaques were significantly different at all three time points ($p < 0.05$). The numbers of GJ plaques measured at each time point were: N = 192 at 0 h, N = 114 at 12 h, N = 85 at 24 h. G) Cumulus-to-cumulus cell GJ plaque shown by method of freeze fracture in an OCC cultured for 12 h. GJ area = 0.26 μm^2. Bar = 200 nm.

Cumulus-to-Oocyte Gap Junctions

At the onset of culture, both immunofluorescence and electron microscopy showed that small Cx43-positive junctions interconnected the cytoplasmic projections of CC with the oolemma (Fig. 4, A and B). Progressive disappearance of these GJ occurred within 6–9 h of culture. No positive staining of Cx43 was found in oocytes cultured longer than 9 h. In contrast, Cx32 became detectable in cytoplasm of oocytes cultured for 6 h (Fig. 4, C and D), its amount increasing progressively up to 24 h of culture. At the ultrastructural level, the labeling with anti-Cx32 antibody coincided with clumps of colloidal gold in cortical ooplasm (not shown). No structures corresponding to GJ were found between corona radiata projections and oolemma at this stage.

18

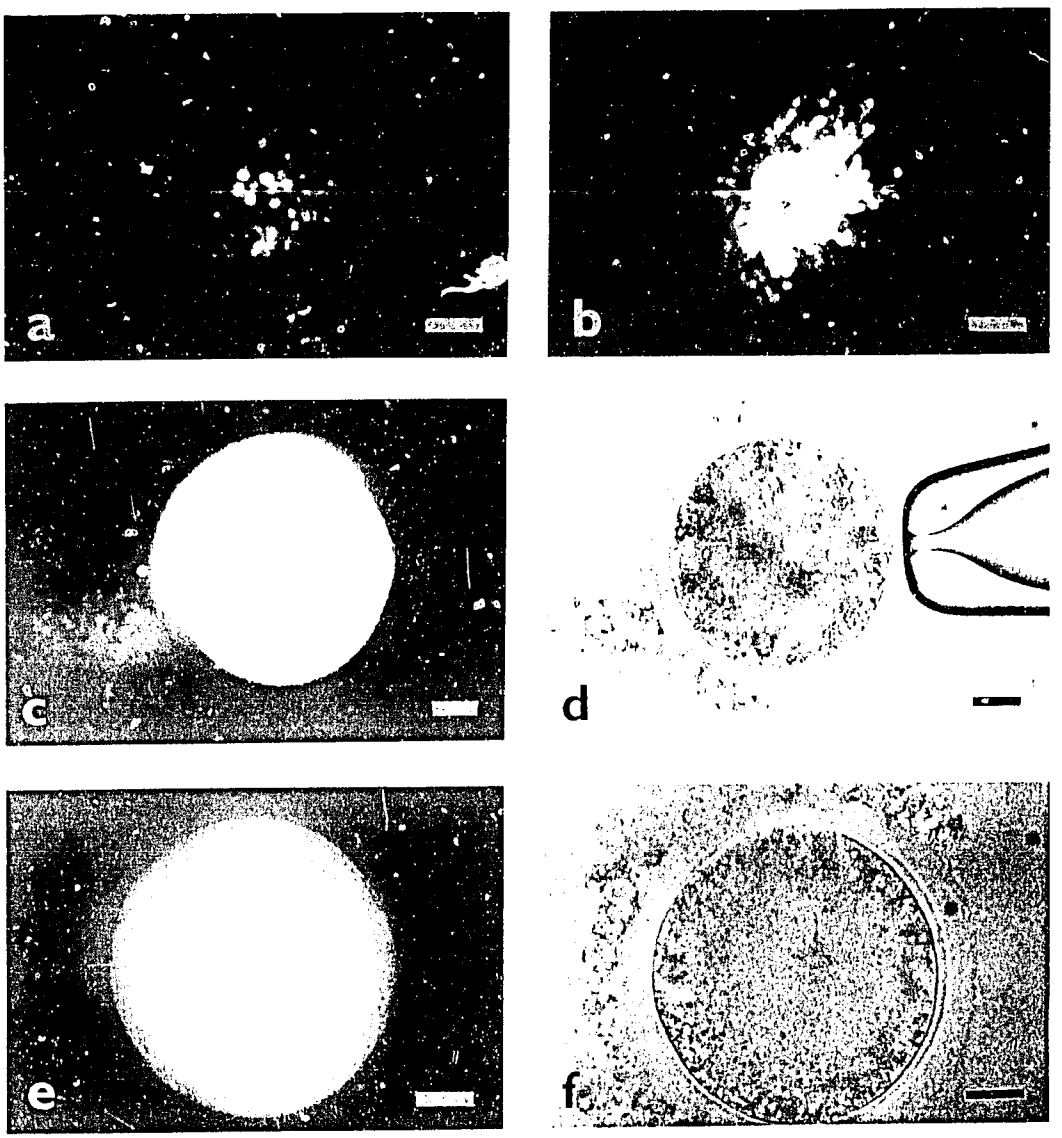

FIG. 5. Injections of fluorescent dye LY into CC (A, B) and into oocytes (C, D, E, F). A, B) Dye spread among CC of an OCC cultured for 24 h: (A) 30 sec, (B) 60 sec after injection. Passage of LY (C) from oocyte to CC in an OCC cultured for 6 h. D) Phase-contrast picture of the same OCC. E, F) No passage of LY was recorded in an OCC cultured for 8 h. All bars = 50 μm.

Dye Coupling Assay

The functional status of both cumulus-to-cumulus and cumulus-to-oocyte GJ was assessed by means of microinjections of fluorescent dye LY, transported exclusively through GJ. During the entire culture time, the injections into CC resulted in the immediate spread of the dye into neighboring cells (Fig. 5, A and B). The passage of LY from oocyte to CC occurred up to 6–9 h of culture (Fig. 5, C and D). After this time point, no transport of LY was observed between CC and oocytes (Fig. 5, E and F).

DISCUSSION

Assembly of F-actin close to the surface of CC within the first 6 h of culture preceded germinal vesicle breakdown

- 19 -

(GVBD), removal of heterologous GJ from oolemma, changes in the staining pattern of homologous GJ, and volumetric cumulus expansion. This phenomenon (F-actin assembly) is thought to participate in the retraction of corona radiata cell projections from the oocyte at the time of meiotic resumption [16]. Larsen et al. [42] demonstrated the association of actin microfilaments with GJ, suggesting that the microfilament-based contractile system is implicated in GJ endocytosis in rat. This initial observation was further supported by the use of actin polymerization inhibitor dihydrocytochalasin B (H$_2$CB), which was found to rescue CC GJ from endocytosis [13] and to inhibit cumulus expansion in isolated rat OCC [28]. However, the same authors showed that the stabilization of actin cytoskeleton by H$_2$CB did not alter the normal course of oocyte meiotic maturation. The inhibitory action of H$_2$CB on F-actin assembly was furthermore demonstrated in cultured granulosa cells [43].

In our study, the actin microfilaments were the most prominent cytoskeletal component of CC cytoplasmic projections interconnecting the cells in expanding cumuli. The assembly of F-actin and membrane ruffling in CC preceded the changes in the distribution and staining pattern of the GJ. Whereas actin microfilaments were frequently found in cytoplasmic projections coupled by GJ to the neighboring cells in cumuli undergoing expansion, no direct association of microfilaments with GJ membranes was observed. In addition, we clearly showed that the GJ in both freshly isolated and fully expanded cumuli were highly active in intercellular transport. Our observations indicate that changes in F-actin distribution in cattle OCC serve to create and maintain rather than disrupt functional intercellular contacts. As occurs similarly in human and rat granulosa cells [44–47], microfilaments of cattle CC provide the first target for gonadotropin-induced cellular differentiation, whereas the networks of microtubules and intermediate filaments remain unaltered [45, 46]. Our findings emphasize an active role of actin cytoskeleton in cumulus expansion and suggest that an interplay between cytoskeleton and extracellular matrix (ECM) synthesis is necessary for this process.

Three sites of possible disruption of cell-to-cell communication have been proposed to participate in triggering the meiotic resumption in rat and hamster OCC: homologous GJ between membrana granulosa cells [1, 18], cumulus-to-cumulus cell GJ [11, 13, 14, 19], and the connections linking CC projections with oolemma [12, 48, 49]. Since the participation of cumulus-to-oocyte GJ and membrana granulosa GJ has been ruled out by quantitative freeze-fracture analysis of rat OCC [1, 11, 14], only the CC GJ seem to be involved in the regulation of oocyte meiotic maturation [10–14].

Ultrastructural studies performed in rats have suggested that the majority of GJ are subjected to the endocytotic process upon the preovulatory LH peak in vivo or upon gonadotropin addition to culture medium in vitro [10–14]. Whereas a decrease in dye coupling between oocyte and corona radiata cells was shown in a study of rat OCC [13], the functional status of homologous CC GJ was not assessed. In our experiments, injections of LY (M_r 457) in the CCs resulted in immediate spread of the dye into neighboring cells at all time points from 0 to 24 h of culture. These observations together with the results obtained via immunofluorescence led us to conclude that the integrity of the cumulus-to-cumulus cell communication was not altered by gonadotropins during in vitro maturation of cattle OCC and that these junctions remained functional until M II. This result coheres with earlier findings of Gilula et al. [20] showing that homologous GJ in rat OCC are conserved until ovulation.

The present study and previous reports on the intercellular communication within bovine OCC in vitro [50] and in vivo [51] demonstrate that the removal of cumulus-to-oocyte GJ from oolemma is temporally correlated with GVBD ([50, 51] and this study) and with the loss of dye coupling between bovine CC and an oocyte (this study). These results may support the involvement of cumulus-to-oocyte GJ in control of oocyte meiotic maturation. In contrast, metabolic coupling assays performed in cattle [23, 26], sheep [27], mice [24, 52], and pigs [21, 53] proved that GVBD in these species occurs before any detectable decrease in transport of small radiolabeled molecules (e.g., ^{3}H-uridine, M_r 244.2 and ^{3}H-choline, M_r 139.5) between CC and oocytes. The reduced degree of transport through the cumulus-to-oocyte pathway is conserved until M II [24, 50, 54]. A possible explanation for these controversial observations could consist in the existence of two transport systems involved in metabolic cooperation between CC and an oocyte. Gap junctions in the oolemma, transporting molecules up to 1 kDa, could be abolished at the onset of meiotic resumption. However, a subsidiary passage could continue through a second hypothetical pathway, permeable for molecules smaller than 400 daltons, after the disruption of heterologous GJ. In agreement with our observations, Cran et al. [9] revealed that gonadotropins partially reduced tritiated choline movement between the oocyte and CC, but not inside the cumulus oophorus. These data suggest that formation of GJ among CC continues during final maturation of cattle OCC in vitro and that the disconnection of the oocytes from enclosing CC is only partial and selective with respect to the molecular weight of transported molecules. Both newly formed and modified junctional contacts maintain the integrity of expanded cumulus and provide the metabolic support required for an oocyte. The importance of CC for normal oocyte maturation in cattle, pigs, and rodents is emphasized by numerous studies [16, 34, 55–58].

The inconsistency of previous findings based on quantitative FF analysis with the results reported here and with metabolic cooperation assay results could be due to several limitations of this method. In FF replicas, the GJ can be missed in highly contoured cellular regions [59] such as ruffled CC membranes in expanded cumulus. In cells pos-

sessing similar architecture, a majority of the fractured membrane surface could belong to the sheets without GJ. However, the correlation of the FF observations with dye coupling assay and immunofluorescence data in our study indicates that this discrepancy could be due to other factors. Primarily, interspecies differences, use of a supporting cell layer, and use of medium containing estrogen may result in an increased GJ synthesis and turnover in our system. In any case, our findings suggest the advisability of strong caution in the interpretation of the results obtained by quantitative FF.

Cx43-positive GJ were recently localized in the rat preovulatory follicle, where their immunofluorescent labeling oscillated from a punctate pattern to regular rings around the cells in some follicular compartments [3]. A positive staining of Cx43 revealed in the mouse zygote by immunoblotting was considered to be a contaminant contributed by residual CC rich in this protein [60]. To date, no GJ containing Cx32 have been localized in the membranes of mammalian oocytes and preimplantation embryos. However, the presence of Cx32 was revealed in the cytoplasm of all preimplantation stages of mouse embryos [61]. Such a cytoplasmic pool of Cx32 was attributed to an inherited oogenetic product [60, 61]. This conclusion is supported by our results localizing Cx32 to the cytoplasm of matured bovine oocytes. Thus we have proved that Cx32 is synthesized during oocyte final maturation. The question whether (or when) this connexin is inserted in oolemma remains to be answered. More detailed ultrastructural analysis in the period of completion of meiotic maturation and preimplantation embryonic development will be necessary for the resolution of this problem.

ACKNOWLEDGMENTS

The authors are very grateful to Dr. D. Gros, Dr. V. Viklický, and Dr. J. Virtanen for the gifts of antibodies and to Dr. J. Fulka for helpful discussion. The technical assistance of Mrs. Solange Delassale and Mr. Jerzi Degrolard and the printing of plates by Miss Lenka Vyohlidová and Miss Lucie Melichárová were very much appreciated. Special thanks to Misses Catherine Chaumontet, Valerie Bex, and Elizabeth Crisians for their help in microinjection experiments and Miss Anne Yvonne Kermabon for editing the manuscript.

REFERENCES

1. Larsen WJ, Wert SE, Brunner GD. Differential modulation of rat follicle cell gap junction populations at ovulation. Dev Biol 1987, 122:61–71.
2. Loewenstein WR. The cell-to-cell channel of gap junctions. Cell 1987, 48:725–726.
3. Risek B, Guthrie S, Kumar N, Gilula NB. Modulation of gap junction transcript and protein expression during pregnancy in the rat. J Cell Biol 1990, 110:269–282.
4. Unwin PNT, Zampigha G. Structure of the junctions between communicating cells. Nature 1980, 283:545–549.
5. Haghighat N, van Winkle LJ. Developmental change in follicular cell-enhanced amino acid uptake into mouse oocytes that depends on intact gap junctions and transport system gly. J Exp Zool 1990, 253:71–82.
6. Lawrence TH, Beers WH, Gilula NB. Transmission of hormonal stimulation by cell to cell communication. Nature 1978, 272:501–506.
7. Albertini DF, Anderson E. The appearance and structure of intercellular connections during the ontogeny of the rabbit ovarian follicle with particular reference to gap junctions. J Cell Biol 1974, 63:234–250.
8. Anderson E, Albertini DF. Gap junctions between the oocyte and companion follicle cells in the mammalian ovary. J Cell Biol 1976, 71:680–686.
9. Cran DG, Moor RM, Crosby IM. Homologous and heterologous cell coupling in mammalian ovarian follicles. Exp Cell Res 1981, 134:251–264.
10. Larsen WJ, Wert SE. Roles of cell junctions in gametogenesis and in early embryonic development. Tissue & Cell 1988, 20:809–848.
11. Larsen WJ, Wert SE, Brunner GD. A dramatic loss of cumulus cell gap junctions is correlated with germinal vesicle breakdown in rat oocytes. Dev Biol 1986, 114:517–521.
12. Larsen WJ, Wert SE, Chen L, Russell P, Hendrix EM. Expansion of the cumulus-oocyte complex during the preovulatory period: possible roles in oocyte maturation, ovulation, and fertilization. In: Familiari G, Makabe S, Motta PM (eds.), Ultrastructure of the Ovary. Dordrecht, Netherlands: Kluwer Academic Publishers, 1991:45–61.
13. Wert SE, Larsen WJ. Meiotic resumption and gap junction modulation in the cultured rat cumulus oocyte complexes. Gamete Res 1989, 22:143–162.
14. Wert SE, Larsen WJ. Precendocytotic alterations in cumulus cell gap junctions precede meiotic resumption in the rat cumulus oocyte complex. Tissue & Cell 1990, 22:827–854.
15. Beyer EC, Kistler J, Paul DL, Goodenough DA. Antisera directed against connexin43 peptides react with a 43 kD protein localized to gap junction in myocardium and other tissues. J Cell Biol 1989, 108:595–605.
16. Dekel N. Regulation of oocyte maturation by cell to cell communication. In: Cell to Cell Communication in Endocrinology. Serono Symp Publ Raven Press 1988, 49:181–194.
17. Racowsky C, Baldwin KV. In vitro and in vivo studies reveal that hamster oocyte meiotic arrest is maintained only transiently by follicular fluid, but persistently by membrana/cumulus granulosa cell contact. Dev Biol 1989, 134:297–306.
18. Racowsky C, Baldwin KV, Larabell CA, De Marais AA, Kazilek CJ. Down-regulation of membrana granulosa cell gap junctions is correlated with irreversible commitment to resume meiosis in golden Syrian hamster oocytes. Eur J Cell Biol 1989, 49:244–251.
19. Racowsky C, Satterlie RA. Decreases in heterologous metabolic and dye coupling, but not in electrical coupling, accompany meiotic resumption in hamster oocyte-cumulus complexes. Eur J Cell Biol 1987, 43:283–292.
20. Gilula NB, Epstein ML, Beers WH. Cell-to-cell communication and ovulation. J Cell Biol 1978, 78:58–75.
21. Modlik J, Fulka J, Flechon JE. Changes in intercellular coupling between pig oocytes and cumulus cells during final maturation in vivo and in vitro. J Reprod Fertil 1986, 76:31–37.
22. Bornslaeger EA, Schultz RM. Regulation of mouse oocyte maturation: effect of elevating cumulus cell cAMP on oocyte cAMP levels. Biol Reprod 1985, 33:698–704.
23. De Loos F, Kastrop P, Van Maurik P, Van Beneden TH, Kruip TAM. Heterologous cell contacts and metabolic coupling in bovine cumulus-oocyte complex. Mol Reprod Dev 1991, 28:255–259.
24. Eppig JJ, Downs SM. Chemical signals that regulate mammalian oocyte maturation. Biol Reprod 1984, 30:1–11.
25. Heller DT, Schultz RM. Ribonucleoside uptake in mouse oocytes: metabolic cooperativity between the fully grown oocyte and cumulus cells. J Exp Zool 1980, 214:355–364.
26. Laurinčík J, Králik P, Hyttel P, Pivko J, Surokin AV. Bovine cumulus expansion and corona oocyte disconnection during culture in vitro. Reprod Nutr Dev 1992, 32:151–161.
27. Moor RM, Smith MW, Dawson RMC. Measurement of intercellular coupling between oocytes and cumulus cells using intracellular markers. Exp Cell Res 1980, 126:15–29.
28. Chen L, Wert SE, Hendrix M, Russel PT, Cannon M, Larsen WJ. Hyaluronic acid synthesis and gap junction endocytosis are necessary for normal expansion of the cumulus mass. Mol Reprod Dev 1990, 26:236–247.
29. Eppig JJ. FSH stimulates hyaluronic acid synthesis by oocyte-cumulus cell complex from mouse preovulatory follicles. Nature 1979, 281:483–484.
30. Eppig JJ. Regulation of cumulus oophorus expansion by gonadotropins in vivo and in vitro. Biol Reprod 1980, 23:545–552.
31. Eppig JJ, Ward Bailey PF. Sulphate aminoglycans inhibit hyaluronic acid synthesizing activity in mouse cumuli oophori. Exp Cell Res 1984, 150:459–466.
32. Salustri A, Yanagishita M, Hascall VC. Mouse oocytes regulate hyaluronic acid synthesis and mucification by FSH-stimulated cumulus cells. Dev Biol 1990, 138:26–32.
33. Salustri A, Yanagishita M, Underhill CB, Laurent TC, Hascall VC. Localization and synthesis of hyaluronic acid in the cumulus cells and mural granulosa cells of the preovulatory follicle. Dev Biol 1992, 151:541–551.

21

34 Buccione R, Schroeder AC, Eppig JJ. Interactions between somatic cells and germ cells throughout mammalian oogenesis. Biol Reprod 1990; 43:543–547.

35 De Loos F, Van Vliet C, Van Maurik P, Kruip TAM. Morphology of immature bovine oocytes. Gamete Res 1989; 24:197–204.

36 Heyman Y, Menezo Y, Chesne P, Camous S, Garner A. In vitro cleavage of bovine and ovine early embryos: improved development using coculture with trophoblastic vesicles. Theriogenology 1987; 27:59–68.

37 El Aoumari A, Fromaget C, Dupont E, Reggio H, Durbec P, Briand JP, Boller K, Kreutman B, Gros D. Conservation of a cytoplasmic carboxy-terminal domain of connexin 43, a gap junctional protein, in mammalian heart and brain. J Membr Biol 1990; 115:229–240.

38 Goodenough DA, Paul DL, Jesaitis LA. Topological distribution of two connexin32 antigenic sites in intact and split rodent hepatocyte gap junctions. J Cell Biol 1988; 107:1817–1824.

39 Viklicky V, Draber P, Hack J, Bartek J. Production and characterization of monoclonal antitubulin antibody. Cell Biol Int Rep 1982; 6:725–730.

40 Virtanen I, Narvanen O, Lehto VP. Differential immunoreactivity and Ca^{2+}-dependent degradation of vimentin in human fibroblast and fibrosarcoma cells. Int J Cancer 1988; 42:256–261.

41 Kruip TAM, Cran DG, van Beneden TH, Dieleman SJ. Structural changes in bovine oocytes during final maturation in vivo. Gamete Res 1983; 8:29–47.

42 Larsen WJ, Tung HN, Murray SA, Swenson CA. Evidence for the participation of actin microfilaments and bristle coats in the internalization of gap junction membrane. J Cell Biol 1979; 83:576–587.

43 Paton AC, Collins WP. Differentiation process of granulosa cells. Obl Rev Reprod Biol 1992; 14:168–223.

44 Amsterdam A, Rotmensch S. Structure-function relationship during granulosa cell differentiation. Endocr Rev 1987; 8:309–337.

45 Anderson E, Selig M, Lee YG, Little B. An in vitro study of the effect of androgens on the cytoskeleton of ovarian granulosa cells with special reference to actin. Tissue & Cell 1988; 20:855–874.

46 Ben Ze'ev A, Amsterdam A. *In vivo* regulation of granulosa cell differentiation: Involvement of cytoskeletal protein expression. J Biol Chem 1987; 262/11:5366–5376.

47 Ben Ze'ev A, Kohen F, Amsterdam A. Gonadotropin-induced differentiation of granulosa cells is associated with the coordinated regulation of cytoskeletal proteins involved in cell contact formation. Differentiation 1987; 34:222–235.

48 Albertini DF. Regulation of meiotic maturation in the mammalian oocyte: interplay between exogenous cues and the microtubule cytoskeleton. Bioessays 1992; 14:97–103.

49 Dekel N, Lawrence TS, Gilula NB, Beers WH. Modulation of cell-to-cell communication in the cumulus oocyte complex and the regulation of oocyte maturation by LH. Dev Biol 1981; 75:247–254.

50 Hytel P. Bovine cumulus oocyte disconnection *in vivo*. Anat Embryol 1987; 176:41–44.

51 Hytel P, Callesen H, Greve T. Ultrastructural features of preovulatory oocyte maturation in superovulated cattle. J Reprod Fertil 1986; 76:645–656.

52 Schultz RM, Montgomery RR, Ward Bailey PF, Eppig JJ. Regulation of oocyte maturation in mouse: possible roles of intercellular communication, cAMP and testosterone. Dev Biol 1983; 95:294–304.

53 Mattioli M, Galeati G, Bacci ML, Seren E. Follicular factors influence oocyte fertilizability by modulating the intercellular cooperation between cumulus cells and oocyte. Gamete Res 1988; 21:223–232.

54 Moor RM, Seamark RF. Cell signalling, permeability, and microvasculatory changes during antral follicle development in mammals. J Dairy Sci 1986; 69:927–943.

55 Ball GD, Leibfried ML, Lenz RW, Ax RL, Bavister BD, First NL. Factors affecting successful in vitro fertilization of bovine follicular oocytes. Biol Reprod 1983; 28:717–725.

56 Galeati G, Modina S, Lauria A, Mattioli M. Follicle somatic cells influence pig oocyte penetrability and cortical granule distribution. Mol Reprod Dev 1991; 29:40–46.

57 Staigmiller RB, Moor RM. Effect of follicle cells on the maturation and developmental competence of ovine oocytes matured outside the follicle. Gamete Res 1984; 9:221–229.

58 Vanderhyden BC, Armstrong DT. Effects of gonadotropins and granulosa cell secretions on the maturation and fertilization of rat oocytes in vitro. Mol Reprod Dev 1990; 26:337–340.

59 Rieske PS, Nagel BA. Gap junction quantification in biological tissues: freeze-fracture replicas versus thin sections. J Microsc 1991; 163:65–78.

60 Valdimarsson G, de Souza OA, Beyer EC, Paul DL, Kidder GM. Zygotic expression of the connexin43 gene supplies subunits for gap junction assembly during mouse preimplantation development. Mol Reprod Dev 1991; 30:18–26.

61 Barron DJ, Valdimarsson G, Paul DL, Kidder GM. Connexin32, a gap junction protein, is a persistent oogenetic product through preimplantation development of the mouse. Dev Genet 1989; 10:318–323.

22

MOLECULAR REPRODUCTION AND DEVELOPMENT 34:58–64 (1993)

Pig Membrana Granulosa Cells Prevent Resumption of Meiosis in Cattle Oocytes

JAROSLAV KALOUS,[1] PETER SUTOVSKY,[1] ZORA RIMKEVICOVA,[1] YASUO SHIOYA,[2] BYONG-LYUL LIE,[3] AND JAN MOTLIK[1]

[1]*Czechoslovak Academy of Sciences, Institute of Animal Physiology and Genetics, Department of Genetics, Libechov, Czechoslovakia;* [2]*National Institute of Animal Industry, Ibaraki, Japan;* [3]*Sagami Chemical Research Centre, Kanagawa, Japan*

ABSTRACT Membrana granulosa was isolated from healthy large antral follicles of prepubertal or cyclic gilts stimulated with PMSG or PMSG and hCG. Ultrastructural observations revealed that pieces of pig membrana granulosa were associated with the basement membrane. The cattle cumulus-enclosed oocytes (COC) were placed in the rolled pieces of the pig membrana granulosa (PMG). After 8 and 24 hr of coculture with PMG from prepubertal gilts,, only 16% and 21% of oocytes underwent GVBD, respectively. PMG from PMSG-stimulated cyclic gilts blocked the resumption of meiosis in all COC. The inhibitory effect of heterologous granulosa cells was fully reversible. When COC were initially incubated for 2 and 4 hr, subsequent culture in PMG prevented GVBD in 100% and 36% of oocytes, respectively. This suggests that functional contact between COC and PMG was established during the first 2 hr of coculture. To follow metabolic cooperation between PMG and COC, PMG was prelabeled with ^{3}H-uridine and cocultured with COC. Autoradiography on semithin sections revealed the intensive passage of ^{3}H-uridine from PMG into the cumulus layer and an oocyte. COC placed in PMG after GVBD (8 and 12 hr of an initial incubation) did not extrude the first polar body. PMG isolated from cyclic gilts after PMSG and hCG stimulation also inhibited GVBD of COC. Since nearly all COC placed in PMG isolated 10 and 12 hr after hCG remained in the GV stage after 24 hr of coculture, the hCG stimulation did not substantially diminish the meiosis inhibiting activity of PMG. During coculture, cattle cumulus cells were closely associated with the basement membrane, but no gap junctions were formed among heterologous granulosa cells. These results suggest that an inhibitory factor secreted by pig granulosa cells is not species specific and it can act in vitro without the mediation of gap junctions. © 1993 Wiley-Liss, Inc.

Key Words: In vitro maturation, Block of meiosis, Domestic animals

INTRODUCTION

In mammalian antral follicles cumulus oophorus is functionally coupled with the membrana granulosa layer by gap junctions. This coupling maintains oocytes in the germinal vesicle stage. The follicular wall of hemisectioned follicles also prevents GVBD in cumulus-enclosed oocytes grafted to the membrana granulosa (Foote and Thibault, 1969; Tsafriri and Channing, 1975; Leibfried and First, 1980b; Meinecke and Meinecke-Tillmann, 1981). However, a lower proportion of denuded pig or hamster oocytes remain in the GV stage after culture on a segment of follicular wall (Leibfried and First, 1980b) or in explanted hamster follicles (Racowsky and Baldwin, 1989). Pig cumulus-enclosed oocytes cultured on follicular walls from which membrana granulosa cells were scraped off resume meiosis (Tsafriri and Channing, 1975). In addition, intrafollicular dislodgement of the hamster cumulus oophorus results in resumption of meiosis of the dislodged oocyte (Racowsky and Baldwin, 1989). All these studies suggest that close association of cumulus and membrana granulosa cells is required to prevent oocyte maturation. Meiotic arrest is overcome by the preovulatory surge of luteinizing hormone (LH) or during culture of follicles in LH or hCG supplemented medium (Lindner et al., 1974).

All pig oocyte cumulus complexes isolated with a piece of membrana granulosa remain in the GV stage (Motlik at al., 1991). Data obtained in vitro with suspension of porcine granulosa cells are conflicting (Tsafriri and Channing, 1975; Leibfried and First, 1980a). Neither suspension of fresh bovine granulosa cells (Leibfried and First, 1980a; Sirard and Bilodeau, 1990b) nor monolayers of bovine granulosa cells prevent germinal vesicle breakdown (GVBD) in cumulus-enclosed bovine oocytes (Sirard and Bilodeau, 1990a). The majority of cattle oocytes did not resume meiosis in only higher concentrations ($0.5–1.0 \times 10^8$/ml) of cattle granulosa cells (Sirard and Bilodeau, 1990b). This inhibitory effect was more pronounced when bovine follicular fluid was added (Sirard et al., 1992). In 2.5×10^7/ml of horse granulosa cells, one half of horse oocytes resumed meiosis (Hinrichs et al., 1992). These data imply that suspended granulosa cells either partly lost their intrafollicular ability to produce the meiotic arrester or they are not able to generate enough intercellular communication to prevent GVBD.

Received November 1, 1992; accepted July 22, 1992.

Address reprint requests to Jaroslav Kalous, Czechoslovak Academy of Sciences, Institute of Animal Physiology and Genetics, Department of Genetics, 277 21 Libechov, Czechoslovakia.

© 1993 WILEY-LISS, INC.

23

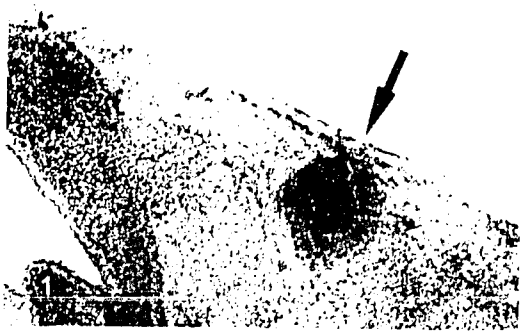

Fig. 1. Cattle cumulus-enclosed oocyte (arrow) situated in the rolled pig membrana granulosa (×60)

Fig. 2. Germinal vesicle (GV) of cattle oocyte cocultured with pig membrana granulosa for 8 hr. Three compact nucleoli (arrowheads) are visible in the vicinity of condensed chromatin (arrow). The nucleolar membrane is out of focus (×1,100)

The present studies were undertaken to evaluate species specificity of the meiotic block induced by pig membrana granulosa (Motlik et al., 1991). Coculture of the pig membrana granulosa cell layer (PMG) with cattle cumulus-enclosed oocytes (COC) proved that the meiosis inhibiting activity is not species specific and it is transmitted through the basement membrane. Surprisingly, the meiosis inhibiting activity of PMG stimulated with hCG was not diminished.

MATERIALS AND METHODS

Isolation of Pig Membrana Granulosa and Cattle Oocytes

Membrana granulosa was isolated from ovaries of slaughtered prepubertal gilts (hybrid line) or from cycling miniature gilts (crosses of the Minnesota and Gottingen strains) treated at day 16 (D16) either with 500 IU PMSG (Antex Leo, Copenhagen) or with PMSG, and 72 hr later with 1,500 IU hCG (Praedyn, Spofa, Praha). Only large antral follicles with transparent, vascularized follicular wall were dissected and hemisectioned. With the help of 2 preparation needles, pieces of the granulosa cell layer were carefully separated from the theca. In the present experiments only large pieces of the pig membrana granulosa (PMG), containing about $3–5 \times 10^5$ granulosa cells, were used.

Ovaries of slaughtered heifers and cows were transferred to the laboratory in phosphate buffered saline (pH 7.4) at 35 C. Antral follicles of 3–5 mm in diameter were aspirated, and isolated oocyte cumulus complexes were repeatedly washed in the culture medium. Only cattle oocytes surrounded with compact cumulus were chosen for coculture experiments.

Coculture of Pig Membrana Granulosa and Cattle Oocytes

Shortly after isolation, the pieces of granulosa tended to roll up with an inside-out orientation. Thus, the COC were placed on the concave surface of the basement membrane (Fig. 1). In each rolled piece of PMG, 3–5 COC were deposited, and these pieces (3–4) of PMG with COC were placed in 1 ml of the equilibrated culture medium under paraffin oil at 38.5 C in 5% CO_2 in air. In the same medium, 10–15 COC were added without any contact with PMG.

The culture medium was modified Parker's medium (M-199, Sevac, Praha) supplemented with 2.92 mM Ca-lactate, 2 mM Na-pyruvate, 33.9 mM Na-bicarbonate, 4.43 mM Hepes buffer, 50 IU/ml penicillin, 50 mg/ml streptomycin sulphate, and 10% heat-treated bovine serum (BOS, Sevac, Praha).

In preincubation experiments, about 20 COC were cultured in 0.25 ml of the medium under the described conditions for 2, 4, 8, and 12 hr before they were placed on the rolled PMG. In reversibility experiments, COC liberated from PMG were cultured either in the control medium or in the medium supplemented with 0.5 IU FSH/ml (Folicotropin, Spofa, Praha). To test the possible nonspecific effect of PMG upon the resumption of meiosis in cattle, the rolled pieces of PMG were mechanically opened after 1 hr of coculture, when contact of COC with the basement membrane was established. The COC were subsequently cultured upon the opened pieces of PMG for 20 hr.

At the end of culture, COC were liberated from the rolled PMG, and cumulus was removed mechanically. The oocytes were then mounted on slides, fixed in acetic acid:alcohol (1:3) for 24 hr, stained with orcein, and examined under a phase-contrast microscope. The frequencies of GVBD in Figs. 3 and 4 were calculated from data pooled from 5 replicate experiments. The frequencies of GVBD (Figs. 3 and 4) in various groups were compared by chi-square analysis. In toto, 912 bovine oocytes were evaluated.

Electron Microscopy

The freshly isolated pig membrana granulosa (PMG) and PMG with COC cultured for 6, 9, 12, and 24 hr were fixed in 4% paraformaldehyde buffered with cacodylate

24

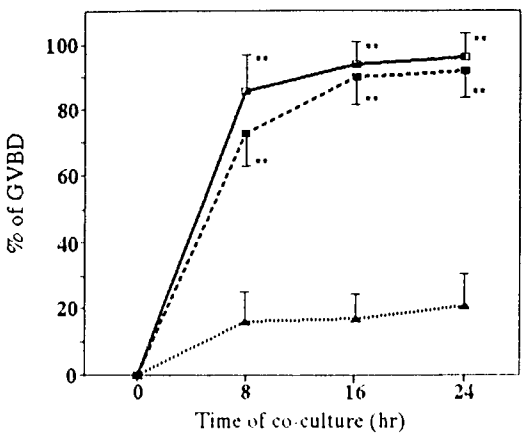

Fig. 3. The effect of pig membrana granulosa (PMG) upon GVBD in cattle cumulus-enclosed oocytes (COC). COC were cultured without PMG (—[ ]—), in medium with PMG but without direct contact with it (—■—), and in rolled pieces of PMG (—▲—) for 8, 16, and 24 hr. Each value represents the mean of 5 replicate experiments. The asterisks denote a significant difference in the percent GVBD of COC cultured without PMG or without direct contact with PMG from the percent GVBD of COC cultured in PMG ($P < 0.01$).

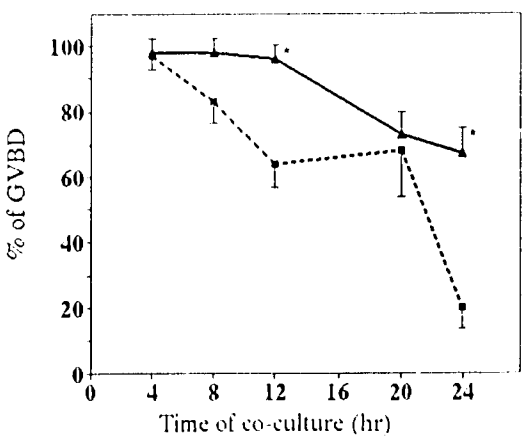

Fig. 4. Reversibility of meiotic block induced by pig membrana granulosa cells (PMG). Cattle oocytes liberated from PMG after 8, 12, 20, and 24 hr were subsequently cultured for 20 hr either in the control medium (—■—) or in the control medium supplemented with 0.5 IU FSH (—▲—). Each value represents the mean of 5 replicate experiments. The asterisk denotes a significant difference in the percent GVBD of COC cultured in the FSH-supplemented medium from the percent GVBD of COC cultured in the control medium ($P < 0.05$).

at pH 7.3 and were postfixed in 1% osmium tetroxide (OsO_4). All samples were treated with 1% tannic acid before dehydratation and embedding in Durcupan (Fluka). The serial thin sections were contrasted with uranyl acetate and lead citrate, examined, and photographed in a Jeol 1200 EX electron microscope.

Autoradiography

The PMG isolated from prepubertal gilts (see above) were placed for 1 hr in the culture medium supplemented with 5-^{3}H-uridine (UVVR, Praha; specific activity 765 Bq/mol) at a final concentration of 3.7 MBq/ml. The labelled granulosa was thoroughly washed in control medium supplemented with cold uridine and was cocultured with intact COC for 3 hr. At the end of culture, PMG with an attached COC was washed in phosphate buffered saline (pH 7.4) and subsequently fixed and embedded (see above) for histological evaluation. The serial semithin sections were coated with Ilford K5 emulsion and exposed for 14 days. The slides were developed by D-19 and stained with toluidine blue.

RESULTS

Effect of Pig Membrana Granulosa (PMG) Upon GVBD in Cattle Oocytes

Cattle cumulus-enclosed oocytes (COC) cultured without PMG underwent GVBD (82%) during 8 hr of culture (Fig. 3). These oocytes reached late diakinesis and metaphase I (94%) after 16 hr and metaphase II (84%) after 24 hr of culture. Similarly, COC cultured in medium with the PMG cells but without direct contact with them resumed meiosis during 8 hr of culture (73% GVBD) and continued to metaphase I (16 hr) and metaphase II (24 hr). When COC were cultured for 24 hr in medium conditioned by 24 hr culture of 5–7 × 10^6/ml PMG cells, more than 90% of COC reached metaphase II (data not shown).

In contrast, GVBD was observed only in 16% of COC placed in the rolled pieces of pig membrana granulosa for 8 hr. The inhibitory effect of PMG was also evident after 16 and 24 hr (17% and 21% GVBD, respectively) of culture. In approximately 50% of GVs, 1–5 nucleoli associated with the condensed chromatin were noticed after 6–24 hr of coculture with PMG (Fig. 2). When rolled pieces of PMG were opened after 1 hr of coculture, the cattle COC remained attached to PMG and 92% of them retained GV after 20 hr of subsequent coculture. A reversibility test revealed that more than 70% of COC inhibited by PMG for 8, 12, and 20 hr were able to undergo GVBD (Fig. 4) and to expel the first polar body. After the longer culture interval (24 hr), reversibility was significantly higher in FSH supplemented medium (20% vs. 67% GVBD). The control medium supported only the expansion of the peripheral layers, while the whole cumulus expanded in the FSH supplemented medium. Results indicate that meiosis inhibiting activity of pig granulosa cell layer is not species specific; it is fully reversible and depends on close contact between the basement membrane of PMG and cattle cumulus granulosa cells.

Effect of Pig Membrana Granulosa on Preincubated Cattle Oocytes

To test the essential time for establishing the inhibitory contact between cumulus and membrana granu-

25

TABLE 1. Inhibition of Meiosis in Preincubated Cattle Oocyte Complexes During Coculture With Pig Membrane Granulosa

Nuclear maturation	2 hr preincubation		4 hr preincubation		8 hr preincubation		12 hr preincubation	
	Preincubation	+ 24 hr coculture	Preincubation	+ 24 hr coculture	Preincubation	+ 24 hr coculture	Preincubation	+ 24 hr coculture
GV III	36	6	18			6		
GV IV	64	94	73	36	7	6	7	
E.D.			9	16	40			
L.D.				46	46	82		
M I				2	7		93	100[a]
T I						6		

Altogether 172 preincubated cattle oocytes were evaluated. Data in columns represent the percentage of oocytes reaching a certain stage of nuclear maturation.
GV III = GV with filamentous chromatin; GV IV = GV with condensed chromatin; E.D. = early diakinesis; L.D. = late diakinesis; M I = metaphase I; T I = telophase I.
[a]Clumps of MI chromosomes.

losa cells, cattle oocytes were preincubated for 2 and 4 hr. Nearly all COC preincubated for 2 and 4 hr were in the GV stage (100% and 91%, respectively). After subsequent culture (24 hr) in PMG, 100% and 36%, respectively, of COC still possessed the GV (Table 1). Thus, the meiosis inhibiting activity exerted by PMG was established during 2 hr of coculture.

All oocytes that underwent GVBD (64%) in the previous experiment (the 4 hr preincubation) were blocked at the early or late diakinesis stage (see Table 1). Cattle oocytes placed in PMG after GVBD (8 hr of preincubation) were also arrested in late diakinesis (82%). The metaphase I COC (12 hr of preincubation) also did not extrude the first polar body during subsequent culture in PMG (24 hr). The metaphase I spindle disappeared and the metaphase I chromosomes clumped (Table 1). We conclude from these experiments that PMG activity is not compatible with function of the meiotic spindle.

Effect of Pig Membrana Granulosa Isolated After PMSG and hCG Stimulation Upon Arrest of Cattle Oocytes

Membrana granulosa isolated from pig preovulatory follicles 72 hr after PMSG stimulation inhibited the resumption of meiosis in all COC after 24 hr of culture. When isolation of membrana granulosa was accomplished 6 and 8 hr after hCG injection, 90% and 73% of COC were still held in the GV stage. Membrana granulosa isolated 9 and 12 hr after hCG was partially luteinized, and it was rather difficult to cover COC in this piece of granulosa. In spite of this, 100% and 97% of oocytes remained in GV stage after 24 hr of culture. Unexpectedly, hCG stimulation does not substantially impair the meiotic inhibitory activity of PMG.

Morphological Cooperation of the Cocultured Pig Membrana Granulosa and Cattle Oocytes

At the time of isolation, pig membrana granulosa was associated with the basement membrane. After 6 hr of coculture, COC sometimes lost contact with PMG due to manipulation before fixation. In the longer intervals (9, 12, and 24 hr), COC were firmly attached to PMG.

The peripheral cumulus cells of COC were in close apposition to the basement membrane, even after 6 hr of culture (Fig. 8). However, no gap junctions were observed between pig granulosa and cattle cumulus cells. Numerous gap junctions were seen between cytoplasmic projections of corona radiata cells and an oocyte (Fig. 5), among PMG cells (Fig. 6) and cattle cumulus cells (Fig. 7). With an increasing time of culture, contact between cattle cumulus cells and the pig granulosa layer became more intimate. The cumulus cells immediately apposed to the basement membrane were attached to it with their large foot projections. Also after 9, 12, and 24 hr, the continuous layer of pig basement membrane prevented the formation of gap junctions (Fig. 9). These ultrastructural findings argue that functional cooperation of PMG and COC is achieved through the basement membrane without the formation of gap junctions.

The ^{3}H-uridine incorporated and taken up with PMG was transported during 3 hr of subsequent coculture with COC. The labelling gradient was observed from intensively labelled cumulus cells that were in close apposition with the basement membrane up to the lightly labelled oocyte (Figs. 10 and 11). The autoradiograms document that ^{3}H-uridine is intensively transported through the basement membrane.

DISCUSSION

After liberation of the pig membrana granulosa layer (PMG) from the follicular wall, the PMG has a strong tendency to roll up, but in an opposite way than in a follicle. This is the reason why COC were added upon the concave surface of basement membrane facing intrafollicularly to the theca layer. The PMG from prepubertal and PMSG-stimulated gilts prevented effectively resumption of meiosis in cattle cumulus-enclosed oocytes. Similarly, the pig oocyte cumulus complexes isolated with a piece of membrana granulosa do not resume meiosis under in vitro conditions (Motlik et al., 1991). Thus, we may conclude that under culture conditions pig granulosa cells continued in their meiosis inhibiting activity in homologous (Motlik et al., 1991) or heterologous system (present results). However, it is

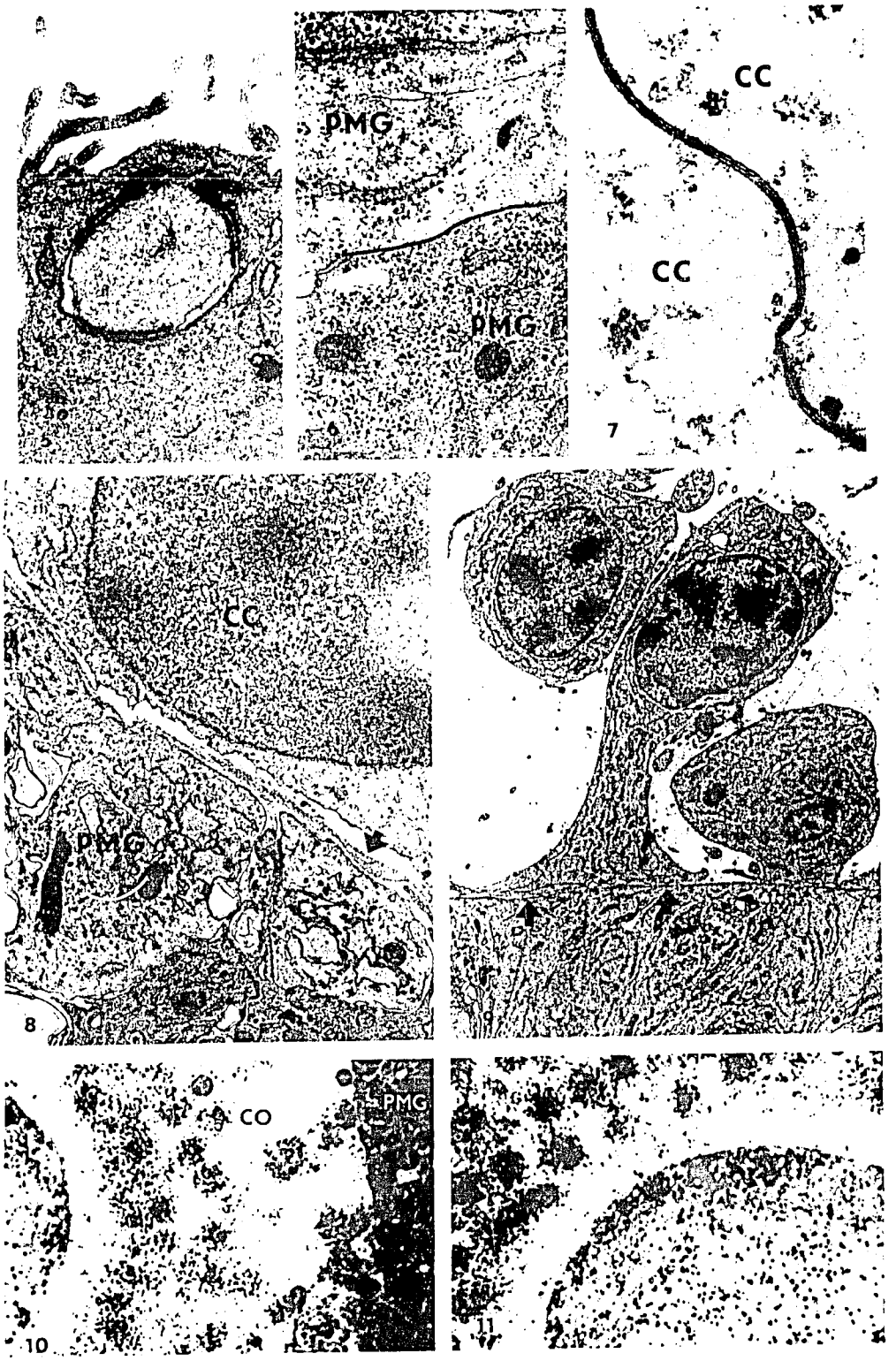

Figs. 5-11.

not known why cattle oocytes isolated with an attached piece (1×10^5 cells) of parietal granulosa (Motlik, unpublished results) cocultured with a suspension of cattle granulosa cells isolated from healthy small antral follicles ($0.5–1.0 \times 10^7$ cells/ml) or upon the cattle granulosa cell monolayer resume meiosis in vitro (Sirard and Bilodeau, 1990a,b). The rapid attachment of cattle COC to the cattle granulosa cells monolayer (Sirard and Bilodeau, 1990a) and to PMG (presented results) prevented cumulus expansion. However, the monolayer prevented GVBD only in 9% and PMG blocked resumption of meiosis nearly in all cattle oocytes. These findings imply that cattle granulosa cells, in contrast to PMG, do not keep their intrafollicular function under in vitro conditions.

The inhibitory effect of heterologous granulosa cells was reversible, while more than 60% of cattle oocytes liberated from pig granulosa after 12 and 20 hr of culture reached metaphase II during the subsequent 24 hr culture. After coculture of cattle oocytes and pig granulosa for 24 hr, reversibility was higher in the FSH-supplemented medium, probably due to the effect upon cumulus expansion. The opening of the rolled PMG after 1 hr coculture allowed free communication of attached oocytes with culture medium and excluded a possible nonspecific effect of PMG upon the resumption of meiosis. These data indicate that neither culture conditions nor pig granulosa cells irreversibly prevent GVBD and the first polar body (FPB) emission in cattle oocytes.

Cattle oocytes put on pig granulosa at late diakinesis or at metaphase I stage did not extrude FPB. The progression of cattle oocytes to metaphase II was significantly affected by coculture with the bovine granulosa cell monolayers as well (Sirard and Bilodeau, 1990a). The results indicate that coculture with homologous and heterologous granulosa cells probably interferes with a function of the first meiotic spindle. The disappearance of the first meiotic spindle and clumping of bivalents was also noticed in the presence of protein synthesis inhibitors (Kubelka et al., 1988; Motlik et al., 1990) or after a multiple fusion of a metaphase I oocyte with growing oocytes (Fulka et al., 1986). These data indicate that the effect of PMG could be related either to changes in the protein synthesis pattern in cattle oocytes or to an interphase status of granulosa cells (see Motlik and Kubelka, 1990). This assumption fits well with the recent findings of Vale (1991) that the cell cycle state controls severing and assembling of microtubules.

Physiologically, LH provides the biological trigger for irreversible commitment to oocyte maturation (Racowsky et al., 1989). LH acts primarily to alter the nature or intensity of the signal from the follicle cells (Moor et al., 1981). At least in the rabbit, sheep, and cattle, de novo hnRNA and protein synthesis in granulosa cells are involved in the resumption of meiosis (Motlik et al., 1989; Moor and Galli, 1991; Kastrop et al., 1991). However, the present data showed that pig membrana granulosa isolated from PMSG and hCG-stimulated follicles still possessed the inhibitory activity. Only few cattle oocytes (10%, 27%, 0%, and 3%) cultured on pig granulosa isolated 6, 8, 10, and 12 hr after hCG injection underwent GVBD, respectively. We demonstrate for the first time that membrana granulosa isolated after hCG stimulation from oestrous gilts did not lose its activity to inhibit the resumption of meiosis in cumulus-enclosed oocytes under in vitro conditions.

Freeze-fracture studies have revealed the downregulation of both cumulus and membrana granulosa gap junctions during the period of GVBD in the rat (Larsen et al., 1986, 1987). The significant loss in gap junctional membrane (50% decrease) was observed 2 hr post-hCG among the hamster membrana granulosa cells that underly the cumulus cell stalk (Racowsky et al., 1989). In this respect it would be of interest to know whether or not granulosa junctional disruption plays a role in signaling meiotic resumption. In cocultures, gap junctions were established between granulosa cells and myocardial cells (Lawrence et al., 1978). However, in the present model pig membrana granulosa was isolated with the basement membrane and cattle oocytes were situated on it. In spite of the fact that cumulus cells were closely associated with the basement membrane and ^{3}H-uridine was efficiently transported through it, no gap junctions were formed among heterologous granulosa cells. The mechanisms by which granulosa cells exert their inhibitory effect is unclear. We may only postulate that an inhibitory factor secreted by pig granulosa cells is not species specific and it can act, at least in vitro, without the mediation of gap junctions.

Fig. 5. The cytoplasmic projections of corona radiata cells are immersed in cattle oocyte cytoplasm. The numerous junctional complexes are visible (×30,000).

Fig. 6. The gap junction between 2 pig membrana granulosa cells (PMG) is similar to the junctional complex in Fig. 7 (×40,000).

Fig. 7. The large junctional complex between 2 cattle cumulus cells (CC) after 6 hr of coculture (×60,000).

Fig. 8. The close apposition of the cattle cumulus cell (CC) to the basement membrane (arrowed) after 6 hr of coculture. PMG — pig membrana granulosa layer (×30,000).

Fig. 9. During coculture, cattle cumulus cells orient their large foot projections against the basement membrane and they are apposed with it in a large area (arrow) (×15,000).

Fig. 10. The passage of ^{3}H-uridine from the prelabelled pig membrana granulosa (PMG) into the cattle oocyte-cumulus complex (CO). The descending gradient of labelling goes from PMG to an oocyte (×350).

Fig. 11. Detail of the cattle cumulus-enclosed oocyte cocultured for 3 hr with prelabelled (^{3}H-uridine) pig membrana granulosa.

ACKNOWLEDGMENTS

The authors thank Professor Richard Schultz and Dr. John Eppig for critical reading of the manuscript. We thank Mr. V. Pech for skillful technical assistance.

REFERENCES

Foote WD, Thibault C (1969): Recherches experimentales sur la maturation in vitro des ovocytes de truie et de veau. Ann Biol Anim Biochim Biophys 9:329–349

28

Fulka J Jr, Motlik J, Fulka J, Crozet N (1986): Activity of maturation promoting factor in mammalian oocytes after its dilution by single and multiple fusions. Dev Biol 118:176–181.

Hinrichs K, Martin MG, Friedman PP (1992): Effect of follicular components on maintenance of meiotic arrest in horse oocytes. Theriogenology 37:223.

Kastrop PMM, Hulshof SCJ, Bevers MM, Destree OHJ, Kruip Th M (1991): The effects of α-amanitin and cycloheximide on nuclear progression, protein synthesis, and phosphorylation during bovine oocyte maturation in vitro. Mol Reprod Dev 28:249–254.

Kubelka M, Motlik J, Fulka J Jr, Prochazka R, Rimkevicova Z, Fulka J (1988): Time sequence of germinal vesicle breakdown in pig oocytes after cycloheximide and p-aminobenzamidine block. Gamete Res 19:423–431.

Larsen WJ, Wert SE, Brunner GD (1986): A dramatic loss of cumulus cell gap junctions is correlated with germinal vesicle breakdown in rat oocytes. Dev Biol 113:517–521.

Larsen WJ, Wert SE, Brunner GD (1987): Differential modulation of rat follicle cell gap junction populations at ovulation. Dev Biol 122:61–71.

Lawrence TS, Beers WH, Gilula NB (1978): Transmission of hormonal stimulation by cell-to-cell communication. Nature 272:501–506.

Leibfried L, First NL (1980a): Effect of bovine and porcine follicular fluid and granulosa cells on maturation of oocytes in vitro. Biol Reprod 23:699–704.

Leibfried L, First NL (1980b): Follicular control of meiosis in the porcine oocyte. Biol Reprod 23:705–709.

Lindner HR, Tsafriri A, Lieberman ME, Zor U, Koch Y, Bauminger S, Barnea A (1974): Gonadotropin action on cultured Graafian follicles: Induction of maturation division of mammalian oocytes and differentiation of the luteal cell. Recent Prog Horm Res 30:79–138.

Meinecke B, Meinecke-Tillmann S (1981): Induction and inhibition of meiotic maturation of follicle-enclosed porcine oocytes in vitro. Theriogenology 15:581–589.

Moor RM, Galli C (1991): Somatic cells and the G_2 to M-phase transition in sheep oocytes. Reprod Nutr Dev 31:127–134.

Moor RM, Osborn JC, Cran DG (1981): Selective effect of gonadotropins on cell coupling, nuclear maturation and protein synthesis in mammalian oocytes. J Embryol Exp Morph 61:347–365.

Motlik J, Kubelka M (1990): Cell-cycle aspects of growth and maturation of mammalian oocytes. Mol Reprod Dev 27:366–375.

Motlik J, Nagai T, Kikuchi K (1991): Resumption of meiosis in pig oocytes cultured with cumulus and parietal granulosa cells: the effect of protein synthesis inhibition. J Exp Zool 259:386–391.

Racowsky C, Baldwin KV (1989): In vitro and in vivo studies reveal that hamster oocyte meiotic arrest is maintained only transiently by follicular fluid, but persistently by membrana/cumulus granulosa cell contact. Dev Biol 134:297–306.

Racowsky C, Baldwin KV, Larabell CA, DeMarais AA, Kazilek CJ (1989): Down-regulation of membrana granulosa cell gap junctions is correlated with irreversible commitment to resume meiosis in golden Syrian hamster oocytes. Eur J Cell Biol 49:244–251.

Sirard MA, Bilodeau S (1990a): Effects of granulosa cell co-culture on in vitro meiotic resumption of bovine oocytes. J Reprod Fertil 89:459–465.

Sirard MA, Bilodeau S (1990b): Granulosa cells inhibit the resumption of the meiosis in bovine oocytes in vitro. Biol Reprod 43:777–783.

Sirard MA, Coenen K, Bilodeau S (1992): Effect of fresh or cultured follicular fractions on meiotic resumption in bovine oocytes. Theriogenology 37:39–57.

Tsafriri A, Channing CP (1975): An inhibitory influence of granulosa cells and follicular fluid upon porcine oocyte meiosis in vitro. Endocrinology 96:922–927.

Vale RD (1991): Severing of stable microtubules by a mitotically activated protein in Xenopus egg extracts. Cell 64:827–839.

29

Reprod Nutr Dev (1993) 33, 419-428
© Elsevier/INRA

Original article

Is cAMP decrease essential for resumption of meiosis in mouse oocytes?

E Nagyová [1], J Kalous [2*], P Šutovský [2], J Motlík [2]

[1] Research Institute of Animal Production, 104-00 Prague 10, Uhříněves;
[2] Institute of Physiology and Genetics of Animals, Czech Academy of Science, 277 21 Liběchov, Czech Republic

(5th Franco-Czechoslovak Meeting, Jouy-en-Josas, December 1992)

Summary — Resumption of meiosis was inhibited in mouse oocyte cumulus complexes (OCC) co-cultured with pig membrana granulosa (PMG). After 3 and 6 h of co-culture these oocytes possessed an intact nuclear envelope and their nucleolar surface was associated with granules ≈ 80 nm in diameter. Preincubation of OCCs for 30, 45, 60 or 90 min followed by co-culture with PMG for 2 h of either OCCs or denuded oocytes resulted in germinal vesicle breakdown (GVBD) in ≈ 0, 30, 70 and 100% mouse OCCs and in ≈ 30, 60, 80 and 100% denuded oocytes, respectively. It seems that the inhibitory contact between mouse oocytes and PMG was established during the first h of co-culture. After isolation from antral follicles the oocytes contained 2.75 fmol cyclic adenosine 3', 5'-monophosphate (cAMP). When OCCs were co-cultured for 1, 2 or 3 h with PMG, the amount of cAMP per oocyte was 1.34, 1.33 and 1.51 fmol, respectively. After culture of OCCs in control medium the amount of cAMP was 1.21, 1.39 and 2.16 fmol, respectively. The present results suggest that the inhibitory activity of PMG is not species-specific. Moreover, PMG prevented resumption of meiosis in mouse oocytes in spite of the cAMP drop in oocyte cytoplasm characteristic of the resumption of meiosis.

mouse oocyte / meiosis / cAMP / pig membrane granulosa

Résumé — La décroissance de l'AMPc est-elle essentielle pour la reprise de la méiose dans les ovocytes de souris ? *La reprise de la méiose a été inhibée dans des complexes ovocyte-cumulus (OCC) de souris cocultivés avec de la «membrana granulosa» de porc (PMG). Ces ovocytes conservent une enveloppe nucléaire après 3 et 6 h de coculture et la surface nucléolaire est associée avec des granules de 80 nm de diamètre. La préincubation des OCCs pendant 30, 40, 60 ou 90 min puis la coculture avec la PMG d'OCCs ou d'ovocytes dénudés aboutit à la rupture de la vésicule germinative (GVBD) dans environ 0, 30, 70 et 100% des OCCs et environ 30, 60, 80 et 100% des ovocytes dénudés, respectivement. Il semble que l'inhibition par contact entre la PMG et les ovocytes s'établisse pendant la première heure de coculture. Après isolement de follicules à l'antrum, les ovocytes contiennent 2,75 fmol d'adénosyl 3'5' monophosphate cyclique (AMPc). Quand les OCCs sont cocultivés pendant 1, 2 ou 3 h avec la PMG, la concentration d'AMPc par ovocyte est respectivement de 1,34; 1,33 et 1,51 fmol. Après culture des OCCs dans le milieu témoin, la concentration d'AMPc est alors de 1,21; 1,39 et 2,16 fmol. Les résultats présents suggèrent que l'activité inhibitrice de la PMG n'est pas limitée à l'espèce. De plus, la PMG empêche la reprise de la méiose d'ovocytes de souris en dépit de la chute d'AMPc, caractéristique de cette reprise, dans le cytoplasme ovocytaire.*

ovocyte de souris / méiose / AMPc / membrana granulosa de porc

---

* Correspondence and reprints

30

INTRODUCTION

The hypothesis that the antral follicles inhibit the resumption of meiosis until the preovulatory gonadotropin surge was first put forward by Pincus and Enzman (1935). Further studies have confirmed that either intrafollicularly or under *in vitro* conditions, the membrana granulosa and cumulus granulosa cells are required for the prevention of oocyte maturation (Foote and Thibault, 1969; Tsafriri and Channing, 1975; Leibfried and First, 1980; Racowsky and Baldwin, 1989). In addition, pig oocytes surrounded by the cumulus with a part of membrana granulosa directly adjacent to the cumulus do not mature in gonadotropin-free medium (Mattioli *et al*, 1988; Motlik *et al*, 1991). We have recently found that under suitable culture conditions a piece of pig membrane granulosa (PMG) is able to prevent resumption of meiosis in cattle oocytes (Kalous *et al*, 1993). This heterologous effect of PMG was used in the present experiments when the mouse OCCs (OCC) were co-cultured with a piece of PMG.

Under *in vitro* conditions, analogs of cAMP and phosphodiesterase inhibitors prevent spontaneous meiotic resumption in mouse (Cho *et al*, 1974; Wassarman *et al*, 1976) and rat oocytes (Magnusson and Hillensjo, 1977; Dekel and Beers, 1978). These findings imply that a drop in the cAMP levels in rodent oocytes is related to germinal vesicle breakdown (GVBD). In fact, a decrease in oocyte cAMP precedes GVBD in mouse (Schultz *et al*, 1983a, b; Vivarelli *et al*, 1983) and rat oocytes (Racowsky, 1984; Aberdam *et al*, 1987).

The present experiments were undertaken to answer 2 questions: first, does PMG prevent resumption of meiosis in oocytes with a rapid time sequence of GVBD? Second, does co-culture with PMG influence cAMP levels in the cytoplasm of the mouse oocytes?

MATERIALS AND METHODS

Oocytes and granulosa cells

Mouse oocytes were isolated from large antral follicles of sexually mature females (strain A) primed 48 h before with 5 IU pregnant mare serum gonadotropin. Only oocytes surrounded by compact cumulus were chosen for these experiments. Membrana granulosa was isolated from ovaries of slaughtered prepubertal gilts. Only large antral follicles (7–10 mm in diameter) with a transparent, vascularized follicular wall were dissected. With the help of 2 preparation needles, large pieces of granulosa layer were carefully separated from the theca. Only pieces of the PMG containing ~ 1–3 x 10^5 granulosa cells were used. A previous ultrastructural study (Kalous *et al*, 1993) revealed that PMG was always isolated with the basement membrane.

Co-culture of mouse oocytes with pig membrana granulosa

In the present experiments modified Parker's culture medium (M-199, Sevac, Prague) supplemented with 2.92 mM Ca–lactate, 2 mM Na–pyruvate, 33.9 mM Na–bicarbonate, 4.43 mM Hepes buffer, 50 IU/ml penicillin, 50 mg/ml streptomycin sulfate, and 10% heat-treated bovine serum (BOS, Sevac, Prague) was used (Pavlok *et al*, 1988).

About 15 mouse OCCs were placed on the basement membrane (concave side) of each piece of PMG and cultured in 0.5 ml Parker's medium under paraffin oil at 38°C under 5% CO_2 in air for 1, 2, 3, or 6 h. In preincubation experiments, ~ 10 OCCs were cultured in 0.1 ml of the medium under the above-described conditions for 30, 45, 60 and 90 min before either oocytes with compact cumulus or oocytes with mechanically removed cumulus (cumulus-free oocytes) were co-cultured for 2 h with PMG.

As a control, mouse OCCs were cultured in the control medium (control I) or in the medium with several pieces of PMG but without direct contact with them (control II). In further control experiments, the PMG basement membrane was covered with a nitrocellulose membrane. Both the adhered membranes and OCCs were

31

situated on the nitrocellulose membrane and were cultured for 3 h.

At the end of the culture period, OCCs were removed from contact with PMG and used either for light and electron microscopic evaluation or for cAMP determination.

Determination of cAMP by radioimmunoassay (RIA)

After isolation (0 h) or incubation (1, 2 or 3 h) the OCCs were transferred to medium containing 1 mM 3-isobutyl-1-methylxanthine (IBMX) to minimize cAMP hydrolysis within the cells. Cumulus cells were mechanically removed from the oocytes. Denuded oocytes were washed 3 times in the medium with IBMX and then transferred into 10 µl 0.5% sodium dodecyl sulfate (SDS, w/v; Racowsky, 1984). When lysis was completed, the samples were capped and stored at −80 C. Before extraction with 100 µl 6% trichloroacetic acid (TCA) at 4 °C, 10 µl bovine serum albumin (10 mg/ml) was added to each microcap to act as carrier protein. The extracted samples were centrifuged at 2 000 *g* for 15 min and supernatants were removed and lyophilized. TCA extracts were diluted and assayed after acetylation. Cyclic AMP was measured by radioimmunoassay using kits (UJVVVR, Prague) (Procházka *et al.* 1991). The sensitivity of the assay was 4 fmol/tube. The intra- and inter-assay coefficients of variation in this RIA were 7.8 and 10.2%. The significance of the differences in cAMP concentrations between experimental groups was assessed using the Student's *t*-test.

Light microscopy

To prepare the OCCs for light microscopy cumulus cells were mechanically removed. Oocytes were mounted on slides, fixed in an acetic acid/alcohol (1:3) mixture for 24 h, stained with orcein and examined under a phase-contrast microscope. Frequency of GVBD in I and II was calculated from data pooled from 3 replicate experiments and the frequency of GVBD between groups was compared by χ^2 analysis.

Electron microscopy

Samples were fixed in a mixture of 0.6% paraformaldehyde and 2.5% glutaraldehyde in 0.2 cacodylate buffer (pH 7.4) for 90 min, washed, postfixed in 1% OsO_4 in cacodylate buffer for 1 h and dehydrated in ascending ethanol series. After infiltration in a mixture composed of propylene oxide and Epon, the samples were embedded in Epon 812. The blocks were cut in Reichert–Jung Ultracut, mounted on grids, contrasted with uranyl acetate and lead citrate, and examined in a Jeol 1200 EX electron microscope.

RESULTS

Co-culture

When the freshly isolated mouse OCCs were cultured on PMG, the OCCs did not resume meiosis during the 3-h (table I) and 6-h (data not shown) co-culture period. The mouse denuded oocytes were also blocked at the GV stage by PMG. In contrast, mouse OCCs cultured in the same drop of medium but without direct contact with PMG matured spontaneously. A sheet of nitrocellulose membrane between PMG and OCCs abolished the inhibitory effect of PMG upon mouse oocytes. It was concluded that the direct contact of the mouse denuded or cumulus-enclosed oocytes with PMG was essential to prevent resumption of meiosis.

Fifty-six percent of the mouse oocytes denuded after the 45-min preincubation period underwent GVBD during the subsequent 2-h co-culture with PMG (table II). The cumulus-enclosed oocytes required 60-min preincubation to undergo GVBD (66%) during the co-culture period. These data indicate that the inhibitory effect of PMG upon GVBD was effective in the commitment period only.

32

Table I. GVBD in mouse OCCs co-cultured with PMG and nitrocellulose membrane.

Type of culture	*No of oocytes*	*Stage of meiosis*		*GVBD (%)*
		GV	*LD/MI*	
Control I	54	2	53	96[a]
Control II	59	3	47	95[a]
OCCs and PMG	46	46	–	0[b]
OCCs and NM	51	1	50	98[a]
OCCs and PMG + NM	47	2	45	96[a]

Mouse OCCs were cultured for 3 h in control medium (control I), in the presence of PMG without contact with PMG (control II), in contact with PMG (OCCs and PMG), in contact with nitrocellulose membrane (OCCs and NM) and in contact with nitrocellulose membrane adhering to PMG (OCCs and PMG + NM). Values with different superscripts are significantly different ($P < 0.05$).

cAMP levels

In the control medium, all oocytes underwent GVBD during 3 h of culture. The alterations in intraoocyte cAMP content in oocytes during culture are shown in table III and figure 1. The oocyte intracellular cAMP content was 2.75 ± 0.24 fmol/oocyte before incubation (0 h). The significant drop in intraoocyte cAMP content, which was detected after 1 h of incubation (1.21 ± 0.07 fmol/oocyte), was followed by GVBD. After co-culture with PMG, the resumption of meiosis was prevented during 1, 2 or 3 h of incubation, but surprisingly the significant cAMP drop was detected in the mouse oocytes (1.34 ± 0.12 fmol/oocyte) after 1 h of co-culture. No significant difference was observed in the intraoocyte cAMP content after 1 h incubation when the control and PMG groups were compared.

Table II. The effect of PMG upon GVBD in preincubated mouse OCCs.

	Cumulus-enclosed oocytes					*Cumulus-free oocytes*				
Min	0	30	45	60	90	0	30	45	60	90
GVBD (%)	0[a]	0[a]	31[b]	66[c]	100[d]	0[a]	34[b]	56[c]	77[d]	100[e]

Mouse OCCs were preincubated for 30, 45, 60 and 90 minutes in control medium and subsequently OCCs (cumulus-enclosed oocytes) and oocytes after mechanical removing of cumulus (cumulus-free oocytes) were co-cultured with PMG for 2 h. Each interval was repeated 3 times and at least 50 oocytes were used. Values with different superscripts are significantly different ($P < 0.05$).

33

Table III. Cyclic AMP levels in oocytes incubated without PMG.

	Group			
	C–	OCC		
Time (h)	0	1	2	3
Mean	2.75*	1.21	1.39	2.16
SEM	0.24	0.07	0.24	0.23

The mouse oocyte cumulus complexes (OCC) were cultured for 1, 2, and 3 h in control medium. The oocytes were denuded (C–) before (time zero) or after incubation in control medium (time 1, 2 and 3 h). Values represent the mean fmol cAMP per oocyte and the SEM from at least 3 independent experiments. * The time zero is significantly different from that of other groups ($P < 0.05$).

Electron microscopy

The co-culture of mouse OCCs with PMG resulted in the close attachment of mouse cumulus cells (CC) to the pig basement membrane (BM) (fig 2). The cells in the mouse cumulus were interconnected by extensive network of gap junctions (GJs) at all time points (0, 3, 6 h of culture) (fig 3A). Similarly, a large number of GJs coupled PMG cells during co-culture (fig 3B). Finally, the cytoplasmic projections of mouse corona radiata cells remained in contact with the oocyte after 6 h co-culture with PMG (fig 4). The direct contact between cytoplasmic membranes of PMG cells and mouse CC was prevented by the presence of the continuous pig BM (fig 5). In no case did the cells from the pig or mouse compartment of the co-culture system penetrate across the BM. In areas where the space between mouse cumulus and pig MG was enlarged, the BM was differentiated into 2 distinguishable layers (lamina rara densa and lamina lucida) (fig 5).

The nuclear ultrastructure of mouse oocytes underwent substantial changes after co-culture with PMG (fig 6). Whereas the nuclear envelope remained intact, the compact nucleoli were surrounded by a conspicuous rim composed of nucleolus-associated chromatin and large granules ≈ 80 nm in diameter. The same granules formed small clusters in the nucleoplasm.

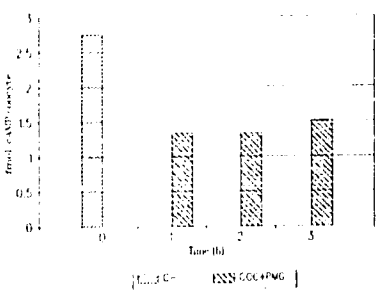

Fig 1. Effect of pig membrana granulosa on the content of cAMP in mouse oocytes. The mouse oocyte cumulus complexes (OCC) were cultured for 1, 2 and 3 h upon pig membrana granulosa (OCC + PMG). The oocytes were denuded of cumulus cells (C–) before (time zero) or after (time 1, 2 and 3 h) the experimental treatment. Bars represent mean fmol cAMP per oocyte and the standard error of the mean from at least 3 independent experiments. The time zero is significantly different from other groups ($P < 0.05$).

34

Fig 2. Composition of 3 serial micrographs showing the experimental model used in this study. Large compact nucleolus (N) is visible inside the intact GV of mouse oocyte cultured for 6 h with pig membrana granulosa (PMG). Mouse cumulus cells (CC) are attached to continuous pig basement membrane (arrowheads) (x 3 000).

In addition, round-shaped clumps of chromatin granules ≈ 20 nm in diameter and numerous nucleolus-like bodies (NLB), were scattered throughout the nucleoplasm. These 3 structures were often associated with the nuclear envelope.

DISCUSSION

The pig cumulus-enclosed oocytes isolated with attached piece of membrana granulosa did not resume meiosis *in vitro* (Motlik *et al*, 1991). The isolated pig membrana granulosa (PMG) effectively and reversibly prevented GVBD in heterologous (cattle) oocytes (Kalous *et al*, 1993). The present data demonstrate that PMG prevented resumption of meiosis in oocytes, also with a rapid GVBD time sequence. Nearly all mouse oocytes retained the GV stage after the 3- and 6-h co-culture. The preincubation of the mouse denuded and cumulus-enclosed oocytes for 45 and 60 min, respectively, significantly abolished the inhibitory effect of PMG. The data suggest that the inhibitory activity of PMG, similarly to

Fig 3a,b. Homologous gap junctions remaining in mouse cumulus cells (A) and pig granulosa cells (B) co-cultured for 6 h (a x 90 000; B x 80 000).
Fig 4. Heterologous contacts (arrowhead) between corona radiata projections and oocyte in mouse OCCs conserved until the end of co-culture (x 27 000).
Fig 5. Pig basement membrane separating the mouse (CC) and pig (PMG) compartment of experimental model. The basement membrane is separated into 2 layers in site of gap between the pig and the mouse cells (asterisk) (x 28 500).

35

3a

3b

4

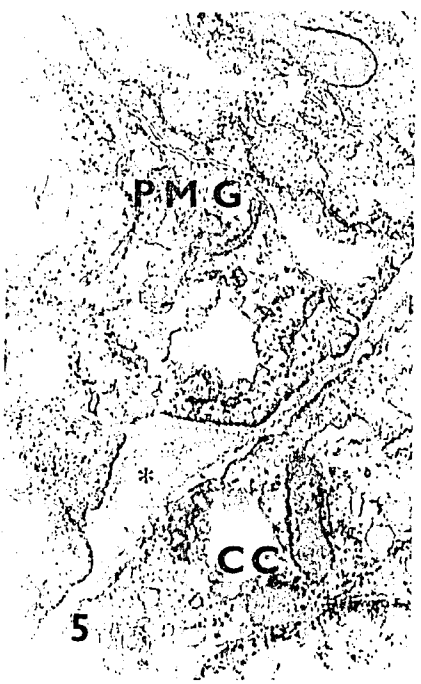
PMG
CC
5

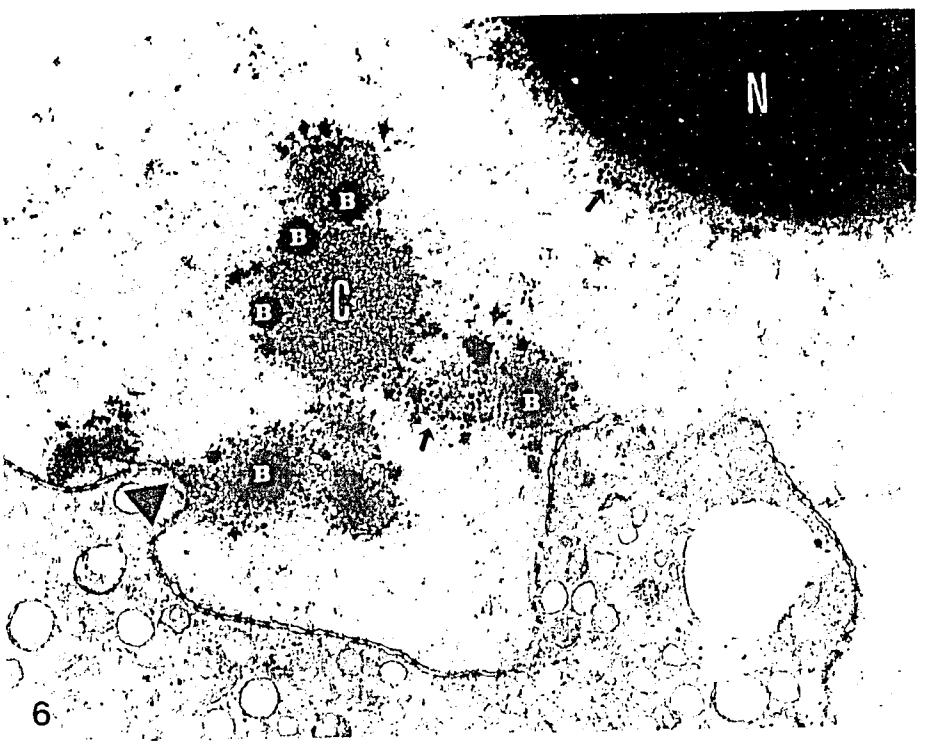

Fig 6. Nuclear ultrastructure of mouse oocyte co-cultured with pig membrana granulosa cells. Large compact nucleolus (N) and small nucleolus-like bodies (B) are surrounded by the rim of chromatin, containing clumps of 80-nm granules (arrows). Note the round-shaped clump of chromatin (C) and the association of nucleolus-like bodies with nuclear membrane (arrowhead) (x 17 500).

the effect of IBMX (Eppig *et al*, 1983), cannot be exerted after irreversible commitment of mouse oocytes to GVBD.

FSH and cholera toxin significantly increase the cumulus-cell cAMP levels. In spite of the fact that it does not result in any detectable rise in oocyte cAMP, resumption of meiosis in mouse oocytes is postponed (Schultz *et al*, 1983b). If cAMP is not transmitted from cumulus cells to oocytes then some factor other than cAMP may be transferred from cumulus cells to the oocyte to inhibit oocyte maturation. The action of FSH in delaying maturation is mediated by the cumulus cells and it is only transient while all oocytes passed GVBD within 4 h (Eppig *et al*, 1983).

The action of FSH, cholera toxin and suboptimal concentrations of dbcAMP in inhibiting mouse oocyte GVBD depends on

37

an intact coupling pathway between the cumulus cells and oocytes (Eppig *et al*, 1983; Schultz *et al*, 1983b). In the present experiments, the pig granulosa cells as well as the mouse cumulus cells and corona radiata cells with the oolemma were tightly coupled by numerous gap junctions. However, both compartments were strictly separated by the basement membrane. This means that a putative maturation inhibiting factor was secreted by the PMG through the basement membrane and was transported in both cumulus-enclosed and denuded oocytes.

The main characteristic of the commitment period in the mouse oocytes is a decrease in oocyte cAMP levels (Schultz *et al*, 1983a; Vivarelli *et al*, 1983; present results). Surprisingly, our experiments also documented this drop in oocytes blocked at the GV stage by PMG. These data could help to answer a question raised by Thibault *et al* (1987): "Is the decrease in the cAMP level a prerequisite to meiosis resumption?" If cAMP dropped similarly in the ooplasm of committed and inhibited oocytes, this significant decrease could be caused by liberation of oocytes from follicular environment to the culture conditions and a putative intrafollicular inhibitor of meiosis could act downstream of the step which is sensitive to the cAMP level.

ACKNOWLEDGMENTS

The authors are grateful to E Markalous for his help with the statistical analyses and L Vyšohlidová and V Pech for skillful technical assistance. This study was supported by the US AID grant No 12.061 E.

REFERENCES

Aberdam E, Hanski E, Dekel N (1987) Maintenance of meiotic arrest in isolated rat oocytes by the invasive adenylate cyclase of *Bordetella pertussis*. *Biol Reprod* 36, 530-535

Cho WK, Stern S, Biggers JD (1974) Inhibitory effect of dibutyryl cAMP on mouse oocyte maturation *in vivo*. *J Exp Zool* 187, 383-386

Dekel N, Beers WH (1978) Rat oocyte maturation *in vitro*: relief of cAMP inhibition by gonadotropins. *Proc Natl Acad Sci USA* 75, 4364-4373

Eppig JJ, Freter RR, Ward-Bailey PF, Schultz RM (1983) Inhibition of oocyte maturation in the mouse: participation of cAMP, steroid hormones and a putative maturation-inhibitory factor. *Dev Biol* 100, 39-49

Foote WD, Thibault C (1969) Recherches expérimentales sur la maturation *in vitro* des ovocytes de truie et de veau. *Ann Biol Anim Bioch Biophys* 9, 329-349

Kalous J, Šutovský P, Rimkevicova Z, Shioya Y, Lie LB, Motlik J (1993) Pig membrana granulosa cells prevent resumption of meiosis in cattle oocytes. *Mol Reprod Dev* 34, 58-64

Liebfried L, First NL (1980) Follicular control of meiosis in the porcine oocyte. *Biol Reprod* 23, 705 709

Magnusson CJ, Hillensjo T (1977) Inhibition of maturation and metabolism of rat oocytes by cyclic AMP. *J Exp Zool* 201, 138-147

Mattioli M, Galeati G, Seren E (1988) Effects of follicle somatic cells during pig oocytes maturation on egg penetrability and male pronucleus formation. *Gamete Res* 20, 177-183

Motlik J, Nagai T, Kikuchi K (1991) Resumption of meiosis in pig oocytes cultured with cumulus and parietal granulosa cells: the effect of protein synthesis inhibition. *J Exp Zool* 259, 336-391

Pavlok A, Torner H, Motlik J, Fulka J, Kauffold P, Duschinski U (1988) Fertilization of bovine oocytes *in vitro*: effect of different sources of gametes on fertilization rate and frequency of fertilization anomalies. *Anim Reprod Sci* 16, 207-213

Pincus G, Enzmann EV (1935) The comparative behaviour of mammalian eggs *in vivo* and *in vitro*. I. The activation of ovarian eggs. *J Exp Med* 62, 665-675

Prochazka R, Nagyova E, Rimkevicova Z, Nagai T, Kikuchi K, Motlik J (1991) Lack of effect of oocytectomy of the porcine cumulus. *J Reprod Fertil* 93, 569-576

38

Racowsky C (1984) Effect of forskolin on the spontaneous maturation and cycli cAMP content of rat oocyte–cumulus complexes. *J Reprod Fertil* 72, 107-116

Racowsky C, Baldwin KV (1989) *In vitro* and *in vivo* studies reveal that hamster oocyte meiotic arrest is maintained only transiently by follicular fluid, but persistently by membrana/cumulus granulosa cell contact. *Dev Biol* 134, 297-306

Schultz RM, Montgomery RR, Belanoff J (1983a) Regulation of mouse oocyte maturation. Implication of a decrease in oocyte cAMP and protein dephosphorylation in commitment to resume meiosis. *Dev Biol* 97, 264-273

Schultz RM, Montgomery RR, Ward-Bailey PF, Eppig JJ (1983b) Regulation of oocyte maturation in the mouse: possible roles of intercellular communication, cAMP, and testosterone. *Dev Biol* 95, 294-304

Tsafriri A, Channing CP (1975) An inhibitory influence of granulosa cells and follicular fluid upon porcine meiosis *in vitro*. *Endocrinology* 96, 922-927

Thibault C, Szöllösi D, Gérard M (1987) Mammalian oocyte maturation. *Reprod Nutr Dev* 27, 865-896

Vivarelli E, Conti M, De Felici M, Siracusa G (1983) Meiotic resumption and intracellular cAMP levels in mouse oocytes treated with compounds which act on cAMP metabolism. *Cell Differ* 12, 271-276

Wasserman PM, Josefowicz WJ, Letourneau GE (1976) Meiotic maturation of mouse oocytes *in vitro*: inhibition of maturation at specific stages of nuclear progression. *J Cell Sci* 22, 531-535

35

DEVELOPMENTAL BIOLOGY 157, 448-454 (1993)

Okadaic Acid Accelerates Germinal Vesicle Breakdown and Overcomes Cycloheximide- and 6-Dimethylaminopurine Block in Cattle and Pig Oocytes

JAROSLAV KALOUS,*[,1] MICHAL KUBELKA,*,† ZORA RIMKEVICOVA,* PIERRE GUERRIER,† AND JAN MOTLIK*

*Department of Genetics, Institute of Animal Physiology and Genetics, Czechoslovak Academy of Sciences, 277 21 Libechov, Czechoslovakia; and †Ecole Normale Supérieure de Lyon, 46 allée d'Italie, 69364 Lyon Cedex 07, France

Accepted January 5, 1993

Pig and cattle oocytes, when released from the follicle, spontaneously resume first meiotic division within 20 or 8 hr, respectively. In oocytes of both species, the activity of histone H1 kinase increases during maturation, exhibiting a maximum in metaphase I. Treatment of these oocytes with okadaic acid results in acceleration of germinal vesicle breakdown (GVBD) and of histone H1 kinase activation. This effect is more important in pig oocytes, in which the acceleration rises for 6 hr, as compared to 2 hr in cattle. Moreover, under these conditions, H1 kinase activity measured after 12 hr of culture appears higher than that observed in control metaphase I oocytes. When added to prophase oocytes, both cycloheximide and 6-DMAP (6-dimethylaminopurine) block GVBD and histone H1 kinase activation. Okadaic acid, at a concentration of 2.5 μM, is able to release the inhibitory effect exerted by cycloheximide on histone H1 kinase activity; however, GVBD occurred only in two-thirds of pig and one-quarter of cattle oocytes after 20 hr of culture. In addition, okadaic acid fully reverses the effect of 6-DMAP on H1 kinase activity and on GVBD in both species. The opposite effects of 6-DMAP and okadaic acid on MPF activation are discussed, as well as the nature of the protein, which has to be synthesized during the first meiotic division and may be involved in the MPF activation cascade. © 1993 Academic Press, Inc.

INTRODUCTION

Okadaic acid (OA), a potent inhibitor of protein phosphatases 1 and 2A (Bialojan and Takai, 1988; Haystead *et al.*, 1989), has been shown to induce a rapid appearance of MPF activity upon microinjection into *Xenopus* (Goris *et al.*, 1989) and starfish oocytes (Picard *et al.*, 1989; Pondaven *et al.*, 1990). In *Xenopus* oocytes, the activation of MPF by OA neither required protein synthesis nor involved cAMP-dependent protein kinase (Rime *et al.*, 1990). Similarly, in mouse oocytes, OA was able to overcome meiotic block induced by dbcAMP (Rime and Ozon, 1990), IBMX, and tumor-promoting phorbol esters (Gavin *et al.*, 1991). These results with mouse oocytes indicate that inhibition of specific phosphatase(s) can bypass the inhibitory effect brought about by protein kinase A or C (Rime and Ozon, 1990; Gavin *et al.*, 1991).

In contrast to rodent oocytes, pig, sheep, and cattle oocytes are very sensitive to cycloheximide or puromycin (Fulka *et al.*, 1986a; Moor and Crosby, 1986; Hunter and Moor, 1987). All of these oocytes are characterized by a slow sequence of events leading to germinal vesicle breakdown (GVBD). However, pig and cattle oocytes are sensitive to these protein synthesis inhibitors only during the first half-period of the time required for GVBD (Fulka *et al.*, 1986a; Motlík *et al.*, 1991). Such protein synthesis requirements, necessary for the initiation of M-phase and also reported in the case of *Xenopus* (Wassermann and Masui, 1976; Gerhart *et al.*, 1984), were formerly interpreted as requirements for cyclin synthesis. However, the latest results obtained by Gautier and Maller (1991) and by Minshull *et al.* (1991) show that cyclin B is already present in *Xenopus* in sufficient amounts before the activation of MPF, which precedes the first and second meiotic divisions. Similarly, our recent experiments with pig oocytes revealed that cyclin B was present in prophase-arrested pig oocytes and did not significantly change its level during first meiotic division (Kubelka *et al.*, unpublished results). Therefore the protein synthesis requirements for the first meiotic division to occur in pig, cattle, and *Xenopus* oocytes may involve another not yet identified protein. This might also apply for the second meiotic division in starfish (Picard *et al.*, 1985) and mouse oocytes (Fulka *et al.*, 1986a), and for the mitotic cell cycles triggered following oocyte fertilization or activation (Gerhart *et al.*, 1984; Clarke and Masui, 1983).

However, OA could activate MPF in cycloheximide-treated *Xenopus* oocytes (Goris *et al.*, 1989) or in mouse

[1] To whom correspondence should be addressed.

0012-1606/93 $5.00
Copyright © 1993 by Academic Press, Inc.
All rights of reproduction in any form reserved.

40

oocytes, which were activated at metaphase II by puromycin and further maintained in the presence of this protein synthesis inhibitor (Rime and Ozon, 1990). This reveals that the absence of this unknown protein can be compensated by the action of OA, suggesting that it is involved in the phosphorylation/dephosphorylation pathway leading to MPF activation.

To investigate the possibility that an inhibition of OA-sensitive protein phosphatases would be capable of inducing the biological effects of MPF in the absence of protein synthesis, pig and cattle oocytes were cultured in media supplemented with OA alone, or with OA plus cycloheximide. Here we report that OA substantially accelerates the kinetics of GVBD along with triggering a premature activation of histone H1 kinase. Furthermore, OA proved to be able to activate H1 kinase in the absence of protein synthesis and in such a way that it overcame the cycloheximide- and 6-DMAP-dependent block of pig and cattle oocytes.

MATERIAL AND METHODS

Source of Oocytes and Culture Procedure

Pig and cattle oocytes were collected at a local slaughterhouse and transported to the laboratory in phosphate-buffered saline (PBS, pH 7.4, 25°C). The oocytes aspirated from small antral follicles (3–5 mm in diameter) were washed in PBS and selected under a stereomicroscope. Only oocytes surrounded by compact cumulus were used for the following culture.

The culture medium was TCM 199 (Sevac, Prague, Czechoslovakia) buffered with 4.43 m*M* Hepes (Sigma, St. Louis), supplemented with bovine inactivated serum (10%, v/v) (Sevac), 2 m*M* sodium pyruvate, 2.92 m*M* calcium lactate, 33.9 m*M* sodium bicarbonate (Serva, Heidelberg, Germany), and antibiotics. About 20 oocytes were cultured in 250 μl of medium under paraffin oil at 38°C (pig oocytes) or at 39°C (cattle oocytes) in humidified air containing 5% CO_2.

In alternate experiments the culture medium was supplemented with okadaic acid (Moana BioProducts Inc., Hawaii) at concentrations 0.5 and 2.5 μM, with 10 μg/ml cycloheximide (Serva, Heidelberg, Germany), or with 2 m*M* 6-dimethylaminopurine (6-DMAP) (Sigma).

At the end of culture, cumulus cells were removed from oocytes by pipetting through a narrow-bore pipette. One part of the oocytes was used for extract preparation (see below); the other was examined morphologically: the oocytes were mounted on slides, fixed in an acetic acid:ethanol (1:3, v/v) mixture for 24 hr, stained with orcein, and examined under a phase-contrast microscope. The frequencies of GVBD were pooled from five replicative experiments with the total of 150 oocytes per group. All data were compared on the basis of χ^2 analysis.

Extract Preparation

For histone H1 kinase assays, the oocytes first incubated in control or drug-supplemented media were freed of cumulus cells and treated with 0.5% pronase (Serva, Heidelberg, Germany) to remove the zona pellucida. They were then washed several times in control medium without bovine serum and transferred in the kinase buffer (Meijer *et al.*, 1989). After several freeze/drying rounds, the oocytes were mechanically homogenized and centrifuged for 10 min at 10,000*g*, at 4°C. Supernatants were used as "crude extracts" for further procedures. About 30 oocytes were used for each extract.

Histone H1 Kinase Assay

H1 kinase activity was tested using a modification of the procedure described previously by Meijer *et al.* (1989).

The reaction mixture contained 5 μl of sample, 0.2 mg/ml histone H1 (Boehringer, Mannheim, Germany), 10 μM PKI-synthetic peptide (Sigma), 2 μCi of [γ-^{32}P]-ATP (110 TBq/mmol, Amersham, PB 10168, England, UK) in 30 μl of the kinase buffer (66 m*M* Na-glycerol-phosphate, pH 7.4, 15 m*M* *p*-nitrophenylphosphate, 5 m*M* EGTA, 15 m*M* MgCl, 1 m*M* dithiothreitol (Sigma). The final concentration of ATP in the reaction mixture was adjusted by nonradioactive ATP to 0.1 m*M*. The mixtures were incubated for 15 min at 30°C and the reaction was stopped by the addition of ½ vol of 3× concentrated electrophoresis sample buffer. The samples were then boiled for 5 min and loaded on 10% SDS-polyacrylamide gels (Laemmli, 1970); dried gels were subjected to autoradiography. The autoradiographs were scanned with LKB Ultroscan XL and the relative H1 kinase activity was plotted against the time of oocyte culture.

RESULTS

OA Accelerates GVBD in Pig and Cattle Oocytes

To study the possible influence of OA upon the time sequence of events leading to GVBD, two concentrations of OA (0.5 and 2.5 μM) were used. In pigs, all control oocytes possessed an intact GV after 6 hr of culture; however, 34 and 76% of the oocyte population underwent GVBD in 0.5 and 2.5 μM OA, respectively. The most prominent difference between control and OA-treated oocytes was detectable after 12 hr of culture, when 88 and 100% of oocytes in the OA group had undergone GVBD, in contrast to only 12% in the control group (Fig. 1). These data imply that OA accelerates significantly

41

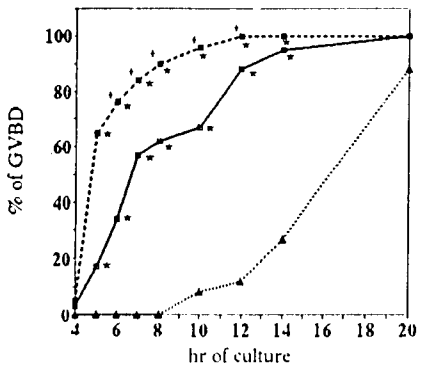

FIG. 1. Effect of OA on time sequence of germinal vesicle breakdown (GVBD) in pig oocytes. Pig cumulus-enclosed oocytes were cultured in control medium (▲) supplemented with 0.5 μM (□) or 2.5 μM (■) OA. At each time interval, the frequency of GVBD was determined in at least five replicate experiments. An asterisk denotes significant difference of OA groups from control ($P < 0.01$). A cross indicates a significant difference between two OA concentrations ($P < 0.01$).

and in a dose-dependent manner the time schedule for GVBD as observed in pig oocytes.

In cattle, the two selected OA concentrations (0.5 and 2.5 μM) increased quite significantly the rate of GVBD after 5 and 6 hr of culture (Fig. 2).

OA Treatment Causes Morphological Changes of the Metaphase I Spindle

In experiments using the lower dose of OA (0.5 μM), the cytological aspects of the metaphase I spindle were checked respectively in cattle and pig oocytes after 6 and 8 hr of culture. Frequently, microtubules were not only oriented toward the two spindle poles, but pointed in several directions (Figs. 3a and 3b). During the longer culture intervals in both pig and cattle oocytes, the abnormal metaphase I spindle disappeared and the highly condensed bivalents, with or without faint remnants of the microtubular network, spread throughout the cytoplasm. Such scattered bivalents remained visible in cytoplasm even after 20 hr of culture.

When the higher concentration of OA (2.5 μM) was used, the highly condensed bivalents of the cattle and pig oocytes were already scattered in the cytoplasm with no remnant of the microtubular network after only 6 and 8 hr of culture, respectively. These results indicate that OA blocks pig and cattle oocytes at the late diakinesis–metaphase I stage. OA at 0.5 μM caused the formation of an atypical, nonfunctional spindle, while the metaphase I spindle could not be formed at all in 2.5 μM OA.

OA Overcomes the Cycloheximide- and 6-DMAP-Dependent Inhibitions of GVBD in Pig and Cattle Oocytes

Nearly all pig and cattle oocytes were blocked at the GV stage with highly condensed bivalents when they were cultured in the presence of 10 μg/ml cycloheximide for 8 and 20 hr, respectively. In a medium containing 10 μg/ml cycloheximide and 2.5 μM OA, 24% cattle (Table 2) and 62% pig oocytes (Table 1) underwent GVBD after 20 hr of culture. Thus, 2.5 μM OA concentration proved able to overcome the cycloheximide block in one-quarter of cattle and two-thirds of pig oocytes.

Pig and cattle oocytes are also blocked at the GV stage when incubated in 2 mM 6-DMAP. In the same medium supplemented with 2.5 μM OA, the inhibitory effect of 6-DMAP upon GVBD of pig oocytes was fully reversed (Table 1) and the time schedule for GVBD was substantially accelerated. OA also counteracted 6-DMAP action in cattle oocytes (Table 2).

OA Induces Premature Activation of Histone H1 Kinase in Pig and Cattle Oocytes and Overcomes the Cycloheximide- and 6-DMAP-Dependent Blocks of H1 Kinase Activity

Using pig and cattle oocytes, which are characterized by a low sequence of events leading to GVBD, we were able to follow premature H1 kinase activation in OA-treated oocytes even during the first meiotic division. As illustrated in Figs. 4 and 7, the H1 kinase activity in pig oocytes begins to increase after 6 hr of culture, reaching a maximum at metaphase I, i.e., after 20 hr of

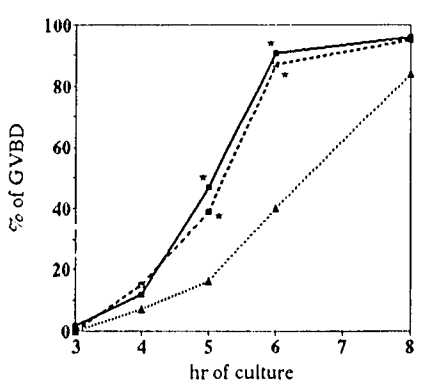

FIG. 2. Effect of OA on time sequence of germinal vesicle breakdown (GVBD) in cattle oocytes. Cattle cumulus-enclosed oocytes were cultured in control medium (▲) supplemented with 0.5 μM (□) or 2.5 μM (■) OA. At each time interval, the frequency of GVBD was determined in at least five replicate experiments. An asterisk denotes significant difference of OA groups from control ($P < 0.01$).

FIG. 3. Cattle oocytes cultured for 6 hr in OA-supplemented (0.5 μM) medium. The highly condensed bivalents are linked to the spindle microtubules, but the microtubules are not oriented to two spindle poles only (× 1000). Two equatorial plates are visible in a (arrowheads); three spindle poles are evident in b (arrowheads). Bars, 10 μm.

culture. When cultured 6 hr in the presence of 2.5 μM OA (Figs. 5 and 7), such pig oocytes exhibit an H1 kinase activity comparable to that observed in control oocytes cultured for 12 hr (Figs. 4 and 7). Moreover, after 12 hr of culture in OA-supplemented medium (Fig. 7), their H1 kinase activity is even higher than that observed in control metaphase I oocytes (Fig. 7). OA produced similar effects when applied to cattle oocytes. In control cattle oocytes, H1 kinase activity is slightly activated after 4 hr of culture (Fig. 8). In OA-treated oocytes, H1 kinase rises sharply during the first 4 hr, then reaches its maximal level after 8 hr of culture (Fig. 8).

Both pig and cattle oocytes possess very low H1 kinase activity, whether treated with cycloheximide or 6-DMAP (Figs. 7 and 8). However, when these media are supplemented with OA (2.5 μM), H1 kinase activity is greatly enhanced. The cycloheximide-dependent block of H1 kinase activity in pig oocytes is already released by OA after 6 hr of culture (Figs. 6A and 7), and after 20 hr H1 kinase is activated to the same extent as observed in control oocytes (Figs. 4, 6A, and 7). Similarly, in cattle oocytes, H1 kinase is activated in cycloheximide-OA-supplemented media (Fig. 8). Furthermore, the 6-DMAP-dependent block of H1 kinase activity could be overcome by OA, both in pig (Figs. 6B and 7) and cattle oocytes (Fig. 8).

Therefore, in both pig and cattle oocytes, OA proved able to provoke an activation of histone H1 kinase and

TABLE 1
THE COMBINED EFFECT OF OA, CYCLOHEXIMIDE, AND 6-DMAP UPON PERCENTAGE (%) OF GVBD IN PIG OOCYTES

Treatment	Duration of culture			
	6 hr	8 hr	12 hr	20 hr
Control medium	0^a	7^a	23^b	93^c
OA	74^b	93^b	100^c	100^c
Cycloheximide		0^a	3^a	5^a
Cycloheximide + OA		17^a	38^b	62^b
6-DMAP	0^a	0^a	—	0^a
6-DMAP + OA	55^b	82^b	—	93^c

Note. After isolation from the follicles the pig oocyte cumulus complexes were cultured in control medium, or in medium enriched with OA (2.5 μM), cycloheximide (10 mg/ml), cycloheximide (10 mg/ml) and OA (2.5 μM), 6-DMAP (2 mM), or 6-DMAP (2 mM) and OA (2.5 μM). At each time point of the culture the GVBD status of the oocytes was evaluated. Figures in columns with different superscripts are significantly different ($P < 0.05$).

TABLE 2
THE COMBINED EFFECT OF OA, CYCLOHEXIMIDE, AND 6-DMAP UPON PERCENTAGE (%) OF GVBD IN CATTLE OOCYTES

Treatment	Duration of culture			
	6 hr	8 hr	12 hr	20 hr
Control medium	5^a	43^b	72^c	94^c
OA	8^a	87^c	96^c	100^c
Cycloheximide	0^a	0^a	0^a	0^a
Cycloheximide + OA	0^a	3^a	8^a	24^b
6-DMAP	0^a	—	0^a	37^b
6-DMAP + OA	8^a	—	31^b	88^c

Note. After isolation from the follicles the cattle oocyte cumulus complexes were cultured in control medium, or in medium enriched with OA (2.5 μM), cycloheximide (10 mg/ml), cycloheximide (10 mg/ml) and OA (2.5 μM), 6-DMAP (2 mM), or 6-DMAP (2 mM) and OA (2.5 μM). At each time point of the culture the GVBD status of the oocytes was evaluated. Figures in columns with different superscripts are significantly different ($P < 0.05$).

43

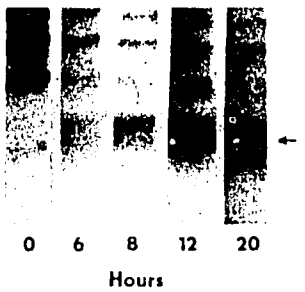

FIG. 4. Time course of H1 kinase activity in pig oocytes cultured for 0, 6, 8, 12, and 20 hr in control medium.

to release the cycloheximide- or 6-DMAP-dependent blocks of H1 kinase activity.

DISCUSSION

In the present experiments, the time sequence of GVBD in cattle oocytes was found to be accelerated by 2 hr in comparison to the kinetics of GVBD observed in control oocytes, matured either *in vivo* (Hyttel *et al.*, 1986) or *in vitro* (Motlík *et al.*, 1978; Hyttel *et al.*, 1987). This phenomenon was more pronounced in pig oocytes in which the OA treatment reduced the time required for GVBD to 8 hr, in comparison with the 16–20 hr necessary to obtain GVBD in oocytes matured after hCG stimulation or under *in vitro* conditions (Motlík and Fulka, 1976). Furthermore, a parallel acceleration of the histone H1 kinase activation could be observed in such OA-treated pig and cattle oocytes. Again, these effects were better expressed in pig oocytes, in which the time corresponding to the beginning of the increase in H1 kinase activity was shortened by 6 hr as compared to 2 hr in cattle oocytes, and in which the activity reached after 12 hr was even higher than that found in control metaphase I oocytes. These results indicate that premature morphological events such as chromosome condensation

FIG. 5. Time course of H1 kinase activity in pig oocytes cultured for 6, 8, and 12 hr in medium with 2.5 μM OA.

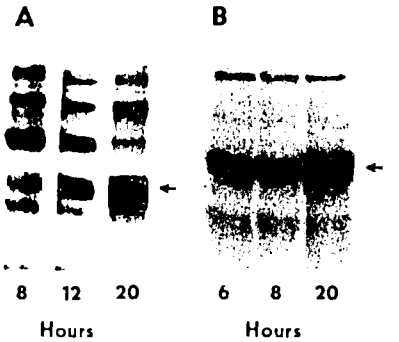

FIG. 6. H1 kinase activity in pig oocytes cultured for 8, 12, or 20 hr in the presence of 10 μg/ml cycloheximide and 2.5 μM OA (A) and for 6, 8, or 20 hr in the presence of 2 mM 6-DMAP and 2.5 μM OA (B).

and GVBD are not caused by nonspecific OA effects, but really depend on MPF activation.

Although OA was found to accelerate GVBD in cattle and pig oocytes, the overall meiotic maturation process did not progress beyond late diakinesis–metaphase I stage. These data confirm previous observations made on *Xenopus* (Rime *et al.*, 1990) and mouse oocytes (Rime and Ozon, 1990; Alexandre *et al.*, 1991), which indicated that the cytoplasm of OA-treated oocytes had lost its capacity to organize a normal pattern of metaphase microtubules. We have observed in cattle and pig oocytes that the effects of OA on spindle formation were dose dependent. While 2.5 μM OA precluded the organization of a metaphase I spindle, 0.5 μM OA produced an abnormal spindle with an apparent multiplication of microtubule organizing centers (MTOCs). These data are in agreement with recent observations of mouse oocytes which showed that OA did not impair the ability of tu-

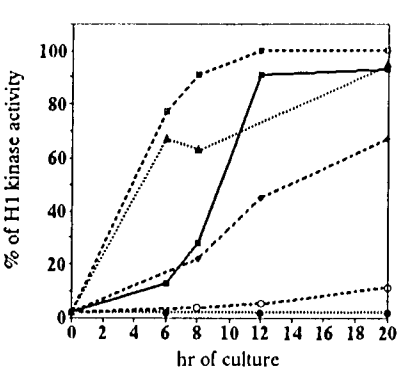

FIG. 7. Quantitative rate of relative H1 kinase activity plotted against time for pig oocytes cultured in control medium (■), or in medium enriched with 2.5 μM OA (□), 10 mg/ml cycloheximide (○), 10 mg/ml cycloheximide and 2.5 μM OA (▲), 2 mM 6-DMAP (●), or 2 mM 6-DMAP and 2.5 μM OA (+).

44

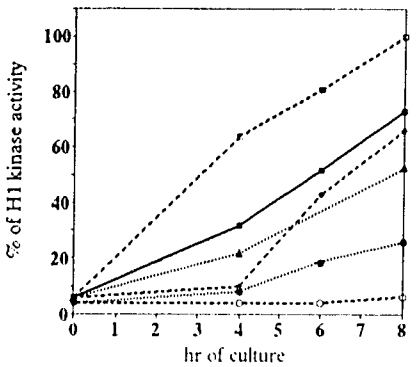

FIG. 8. Quantitative rate of relative H1 kinase activity plotted against time for cattle oocytes cultured in control medium (■), or in medium enriched with 2.5 μM OA (□), 10 mg/ml cycloheximide (○), 10 mg/ml cycloheximide and 2.5 μM OA (▲), 2 mM 6-DMAP (●), or 2 mM 6-DMAP and 2.5 μM OA (+).

bulin to polymerize, but interfered with the establishment of focal MTOCs (Alexandre *et al.*, 1991). Similarly, Vandré and Wills (1992) showed the occurrence of the abnormal mitotic spindle in porcine kidney (LLC-PK) cells blocked in mitosis by OA.

Pig and cattle oocytes, which normally mature spontaneously when taken out of the follicle, cannot resume meiosis in media supplemented with protein synthesis inhibitors (Fulka *et al.*, 1986a; Hunter and Moor, 1987; Sirard *et al.*, 1989; Motlík *et al.*, 1991). However, in contrast to what occurs in *Xenopus*, cycloheximide precludes the amplification of MPF in those mammalian oocytes which have been fused (Fulka *et al.*, 1986b, 1988) or microinjected (Procházka *et al.*, 1989). It has also been shown that the microinjection of active $p34^{cdc2}$ kinase into starfish (*Astropecten*) prophase oocytes failed to trigger GVBD, suggesting that another component may exert a negative control on the amplification step (Picard *et al.*, 1991). The action of this neutralizing factor could be reversed by another factor originating from the nucleus, as revealed in experiments, in which the MPF amplification was induced by injecting the kinase into the nucleus or by injecting nuclear content into recipient cytoplasm. Requirements for this nuclear factor could be overcome by an inhibition of type 2A phosphatase, mediated by the microinjection of OA, whereas the microinjection of phosphatase 1 inhibitors had no effect. Therefore, the inactivation of microinjected $p34^{cdc2}$ kinase within the recipient cytoplasm was presumably due to its rephosphorylation, the unknown nuclear factor acting most likely by inhibiting type 2A phosphatase (Picard *et al.*, 1991).

If we suppose that such a factor, necessary for MPF activation, is synthesized only during first meiotic division in pig and cattle oocytes, one may understand why inhibition of type 2A phosphatase may bypass the cycloheximide block of these oocytes. And, actually, we found that OA was able to reverse the effect of cycloheximide and to induce H1 kinase activation with kinetics similar to those found in control oocytes. This indicates that the relevant protein, synthesized at the beginning of the first meiotic cell cycle in pig and cattle oocytes, can activate $p34^{cdc2}$ kinase most probably by influencing its phosphorylation/dephosphorylation state. The differences between H1 kinase activity and the percentage of GVBD under the same culture conditions could support the idea, already pronounced by several authors, that the histone H1-$p34^{cdc2}$ kinase activity and MPF activity need not present the same entity.

6-DMAP, an inhibitor of serine/threonine protein kinases (Meijer and Pondaven, 1988; Néant and Guerrier, 1988), was also found to provoke a rephosphorylation of $p34^{cdc2}$ on tyrosine, when applied to *Xenopus* oocytes at GVBD (Jessus *et al.*, 1991). Such a rephosphorylation process correlated with the disappearance of MPF, the partial inactivation of H1 kinase, and reentry into interphase. OA, which is supposed to control MPF activation by modulating the tyrosine phosphorylation level of $p34^{cdc2}$ (Rime *et al.*, 1991), proved able to reverse the action of 6-DMAP in such *Xenopus* oocytes (Jessus *et al.*, 1991).

In accordance with recent data on mouse oocytes (Alexandre *et al.*, 1991), we show that the effects of 6-DMAP on pig and cattle oocytes (block in the prophase stage accompanied by an inhibition of H1 kinase activation) can be reversed by OA. H1 kinase activation takes place with nearly the same kinetics as observed in control nontreated oocytes, suggesting that MPF is fully activated in 6-DMAP-OA-treated oocytes and it induces its biological effects in more than 90% of the oocyte population.

Taken together, our data therefore suggest that in pig and cattle as well as in *Xenopus* oocytes, OA and 6-DMAP may positively and negatively regulate MPF activation, probably by influencing the phosphorylation/dephosphorylation state of $p34^{cdc2}$ most likely via the involvement of a still unknown protein regulator. Experiments are now in progress to test the value of this new working hypothesis.

We thank Mrs. L. Koberova for excellent technical assistance. This work was partially supported by Grant 6145 from ARC and 9100708 from INSERM. M.K. was supported by Postdoctoral Grant 053224K from MRT, France. The project was further supported by U.S. A.I.D. Grant 12.061E.

REFERENCES

Alexandre, H., Vancauwenberge, A., Tsukitani, Y., and Mulnard, J. (1991). Pleiotropic effect of okadaic acid on maturing mouse oocytes. *Development* 112, 971–980.

45

Bialojan, C., and Takai, A. (1988). Inhibitory effect of marine-sponge toxin, okadaic acid, on protein phosphatases. *Biochem. J.* **256**, 283–290.

Clarke, H. J., and Masui, Y. (1983). The induction of reversible and irreversible chromosome decondensation by protein synthesis inhibition during meiotic maturation of mouse oocytes. *Dev. Biol.* **97**, 291–301.

Fulka, J., Jr., Flechon, J. E., Motlik, J., Fulka, J., and Jilek, F. (1986a). Effect of cycloheximide on nuclear maturation of pig and mouse oocytes. *J. Reprod. Fertil.* **77**, 281–285.

Fulka, J., Jr., Motlik, J., Fulka, J., and Crozet, N. (1986b). Activity of maturation promoting factor in mammalian oocytes after its dilution by single and multiple fusions. *Dev. Biol.* **118**, 176–181.

Fulka, J., Jr., Fléchon, J. E., Motlik, J., and Fulka, J. (1988). Does autocatalytic amplification of maturation promoting factor (MPF) exist in mammalian oocytes? *Gamete Res.* **21**, 185–192.

Gautier, J., and Maller, J. L. (1991). Cyclin B in *Xenopus* oocytes: Implifications for the mechanism of pre-MPF activation. *EMBO J.* **10**, 177–82.

Gavin, A. C., Tsukitani, Y., and Schorderet-Slatkine, S. (1991). Induction of M-phase entry of prophase-blocked mouse oocytes through microinjection of okadaic acid, a specific phosphatase inhibitor. *Exp. Cell Res.* **192**, 75–81.

Gerhart, J., Wu, M., and Kirschner, M. W. (1984). Cell cycle dynamics of an M-phase specific cytoplasmic factor in *Xenopus laevis* oocytes and eggs. *J. Cell Biol.* **98**, 1247–1255.

Goris, J., Hermann, J., Hendrix, P., Ozon, R., and Merlevede, W. (1989). Okadaic acid, a specific protein phosphatase inhibitor, induces maturation and MPF formation in *Xenopus laevis* oocytes. *FEBS Lett.* **245**, 91–94.

Haystead, T. A. J., Sim, A. T. R., Carling, D. C., Honnor, R. Y. C., Tsukutami, Y., Cohen, P., and Hardie, D. G. (1989). Effects of the tumour promoter okadaic acid on intracellular protein phosphorylation and metabolism. *Nature* **337**, 78–81.

Hunter, A. G., and Moor, R. M. (1987). Stage-dependent effects of inhibiting ribonucleic acids and protein synthesis on meiotic maturation of bovine oocytes *in vitro*. *J. Dairy Sci.* **70**, 1646–1651.

Hyttel, P., Xu, K. P., Smith, S., and Greve, T. (1986). Ultrastructure of *in vitro* oocyte maturation. *J. Reprod. Fertil.* **78**, 645–656.

Hyttel, P., Xu, K. P., Smith, S., Callesen, H., and Greve, T. (1987). Ultrastructure of the final nuclear maturation of bovine oocytes *in vitro*. *Anat. Embryol.* **176**, 35–40.

Jessus, C., Rime, H., Haccard, O., van Lint, J., Goris, J., Merlevede, W., and Ozon, R. (1991). 6-DMAP and okadaic acid control the level of MPF activity and tyrosine phosphorylation of $p34^{cdc2}$ antagonistically in *Xenopus* oocyte. *Development* **111**, 813–820.

Laemmli, U. K. (1970). Cleavage of structure proteins during the assembly of the head of bacteriphade T4. *Nature* **227**, 680–685.

Meijer, L., and Pondaven, P. (1988). Cyclic activation of histone H1 kinase during sea urchin egg mitotic divisions. *Exp. Cell Res.* **174**, 116–29.

Meijer, L., Arion, D., Golstein, R., Pines, J., Brizuela, L., Hunt, T., and Beach, D. (1989). Cyclin is a component of the sea urchin egg M-phase specific histone H1 kinase. *EMBO J.* **8**, 2275–2282.

Minshull, J., Murray, A., Colman, A., and Hunt, T. (1991). *Xenopus* oocyte maturation does not require new cyclin synthesis. *J. Cell Biol.* **114**, 767–772.

Moor, R. M., and Crosby, I. M. (1986). Protein requirements for germinal vesicle breakdown in ovine oocytes. *J. Embryol. Exp. Morphol.* **94**, 207–220.

Motlik, J., and Fulka, J. (1976). Breakdown of the germinal vesicle in pig oocytes *in vivo* and *in vitro*. *J. Exp. Zool.* **198**, 155–162.

Motlik, J., Koefoed-Johnsen, H. H., and Fulka, J. (1978). Breakdown of the germinal vesicle in bovine oocytes. *J. Exp. Zool.* **205**, 377–383.

Motlik, J., Nagai, T., and Kikuchi, K. (1991). Resumption of meiosis in pig oocytes cultured with cumulus and parietal granulosa cells: The effect of protein synthesis inhibition. *J. Exp. Zool.* **259**, 386–391.

Néant, I., and Guerrier, P. (1988). 6-Dimethylaminopurine blocks starfish oocyte maturation by inhibiting a relevant protein kinase activity. *Exp. Cell Res.* **176**, 68–79.

Picard, A., Peaucellier, G., Boulfant, P., Peuch, C., and Dorée, M. (1985). Role of protein synthesis and proteases in production and inactivation of maturation promoting activity during meiotic maturation of starfish oocytes. *Dev. Biol.* **109**, 311–320.

Picard, A., Capony, J. P., Brautigan, D. L., and Dorée, M. (1989). Involvement of protein phosphatases 1 and 2A in the control of M phase-promoting factor activity in starfish. *J. Cell Biol.* **109**, 3347–3354.

Picard, A., Labbé, J.-C., Barakat, H., Cavadore, J.-C., and Dorée, M. (1991). Okadaic acid mimics a nuclear component required for cyclin B-cdc2 kinase microinjection to drive starfish oocytes into M phase. *J. Cell Biol.* **115**, 337–344.

Pondaven, P., Meijer, L., and Bialojan, C. (1989). La microinjection d'acide okadaique, un inhibiteur dephosphoproteine phosphatases, induit la maturation de l'ovocyte d'etoile de mer. *C. R. Acad. Sci. Paris* **309**, 563–569.

Procházka, R., Motlik, J., and Fulka, J. (1989). Activity of maturation promoting factor in pig oocytes after microinjection and serial transfer of maturing cytoplasm. *Cell Differ. Dev.* **27**, 175–182.

Rime, H., and Ozon, R. (1990). Protein phosphatases are involved in the *in vivo* activation of histone H1 kinase in mouse oocyte. *Dev. Biol.* **141**, 115–22.

Rime, H., Huchon, D., Jessus, C., Goris, J., Merlevede, W., and Ozon, R. (1990). Characterization of MPF activation by okadaic acid in *Xenopus* oocytes. *Cell Differ. Dev.* **29**, 47–58.

Rime, H., van Lint, J., Goris, J., Merlevede, D., Jessus, C., and Ozon, R. (1991). OA-sensitive protein phosphatase and cyclin regulate *in vivo* the level of tyrosine phosphorylation of $p34^{cdc2}$ during first meiotic division of *Xenopus* oocyte. Submitted for publication.

Sirard, M. A., Florman, H. M., Leibfried-Rutledge, M. L., Barnes, F. L., Sims, M. L., and First, N. L. (1989). Timing of nuclear progression and protein synthesis necessary for meiotic maturation of bovine oocytes. *Biol. Reprod.* **40**, 1257–1264.

Vandré, D. D., and Wills, V. L. (1992). Inhibition of mitosis by okadaic acid: Possible involvement of a protein phosphatase 2A in the transition from metaphase to anaphase. *J. Cell Sci.* **101**, 79–91.

Wassermann, W. J., and Masui, Y. (1976). A cytoplasmic factor promoting oocyte maturation: Its extraction and preliminary characterization. *Science* **191**, 1266–1268.

46

Biol Cell (1993) 77, 173–180
© Elsevier, Paris

Original articl

Ultrastructural cytochemistry of the nucleus and nucleolus in growing rabbit oocytes

Peter Šutovský [a], Ladislava Jelínková [a], Libuše Antalíková [b], Jan Motlík [a]

[a] *Institute of Animal Physiology and Genetics, 277 21 Liběchov;* [b] *Research Institute of Animal Production, Praha 10 Uhříněves, Czech Republic*

(Received 27 October 1992; accepted 19 January 1993)

Summary – Ultrastructural changes of the germinal vesicle during the growth of rabbit oocytes were studied by means of light and electron microscopy, ^{3}H-uridine autoradiography, Ag-NOR staining and E-PTA staining. Particular interest was paid to the nucleologenesis and condensation of chromatin. In contrast to other mammalian species, chromosome condensation in rabbit oocytes occurred concomitantly with rRNA synthesis-dependent nucleolar compaction and preceded nuclear envelope breakdown and resumption of meiosis.

nucleolus / chromosome condensation / oocyte / rabbit / rRNA synthesis

Introduction

Mammalian follicles leaving the follicular pool enter in the growth phase. The follicular growth, characterised by progressive differentiation of follicular cells, is paralleled by oocyte growth [14]. In oocyte nucleus, germinal vesicle (GV), diplotene chromosomes are decondensed and the fibrillo-granular nucleolus contains numerous small fibrillar centers (FC) [1, 35, 37].

The increase of nucleolar rRNA synthesis is considered to be the first event in the initiation of oocyte growth [7, 23]. During further oocyte growth, both the nucleclar structure as well as the high ^{3}H-uridine incorporation in the nucleoplasm and nucleolus indicate that growing oocytes are engaged in intense hnRNA and rRNA synthesis [12, 13]. The active transcription of the highly decondensed genome enables a steady accumulation of tRNA and rRNA throughout the oocyte growth period [16, 18].

When the oocytes reach full size, substantial changes of the nucleolar ultrastructure lead to the compaction of the nucleolus, which is accompanied by gradual cessation of rRNA synthesis [10, 27]. However, some hnRNA synthesis takes place in mammalian oocytes up to the resumption of meiosis [27, 32, 39].

In the majority of mammalian species, the chromosome condensation occurs after resumption of meiosis, concomitantly with breakdown of the nuclear envelope. Surprisingly, the GV of fully grown rabbit oocytes is filled with highly condensed bivalents [26]. This fact suggests that chromatin condensation in this species is not dependent upon meiotic stimulus.

In the present study, growing and fully grown rabbit oocytes were investigated using autoradiography and ultrastructural cytochemistry. We report here for the first time that in rabbit oocytes, in contrast to all mammalian species so far studied, the process of nucleolar compaction and chromosome condensation occur concomitantly.

Materials and methods

Oocyte collection and light microscopic observations

In adult rabbit females, pseudopregnancy was induced by 150 IU hCG (Praedyn, Spofa, Czech Republic). At the 17th, 18th and 19th day of pseudopregnancy, the females were injected twice daily with 5.7 IU of FSH (Folicotropin, Spofa, Czech Republic). 1 day later, the rabbits were killed, and the follicles and pieces of ovarian cortex were isolated under dissection microscope. The follicles were measured by light microscope with measuring attachement. Oocyte cumullus complexes (OCCs) were collected by rupturing of the follicular wall, the oocytes were denuded by pipetting, measured and divided according to the follicle diameter into the following categories:
i) category A: oocytes from preantral follicles (follicle and oocyte diameters were not measured); ii) category B: oocytes from small antral follicles 0.2–0.5 mm in diameter (oocyte diameter 95–122 μm); iii) category C: oocytes from middle antral follicles 0.5–1.0 mm in diameter (oocyte diameter 122–138 μm); and iv) category D: oocytes from large antral follicles 1.0–1.8 mm in diameter (oocyte diameter 140–153 μm).

Numbers of oocytes and pieces of ovarian cortex used in present study were: for electron microscopy: 56 oocytes and 12 pieces of ovarian cortex; for light microscopic autoradiography: 15 oocytes; for Ag-NOR staining: 19 oocytes and seven pieces of ovarian cortex; and for E-PTA staining: 16 oocytes and eight pieces of ovarian cortex.

Light microscopic autoradiography

The OCCs were incubated for 20 min in culture medium containing 92 ml isotonic M 199 (Usol, Prague), 25 mg calcium lac-

Abbreviations: GV, germinal vesicle; FC, fibrillar center; OCC, oocyte cumullus complex; GC, granular component; DFC, dense fibrillar component; NAC, nucleolus associated chromatin; NV, nucleolar vacuole; E-PTA, ethanol-phosphotungstic acid.

tate, 25 mg sodium pyruvate, 150 mg Hepes, 3 mg penicillin, 5 mg streptomycin, 3.9 ml 1.45% $NaHCO_3$ + 0.002% phenol red and 5-^{3}H-uridine (UVVVR, Prague, Czech Republic; specific activity 765 GBq/mol, final concentration 3.7 MBq/ml). Then the OCCs were washed, fixed and embedded in Epon 812. Semithin sections on glass slides were coated with Ilford K 5 autoradiographic emulsion and exposed for 14 days at 4°C. After developing in D19 developer the sections were stained by toluidine blue and examined in light microscope.

Electron microscopy

OCCs from antral follicles and small pieces of ovarian cortex containing preantral follicles were fixed in 0.6% paraformaldehyde and 2.5% glutaraldehyde mixture for 90 min. After brief washing and postfixation in 1% osmium tetroxide, the samples were dehydrated and embedded in Epon 812. Ultrathin sections were stained by uranyl-acetate and lead citrate and examined in Jeol 1200 EX electron microscope.

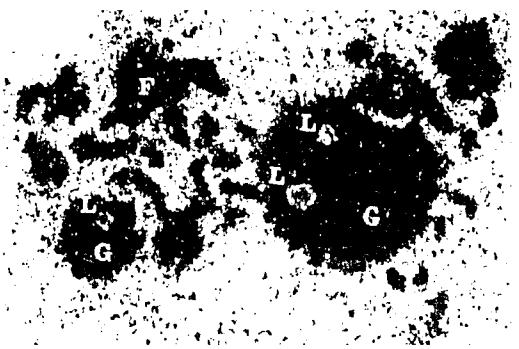

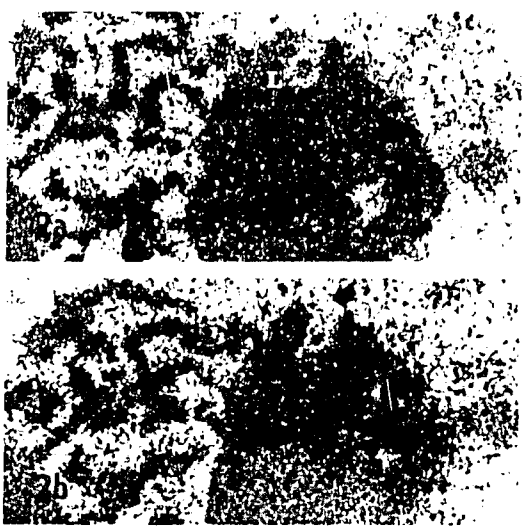

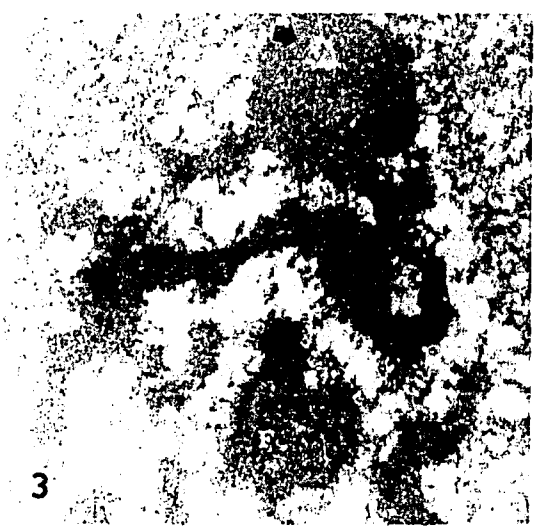

Figs 1–3. 1. Ultrathin section of the nucleolus in an oocyte from unilaminar follicle as demonstrated by uranyl acetate/lead citrate staining. The large round shaped areas of the granular component (G) possess the lacunas filled with fine filamentous material (L). The strands of dense fibrillar component link the granular areas with fibrillar center (F); × 15000. **2. a.** Serial sections of the granular area with the lacuna (L), located closely to the periphery. **b.** The material inside nucleolar lacuna is connected with perinucleolar chromatin (arrow). The sections were stained by uranyl acetate and lead citrate; × 30000. **3.** Nucleolus of an unilaminar stage oocyte after Ag-NOR staining. Fibrillar center (F) and dense fibrillar components are densely covered by silver grains. The granular components and the lacuna (arrow) are not silver positive; × 40000.

48

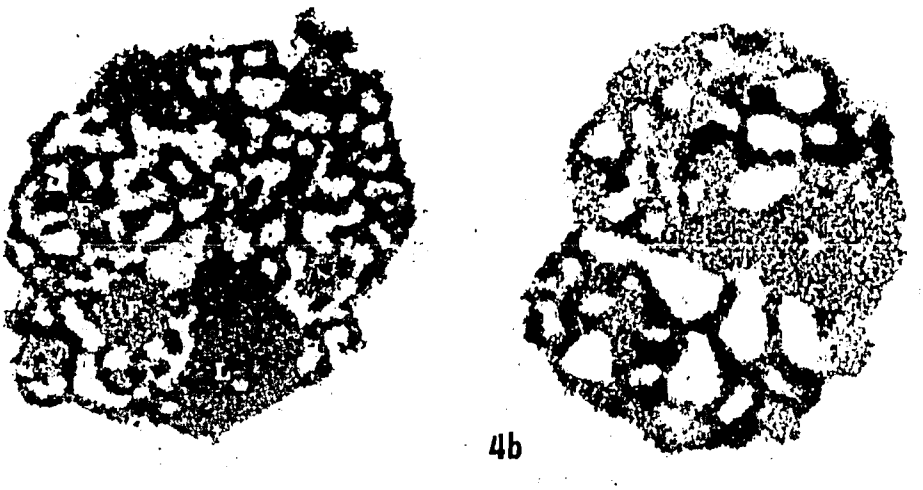

Fig 4. Nucleolus of an oocyte from plurilaminar follicle with a large amount of dense fibrillar components. **a.** Fibrillar centers (F) are scattered in the nucleolonema. The area of granular components with small lacuna is visible (arrow) in this section stained by uranyl acetate and lead citrate; × 17000. **b.** After E-PTA treatment, the dense fibrillar components are strongly stained. × 26000.

E-PTA staining

E-PTA staining of basic, lysine-rich proteins associated with DNA was used for distinction of DNA and RNA created particles in the nucleoli. The oocytes were fixed by 1.6% glutaraldehyde in phosphate buffer, dehydrated and immersed in 2% phosphotungstic acid in ice-cold absolute alcohol overnight according to Antoine *et al* [3]. After rinsing in absolute alcohol and washing in propylene oxide, the samples were embedded in Epon, sectioned and examined without further contrast.

Ag-NOR staining

The Ag-NOR staining method was used for ultrastructural localization of acidic non-histone proteins involved in rDNA transcription and early processing.

The oocytes were fixed for 20 min in glutaraldehyde, washed in 0.2 M cacodylate buffer, postfixed in the mixture of ethanol and acetic acid for 10 min and then washed carefully in deionized water. The silver staining technique described by Likovsky and Smetana [22] was used. Finally, the samples were dehydrated in ascending series of ethanol, infiltrated and embedded in Epon 812. Ultrathin sections were contrasted by uranyl acetate and evaluated.

Results

Category A

In unilaminar follicles, the oocytes possessed the reticulated nucleoli with round shaped sheets of granular components (GC). Small lacunas filled with finely filamentous material were often embedded in GCs (fig 1). Occasionally, these lacunas were located at the periphery and linked with nucleolus associated chromatin (NAC) (fig 2a,b). The cords of dense fibrillar components (DFC), often attached to GCs, and fibrillar centers (FC) were strongly positive for silver after Ag-NOR staining (fig 3). The DFCs and NAC were highly contrasted in E-PTA stained sections, whereas FCs, GCs and material in nucleolar lacunas stained only weakly.

Concomitantly with the multiplication of follicle cells in plurilaminar follicles, the nucleolonemas formed round-shaped nucleoli with numerous irregular nucleolar vacuoles (NV). The increased amount of DFCs created a large meshwork of anastomosing cords. Numerous small FCs were scattered in nucleolonemas. The strands of GCs were shifted to the periphery and still possessed several lacunas (fig 4a).

The above described distribution of nucleolar components was confirmed by Ag-NOR staining. The DFCs and small FCs were densely covered by silver grains, whereas GCs and lacunas were completely devoid of silver. The E-PTA staining emphasized the large masses of DFC and clusters of NAC (fig 4b).

Category B

Oocytes isolated from small antral follicles were highly active in rRNA and hnRNA synthesis, as shown by light microscopical autoradiography (fig 9a). Besides numerous small vacuoles, several large NVs appeared in round-shaped nucleolonemas of those oocytes. The FCs, sometimes located at the nucleolar periphery and linked with clusters of NAC, begun to extend in diameter (fig 5a). The DFCs, visualized by Ag-NOR staining penetrated by numerous protrusions from FCs into nucleolonemas (fig 6a). GSc formed large sheets and thick cords among nucleolar vacuoles.

Usually, the nucleoli were surrounded by the bound of NAC, sometimes penetrating into peripherally located nucleolar vacuoles. Small clusters of the same material were found inside several vacuoles, particularly around FCs (fig 5b). Some of these clusters, both on the rim of NAC and the DFCs were strongly stained by E-PTA (fig 6b). The first signs of chromosome condensation appeared in the nucleoplasm.

49

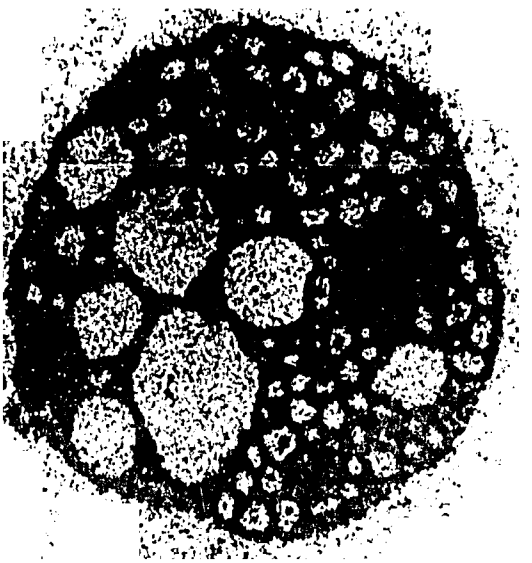

5b

6a

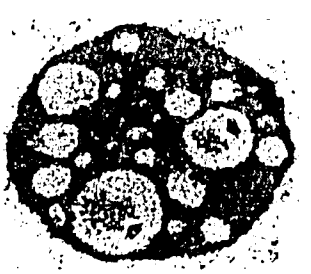

5

Category C

Oocytes isolated from middle antral follicles reached nearly full size (see *Materials and methods*). Owing to a chromosome condensation, the ^{3}H-uridine incorporation in nucleoplasm substantially decreased. The labelling of nucleoli was visible as peripherally localized caps, corresponding with the position of FCs in ultrastructural observations (fig 9b).

The large nucleolar vacuoles extended to maximal size, giving a lattice-like shape to the nucleolonemas. Considerable clusters of NAC were arranged at the periphery and similar material was found inside the vacuoles. The number of DFCs and FCs decreased and the nucleolonema was predominantly created by GCs. However, the diameter of FCs substantially increased (fig 7a). They were located at the periphery and contained only small amounts of silver grains after Ag-NOR staining. The protrusions of silver deposits from FCs to nucleolonema disappeared (fig 8).

E-PTA staining showed a continuous rim of NAC at the nucleolar periphery and a decreased amount of DFC in nucleolonemas. Some of the granular clusters inside vacuoles and small clumps of condensed chromatin in nucleoplasm were well stained too (fig 7b).

Category D

The fully grown oocytes were weakly labelled after the ^{3}H-uridine autoradiography (fig 9c).

Nucleolar compaction and the segregation of nucleolar components beginning in this stage caused the shrinking and gradual disappearence of nucleolar vacuoles (fig 10). In some oocytes, both compact and vacuolated nucleoli were found.

The compact nucleoli were composed of a homogenous mass of fine filaments. The FCs, DFCs and GCs disappeared. Sometimes, the lenticles of silver positive material were found at the nucleolar periphery (fig 12b). Highly condensed chromosomal bivalents appearing in the nucleoplasm were linked at several points with compact nucleoli. Numerous small beads were often associated with the periphery of condensed chromatin (fig 11).

E-PTA staining emphasized the peripheral rim of NAC and highly condensed chromosomal bivalents. The lenticles were well stained too. Homogenous nucleolar mass was bleached (fig 12a).

Discussion

Diplotene stage oocytes in primordial follicles of the mouse [10], rat [1], hamster [41], cow [24] and man [9] exhibit a reticulated type nucleolus that predominantly consists of strands of DFCs, small FCs and aggregates of GC. In rabbit primordial follicles studied here, the large, round-shaped sheets of GCs were the predominant structure of reticulated nucleoli. Besides all usual nucleolar components (review in [17]), numerous small structures, containing the clumps of fine filamentous material were embedded in GCs. They seem to arise from the penetration of perinucleolar chromatin into nucleolonemas, as shown in figure 2a,b. To better distinguish these structures from other nucleolar components, we designated them nucleolar lacunas. Similar structures were described as nucleolar microspherules in the nucleoli of supraoptic neurons without any suggestion about their function [21]. After uranyl acetate/lead citrate staining, fibrillar material in nucleolar lacunas resembles the material observed in FCs. However, the lacunas do not touch directly the DFCs, from which they are separated by a large mass of GC and they lack other typical features of FC such as the positivity to silver staining. The disappearance of nucleolar lacunas before the fall of rRNA synthetic activity in oocytes isolated from antral follicles could be considered as one of the first steps in the process of nucleolar component segregation. The question remains to be answered if the lacunas contain rDNA.

The presented autoradiographic data on rabbit oocytes are in agreement with previous findings that rRNA synthesis gradually increases after beginning of the growth period in mammalian oocytes and diminishes concomitantly with achievement of their full size [12, 13]. The amount of DFC protrusions around FCs in rabbit oocyte nucleoli, visualised by Ag-NOR staining increased in direct relation to rRNA synthesis. The same phenomenon was described in stimulated somatic cells [31, 40]. Similarly, the tendency of rabbit oocytes to rise the number and diminish the diameter of FCs concomitantly with the increase of rRNA synthesis is well known from the experiments with stimulated human lymphocytes [15]. Such results are in contrast with the recent suggestion that there is no direct relationship between silver staining and rRNA synthesis [6]. Perhaps, the quantity of Ag-NOR proteins is enlarged after the increase of rRNA synthesis, but a certain amount of these proteins is still present in inactive nucleoli.

We demonstrated the penetration of NAC into peripherally localized nucleolar vacuoles. Presence of this material, well stained after E-PTA staining, both in small and large nucleolar vacuoles, could imply that the non-transcribed rDNA is situated in nucleolar vacuoles of rabbit growing oocytes. After the disappearence of NVs, the compact nucleoli were still linked with condensed chromatin. Similarly, the connection of chromatin bivalents with the nucleolus was confirmed both by electron microscopy [34] and Ag-NOR staining of chromosome preparations [33].

Nucleolar compaction, accompanied by gradual cessation of rRNA synthesis [11, 39] could play a key role in achievement of full meiotic competence of mammalian oocytes [26]. This process seems to be a general feature

Figs 5, 6. 5. Nucleolus of an oocyte obtained from small antral follicle. Uranyl acetate/lead citrate staining. **a.** The fibrillar centers (F) are surrounded by the clumps of a dense fibrillar component. The peripherally located fibrillar center is connected with clusters of nucleolus associated chromatin (arrow). Several small vacuoles are filled with similar material. Some vacuoles increased profoundly in size; × 12000. **b.** Considerable clusters of nucleolus associated chromatin are characteristic for those oocytes. The penetration of nucleolus associated chromatin into the nucleolar vacuoles is arrowed; × 16000. **6.** Nucleolus of an oocyte from small antral follicle. **a.** Ag-NOR staining shows strongly positive fibrillar centers. Numerous protrusions of silver deposits penetrate from fibrillar centers into nucleolonema; × 20000. **b.** E-PTA staining emphasises the peripheral rim of nucleolus associated chromatin and the dense fibrillar components. E-PTA positive granules are visible inside the nucleolar vacuoles (arrowed); × 10000.

51

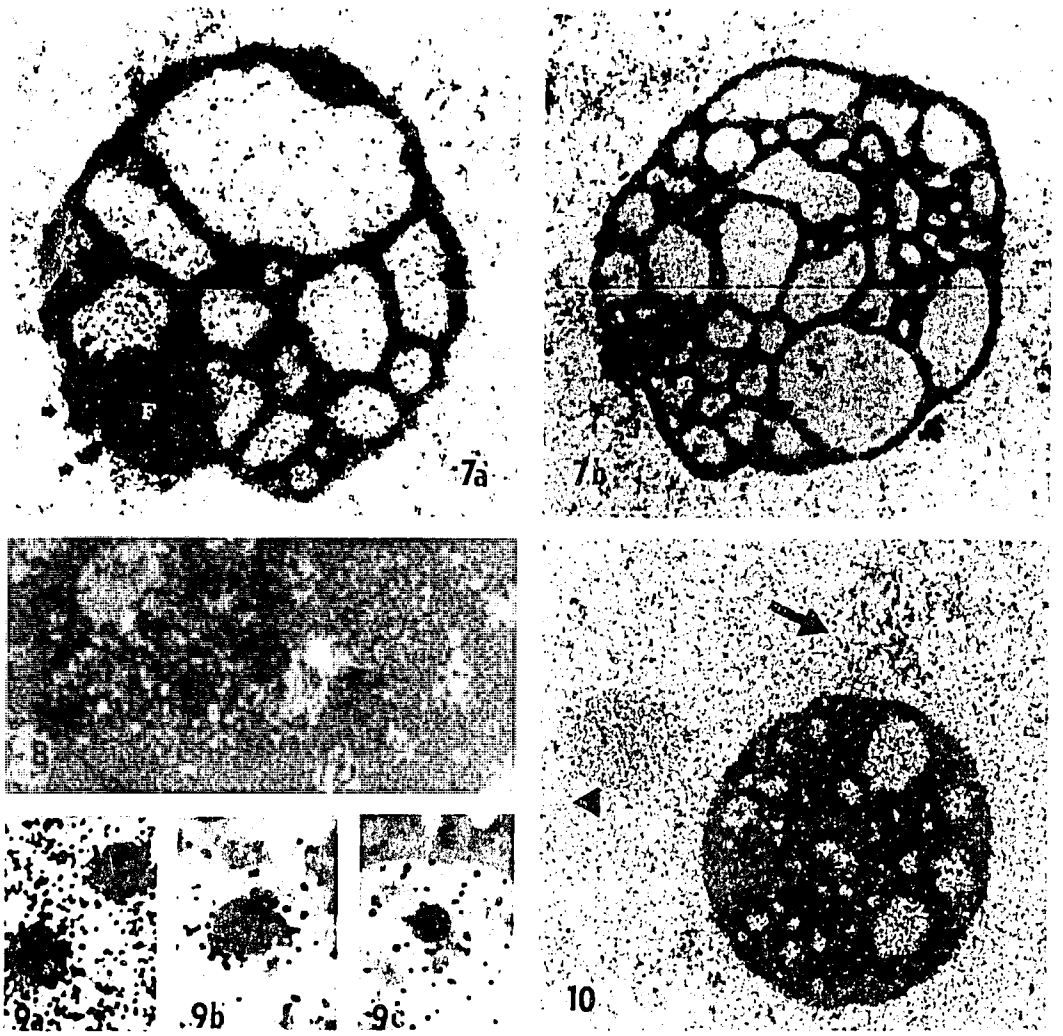

Figs 7–10. 7. Uranyl acetate/lead citrate staining of the nucleolus in an oocyte isolated from a middle-sized antral follicle. a. Extended nucleolar vacuoles give a lattice-like shape to the nucleolus predominantly formed by granular components. The clusters of nucleolus associated chromatin (arrows) are attached to large fibrillar center (F), moved to the nucleolar periphery; × 15000. b. After E-PTA staining, the rim of nucleolus associated chromatin is more conspicuous in comparison with previous stage. Dense fibrillar components are well stained too; × 10000. 8. Ag-NOR staining of an oocyte from middle-sized antral oocyte. The sensitivity of fibrillar centers to silver decreases and the protrusions of silver positive material disappear; × 30000. 9. ^{3}H uridine autoradiography. a. Autoradiogram of an oocyte from small antral follicle. The intensive labelling is visible both over the nucleoplasm and the nucleoli; × 650. b. Germinal vesicle of an oocyte isolated from a middle sized antral follicle. The incorporation of ^{3}H uridine is concentrated in two caps at the nucleolar periphery. The nucleoplasm is labelled less intensively; × 500. c. The compact nucleolus of an oocyte obtained from large antral follicle is weakly labelled only. The labelling of nucleoplasm is at the level of background; × 400. 10. In an oocyte from large antral follicle, the nucleolus undergoes compaction. The nucleolar vacuoles are shrinked, condensed chromatin (arrow) and expulsed granular components (arrowhead) are visible in the nucleoplasm. An ultrathin section was stained by uranyl acetate and lead citrate; × 12000.

of mammalian oogenesis but it does not occur at the same follicular stage in individual species. While nucleoli of mouse oocytes are exclusively compact before antrum formation [10], the rat [1] and hamster [36] oocyte nucleoli become a compact homogenous mass at the antral follicle stage. Nucleoli of the pig and cattle oocytes are compact also in small antral follicles when the full size is achieved [25]. We found the compact nucleoli in oocytes isolated from large antral follicles, similarly to human oocytes [38].

The process of nucleolar compaction was described in the oocytes of viviparous teleost [5], in mollusc *Helcion pellucidus* [4] and in cow oocytes [12] as enlargement of the central nucleolar vacuole with subsequent segregation of nucleolar components. In mice [10], rat [1] and pig [13], a new nucleolar structure, the compact, homogenous mass

52

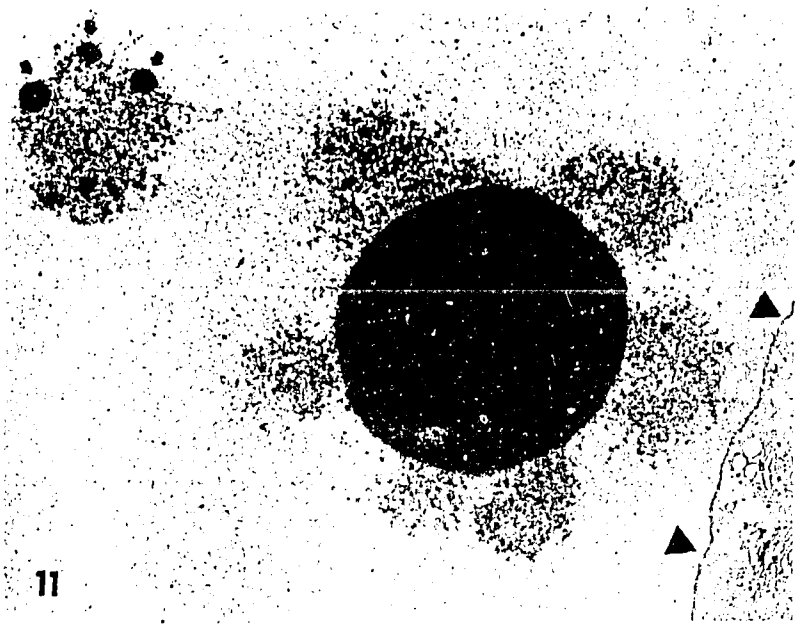

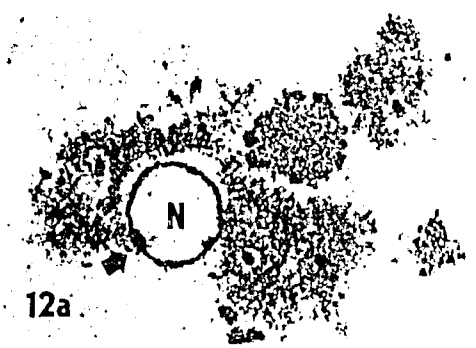

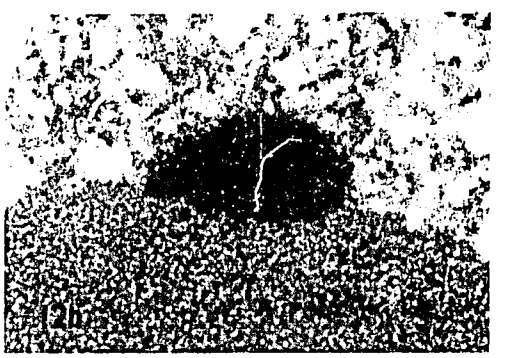

Figs 11, 12. 11. The compact nucleolus of an preovulatory oocyte consists of a homogenous fibrillar mass. The condensed bivalents are either linked with compact nucleolus or located separately in the nucleoplasm (C). Small dense beads are arrowed. The nuclear enveloppe (arrowhead) is still intact. Section stained by uranyl acetate/lead citrate; × 6000. **12.** The nucleolus of large antral stage oocyte. **a.** After E-PTA treatment, the homogenous nucleolar mass (N) is bleached, the nucleolar periphery together with highly condensed bivalents is well stained. Note the strongly stained lenticle at the nucleolar periphery (arrow); × 5000. **b.** Ag-NOR staining revealed that such lenticles, attached to the exclusivelly compact nucleolus, are strongly positive to silver; × 60000.

of fine fibrills, gradually growing from the center of nucleolus, is involved in process of nucleolar compaction. In rabbit oocytes, the compaction was realized by shrinking and gradual disappearence of nucleolar vacuoles.

The compact nucleoli are formed by a fibrillar mass rich in basic E-PTA positive proteins, believed to be the remnants of DFCs [13, 35, 36]. In some works, the presence of acidic phosphoproteins, which are not silver-stainable, was detected in compact nucleoli [2]. In our results, the E-PTA staining was strongly positive at NAC, but only the peripheral part of compact nucleoli was stained. However, the presence of basic proteins cannot be excluded because of insufficient penetration of E-PTA into the compact nucleolar mass, shown previously [36].

The germinal vesicles of fully grown mammalian oocytes possess compact nucleoli surrounded by highly condensed NAC [8]. However, no condensed chromatin is visible in nucleoplasm before the endogenous LH peak, exogenous hCG stimulation or at the beginning of *in vitro* culture [19]. In this study, the first signs of chromatin condensation were found in the nucleoplasm of growing rabbit oocytes isolated from small antral follicles. In middle-sized antral follicles, the progressive condensation of NAC as well as chromatin in nucleoplasm was noticed. The highly condensed bivalents together with an intact nuclear envelope characterized rabbit oocytes in pre-ovulatory follicles. Interestingly, a similar morphology of the GV was seen in pig and cattle oocytes cultured in protein synthesis inhibitors [20, 28] and in the mouse oocytes subsequently treated with 6-dimethylaminopurine and cycloheximide [29].

Altogether, these results confirm the conclusion of Newport and Spann [30] that nuclear envelope breakdown and

chromosome condensation are separable and independent processes. Further biochemical studies are required to clarify preconditions for initiation of chromatin condensation in growing rabbit oocytes.

Acknowledgments

We are very grateful to Prof Karel Smetana and Dr Josef Fulka for the valuable discussion. We thank also Mr Vaclav Pech for excellent technical assistence and Miss Lucie Melicharova for the preparation of manuscript. This work was partially supported by AID grant number 12.061E.

References

1 Antoine N, Lepoint A, Baeckeland E, Goessens G (1987) Evolution of the rat oocyte nucleolus during follicular growth. *Biol Cell* 59, 107–112
2 Antoine N, Lepoint A, Baeckeland E, Goessens G (1988) Ultrastructural cytochemistry of the nucleolus in rat oocytes at the end of the folliculogenesis. *Histochemistry* 89, 221–226
3 Antoine N, Thiry M, Goessens G (1989) Ultrastructural and cytochemical studies on extranucleolar bodies in rat oocytes at the preovulatory follicle stage. *Biol Cell* 65, 61–66
4 Azvedo C, Castilho F, Coimbra A (1984) Fine structure and cytochemistry of the oocyte nucleolus in the mollusc *Helcion pellucidus* (Prosobranchia). *J Ultrastruct Res* 89, 1–11
5 Azvedo C, Coimbra A (1980) Evolution of nucleoli in course of oogenesis in viviparous teleost *(Xiphophorus helleri). Biol Cell* 38, 43–48
6 Biggiogera M, Kaufmann SH, Shaper JH, Gas N, Almaric F, Fakan S (1991) Distribution of nucleolar proteins B23 and nucleolin during mouse spermatogenesis. *Chromosoma* 100, 162–172
7 Buccione R, Ceccioni S, Tatone C, Mangia F, Colona R (1987) Follicle cell regulation of mammalian oocyte growth. *J Exp Zool* 242, 351–355
8 Calarco PG, Donahue RP, Szollosi D (1971) Germinal vesicle breakdown in the mouse oocyte. *J Cell Sci* 10, 1–17
9 Cataldo C, Souchier C, Vasserot M, Calisti A, Vagner-Capodano AM, Stahl A (1985) Three-dimensional analysis of fibrillar centers and associated chromatin in the nucleolus of human oocytes in primordial follicles. *Biol Cell* 54, 191–195
10 Chouinard LA (1971) A light and electron microscope study of the nucleolus during growth of the oocyte in the prepubertal mouse. *Biol Cell* 41, 35–42
11 Crozet N (1983) Effects of actinomycin D and cycloheximide on the nucleolar ultrastructure of porcine oocytes. *Biol Cell* 48, 25–30
12 Crozet N, Kanka J, Motlik J, Fulka J (1986) Nucleolar fine structure and RNA synthesis in bovine oocytes from antral follicles. *Gamete Res* 14, 65–73
13 Crozet N, Motlik J, Szollosi D (1981) Nucleolar fine structure and RNA synthesis in porcine oocytes during the early stages of antrum formation. *Biol Cell* 41, 35–42
14 Greenwald GS, Terranova PF (1988) Follicular selection and its control. *In: The Physiology of Reproduction. Vol 1* (Knobil E, Neil JD, eds) Raven Press Ltd, New York, 387–445
15 Hozak P, Novak JT, Smetana K (1989) Three-dimensional reconstructions of nucleolus-organizing regions in PHA-stimulated human lymphocytes. *Biol Cell* 66, 225–229
16 Jahn CL, Baran MM, Bachvarova R (1976) Stability of RNA synthesized by the mouse oocyte during its major growth phase. *J Exp Zool* 197, 161–172
17 Jordan GE (1991) Interpreting nucleolar structure: where are the transcribing genes? *J Cell Sci* 98, 437–442
18 Kanlan G, Abreuand SL, Bachvarova R (1982) rRNA accumulation and protein synthetic patterns in growing mouse oocytes. *J Exp Zool* 220, 361–370
19 Kruip TAM, Cran PG, van Beneden TH, Dielemann SJ (1983) Structural changes in bovine oocytes during final maturation *in vivo. Gamete Res* 8, 29–47
20 Kubelka M, Motlik J, Fulka J Jr, Prochazka R, Rimkevicova Z, Fulka J (1988) Time sequence of germinal vesicle breakdown in pig oocytes after cycloheximide and p-aminobenzidine block. *Gamete Res* 19, 423–431
21 Lafarga M, Andres MA, Berciano MT, Maquiera E (1991) Organization of nucleoli and nuclear bodies in osmotically stimulated supraoptic neurons of the rat. *J Comp Neurol* 308, 329–339
22 Likovsky Z, Smetana K (1981) Further studies on the cytochemistry of the standardized silver staining of interphase nucleoli in smear preparatios of Yoshida ascitic sarcoma cells in rats. *Histochemistry* 72, 301–313
23 Lintner-Moore S, Moore GPM (1979) The initiation of oocyte growth in the mouse ovary. *Ann Biol Anim Biochem Biophys* 19, 1399–1407
24 Mhawi AJ, Kanka J, Motlik J (1991) Follicle and oocyte growth in early postnatal calves: cytochemical, autoradiographic and electron microscopic studies. *Reprod Nutr Develop* 31, 115–126
25 Motlik J, Fulka J (1986) Factors affecting meiotic competence in pig oocytes. *Thieriogenology* 25, 87–96
26 Motlik J, Fulka J Jr, Prochazka R, Rimkevicova Z, Kubelka M, Fulka J (1989) RNA and protein synthesis requirements for the resumption of meiosis in rabbit oocytes: the role of cumulus cells. *Reprod Nutr Develop* 29, 601–609
27 Motlik J, Kopecny V, Travnik P, Pivko J (1984) RNA synthesis in pig follicular oocytes. Autoradiographic and cytochemical study. *Biol Cell* 50, 229–236
28 Motlik J, Lie B, Shioya Y (1990) Two sensibility levels of cattle oocytes to puromycin. *Biol Reprod* 43, 994–998
29 Motlik J, Rimkevicova Z (1990) Combined effect of protein phosphorylation and protein synthesis inhibitors on maturation of mouse oocytes *in vitro. Mol Reprod Dev* 27, 230–234
30 Newport J, Spann T (1987) Disassembly of nucleus in mitotic extracts: Membrane vesicularization, lamin disassembly and chromosome condensation are independent processes. *Cell* 48, 219–230
31 Pession A, Farabegoli F, Trere D, Novello F, Montanaro L, Sperti S, Rambelli F, Derenzini M (1991) The Ag-NOR proteins and transcription and duplication of ribosomal genes in mammalian cell nucleoli. *Chromosoma* 100, 242–250
32 Rodman TC, Bachvarova R (1976) RNA synthesis in preovulatory mouse oocytes. *J Cell Biol* 70, 251–257
33 Schwarzacher T, Mayr B, Schweizer D (1984) Heterochromatin and nucleolus-organizer-region behaviour at male pachytene of *Suscrofa domestica. Chromosoma* 91, 12–19
34 Stahl A, Mirre C, Hartung M, Knibiehler B (1980) Localisation, structure et activité des gènes ribosomiques dans le nucléole de l'ovocyte en prophase de meiose. *Reprod Nutr Develop* 20, 469–483
35 Takeuchi IK (1986) Etanol-phospotungstic acid staining of basic proteins in the nucleolar condensation occurring in growing mouse oocytes. *J Electron Microsc* 35, 173–184
36 Takeuchi IK, Sonta S, Takeuchi YK (1984) Association of perichromatin granules with nuclear pores of growing Chinese hamster oocytes. *J Electron Microsc* 33, 388–394
37 Takeuchi IK, Takeuchi YK (1986) Ultrastructural localization of Ag-NOR proteins in fully grown oocytes and preimplantation embryos of mice. *J Electron Microsc* 35, 280–287
38 Tesarik J, Travnik P, Kopecny V, Kristek F (1983) Nucleolar transformations in the human oocyte after completion of growth. *Gamete Res* 8, 267–277
39 Wasserman WJ, Letourneau GE (1976) RNA synthesis in fully-grown mouse oocytes. *Nature* 261, 73–74
40 Zacepina O, Novak J, Smetana K, Schwarzacher HG, Wachtler F (1984) Studies on nucleolar silver stained proteins in nucleoli of human normal, stimulated and leucemist lymphocytes. *Mikroskopie* 41, 278–284
41 Zybina EU, Grischenko TA, Semionov VM (1984) Ultrastructure of the fibrillar center in oocyte nuclei at diplotene stage in golden hamster. *Tsitologia* 26, 1246–1249

54

MOLECULAR REPRODUCTION AND DEVELOPMENT 38:91–93 (1994)

Rapid, Nonradioactive, and Quantitative Method to Analyze Zona Pellucida Modifications in Single Mouse Eggs

JIRI MOOS,[1,2] PETR KALAB,[1] GREGORY S. KOPF,[1] AND RICHARD M. SCHULTZ[2]
Division of Reproductive Biology, Departments of [1]Obstetrics and Gynecology, and [2]Biology, University of Pennsylvania Philadelphia

ABSTRACT A rapid, nonradioactive method to monitor the ZP2 to $ZP2_f$ conversion in the zona pellucida of single mouse eggs has been developed. This assay is based on the chemiluminescent detection of biotinylated ZP2 and $ZP2_f$ following electrophoresis under reducing conditions and electrophoretic transfer to Immobilon P. This method is about 10 times faster and detects similar extents of ZP2 to $ZP2_f$ conversion following A23187-induced egg activation, when compared to the commonly used radioiodination procedures. © 1994 Wiley-Liss, Inc.

Key Words: Zona pellucida, Egg activation, Mouse

INTRODUCTION

The zona pellucida (ZP) of mouse eggs is composed of three glycoproteins, ZP1, ZP2, and ZP3 (Wassarman, 1990). ZP3 binds acrosome-intact sperm and subsequently induces the acrosome reaction of those bound sperm. Acrosome-reacted sperm then interact with ZP2. Following fertilization-induced cortical granule exocytosis, the contents of the granules modify ZP2 and ZP3, such that they lose these aforementioned biological activities. These modifications of the ZP constitute a block to polyspermy.

The modification of ZP3, which results in a form called $ZP3_f$, does not result in any apparent change in its electrophoretic mobility. In contrast, the modification of ZP2 to $ZP2_f$, which is due to a specific proteolytic cleavage, results in a change in electrophoretic mobility from $M_r = 120{,}000$ (ZP2) to $M_r = 90{,}000$ ($ZP2_f$) under reducing conditions (Bleil et al., 1981). The electrophoretic mobility shift associated with the ZP2 to $ZP2_f$ conversion can, therefore, serve as a quantitative index of early events of egg activation, since a positive correlation exists between the extent of cortical granule exocytosis and the conversion of ZP2 to $ZP2_f$ (Ducibella et al., 1993).

At present, the ZP2 to $ZP2_f$ conversion is quantified by a method that is based on radioiodination of the intact ZP (Bleil et al., 1981) and this method can be used on the ZP from single eggs (Kurasawa et al., 1989). Briefly, isolated ZP are radioiodinated using chloramine T and subjected to electrophoresis under nonreducing conditions (Schroeder et al., 1990). Under these conditions, ZP2 and $ZP2_f$ have similar electrophoretic mobilities, which differ from those of ZP1 and ZP3. The position of the $[^{125}I]ZP2/ZP2_f$ is located by autoradiography of the nondried gel, and when individual ZP are analyzed, this exposure takes 3–7 d. The portion of the gel corresponding to $[^{125}I]ZP2/ZP2_f$ is then excised and subjected to gel electrophoresis under reducing conditions. (Under reducing conditions, a disulfide bond that stabilizes the proteolytic cleavage product is reduced and results in the release of that product and the formation of $ZP2_f$.) The positions of ZP2 and $ZP2_f$ are again located following autoradiography of a dried gel, the bands excised from the gel, and subjected to gamma counting to quantify the extent of the ZP2 to $ZP2_f$ conversion. When individual ZP are analyzed, this exposure takes 3–5 d.

Although this method provides accurate and quantitative data, it has two main drawbacks. First, when analyzing individual ZP, the time that it takes to complete this analysis is about 10–14 d. Second, the use of $[^{125}I]NaI$ has associated health and disposal concerns. We report here a nonradioactive method to analyze quantitatively the ZP2 to $ZP2_f$ conversion of individual ZP. This method, which is based on enhanced chemiluminescent (ECL) detection of biotinylated ZP, yields data that are comparable to that obtained by radioiodination and can be performed in 1 d.

MATERIALS AND METHODS

Collection and Ionophore Treatment of Mouse Eggs

Ovulated metaphase II–arrested eggs were isolated from superovulated 6 week old CF-1 female mice as previously described (Kurasawa et al., 1989); cumulus cells were dispersed by hyaluronidase treatment. The eggs were washed in minimal essential medium containing 25 mM HEPES, pH 7.4, and 3 mg/ml polyvinylpyrrolidone (MEM/PVP) and then incubated in

Received July 29, 1993; accepted October 6, 1993.
Address reprint requests to Richard Schultz, Department of Biology, University of Pennsylvania, Philadelphia, PA 19104-6018.
P. Kalab's present address is The Institute of Animal Physiology and Genetics, Department of Genetics, 27721 Libechov, Czech Republic.
J. Moos is on leave from Institute of Molecular Genetics, Department 227, 14220, Videnska 1083, Prague, Czech Republic.

© 1994 WILEY-LISS, INC.

MEM/PVP in the presence or absence of 5 μM calcium ionophore A23187 (Calbiochem). Eggs were removed at various periods of time and intact ZPs were isolated as described below.

ZP Isolation, Radioiodination, and Biotinylation

Intact single ZP were isolated, washed, and radioiodinated as previously described (Kurasawa et al., 1989). Single ZP were biotinylated using the water soluble sulfosuccinimidyl-6 (biotinamido) hexanoate (NHS-LC-Biotin, Pierce, Il). NHS-LC-Biotin was dissolved in 0.1 M $NaHCO_3$, pH 8.3, to a concentration of 1 μM and three volumes of this solution were mixed with one volume of a buffer containing 20 mM HEPES, pH 7.4, 150 mM NaCl, 3 mg/ml PVP, and the isolated ZPs. The samples were incubated for 60 min at 20°C, washed five times with MEM/PVP, and individually analyzed by SDS-PAGE and Western blotting (see below).

Electrophoresis/Western Blotting, Autoradiography, and Chemiluminescent Detection

Two-dimensional reduction electrophoresis of radioiodinated ZP, autoradiography, and quantification of the ZP2 to $ZP2_f$ conversion were performed as previously described (Schroeder et al., 1990).

Biotinylated ZP were subjected to SDS-PAGE on a 9% gel under reducing conditions (Laemmli, 1970). ZP glycoproteins were transferred electrophoretically onto an Immobilon P membrane (Millipore) (Towbin et al., 1979) for 90 min at 50 volts. (Although we have limited experience using nitrocellulose, it is suitable under the described conditions for transfer.) Following electrophoretic transfer, the membranes were blocked by an overnight incubation with teleostean skin gelatin (30 ml/l) (Sigma, G-7765) in a buffer containing 150 mM NaCl, 0.05% Tween-20, and 20 mM Tris-HCl, pH 7.4 (TBS-Tween-gelatin). The membrane was then incubated for 45 min at 20°C with avidin-biotinylated peroxidase complex (Vectastain ABC kit, Vector Laboratories, Inc., CA) in TBS-Tween-gelatin according to the manufacturer's instructions. The membranes were first briefly washed three times with TBS-Tween, followed by three additional washes over a 2 hr period at room temperature. The bound peroxidase was then detected using an Amersham ECL detection kit according to the manufacturer's instructions and Kodak XAR X-ray film. The exposure times were typically 20 sec to 3 min. The extent of the conversion of biotinylated ZP2 to $ZP2_f$ was quantified using an Image I/AT image processor (Interactive Video Systems, Inc.; Concord, MA).

RESULTS AND DISCUSSION

The major component of the mouse ZP detected by ECL following biotinylation according to the methods described above was ZP2 (Fig. 1, lane 1); ZP1 and ZP3 were either not detected or were barely discernible. In addition, the presence of ZP2 as the major biotinylated product was also observed following electrophoresis under non-reducing conditions (data not shown). These

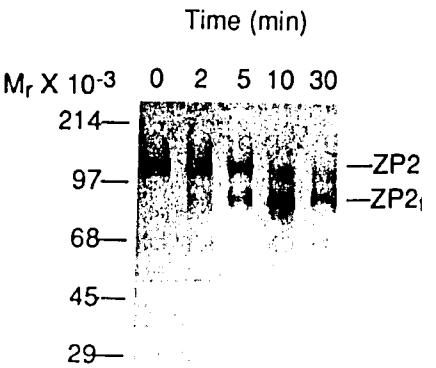

Fig. 1. Time course of the ZP2 to $ZP2_f$ convers.on detected following A23187 treatment. Metaphas[illegible] [illegible]rrested eggs were with A23187 and the ZP2 to $ZP2_f$ conversion analyzed by biotin and ECL as described under Materials and Methods. Each lan sents the profile from a single isolated ZP. The exposure tim X-ray film was 20 sec.

patterns contrast those observed following e phoretic analysis of radioiodinated ZP where all ZP glycoproteins are observed. The failure to ol biotinylated ZP3 facilitates the analysis of the Z $ZP2_f$ conversion, when compared to analysis usi dioiodinated ZP, since only electrophoresis und ducing conditions is required. The reason for this $ZP2_f$ co-migrates with ZP3 (M_r = 83,000) under ing conditions and this necessitates electroph first under nonreducing conditions to resolve ZP from ZP3.

At this juncture two qualifications must be er sized. First, we do not know if other PVDF memb will substitute for immobilon P. Second, it mu stressed that if this method is used for ZP analy other species, the electrophoretic profile of the bi lated ZP must first be established under nonred conditions to insure that the mobility of a ZP component is not similar to that of a ZP3-like co nent. If two-dimensional reduction gel electroph is required, a brief capillary transfer (15–30 min) ZP proteins from the gel to the Immobilon P is cient to detect analytically the position of the resp bands in the nonreducing gel by ECL (data not sh the appropriate band may then be excised from th and run under reducing conditions.

When mouse eggs were treated with the calciu ophore A23187 to induce cortical granule exoc and the associated ZP modifications that normal company fertilization, a time-dependent increase conversion of ZP2 to $ZP2_f$ was observed (Figs. 1 a The time course and extent of the ZP2 to $ZP2_f$ co sion were similar to that observed when a parall periment was performed and the ZP2 to $ZP2_f$ co sion monitored by the radioiodination protocol (F

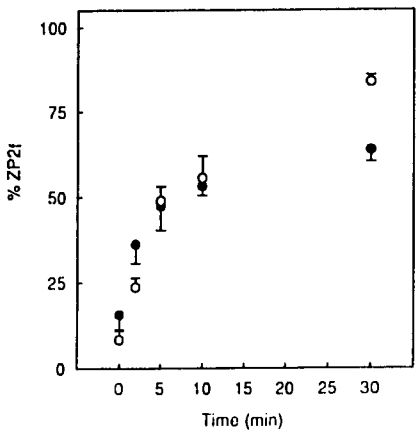

Fig. 2. Comparison of the extent of the ZP2 to $ZP2_f$ conversion by either radioiodination or biotinylation following A23187 treatment. ○, biotinylation; ●, radioiodination. Each point represents the mean ± SEM (*n* ranges from 3–7 individually assayed ZP at each time point).

Linear regression analysis of the ZP2 conversion at each time point comparing both methods yielded an $r^2 = 0.92$, which indicates that the results obtained from both methods are highly correlated with each other. This method has also been used to monitor the extent of the ZP2 to $ZP2_f$ conversion following fertilization in vitro and has yielded results similar to that obtained with the radioiodination protocol (data not shown).

In summary, we report here a simple, rapid (about 10 times faster than the radioiodination procedure with no loss in sensitivity), safe, and cost-effective method to analyze quantitatively changes in the ZP composition of single mouse eggs. This method is also likely to be applicable to the analysis of ZP and ZP conversions in other species.

ACKNOWLEDGMENTS

This research was supported by a grant from the NIH (HD 28514 to R.M.S. and G.S.K.), part of the National Cooperative Program on Non-Human In Vitro Fertilization and Preimplantation Development. J.M. is supported by a grant from the Agency for International Development (12.061E).

REFERENCES

Bleil JD, CF Beall, PM Wassarman (1981): Mammalian sperm–egg interaction: Fertilization of mouse eggs triggers modification of the major zona glycoprotein, ZP2. Dev Biol 86:189–197.

Ducibella T, Kurasawa S, Duffy P, Kopf GS, Schultz RM (1993): Regulation of the polyspermy block in the mouse egg: Maturation-dependent differences in cortical granule exocytosis and zona pellucida modifications induced by inositol 1,4,5-trisphosphate and an activator of protein kianse C. Biol Reprod 48:1251–1257.

Kurasawa S, Schultz RM, Kopf GS (1989). Egg-induced modifications of the zona pellucida of the mouse egg: Effects of microinjected inositol 1,4,5-trisphosphate. Dev Biol 133:295–304.

Laemmli UK (1970): Cleavage of structural proteins during the assembly of the head of bacteriophage T4. Nature 227:680–685.

Schroeder AC, Schultz RM, Kopf GS, Taylor FR, Becker R, Eppig JJ (1990): Fetuin inhibits zona pellucida hardening and conversion of ZP2 to $ZP2_f$ during spontaneous mouse oocyte maturation in vitro in the absence of serum. Biol Reprod 43:891–897.

Towbin H, Staehelin T, Gordon J (1979): Electrophoretic transfer of proteins from polyacrylamide gels to nitrocellulose sheets: Procedure and some applications. Proc Natl Acad Sci USA 76:4350–4354.

Wasserman PM (1990): Profile of a mammalian sperm receptor. Development 108:1–17.

51

THE EFFECT OF MEMBRANA GRANULOSA CELLS ON HISTONE H1 AND MAP KINASE ACTIVITY IN MAMMALIAN OOCYTES.

Peter SUTOVSKY[1,#] Jaroslav KALOUS[1], Petr KALAB[1], Michal KUBELKA[1], Jiri MOOS[2], Richard M. SCHULTZ[3], and Jan MOTLIK[1].

[1]*Institute of Physiology and Genetics of Animals, 277 21 LIBECHOV, Czech Republic.*

[2]*Institute of Molecular Genetics, Prague, Czech Republic*

[3]*University of Pensylvania, Philadelphia, USA*

#Present and correspondence address: Department of Zoology, University of Wisconsin, 1117 West Johnson Street, Madison, WI 53706, USA

Phone: (608) 262 2048

Fax: (608) 262 7319

E-mail: PSUTY@MACC.WISC.EDU

Submitted : Developmental Biology

58

ABSTRACT

Cattle cumulus-enclosed oocytes (OCCs), initially cultured up to diakinesis or metaphase I stage, possessing high H1 kinase and MAP kinase activities, were subsequently cocultured with pig membrana granulosa (PMG) cells for 6 h. In the diakinesis stage oocytes, PMG cells caused aggregation of chromosome bivalents into one or several chromatin clumps and the process of nuclear envelope disassembly was interrupted. In OCCs initially cultured up to metaphase I, PMG cells also induced clumping of bivalents and, moreover, destruction of microtubules of meiotic spindle was observed. In both diakinesis and metaphase I oocytes, chromatin clumping was accompanied by a dramatic decrease of H1 and MAP kinase activities within 6 hours of coculture. After release from coculture, the diakinesis oocytes continued in meiosis progression with a concomitant increase of histone H1 and MAP kinase activities up to the level characteristic to MI oocytes. This complete reversibility of granulosa cell derived block was never observed in the cocultured metaphase I oocytes. These results suggest that granulosa cells possess a meiosis inhibiting activity incompatible with high H1 and MAP kinase activity in maturing oocytes. These studies indicate that also under in vitro conditions, PMG cells control progression of meiosis by modulating the protein kinase activity.

59

INTRODUCTION

Mammalian oocytes released from their intrafollicular environment resume meiosis in a time sequence that is species specific (Motlik, 1989) and depends on activation of cytoplasmic maturation promoting factor (MPF) (see Motlik and Kubelka, 1990). In the cytoplasm of fully grown oocytes, both MPF components, protein $p34^{cdc2}$ and cyclin B are present and assembled into inactive MPF (Lohka et al., 1988). Activation of $p34^{cdc2}$ kinase requires dephosphorylation of $p34^{cdc2}$ on Tyr-15 and Thr-14 (Solomon et al., 1992). These dephosphorylations are catalyzed by cdc25, a protein phosphatase containing both tyrosine and serine/threonine phosphatase activity (Gautier et al., 1992).

The active MPF phosphorylates several substrates including nuclear lamins (Dessev et al., 1991), histone H1 (Langan et al., 1989), tubulins of meiotic spindle (Verde et al., 1990) and proteins associated with microtubule organizing centers (MTOCs) (Buendia et al., 1992; Centonze and Borisy, 1990; Verde et al., 1990). Phosphorylation catalyzed by MPF initially leads to germinal vesicle breakdown (GVBD), a complex event including condensation and individualization of chromosomal bivalents, disassembly of nuclear envelope and formation of meiotic spindle (Calarco et al., 1972).

The mitogen-activated protein (MAP) kinase is stimulated during meiotic maturation of clam (Shibuya et al., 1992), Xenopus (Ferrel et al., 1991; Gotoh et al., 1991b; Posada and Cooper 1992) and mouse oocytes (Verlhac et al., 1993). MAP kinase activation in Xenopus oocytes starts at the time of GVBD and it coincides with the rise of H1 kinase activity

60

(Gotoh et al., 1991a; Posada et al., 1991). For in vitro matured mouse oocytes, the rise of MAP kinase occurs about 2 h after H1 kinase activation (Verlhac et al., 1994).

We recently demonstrated that the isolated PMG cells maintain their intrafollicular function to inhibit resumption of meiosis in cocultured pig (Motlik et al., 1991) cattle (Kalous et al., 1993) and mouse oocytes (Nagyova et al., 1993). The present study describes morphological and biochemical alterations that occur in bovine oocytes initially cultured up to diakinesis or metaphase I stage, and subsequently exposed to the inhibitory effect of PMG cells. In both cases, this coculture caused the block of meiosis, and was paralleled by a fall of H1 and MAP kinase activity, clumping of chromosomal bivalents, interruption of nuclear envelope disassembly (diakinesis oocytes) and disappearance of meiotic spindle (M I oocytes). Whereas diakinesis stage oocytes were able to complete the first meiotic division when released from coculture, no reversibility was observed in metaphase I oocytes. These observations suggest that the meiosis inhibiting activity of PMG cells modulates the protein kinase activity in oocyte cytoplasm.

MATERIALS AND METHODS

Isolation of Pig Membrana Granulosa Cells and Bovine Oocytes

Pig and cattle ovaries were collected at a local slaughterhouse and transported to the laboratory in phosphate-buffered saline (PBS, pH 7.4, 25°C). Bovine oocytes aspirated from small antral follicles (3-5 mm in diameter) were washed in PBS and selected under stereomicroscope. Only those oocytes surrounded with multiple layered compact cumulus were used for further experiments.

Membrana granulosa cells were isolated from the ovaries of slaughtered prepubertal gilts (hybrid line). Large antral follicles with transparent, vascularized follicular walls were dissected and hemisectioned. With the help of two preparation needles, the large pieces of granulosa cell layer were carefully separated from the theca, washed in PBS and transferred into culture medium.

Culture of Bovine Oocytes

Isolated bovine OCCs were washed and initially cultured for 8 h (diakinesis) or 12 h (metaphase I) in modified Parker's medium (M-199, Sevac, Prague), supplemented with 2.92 mM Ca-lactate, 2 mM Na-pyruvate, 33.9 mM Na-bicarbonate, 4.43 mM Hepes buffer pH 7.2, 50 IU/ml penicillin, 50 mg/ml streptomycin sulphate, and 10% heat-treated bovine serum (BOS, Sevac, Prague), under paraffin oil at 38.5°C in 5% CO_2 in air.

62

Coculture of Bovine OCCs with PMG

Since the PMG cells were always isolated with the underlying basement membrane and these pieces tended to roll up with an inside-out orientation, the OCCs were placed on concave surface of this basement membrane. The bovine OCCs, initially cultured up to diakinesis or metaphase I stage, were put in the rolled pieces of PMG and co-cultured for 6 h under the conditions described above. In each rolled piece of PMG cells, 8-10 OCCs were deposited and 3-4 pieces of PMG cells with OCCs were placed in 1 ml of the equilibrated culture medium. The control OCCs were added in every culture dish and cultured outside the PMG. After 6 h of coculture, the OCCs were liberated from the rolled PMG cells and a portion was further cultured in hormone free culture medium in order to assess the reversibility of the meiotic arrest caused by coculture with PMG cells. At the end of culture, the control and co-cultured OCCs were stripped of cumulus cells and processed as described bellow. In total, above 1000 bovine oocytes were evaluated.

MBP and histone H1 kinase double assay

At selected times, groups containing 10 oocytes each were removed from culture and transferred in a minimal volume of buffer to an Eppendorf tube and freezed immediately at -70°C. Before assay, tubes were placed on ice and 4 µl of buffer A (15 mM para-nitrophenyl phosphate, 60 mM beta-glycerophosphate, 15 mM EGTA, 0.1 mM EDTA, 1 mM DTT, 0.25 mM Na_3VO_4, 60 fg/ml leupeptin and 60 fg/ml aprotinin) was

63

added. Tubes were briefly vortexed, centrifuged at 10,000g for 15 sec and then the kinase reaction was initiated by addition of 5 µl of buffer B (25 mM HEPES, pH 7.2, 5 mM para-nitrophenylphosphate, 60 mM beta-glycerophosphate, 25 mM $MgCl_2$, 15 mM EDTA, 0.1 mM EGTA, 20 fM cAMP dependent protein kinase inhibitor (Sigma). 60 µg/ml leupeptin and aprotinin, 600 fM ATP, 2 mg/ml histone H1 (Boehringer) and 3 mg/ml MBP (Sigma) and 500 fCi/ml ^{32}P gamma ATP (Amersham). The reaction was allowed to proceed for 30 min at 30°C and was stopped by the addition of 15 µl of double-concentrated sample buffer. Samples were boiled for 3 minutes and separated on 15% SDS PAGE gel (Laemmli, 1970). Gels were stained with Coomassie Blue R250 (Serva), destained overnight, dried and after autoradiography, the regions containing 32P labelled histone H1 and MBP were cut out and scanned with LKB Ultroscan XL. The relative H1 kinase and MAP kinase activity were plotted against the time of oocyte culture.

Phase contrast and electron microscopy

To evaluate the rate of meiotic maturation, the cumulus free oocytes were mounted on slides, fixed for 24 h in ethanolic acetic acid, stained with orcein, and examined under a phase-contrast microscope. The frequencies of GVBD were pooled from three replicative experiments. The obtained data were evaluated using chi-square analysis.

For transmission electron microscopy, the OCCs were fixed in mixture of 0.6% paraformaldehyde and 2.5% glutaraldehyde, then postfixed in 1% osmium tetroxide, dehydrated by an ascending series of ethanol and

embedded in Epon 812 (Serva, Heidelberg, Germany). The blocks were sectioned in Reichert-Jung Ultracut E, contrasted by uranyl acetate and lead citrate and observed in Jeol 1200 EX electron microscope.

Immunofluorescence

The oocytes, devoid of the cumulus oophorus and zona pellucida, were fixed for 20 min in 2.5% paraformaldehyde in 0.1 M PBS (pH 7.3, room temperature), then incubated for 1 h in the solution of 50 mM ammonium chloride, washed and placed in 0.1 M PBS containing 0.05% sodium azide (NaN_3) and 1 mM PMSF. The immunofluorescence protocol (Sutovsky et al., 1993) included blockage of nonspecific reactions by preincubation in 0.1 M PBS, containing 2% BSA, NaN3 and saponin. The samples were then incubated with anti-α-tubulin TU-01 mouse monoclonal antibody (Viklicky et al. 1982), washed and treated with FITC conjugated anti-mouse IgG and Hoechst 33258 (5 μg/ml). After repeated washing, the samples were mounted on slides in a mixture of Mowiol V 4-88 and n-propyl gallate and observed in Leitz axiophot epifluorescence microscope. Controls were performed by omitting first antibody.

65

RESULTS

Co-culture of late diakinesis oocytes with PMG cells

Bovine oocytes initially cultured for 8 h reached diakinesis stage of the first meiotic division and displayed typical signs of GVBD. The individual chromosomal bivalents were formed (Figs.1A and 1B) and they were surrounded by deeply folded nuclear envelope (NE), which exhibited numerous loops, blebs and quadruplexes (Fig.1A). The co-culture of these oocytes with PMG resulted in aggregation of individual bivalents into one or more clumps of highly condensed chromatin that were surrounded by the remnants of NE (Figs.1C and 1D). Frequently, this compact mass of chromatin contained several bright areas, probably composed of centromere heterochromatin (Fig.1C). The percentage of GVBD in OCCs initially incubated for 8 hr and subsequently co-cultured with PMG for 6 hr was not significantly different from OCCs initially incubated for 8 hr only (81% and 76%, respectively; Table 1A). When diakinesis oocytes were withdrawn from contact with PMG cells, block of meiosis was fully reversible, and the majority of oocytes reached metaphase II during 20 h (Table 1A, Figs.1E and 1F) or 30 h (data not shown) of subsequent culture.

Coculture of metaphase I oocytes with PMG

After 12 h of preincubation, 89% of bovine oocytes underwent GVBD and two thirds of them exhibited typical metaphase I appearance with condensed bivalents in the longitudinally arranged microtubules of the

66

meiotic spindle (Table 1B, Figs.2A,2B and 2C). During the subsequent coculture for 6 h with PMG cells, the incidence of GVBD did not increase (Table 1B) and chromosomal bivalents clumped similarly as observed for diakinesis oocytes (Figs.2D and 2E). Moreover, the coculture caused depolymerization of microtubules and subsequent disappearance of meiotic spindle. Bundles of disordered microtubules were found, however, in association with chromatin clumps (Figs.2F and 2G). Concomitantly, the structures similar to the dense pericentriolar material assembled by parthenogenetically activated rabbit embryos (Szollosi and Ozil, 1991) appeared in the perinuclear region of cocultured oocytes. No centrioles were found inside these structures that were apparently derived from Golgi vesicles (Fig.2H). These results suggest that meiosis in OCCs initially cultured for 12 h was irreversibly blocked during 6 h of co-culture with PMG.

H1 and MAP kinase assay

Both diakinesis and metaphase I oocytes possessed high histone H1 and MAP kinase activity (Figs. 3A and 3B; 4A and 4B). A dramatic fall in H1 and MAP kinase activity occurred within the 6 hours of coculture in all of the experiments performed. There were differences, however, in the kinetics of the decrease of H1 kinase activity as compared to the activity of MAP kinase. The decrease of histone H1kinase activity appeared to be more linear, while that of MAP kinase activity displayed a more abrupt decline within the first 4 h of co-culture, in some experiments the initial dramatic decrease was followed by a moderate increase within this period

67

(see Fig.3B, lane 3 and 4). When diakinesis stage oocytes were released from coculture, the reappearance of H1 and MAP kinase activity was evident within 2 h and their values further rose after 4 h and 6 h of culture (Figs. 3A and 4A) to levels typical for metaphase I oocyte. Such a complete reactivation was accompanied by progression of meiosis (Table 1A). In contrast, only partial restoration of H1 and MAP kinase activity was observed in metaphase oocytes within 6 hours after removal from the coculture with granulosa (Fig. 4B and Fig. 3B, lanes 7 and 8). This moderate increase of H1 and MAP kinase, however, was never accompanied by progression of meiosis (Table 1B), even when the culture periods was extended up to 30 h (data not shown).

DISCUSSION.

In the present study, we have shown the ability of PMG cells to modulate the level of histone H1 kinase and MAP kinase activity in co-cultured bovine oocytes. These oocytes, initially cultured up to diakinesis or metaphase I stage possessed high histone H1 and MAP kinase activity, each of which was dramatically reduced by coculture with PMG cells. Thus, it is likely that the specific dephosphorylation of $p34^{cdc2}$ (Solomon et al., 1990) and phosphorylation of MAP kinase on threonine and tyrosine residues (Anderson et al., 1990; Posada and Cooper, 1992) were abolished by this co-culture. Whereas the activation of MAP kinase in mouse oocytes is evident not earlier than 3 h after GVBD (Verlhac et al., 1994), the present data show high MAP kinase activity in cattle oocytes prior to GVBD. Following co-culture with PMG cells, the decrease of MAP kinase activity was more abrupt in comparison with relatively linear decline of histone H1 kinase activity. During the natural MI to MII transition, histone H1 kinase activity drops (Kubiak et al., 1992; Verlhac et al., 1993) although MAP kinase activity remains high (Verlhac et al., 1993; 1994). Also, the activation of ovulated mouse eggs results in a sharp decrease of histone H1 kinase activity while MAP kinase activity declines very slowly. Similarly, the decrease of MAP kinase activity in activated *Xenopus* oocytes occurs only after MPF inactivation (Posada et al., 1991; Nebreda and Hunt, 1993). Consistent with these results, our results clearly show that the kinases responsible for MBP and histone H1 phosphorylation behave independently and therefore MBP phosphorylation is not due to the activity of $p34^{cdc2}$ kinase.

An initial incubation of mouse oocytes for 45 and 60 min

significantly abolished the inhibitory effect of PMG cells on GVBD (Nagyova et al., 1993) This suggests that the inhibitory activity of PMG, similarly to the effect of IBMX (Eppig et al., 1983), cannot be exerted after irreversible commitment of mouse oocytes to GVBD. In contrast with these observations, both histone H1 and MAP kinase activities reappeared in bovine diakinesis oocytes within 2 h after termination of coculture with PMG cells. Further increase of histone H1 and MBP phosphorylation up to the level characteristic for MI was accompanied by progression in oocyte maturation. This would suggest that the effect of PMG cells on diakinesis oocytes was reversible from both biochemical and morphological aspects.

Only moderate increase of histone H1 and MAP kinase activity occurred in metaphase I oocytes released from co-culture with PMG and this increase was not accompanied by either reformation of meiotic spindle or progression of meiosis. The observation that MAP kinase may regulate microtubule dynamics at metaphase (Gotoh et al., 1991b) could account for the failure of metaphase oocytes to reassemble meiotic spindle after the termination of co-culture since MAP kinase activity is low in these oocytes.

Protein synthesis, rather than protein phosphorylation, seems to be a prerequisite for maintaining metaphase chromosomes in a condensed form (Clarke and Masui, 1983; Hashimoto and Kishimoto, 1988). Indeed, the chromosomes of prometaphase stage murine oocytes decondense in presence of puromycin, a drug affecting both protein synthesis and phosphorylation, whereas the chromosomes remain condensed when exposed to 6-DMAP, an inhibitor of protein phosphorylation (Rime et al.,

70

1989; Szollosi et al., 1991). Our results are consistent with the meiosis inhibiting influence of PMG cells not affecting protein synthesis in co-cultured oocytes. Moreover, the finding of MTOC-like structures in cocultured metaphase oocytes suggests the de novo synthesis of MTOC proteins throughout the co-culture period.

The disruption of interphase-like network of microtubules and the enucleation of microtubules around MTOCs occurs as a consequence of oocyte MPF activation (Maro et al., 1990). Generally, the MTOCs are composed of a pair of centrioles embedded in dense pericentriolar material (PCM), within which the microtubule nucleating activity seems to be located (Gould and Borisy, 1977). Surprisingly, no centrioles are found in the MTOCs at the spindle poles of mammalian oocytes throughout first and second meiotic division (Szollosi et al., 1972) and the centrioles found in blastomeres during first mitotic cycles are thought to be of paternal origin (Le Guen and Crozet, 1989; Schatten et al., 1986). Similarly, the centrioles are absent from the MTOCs found in parthenogenetically activated rabbit oocytes (Szollosi and Ozil, 1991). The MTOC-like structures, described in our study, are morphologically reminiscent to the acentriolar MTOCs found in those parthenogenetically activated embryos and in meiotic spindles of ruminant oocytes (Thibault et al., 1987). Moreover, the association with Golgi vesicles is observed in all these studies and the emergence of MTOC-like structures in bovine oocytes (this study) coincides with the depolymerization of spindle microtubules. These observations are consistent with Boveri's theory on paternal centrosome inheritance (Boveri, 1901), suggesting that the centrioles are introduced in the zygote by sperm at the time of

71

fertilization. Despite of the lack of centrioles, bovine oocytes themself seem to have an ability to generate pericentriolar material.

The occurrence of polymerized microtubules associated with clumped chromosomal bivalents in metaphase oocytes is of a particular interest since the spindle microtubules in those oocytes are depolymerized after coculture with PMG. This fact could be explained by the known eff ct of mitotic chromatin on microtubule polymerization (Karsenti et al., 1984). In addition, the ability of histone H1, a protein involved in chromatin condensation, to stabilize microtubules, provides further support for the role of chromatin in the assembly of mitotic (meiotic) spindle (Multinger et al., 1992).

Taken together, the present data imply that PMG cells regulate the activity of oocyte protein kinases (histone H1 kinase and MAP kinase) and thus influence the resumption and progression of meiotic maturation. The ultrastructural observations on behavior of spindle microtubules and MTOCs s provide the opportunity for further characterization of factors involved in organization of meiotic apparatus.

ACKNOWLEDGEMENTS

The authors wish to thank Dr. V. Viklicky for kind gift of TU-01 antibody. The use of light microscopy facilities of Dr. L. Veselsky is gratefully acknowledged. We strongly appreciate the technical assistance of Mr. Vaclav Pech and the printing of figures by Miss Lenka Vysohlidova . The work was supported by grant number 12.061-E from Agency for International Development (Washington; USA) and grant Z-503 from Czech Ministry of Economics.

72

TEXT TO THE FIGURES

Fig. 1. Reversible inhibition of meiotic maturation in bovine oocytes precultured up to late diakinesis and subsequently put in co-culture with PMG cells. **A** control oocyte cultured for 8 hdisplays typical signs of germinal vesicle breakdown, including folded nuclear envelope (arrows) and condensation of chromatin (arrowheads). Bar represents 2 μm. **B** Condensed chromosomal bivalents demonstrated by fluorescent staining with Hoechst 33258. Bar represents 15 μm. **C** Diakinese stage oocytes after the coculture with pig membrana granulosa cells. The quadruplets of nuclear envelope (arrowheads) are assembled around clumped chromosomal bivalents. Bar represents 1 μm. **D** A clump of disordered chromosomes in the diakinesis stage oocyte cocultured with PMG and stained by Hoechst 33258. Bar represents 15 μm. **E, F** Double fluorescence labelling with Hoechst 33258 (E) and anti-α-tubulin (F) antibody shows the metaphase II chromosomes (E) and meiotic spindle (F) in a diakinese stage oocyte, cocultured for 6 h with PMG and subsequently cultured for 30 h in absence of PMG cells. Bar represents 15 μm.

Fig. 2. Coculture of metaphase I stage bovine oocytes with PMG cells irreversibly blocked the progression of meiotic division. **A** Electron micrograph of a control oocyte cultured for 12 h. The microtubules (arrowheads) start to form meiotic spindle around the condensed chromosomal bivalents (Ch). Bar represents 1 μm. **B,C** Double immunofluorescence labelling of a metaphase I oocyte with Hoechst 33258 (B) and anti-α-tubulin antibody (C) shows the formation of

metaphase plate and meiotic spindle. Bars represent 10 μm. **D** A metaphase stage oocyte cultured for 6 h with PMG. The meiotic spindle disappeared and the condensed bivalents are clumped. Bar represents 1 μm. **E,F** Double fluorescence labellingof a metaphase oocyte exposed to the coculture with PMG. The bundle of disordered microtubules, shown by anti-α-tubulin antibody (F) coincides with clumped chromatin, demonstrated by Hoechst 33258 (E). Bars represent 10 μm. G A metaphase I bovine oocyte cocultured for 6 h with PMG. Whereas the meiotic spindle was destructed, large individual microtubules (arrowheads) appeared inside the ring of clumped chromosomal bivalents. Bar represents 0.5 μm. H A detail of the microtubule organizing center-like structure, apparently derived from Golgi vesicles (arrowheads). These structures, reminisce to pericentriolar material of embryonic MTOCs, were regularly found in the perinuclear region of metaphase oocytes cocultured with PMG. Bar represents 0.3 μm.

Fig 3. A The H1 and MAP kinase activity in cattle oocytes precultured for 8 hr. The oocytes were cultured for 0 h (lane 1) and 8 h (lane 2) in control conditions. The precultured oocytes were cocultured with PMG for 2 h (lane 3), 4 h (lane 4) and 6 h (lane 5). After 6 h of coculture the oocytes were released from the contact with PMG and subsequently cultured in control medium for 2 h (lane 6), 4 h (lane 7) and 6 h (lane 8). **B** The H1 and MAP kinase activity in cattle oocytes precultured for 12 h. The oocytes were cultured for 0 h (lane 1) and 12 h (lane 2) in control conditions. The precultured oocytes were cocultured with PMG for 2 h (lane 3), 4 h (lane 4) and 6 h (lane 5). After 6 h of coculture the oocytes were released from the

74

contact with PMG and subsequently cultured in control medium for 2 h (lane 6), 4 h (lane 7) and 6 h (lane 8).

Fig 4. Relative histone H1 (,) and MAP (Δ,Δ) kinase activity in bovine oocytes precultured for 8 h (K 8)(Fig. 4A) and 12 h (K 12)(Fig. 4B) prior to coculture with PMG for 2 h, 4 h, and 6 h (Gr 2, Gr 4, and Gr 6) and cultured for 2 h, 4 h, and 6 h after coculture (R 2, R 4, and R 6). K0 corresponds to freshly isolated oocytes. Experiments were performed twice whereby autoradiograms corresponding to data denoted by filled symbols (,Δ) are shown on Fig. 3A and Fig. 3B, respectively.

15

REFERENCES

Anderson, N.G., Maller, J.L., Tonks, N.K., and Sturgill,T.W. (1990). Requirement for integration of signals from two distinct phosphorylation pathways for activation of MAP kinase. Nature 343, 651-653.

Boweri, T., (1901) Zellen-studien: Ueber die natur der centrosomen. Fisher Verlag, Jena, Germany

Buendia, B., Draetta, G., and Karsenti, E. (1992). Regulation of microtubule nucleating activity of centrosomes in Xenopus egg extracts. J. Cell. Biol. 116, 1431-1442.

Centonze, V.E. and Borisy, G.G.(1990). Nucleation of microtubules from mitotic centrosomes is modulated by a phosphorylated epitope. J. Cell Sci. 95, 405-411.

Calarco, P.G., Donahue, R.P., Szollosi, D. (1972). Germinal vesicle breakdown in the mouse oocyte. J. Cell Sci. 10, 369-385.

Clarke, H.J., Masui, Y. (1983). The induction of reversible chromosome condensation by protein synthesis inhibition during meiotic maturation of mouse oocytes. Dev. Biol. 97, 291-301.

Dessev, G., Ivcheva-Dessev, C., Bischoff, J., Beach, D., Goldman, R. (1991). A complex containing p34cdc2 and cyclin B phosphorylates the nuclear lamin and disassembles the nuclei of clam oocytes in vitro. J. Cell. Biol. 112, 523-533.

Eppig, J.J., Freter, R.R., Ward-Bailey, P.F., Schultz, R.M.

76

(1983). Inhibition of oocyte maturation in the mouse: participation of cAMP, steroid hormones and a putative maturation-inhibitory factor. Dev.Biol 100, 39-49.

Ferrel, J.E., Jr., Wu, M., Gerhart, J.C., and Martin, G.S.(1991). Cell cycle tyrosine phosphorylation of p34cdc2 and a microtubule-associated protein kinase homolog in Xenopus oocytes and eggs. Mol. Cell. Biol. 11, 1965-1971.

Gautier, J., Solomon, M.J., Boother, R.N., Bazan, J.F., Kirschner, M.W. (1992) Oscillation of MPF is accompanied by periodic association between cdc25 and cdc2-cyclin B. Cell 67, 197-211.

Gotoh, Y., Moriyama, K., Matsuda, S., Okumura, E., Kishimoto, T., Kawasaki, H., Suzuki, K., Yahara, I., Sakai, H. and Nishida, E. (1991a). Xenopus M phase MAP kinase: isolation of its cDNA and activation by MPF. EMBO J. 10, 2661-2668.

Gotoh, Y., Nishida, E., Matsuda, S., Shiina, N., Kosako, H., Shiokawa, K., Akiyama, T., Ohta, K., and Sakai, H.(1991b). In vitro effects on microtubule dynamics of purified Xenopus M phase-activated MAP kinase. Nature 349, 251-254.

Gould, R.R., and Borisy, G.G. (1977). The pericentriolar material in chinese hamster ovary cells nucleates microtubule formation. J. Cell Biol. 73, 601-615.

Hashimoto, N., and Kishimoto, T., (1988). Regulation of meiotic metaphase by a cytoplasmic maturation-promoting factor during mouse oocyte maturation. Dev. Biol. 126, 242-252.

Kalous, J., Sutovsky, P., Rimkevicova, Z., Shioya, Y., Lie, B.L.,

-77-

and Motlik, J. (1993). Pig membrana granulosa cells prevent resumption of meiosis in cattle oocytes. Mol. Reprod. Dev. 34, 58-64.

Karsenti, E., Newport, J., Hubble, R., and Kirschner, M. (1984). Interconversion of metaphase and interphase microtubule arrays, as studied by the injection of centrosomes and nuclei in Xenopus eggs. J.Cell.Biol. 98, 1730-1745.

Kubiak, J.Z., Weber, M., G raud, G., and Maro, B. (1992). Cell cycle modification during the transition between meiotic M-phases in mouse oocytes. J.Cell.Sci. 102, 457-467.

Laemmli, U.K. (1970). Cleavage of structural proteins during the assembly of the head of bacteriophage T4. Nature 227, 11713-11720.

Langan, T.A., Gautier, J., Lohka, M., Hollingsworth, R., Moreno, P.N., Nurse, P.N., Maller, J.L., and Sclafani, R. (1989). Mammalian growth-associated H1 histone kinase: a homolog of cdc2+/CDC28 protein kinase controlling mitotic entry in yeast and frog cells. Mol. Cell. Biol. 9, 3860-3868.

Le Guen, P., and Crozet, N., (1988) Microtubule and centrosome distribution during sheep fertilization. Eur. J. Cell Biol. 48, 239-249

Lohka, M.J., Hayes, M., and Maller, J.L. (1988). Purification of maturation-promoting-factor, an intracellular regulator of early mitosis events. Proc. Natl. Acad. Sci. USA 85, 3009-3013.

Maro, B., Kubiak, J.Z., Gueth, C., De Pennart, H., Houliston, E., Weber, M., Antony, C., Aghion, J. (1990). Cytoskeleton

organization during oogenesis, fertilization and preimplantation development of the mouse. Int. J. Dev. Biol. 34, 127-137.

Motlik, J. (1989). Cytoplasmic aspects of oocyte growth and maturation in mammals. J. Reprod. Fert. 38, 17-25.

Motlik, J., and Kubelka, M. (1990). Cell-cycle aspects of growth and maturation of mammalian oocytes. Mol. Reprod. Dev. 27, 366- 375.

Motlik, J., Nagai, T., and Kikuchi, K. (1991). Resumption of meiosis in pig oocytes cultured with cumulus and parietal granulosa cells: The effect of protein synthesis inhibition. J. Exp. Zool. 259, 386-391.

Multinger, L., Gagnon, J.. Van Dorsselaer, A., Job, D. (1992), Stabilization of sea urchin flagellar microtubules by histone H1. Nature 360, 33-39.

Nagyova, E., Kalous, J., Sutovsky, P., Motlik, J. (1993). Is cAMP decrease essential for resumption of meiosis in mouse oocytes? Reprod. Nutr. Develop. 33, 419-428.

Nebreda, A.R. and Hunt, T. (1993). The c-mos proto-oncogene protein kinase turns on and maintains the activity of MAP kinase, but not MPF, in cell-free extract of Xenopus oocytes and eggs. EMBO J. 12, 1979-1986.

Posada, J. and Cooper, J.A. (1992). Requirements for phosphorylation of MAP kinase during meiosis in Xenopus oocytes. Science 255, 212-215.

Posada, J., Sanghera, J., Pelech, S., Aebersold, R., and Cooper,

J.A.(1991). Tyrosine phosphorylation and activation of homologous protein kinases during oocyte maturation and mitogenic activation of fibroblasts. Mol. Cell. Biol. 11, 2517-2528.

Rime, H., Neant, J., Guerrier, P., Ozon, R, (1989). 6-Dimethyl-aminopurine (6-DMAP), a reversible inhibitor of the cytoplasmic maturation promoting factor(MPF) during the first maturation division of the mouse oocyte. Dev. Biol. 133, 169-179.

Sathanathan, A.H., Kola, I., Osborne, J., Trounson, A. (1991). Centrioles in the beginning of human development. Proc. Natl. Acad. Sci. USA 88, 4806-4810.

Schatten, G., Schatten,H., Mazia, D., Balczon, C., and Simerly, C., (1986) Behavior of centrosomes during fertilization and cell division in mouse oocytes and in sea urchin eggs. Proc. Natl. Acad. Sci. USA 83, 105-109

Shibuya, E.K., Boulton, T.G., Cobb, M.H., and Ruderman, J.V. (1992). Activation of p42 MAP kinase and the release of oocytes from cell cycle arrest. EMBO J. 11, 3963-3975.

Solomon, M.J., Glotzer, M., Lee, T.H., Philippe, M., and Kirschner, M.W. (199O). Cyclin activation of p34cdc2. Cell 63, 1013-1024.

Sutovsky, P., Flechon, J.E., Flechon, B., Motlik, J., Peynot, N., Chesne, P., and Heyman, Y. (1993). Dynamic changes of gap junctions and cytoskeleton during in vitro culture of cattle oocyte cumulus complexes. Biol. Reprod. 49, 1277-1287.

Szollosi, D., Calarco, P., and Donnahue, R.P. (1972). Absence of centrioles in the first and second meiotic spindles of mouse oocytes. J. Cell Sci. 11, 521-541

Szollosi, D., and Ozil, J.P. (1991). De novo formation of centrioles in parthenogenetically activated, diploidized rabbit embryos. Biol. Cell. 72, 61-66.

Szollosi, M., Debey, P., Szollosi, D., Rime, H., Vautier, D. (1991). Chromatin behaviour under influence of puromycin and 6-DMAP at different stages of mouse oocyte maturation. Chromosoma 100, 339-354 .

Thibault, C., Szollosi, D., Gerard, M. (1987). Mammalian oocyte maturation. Reprod. Nutr. Develop. 27, 865-896.

Verde, F., Labb , J-C., Dor , M., Karsenti, E. (1990). Regulation of microtubule dynamics by cdc2 kinase in cell-free extracts of Xenopus eggs. Nature 343, 233-238.

Verlhac, M.L., De Pennart, H., Maro, B., Cobb, M.H., and Clarke, H.J.(1993). MAP kinase becomes stably activated at metaphase and is associated with microtubule-organizing centers during meiotic maturation of mouse oocytes. Dev.Biol. 158, 330-340.

Verlhac, M.L., Kubiak, J.Z., Clarke, H.J., Maro, B.(1994). Microtubule and chromatin behavior follow MAP kinase activity but not MPF activity during meiosis in mouse oocytes. Development 120, 1017-1025.

Viklicky, V., Draber, P., Hasek, J., Bartek, J. (1982). Production and characterization of monoclonal antitubulin antibody. Cell Biol. Int. Rep. 6, 725-730

4\

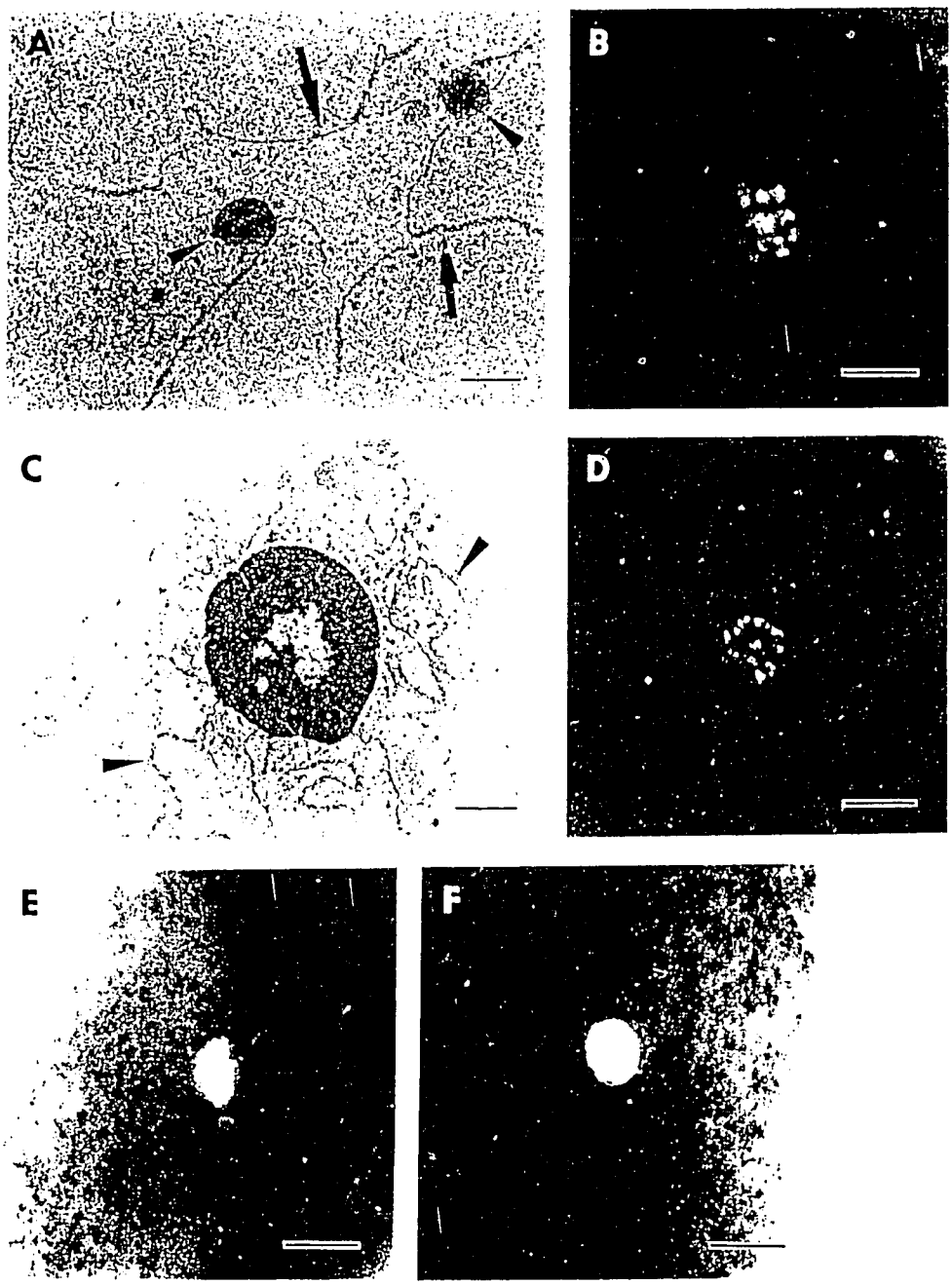
A
B
C
D
E
F

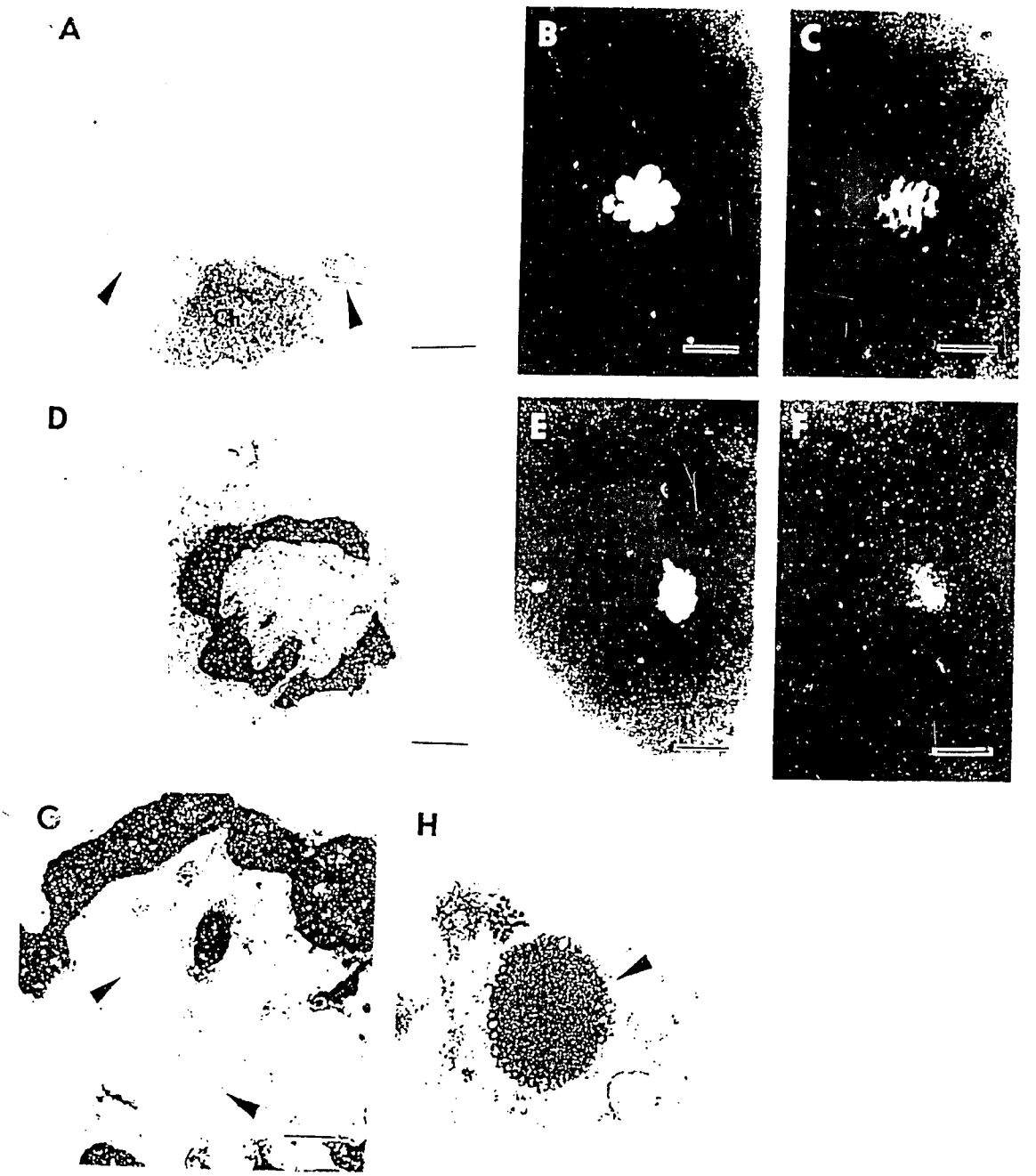
A
B
C
D
E
F
G
H

Fig. 3A

Fig. 3B

myelin basic protein

58

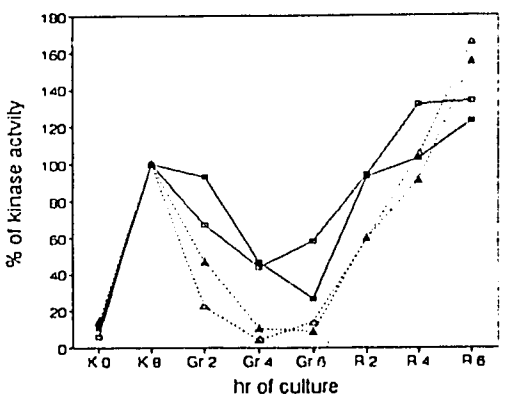

Fig. 4A

Šutovský et al.: The effect
of membrana granulosa

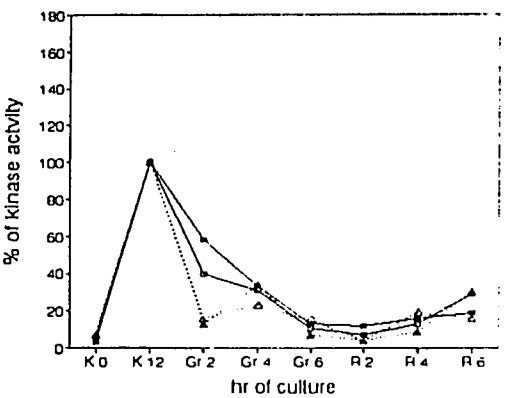

Fig. 4B

Šutovský et al.: The effect
of membrana granulosa ...

Table 1A Meiotic maturation of cocultured cattle oocytes preincubated for 8 h

Culture procedure				Stage of meiosis [number of oocytes(percentage)]					Total Number of OCCs
Preincu-bation 8 h	Coculture with PMG 6 h	Subsequent culture 10 h	20 h	GV	LD	MI	MII	GVBD	
+	-	-	-	15(23)	45(73)	-	2 (3)	48(76)[a]	62
+	+	-	-	11(29)	43(77)*	1 (2)*	1 (2)*	45(81)	56
+	+	+	-	9(13)	52(73)	9(13)	1 (1)	62(87)	71
+	+	-	+	5 (7)	15(25)	8(12)	36(56)	59(93)[a]	64

Note: * - chromatin condensed during coculture with PMG
a - these values are significantly different ($P<0.05$)

Table 1B Meiotic maturation of cocultured cattle oocytes preincubated for 12 h

Culture procedure				Stage of meiosis [number of oocytes(percentage)]					Total Number of OCCs
Preincu-bation 12 h	Coculture with PMG 6 h	Subsequent culture 10 h	20 h	GV	LD	MI	MII	GVBD	
+	-	-	-	6(11)	12(21)	35(61)	4 (7)	51(89)	57
+	+	-	-	7(15)	11(24)*	24(54)*	3 (7)*	38(85)	45
+	+	+	-	7(15)	8(17)*	30(64)*	2 (4)*	40(85)	47
+	+	-	+	6(10)	15(25)*	38(62)*	2 (3)*	55(90)	61

Note: * - chromatin condensed during coculture with PMG

Porcine Cumulus and Mural Granulosa Cells Secrete Cumulus Expansion Enabling Factor (CEEF)[1]

Radek Procházka, Eva Nagyová and Jan Motlík

Academy of Sciences of the Czech Republic
Institute of Animal Physiology and Genetics
277 21 Liběchov, Czech Republic

Short title: CEEF secretion in the pig follicle

Key words: pig, oocyte, cumulus, expansion, granulosa cells

Address for correspondence:
Radek Procházka, Academy of Sciences of the Czech Republic, Institute of Animal Physiology and Genetics, 277 21 Liběchov, Czech Republic
Fax: +42-206-69 71 86; Telephone: +42-206-69 70 24

---

[1]This research was supported by grant A745 401 from Academy of Sciences of the Czech Republic; grant 12.061E, Program in Science and Technology Cooperation from U.S. Agency for International Development; and grant GZ 45.379/1-IV/3a/94 from Austrian Ministry of Science.

88

ABSTRACT

The objectives of this study were 1) to assess production of CEEF by porcine oocytes during their growth and differentiation and 2) to find out whether porcine cumulus cells and mural granulosa cells can secrete CEEF. Culture drops of M-199 medium were conditioned by denuded oocytes in different stages of their development (1 oocyte/μl), oocytectomized complexes (OOX) representing cumulus cells (1 OOX/μl) or pieces of mural granulosa cells (MGC) or porcine oviductal cells (POC) (1000 cells/μl). The production of CEEF was assessed by addition of mouse OOX and FSH (1μg/ml) into the conditioned medium. Expansion of the mouse OOX, resistance to mechanical disruption and mucification of the cumulus were assessed 16-18 h later by a subjective scoring system (0-4). Mouse OOX did not expand in non-conditioned FSH supplemented medium. Growing GVBD incompetent porcine oocytes (diameter <100 μm), growing GVBD competent oocytes (diameter $=110$ μm), and fully grown immature oocytes (120 μm) stimulated 3-4 expansion of the mouse OOX which is the same degree of expansion that was observed in intact oocyte-cumulus complexes (OCC). The expanded cumuli were highly mucified and extremely resistant to mechanical disruption. Metaphase I, metaphase II, activated and pronuclear oocytes also caused dispersion of the mouse OOX. However, the cumuli were not mucified and were easy to remove by pipetting. We conclude that 1) immature porcine oocytes produce CEEF regardless of their GVBD competence; 2) the production of CEEF persists during the transition to metaphase I oocytes; oocytes that progressed to and beyond metaphase I produce factor(s) that appears to be different from CEEF. All porcine granulosa cells regardless of their position in the medium size follicles

(cumulus or mural granulosa cells) responded in vitro to FSH treatment by expansion. Moreover,these granulosa cells secreted CEEF. In preovulatory follicles (after PMSG or PMSG and hCG treatment), the mural granulosa lost the above mentioned properties and only cumulus granulosa cells and the limited area of the mural granulosa attached to the cumulus oophorus still secreted CEEF and responded to FSH by expansion. We conclude that porcine cumulus cells constitutively produce CEEF in vitro. Mural granulosa cells from medium size follicle do so only when they are stimulated by FSH.

INTRODUCTION

In the fetal mammalian ovary, dictyate oocytes become enclosed in a single layer of flattened pregranulosa cells and form primordial follicles. In follicles selected for growth, the granulosa cells undergo a series of mitotic divisions and, following antrum formation, differentiate in two populations: cumulus cells, surrounding the oocytes, and mural granulosa cells (MGC) representing the innermost layer of the follicle wall. The granulosa cells, cumulus cells and the oocytes communicate via gap junctions [1] and also by secretion of paracrine factors [2,3]. This communication is bidirectional. The granulosa cells appear essential for oocyte growth [4,5] and regulation of oocyte maturation [3,6]; the oocyte is essential for proliferation, differentiation and function of granulosa cells [3,7].

The cumulus cells undergo expansion following the preovulatory surge of gonadotropins. The expansion involves dispersion of cumulus cells due to deposition of hyaluronic acid in the extracellular matrix [8]. In vitro, cumulus

expansion can be induced by chemicals that increase intracellular cAMP like FSH [9,10] or activators of adenylcyclase [11,12] and also by an activator of tyrosine kinase, EGF [13]. In the mouse, oocyte plays an important role in regulation of cumulus expansion. Removal of the oocyte from OCC inhibits FSH and EGF induced expansion of the cumulus [14,15]. This inhibition occurs independently or downstream of the cAMP regulation since cAMP levels are comparable in both intact and oocytectomized complexes [14]. Conditioning of the culture medium with denuded oocytes reverses the inhibitory effect of oocytectomy on expansion of cumulus cells [14]. This indicates that mouse oocytes produce a soluble factor enabling expansion of the cumulus (CEEF). Mouse oocytes acquire the ability to secrete CEEF during the growth period, at the time of acquisition of the competence to undergo germinal vesicle breakdown. The oocyte ability to secrete CEEF is lost after fertilization [16].

Porcine oocytes also produce CEEF since they enable the FSH stimulated expansion of mouse OOX [17,18]. However, oocytectomy does not affect FSH induced expansion of the porcine cumulus in vitro [11,17,18]. The ability of the OOX to expand is not due to persistence of CEEF of oocyte origin within cumulus cells since they expanded even with a 32 h delay before FSH stimulation [18]. A hypothesis was proposed that the oocyte CEEF induces a permanent change in the cumulus cells that enables them to undergo expansion whenever the appropriate hormonal stimulus occurs [18]. An alternative possibility could exist that the CEEF is not produced exclusively by the oocyte in the pig follicle. Porcine granulosa cells produce different paracrine factors including EGF [19], TGF-beta [20] and IGF I [21]. An autocrine or paracrine production of CEEF by the porcine cumulus cells would also explain the FSH

stimulated expansion of oocytectomized complexes.

To understand more the regulation of expansion of the porcine cumulus we decided 1) to assess production of CEEF by porcine oocytes during their growth and differentiation and 2) to find out whether porcine cumulus cells and other populations of granulosa cells can secrete CEEF.

MATERIALS AND METHODS

Source of oocytes and culture

Gilts from crosses between Minnesota and Göttingen strains of miniature pigs were stimulated with 500 IU pregnant mares' serum gonadotrophin (PMSG) (Bioveta, Ivanovice na Hané, Czech Republic) on Day 16 of the cycle; 66 h later, the gilts were slaughtered, ovaries were excised, put in a thermos and transferred to laboratory. The preovulatory follicles were cut out from ovarian tissue, opened and membrana granulosa was released in PBS by scraping the inner surface of the follicular wall. OCC and OCC with an attached piece of membrana granulosa were collected and washed three times in culture medium. PBS containing the pieces of mural granulosa cells was collected in 15 ml testubes. The cells were let to settle and then washed three times in culture medium. Pieces of the membrana granulosa containing about 1000 cells were used for medium conditioning. The same procedures were used for the isolation of OCC and granulosa cells from medium size (2-5 mm in diameter) follicles of slaughtered prepubertal gilts.

Growing pig oocytes were obtained by the above described procedure from small antral follicles (<0.7 mm; GVBD incompetent oocytes, oocyte diameter

1 < 100 μm) and from 1.6 mm follicles (GVBD competent growing oocytes, oocyte
2 diameter = 110 μm). The competence of the oocytes to undergo GVBD was
3 verified following 48 h of culture in vitro. Metaphase II oocytes were obtained
4 by culture of fully grown oocytes (120 μm) in vitro for 42 h. Activated oocytes
5 were obtained by stimulation of the M II oocytes by a single 100 μs electrical
6 pulse of 1.75 kV/cm [22]. Pronuclear oocytes were produced by overnight (16 h)
7 culture of the activated oocytes. Maturing oocytes surrounded with an expanded
8 cumulus were also collected from preovulatory follicles of minipigs stimulated
9 by PMSG and 66 h later by hCG (1000 iu). The oocytes were collected 20 h
10 following administration of hCG.

11 Pig oviductal cells (POC) were isolated by the method described previously
12 for bovine oviductal cells [23]. Briefly, POC were transferred to 15 ml conical
13 tube and washed 3 times with M-199. The cells were transferred to a 60 mm
14 culture dish with 10 ml M-199 with 10% FCS and cultured overnight. The
15 ciliated cell aggregates were used for conditioning.

16 Mouse OCC were isolated from ovaries of 4-6 weeks old ICR mice, stimulated
17 44-46 h previously with 10 i.u. PMSG. The complexes were released from
18 follicles by a puncture of the follicular wall with fine needles in M-199 medium,
19 washed and immediately used for culture or oocytectomy.

20 The culture medium was TCM 199 (Sevac, Prague, Czech Republic) buffered
21 with 20 mM $NaHCO_3$ and 6,25 mM Hepes, supplemented with fetal calf serum
22 (FCS) (10%, v/v), 0.91 mM sodium pyruvate, 1.62 mM calcium lactate and
23 antibiotics [24]. This medium was supplemented by 1.0 μg/ml FSH (Bioproduct
24 Belgium) when used for production of matured oocytes. The culture drops were
25 placed in 35 mm Petri-dishes and covered by light mineral oil (Sigma

Chemicals). The dishes were cultured at 38,5°C in air containing 5% CO_2.

Oocytectomy

Some of the mouse and pig OCC were deprived of the oocyte (oocytectomized) by the method described previously [14,11]. Briefly, each OCC was attached to a holding pipette. A glass needle was then introduced through the cumulus cells and the oocyte into the holding pipette. After withdrawal of the needle, the ooplasm was aspirated into the holding pipette by a burst of negative pressure. A set of about 15 oocytectomized complexes (OOX) was prepared within 20 min and immediately placed into culture.

Preparation of conditioned media and assessment of the cumulus expansion

Conditioned media were prepared by a culture of 50 denuded oocytes, OOX (cumulus cells), pieces of granulosa cells or aggregates of POC in 50 μl of the culture medium for 24 h. Afterwards, 40 μl of the conditioned medium was collected, supplemented by 1.0 μg/ml FSH provided that FSH was not previously included in the culture medium during the period of conditioning. To assess production of CEEF, about 15 mouse OOX were added to the culture drop of the conditioned medium and expansion of the cumulus cells was assessed 18 h later, according to the subjective scoring system (0-4) described previously [14]. Briefly, 0 indicates no detectable response, while 1 indicates the minimum observable response, peripheral cumulus cells have a glistening appearance ; 2 indicates expansion of the peripheral layers of the cumulus; 3 indicates expansion of all layers of the cumulus except corona radiata cells and

4 indicates expansion of the cumulus including corona radiata cells. Following assessment of cumulus expansion, the cumuli were passed several times through a glass pipette and assessed for mucification (0-4) and resistance to mechanical disruption (0 - all layers of the cumulus and corona cells were easily removed by pipetting; 1 - indicates that cumulus cells but not corona cells were removed; 2 - indicates that outer half of the cumulus cells was removed mechanically; 3 - only peripheral layers were removed; 4 - no or few cells could have been removed). Sensitivity to hyaluronidase was assessed by exposing several expanded cumuli to 200 IU/ml hyaluronidase (Sevac, Prague) in the culture medium for 10 min [11].

RESULTS

Production of CEEF by pig oocytes during their development

Intact mouse OCCs underwent 3-4 expansion when cultured in medium supplemented with FSH and FCS. On the other hand, expansion did not occur in OOX cultured under the same conditions (Table 1). However, 3-4 expansion occurred in both OCC and OOX in the medium conditioned by growing pig oocytes with or without GVBD competence or by fully grown oocytes (Table 1, Fig. 1). In all these situations, the expanded cumuli were mucified, elastic, highly resistant to mechanical disruption and sensitive to hyaluronidase. The metaphase I, metaphase II, activated and pronuclear pig oocytes also induced 3-4 expansion of the mouse OOX. However, the cumuli were fragile, not mucified, insensitive to hyaluronidase and exhibited no or low resistance to mechanical disruption (Fig.2). Nevertheless, these cumuli essentially differed from those

cultured in non-conditioned medium which were compact and firmly attached to the bottom of the culture dish (Fig.3). Thus, it can be concluded that CEEF is produced by growing pig oocytes regardless of their GVBD competence and by fully grown GV oocytes during their transition to M I. Matured, activated and pronuclear oocytes produce factors which prevent attachment of cumulus cells to bottom and induce disintegration of the cumulus. However, due to absence of mucification of the cumulus, the factors appear to be different from CEEF.

Production of CEEF by cumulus granulosa cells

To assess the hypothesis that expansion of porcine OOX may be supported by autocrine production of CEEF by cumulus cells, we conditioned medium with porcine cumulus cells stimulated by FSH. As shown in Table 2, the porcine OOX originating from medium size follicles and also from large preovulatory (PMSG treated) follicles stimulated 2-3 expansion in the mouse OOX (Fig.4), compared to 0 expansion in control groups (unconditioned or conditioned by evacuated zonae). Identical results were obtained when the medium was conditioned by the pieces of MGC attached to the cumulus which also possess the ability to undergo expansion [11].

We assessed production of CEEF by cumulus and the attached piece of MGC undergoing expansion in vivo following PMSG and hCG administration. The mass of expanded cells isolated from a single follicle (Fig. 5) was sufficient to condition 50 μl of the culture medium (Table 2).

The above data indicate that expansion of the porcine cumulus is accompanied by secretion of CEEF or CEEF like molecule. To exclude a possibility that the CEEF was not produced by the cumulus cells, but

represented CEEF of the oocyte origin accumulated in cumulus cells, we first cultured the porcine OOX in a large volume of culture medium (1 ml) for 16 h and then allowed the complexes to condition a drop of culture medium. The production of CEEF was preserved after 16 h delay (Table 2). Next, we assessed whether the CEEF is produced by cumulus cells only as a response to FSH stimulation. The data of Table 1 show that CEEF is produced in both FSH stimulated and FSH non-stimulated cumulus. In other words, both compact and expanding cumuli produce CEEF.

Production of CEEF by MGC

As shown in Table 2, MGC of medium size pig follicles (2-5 mm) stimulated 2-4 expansion of mouse OOX, however, only when FSH was added to the medium during the period of conditioning. The FSH stimulated MGC of the medium size follicles underwent extensive expansion within the culture period of 24h (Fig. 6). This was in contrast to the behaviour of MGC isolated from preovulatory follicles of PMSG treated animals, which did not expand within 24 h of culture (Fig. 7) and did not produce the CEEF even after FSH stimulation (Table 2). MGC of PMSG and hCG treated preovulatory follicles also did not stimulate expansion of mouse OOX.

Medium conditioned by POC does not stimulate cumulus expansion of mouse OOX. When FSH was added to POC during the period of conditioning, the medium induced 1-2 expansion in the OOX, however the cumuli were fragile and displayed no or low mucification (Table 2).

DISCUSSION

In the mouse oocytes, the onset of CEEF production coincides with the time of acquisition of GVBD competence [16]. However, this coincidence is only temporal but not functional. It has been shown that the secretion of CEEF by mouse oocytes is independent of oocyte growth and competence to undergo GVBD [25]. Our results also document that there is not a casual relationship between acquisition of GVBD competence and production of CEEF in porcine oocytes, since CEEF is secreted by oocytes which did not possess GVBD competence. The pattern of CEEF production differs from that observed in the mouse in other aspects. In mouse oocytes, CEEF secretion continues throughout the periods of growth and maturation [16]. In pig oocytes, secretion of CEEF occurs only in oocytes in GV stage and during GV to MI transition. Oocytes which progressed to and beyond metaphase I appear to produce factor(s) that is (are) different from CEEF at least in its physiological effect on mouse cumulus cells. Instead of mucification of the cumulus, these factors promoted, in combination with FSH, rather disaggregation of cumulus cells. We observe identical situation in mouse oocyte-cumulus complexes stimulated by FSH and cultured in serum free media. Under these condition, the produced hyaluronic acid cannot be incorporated in the extracellular matrix [26,27]. Recently, the serum factor responsible for retaining hyaluronic acid in the expanding cumulus was identified as a member of inter-α-trypsin inhibitor family [28]. We may thus speculate that pig oocytes beyond M I, in contrast to GV oocytes, do not produce this factor. Another possibility is that these oocytes do not stimulate synthesis of hyaluronic acid in mouse OOX. Further experiments are necessary to differ between these possibilities.

98

Our results document that under in vitro conditions CEEF was not produced exclusively by oocytes. The porcine cumulus cells and also MGC of medium size capable of CEEF secretion. This is the first demonstration of CEEF secretion by somatic cells. The failure of POC to stimulate expansion and mucification of the mouse cumulus suggests that production of CEEF is not a common feature of somatic cells but this property is limited perhaps only to granulosa and cumulus cells. In the mouse, any of the assayed somatic cell types, including granulosa and Sertoli cells, did not secrete CEEF in sufficient concentrations (expansion 1 was observed in all tests) [14]. This discrepancy may by caused by species differences or by different preparation of the cells for conditioning of the culture medium. So far, we do not know whether CEEF secreted by granulosa cells is the same as the CEEF secreted by oocytes. If it is true, the purification and characterization of CEEF would be greatly facilitated, since it is extremely difficult to obtain enough material from oocytes.

We show in this study that both cumulus and MGC of medium size follicles have the ability to undergo expansion following FSH stimulation. This ability persists until the preovulatory surge of gonadotropins. So far, there is only fragmentary information in the literature about an ability of mural granulosa to expand. The porcine MGC attached to the cumulus were observed to undergo expansion in vivo and in vitro [29,11]. In mouse PMSG and hCG primed follicles, the MGC neighbouring the cumulus and also the antral layer of the mural granulosa cells were shown to secrete hyaluronic acid [30] and thus altogether participate on cumulus expansion in vivo. In our study, we observed expansion of not only superficial but all layers of the mural granulosa under in vitro conditions. However, only MGC of medium size follicles are capable of

expansion. Pieces of MGC isolated from PMSG treated follicles do not undergo expansion, as we [11] and others [18] postulated previously.

Our data suggest that CEEF is constitutively produced by porcine oocytes and cumulus cells during folliculogenesis. MGC were found, in our experiments, to produce CEEF only during FSH induced expansion in vitro. Since such an expansion does not occur during follicle development in vivo, we cannot confirm that MGC produce CEEF under in vivo conditions. For this reason, physiological significance of the production of CEEF by MGC cannot be defined at the present time. Nevertheless, it is noteworthy in this respect that pig preovulatory follicle has an internal volume 200 μl which is strikingly different from the mouse follicle, whose volume is below 1 μl. If intrafollicular concentration of CEEF plays a role in regulation of cumulus expansion or in other yet unknown processes, it is conceivable that production of CEEF by cumulus and MGC may be essential for achievement of sufficient concentration of CEEF in large volume follicles.

Following preovulatory surge of gonadotropins, the ability to undergo expansion and to secrete CEEF remains limited only to cumulus cells and attached piece of MGC. Our results suggest that auto- or paracrine production of CEEF by these cells is sufficient to drive the cumulus expansion. This opinion is justified by the finding that both intact and oocytectomized complexes undergo the same degree of expansion [11,18,17]. Nevertheless, the cumuli may, under in vitro condition, secrete less CEEF than the oocytes, since the expansion of mouse OOX was somewhat lower in medium conditioned by the cumuli compared to the same number of denuded oocytes.

We conclude that 1) the onset of production of CEEF by porcine oocytes does

not depend on the acquisition of GVBD competence; 2) CEEF appears to be produced only by oocytes in GV stage and during GV-MI transition; 3) in vitro, CEEF is constitutively produced by porcine cumulus and by FSH stimulated MGC of growing follicles; 4) MGC of medium size follicles stimulated by FSH undergo expansion and produce CEEF.

Acknowledgements

We thank Mrs. Miloslava Hoření for excellent technical assistance and typing the manuscript. Drs. J. J. Eppig and P. Šutovský are thanked for critical reading the manuscript and their valuable suggestions.

REFERENCES

1. Albertini DF, Anderson E. The appearance and structure of the intercellular connections during the ontogeny of the rabbit ovarian follicle with special reference to gap junctions. J Cell Biol 1974; 63:680-686.
2. Tsafriri A. Local nonsteroidal regulators of ovarian function. In: Knobil E, Neill J (eds.). The physiology of Reproduction. New York: Raven Press, Ltd.; 1988:527-567.
3. Buccione R, Schroeder AC, Eppig JJ. Interactions between somatic cells and germ cells throughout mammalian oogenesis. Biol Reprod 1990; 43:543-547.
4. Eppig JJ. Mouse oocyte development in vitro with various culture systems. Dev Biol 1977; 60:371-388.
5. Eppig JJ. A comparison between oocyte in coculture with granulosa cells

and oocytes with granulosa cell-oocyte junctional contact maintained in vitro. J Exp Zool 1979; 209:345-353.

6. Thibault C, Szöllösi D, Gerard M. Mammalian oocyte maturation. Reprod Nutr Develop 1987; 27:865-896.

7. Salustri A, Hascall VC, Camaioni A, Yanagishita M. Oocyte-granulosa cell interactions. In: Adashi EY, Leung PCK (eds). The Ovary. New York: Raven Press Ltd.; 1993:209-225.

8. Eppig JJ. FSH stimulates hyaluronic acid synthesis by oocyte-cumulus cell complexes from mouse preovulatory follicles. Nature 1979; 281:483-484.

9. Dekel N, Kraicer PF. Inductions in vitro of mucification of rat cumulus oophorus by gonadotrophin and adenosine 3',5'-monophosphate. Endocrinology 1978; 102:1797-1802.

10. Thibault C. Final stages of mammalian meiotic maturation. In: Biggers JD, Schuetz AW (eds). Oogenesis. Baltimore: University Park Press; 1972:397-411.

11. Procházka R, Nagyová E, Rimkevičová Z, Nagai T, Kikuchi K, Motlík J. Lack of effect of oocytectomy on expansion of the porcine cumulus. J Reprod Fert 1991; 93:569-576.

12. Racowsky C. Effects of forskolin on maintenance of meiotic arrest and stimulation of cumulus expansion, progesterone and cyclin AMP production by pig oocyte-cumulus complexes. J Reprod Fert 1985; 74:9-21.

13. Downs SM. Specificity of epidermal growth factor action on maturation of the murine oocyte and cumulus oophorus in vitro. Biol Reprod 1989; 41:371-379.

14. Buccione R, Vanderhyden BC, Caron PJ, Eppig JJ. FSH-induced

102

expansion of the mouse cumulus oophorus in vitro is dependent upon a specific factor(s) secreted by the oocyte. Dev Biol 1990; 138:16-25.

15. Salustri A, Yanagishita M, Hascall VC. Mouse oocytes regulate hyaluronic acid synthesis and mucification by FSH-stimulated cumulus cells. Dev Biol 1990; 138:26-32.

16. Vanderhyden BC, Caron PJ, Buccione R, Eppig JJ. Developmental pattern of the secretion of cumulus expansion-enabling factor by mouse oocytes and the role of oocytes in promoting granulosa cell differentiation. Dev Biol 1990; 140:307-317.

17. Singh B, Zhang X, Armstrong DT. Porcine oocytes release cumulus expansion-enabling activity even though porcine cumulus expansion in vitro is independent of the oocyte. Endocrinology 1993; 132:1860-1862.

18. Vanderhyden BC. Species differences in the regulation of cumulus expansion by an oocyte-secreted factor(s). J Reprod Fert 1993; 98:219-227.

19. Singh B, Rutledge JM, Armstrong DT. Epidermal growth factor and its receptor gene expression and peptide localization in porcine ovarian follicles. Mol Reprod Dev 1995; 40:391-399.

20. May JV, Turzcynski CJ, Ramos L, Mau YH. Differential involvement of protein kinase C in the regulation of transforming growth factor-beta (TGF-beta) secretion by porcine theca and granulosa cells in vitro. Endocrinology 1995; 136:3-11.

21. Hammond JM, Baranao JL, Skaleris DA, Rechler MM, Knight AP. Somatomedin (Sm) production by cultured porcine granulosa cells (GC). J Steroid Biochem 1984; 20:1597 (abstr. 128).

22. Procházka R, Kaňka J, Šutovský P, Fulka J, Motlík J. Development of pronuclei in pig oocytes activated by a single electric pulse. J Reprod Fert 1992; 96:725-734.

23. Eyestone WH, First NL. Co-culture of early cattle embryos to the blastocyst stage with oviductal tissue or in conditioned medium. J Reprod Fert 1989; 85:715-720

24. Pavlok A, Torner H, Motlík J, Fulka J, Kauffold P, Duschinski U. Fertilization of bovine oocytes in vitro: effect of different sources of gametes on fertilization rate and frequency of fertilization anomalies. Anim Reprod Sci 1988; 16:207-213.

25. Eppig JJ, Wigglesworth K, Chesnel F. Secretion of cumulus expansion enabling factor by mouse oocytes:Relationship to oocyte growth and competence to resume meiosis. Dev Biol 1993; 158:400-409.

26. Eppig JJ. Role of serum in FSH stimulated cumulus expansion by mouse oocyte-cumulus cell complex in vitro. Biol Reprod 1980; 22:629-633.

27. Salustri A, Yanagishita M, Hascall VC. Synthesis and accumulation of hyaluronic acid and proteoglycans in the mouse cumulus cell-oocyte complex during follicle stimulating hormone-induced mucification. J Biol Chem 1989; 264:13840-13847.

28. Chen L, Mao SJT, Larsen WJ. Identification of a factor in fetal bovine serum that stabilizes the cumulus extracellular matrix. A role for a member of inter-α-trypsin inhibitor family. J Biol Chem 1992; 267:12380-12386.

29. Motlík J, Fulka J, Flechon JE. Changes in intercellular coupling between

1 pig oocytes and cumulus cells during maturation in vivo and in vitro. J
2 Reprod Fert 1986; 72:107-116.
3 30. Salustri A, Yanagishita M, Underhill CB, Laurent TC, Hascall VC.
4 Localization and synthesis of hyaluronic acid in the cumulus cells and
5 mural granulosa cells of the preovulatory follicle. Dev Biol 1992; 151:541-
6 551.

Table 1. Expansion of mouse intact and oocytectomized oocyte-cumulus complexes in culture medium conditioned by oocytes in different stage of development.

Type of oocytes used for conditioning	Type of complexes	Degree of expansion	Res/ mucif	Number of complexes
None (M-199)	Intact	0	1-2/0	40
	OOX	0	1-2/0	40
None (M-199+FSH)	Intact	3-4	4/4	45
	OOX	0	1-2/0	45
Fully-grown oocytes	Intact	3-4	4/4	60
	OOX	3-4	4/4	60
Growing oocytes, GVBD incompetent	Intact	3-4	4/4	45
	OOX	3-4	4/4	45
Growing oocytes, GVBD competent	Intact	3-4	4/4	45
	OOX	3-4	4/4	45
Maturing (MI) oocytes	Intact	3-4	4/4	45
	OOX	3-4	0/0-1	45
Matured (MII) oocytes	Intact	3-4	4/4	45
	OOX	3-4	0/0-1	45
Activated oocytes	Intact	3-4	4/4	45
	OOX	3	0/0-1	45
Pronuclear oocytes	Intact	3-4	4/4	45
	OOX	3	0/0	45

Res-resistance to mechanical disruption; Mucif-mucification of the cumulus. GVBD-germinal vesicle breakdown; MI-metaphase I; MII-metaphase II.

Table 2. Expansion of mouse oocytectomized[1] oocyte-cumulus complexes in culture medium conditioned by cumulus, granulosa and oviductal cells.

Type of cells used for conditioning	Degree of expansion	Degree of resistance/ mucification	Number of complexes
Cumulus cells	2-3	3/3	30
Cumulus cells (16 h delay)	2-3	3/3	30
Cumulus cells+FSH	2-3	3/3	30
Cumulus cells from PMSG follicles	2-3	3/3	30
Cumulus cells from PMSG follicles+FSH	2-3	3/3	30
MGC from medium follicles(2-5mm)	0-1	1/0	30
MGC from medium follicles+FSH	2-4	3/3	40
MGC from PMSG follicles	0	1/0	40
MGC from PMSG follicles+FSH	1	1/1	40
MGC from PMSG and HCG follicles	1	1/1	40
Pig oviductal cells	0-1	0/0-1	30
Pig oviductal cells+FSH	1-2	0/0-1	30

[1]Intact oocyte-cumulus complexes cultured under the listed conditions displayed a uniform response: expansion 3-4, resistance to mechanical disruption 3-4, mucification 3-4.

Cumulus Expansion in Mammals: Cumulus Granulosa Cell Cytoskeleton / Extracellular Matrix / Oocyte Secretion Interactions

P. Šutovský and J. Motlík

Institute of Physiology/Genetics of Animals, Czech Academy of Sciences, 277 21 Liběchov, CZECH REPUBLIK

Correspondence to: Integrated Microscopy Resource, University of Wisconsin, WI 53706, USA

Abstract

Cumulus expansion is a final step in the process of cumulus granulosa cell differentiation, including cytoskeletal remodelling, alterations of protein synthesis and steroidogenesis, deposition of cumulus ECM, and modification of the pathway interconnecting an oocyte and somatic follicle cells. Although the recent data threw light on some of these particular processes, cumulus expansion still raises many questions. Among others, the oocyte secreted expansion enabling factor awaits precise characterization. This investigation was conducted to evaluate the interaction between oocyte-secreted factor(s) and the cytoskeleton of CGC, and the possible stimulating influence on ECM synthesis. Similarly, little is known about the differential response of cumulus and parietal granulosa cells to LH stimulus. There is the distinct cytoskeletal organization of these two follicular compartments. There is also a descending gradient of oocyte secreted factors from cumulus to peripheral granulosa layers. In spite of the recent findings on regulation of oocyte meiosis by metabolic activity of granulosa cells, doubts still exist about the role of cumulus expansion related processes (e.g. GJ endocytosis) in regulation of oocyte meiosis. The resolution of these problems play a key role in developing the reliable technology of *in vitro* maturation/fertilization.

Abbreviations

CEEF	cumulus expansion enabling factor
CGC	cumulus granulosa complex
ECM	extracellular matrix
EGF	epidermal growth factor
F-actin	filament actin
FGF	fibroblast growth factor
GF	growth factors
GJ	gap junction
HA	hyaluronic acid
IF	intermediate filament
IGF	insulin-like growth factor
IαI	inter-α trypsin inhibitor
OCC	oocyte cumulus complex

I. Introduction

In most mammalian species, the oocytes, reaching metaphase of the second meiotic division, are released from ovarian follicles together with the expanded cumulus oophorus (CO). Gonadotropin-stimulated expansion of cumulus cell-oocyte complex is instrumental for ovulation (Dekel et al, 1979; Eppig 1979) since inhibition of cumulus expansion prevents the rupture of follicular wall and the release of an oocyte into oviductal infundibulum (Chen et al, 1990). The presence of expanded cumulus around the ovulated oocyte substantially influences its transport throughout the oviduct (Larsen 1988).

Under in vitro conditions, the cumulus expansion is often taken as a major criterion for both human and domestic animal in vitro fertilization protocols. The oocytes matured and fertilized with their enclosing cumulus oophorus display clearly higher rates of fertilization, pronuclear formation and embryonic development (Pavlok/McLaren 1972; Ball et al, 1983; Staigmiller/Moor 1984).

Until now, cumulus expansion has been defined as a process of spatial separation of cumulus cells due to the increased secretion and deposition of a mucoelastic extracellular matrix rich in hyaluronic acid (Dekel et al, 1979; Eppig 1979). Recent studies brought new important data about composition of cumulus ECM, intercellular communications, involvement of cytoskeleton and interactions between oocyte and cumulus cells throughout the preovulatory period. The present review takes profit from all these recent findings. The significance of cumulus expansion for oocyte maturation, fertilization and initial period of embryonic development will be discussed as well.

II. Oocyte-cumulus Complex in Preovulatory Follicle before LH Surge

A. Origin / Morphology of cumulus granulosa cells

Membrana granulosa cells (GC), probably issued from embryonic rete ovarii (Byskov 1974) form one layer of flattened cells in the primordial ovarian follicle. During the FSH-controlled period of follicle and oocyte growth, the GC undergo intensive proliferation, giving rise to several distinct cellular population. The peripheral layer, termed mural or parietal granulosa, is attached to the follicular basement membrane, constituting a selective barrier between vascular and avascular compartments of the follicle. Around the oocyte, multiple layers of cumulus granulosa cells (CGC) form the cumulus oophorus. The innermost layer of cumulus granulosa cells, designated corona radiata, penetrates by long cytoplasmic projections through zona pellucida and interacts with oocyte cytoplasmic membrane (Thibault et al, 1987)

Generally, parietal and cumulus granulosa cells in nonovulatory antral follicles display uniform morphology (Figure 1). This is characterized by round shape, large nucleus and the cytoplasm containing numerous mitochondria and poorly developed Golgi and endoplasmic reticulum (Amsterdam/Rotmensch, 1989). Such GC contain typical interphase network of microtubules (MT) and intermediate filaments (IF), built of cytokeratin and/or vimentin (Ben-Ze'ev/Amsterdam, 1989; Šutovský et al, 1993). The filamenous actin (F-actin- or microfilaments (MF) are regularly disturbed along cytoplasmic membranes of such cells.

B. Intercellular communication in preovulatory follicle

The cells inside antral follicle communicate through an extensive network of gap junctions (GJ), interconnecting the individual populations of somatic follicle cells with one another and with the oocyte (Gillula et al, 1978; Larsen et al, 1987). These transmembrane structures arise from the assembly of permeable channels called **connexons**, which are the **hexamers** of proteins belonging to the **connexin** family (Risek et al, 1990). GJs allow bidirectional exchange of ions and molecules up to 1 kDa. Formation and activity of **GJs** is regulated by differential phosphorylation of connexin molecules (Musil et al, 1990). In cattle oocyte cumulus complexes (OCC), these GJs are formed exclusively by connexin43 (Figure 2), whereas mouse granulosa cells contain also connexin32 (Šutovský et al, 1993; Validmarrson et al, 1993). The communication between oocyte and corona cells is mediated by Cx43 positive cumulus-to-oocyte GJs, found at the tips of zona spanning cytoplasmic projections (Šutovský et al, 1993).

Besides the GJs, the desmosomes, tight and intermediate junctions are present in cumulus and parietal granulosa. Similarly, the intermediate junctions interconnect the bulbous ending of the zona spanning projections of corona radiata cells with an oocyte (Paton/Collins, 1992; Thibault et al, 1987).

C. Granulosa cells/Oocyte interaction

Several transport mechanisms, established during folliculogenesis allow bidirectional exchange of metabolic and signal molecules between somatic and germinal compartment of ovarian follicle. Indeed, GCs uptake aminoacids for the oocyte and produce other metabolites necessary for oocyte growth (Haghighat/Van Winkle, 1990). GCs also seem to be a major source of substances maintaining the oocyte in meiotic arrest (Sirard/Bilodeau, 1990). Inversely, the oocyte generated signals are necessary for follicle development (Nekola/Nalbandov, 1974). Differentiation of granulosa cells to functional cumulus cells competent to synthesize ECM is critically influenced by the oocyte (Moriya et al, 1988; Vanderhyden et al, 1990).

Cumulus expansion, which is mediated through the cAMP pathway (Eppig 1989), is dependent upon a specific cumulus expansion-enabling factor (CEEF) secreted by mouse oocyte (Buccione et al, 1990; Salustri et al, 1990). It allows the cumulus cells to synthesize hyaluronic acid and undergo cumulus expansion in response to FSH or EGF (Buccione et al, 1990). The CEEF is secreted by the mouse fully grown, meiosis-arrested oocytes, maturing oocytes and metaphase II oocytes. Intrafollicularly, it causes a descending gradient of ECM synthesis from oocyte to peripheral granulosa layers (Sallustri et al, 1992). The innermost granulosa cells synthesize and deposit extracellular matrix also in the pig preovulatory follicles after LH surge. Thereafter, a limited area of the parietal granulosa is expanded and connected with the mucified cumulus (Motlík et al, 1986). Furthermore, both the ability for the cumulus oophorus to expand and the capacity for the oocytes to secrete enabling factor are temporally linked to the acquisition of competence for germinal vesicle breakdown (Vanderhyden et al, 1990).

Whereas mouse OCCs fail to expand when deprived of their included oocyte (Buccione et al, 1990), oocytectomy does not influence expansion of the porcine cumulus (Procházka et al, 1991). These data could imply that cumulus expansion does not depend on the presence of oocyte in this species. However, pig oocytes secrete a factor that enables the expansion of

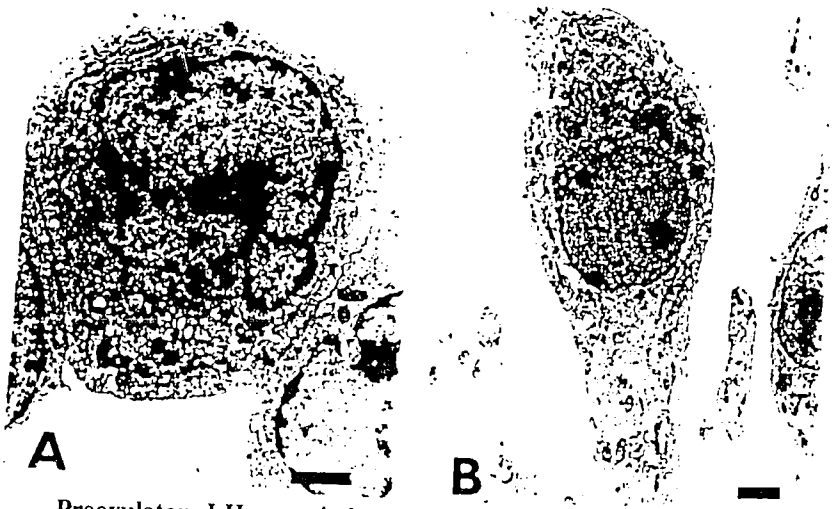

Figure 1: Preovulatory LH surge induced substantial changes in morphlogy of cumulus granulosa cells.

A) Round shaped cells in bovine cumulus oophorus isolated from preovulatory follicle before LH stimulation. The cytoplasm is regularly distributed around the nucleus and contain numerous mitochondria and poorly developed Golgi and endoplasmic reticulum (Bar = 1 μm).

B) LH-stimulated cell in an expanded cumulus oophorus forms large projection anchored at zona pellucida. The opposite pole of cytoplasm is filled with well developed ER and Golgi apparatus (Bar = 1 μm).

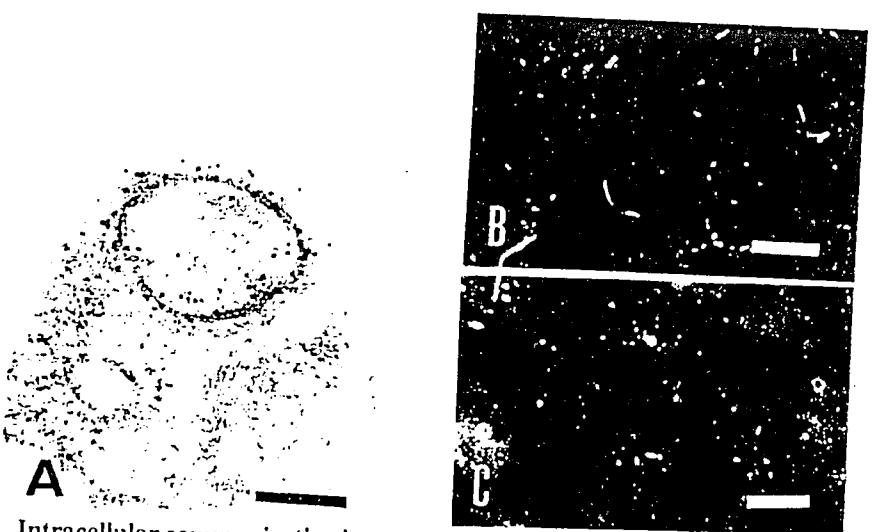

Figure 2: Intracellular communication between bovine cumulus cells is mediated by gap junctions containing connexin43.

A) A circular gap junction labelled with anti-Cx43 mouse monoclonal antibody and 10 μm colloidal gold-conjugated anti-mouse IgG (Bar = 500μm).

B, C) Indirect immunofluorescence with anti-Cx43 antibody demonstrates the redistribution of cumulus cell GJs. Where as large linear GJs interconnect the cells in unstimulated cumulus oophorus (B), dot-lik GJs are found in fully expanded one (C). (Bar = 10 μm)

111

mouse and rat oocytectomized complexes (Vanderhyden 1993). The function of this factor in promoting cumulus expansion seems to be different in rodent and pig OCCs. Even though porcine cumulus expansion in vitro is not dependent on the oocyte, the porcine oocyte is capable of secreting CEEF. In rodents the cumulus granulosa cells require to be continuously supplied with CEEF while porcine cells once primed with CEEF do not need its presence during in vitro culture and expansion induced by cAMP-elevating drugs.

III. LH-induced Expansion of Cumulus Oophorus/Rearrangement of Cumulus Cell Cytoskeleton/Secretion of Extracellular Matrix

A. Preovulatory LH peak induces multiple responses in cumulus cells

The changes in the morphology and function of GC, elicited by LH stimulation, represent final step in their differentiation (Paton/Collins, 1993). Whereas alterations of cellular metabolism occur in all layers of GC, the morphological consequences of preovulatory LH discharge are most distinct in cumulus and corona radiata cells. An initial event following LH stimulation is the assembly of microfilaments in cumulus cell cytoplasm (Figure 3). This results in the ruffling of cytoplasmic membranes and subsequent formation of small cellular projections, interconnecting cumulus granulosa cells (CGC) one with another, and long projections, anchoring them at the surface of zona pellucida (Dekel et al, 1988; Šutovský et al, 1993).

The reorganization of the microfilament network inside cumulus cell cytoplasm is followed by the redistribution of microtubules and intermediate filaments (Allworth/Albetini, 1993; Šutovský et al, 1993). Such a cooperation of individual cytoskeletal components causes the cumulus cells to acquire an elongated shape with the cytoplasmic projections oriented towards the oocyte. Gonadotropin induced rearrangement of cytoskeleton has been also shown in cultured granulosa cells (Ben-Ze'ev/Amsterdam, 1989). Concomitantly with the elongation of CGC and volumetric expansion, the GJ network undergoes substantial reorganization. Although cumulus-to cumulus cell GJs decrease in size, their number increases concomitantly with the progression of cumulus expansion. On the contrary, the GJs linking transzonal processes of CC with oolemma are removed approximately at the time of GVBD and the oocyte starts to generate cytoplasmic stores of connexin32 (Barron et al, 1980; Šutovsky et al, 1993). These events coincide with the expulsion of the bulbous endings of transzonal projections from cortical ooplasm, probably due to the actin assembly in CC and redistribution of microfilaments in oocyte cortex (Maro et al, 1984).

The cytoskeletal rearrangement in cumulus cells is accompanied by an increased secretion and deposition of cumulus extracellular matrix (ECM), rich in hyaluronic acid (Salustri et al, 1992). The increased synthesis and secretion of cumulus ECM is reflected by the development of RER and Golgi apparatus. Whereas these are poorly developed in unstimulated GC, the cells in expanded cumulus contain large stacks of Golgi and well developed RER (Rotmensch et al, 1986; Šutovský et al, 1994). The acquisition of final phenotype by cumulus granulosa cells is paralleled by the conversion of steroid metabolism from estrogen to progesterone, due to the LH-induced increase in steroidogenic activity of cholesterol side-chain cleavage enzyme P-450scc (Funkenstein et al, 1984).

112

At the ultrastructural level, the enhanced steroidogenesis and the increased turnover of steroid precursor molecule cholesterol cause the appearance of lipid droplets inside the cytoplasm (Rigby et al, 1986). Frequently, these are associated with intermediate filaments. The process of cumulus expansion is accomplished at the time when the oocyte reaches metaphase of second meiotic division. Fully expanded OCC reaches metaphase of second meiotic division. The fully expanded OCC occupies about two time-higher area than before LH stimulation (Chen et al, 1990).

B. Role of F-actin in regulation of cumulus expansion

The rearrangement of CC cytoskeleton is one of most striking events induced by LH and probably plays an essential role in determination of cumulus cell phenotype. However, the individual cytoskeletal components contribute in different ways to cumulus expansion.

Stimulation of cultured granulosa cells with FSH causes the decrease of synthesis of tubulin and vimentin remain at the level of unstimulated control. These cells remain attached to the substrate and form tight multilayered aggregates. Whereas comparable patterns of protein synthesis were found in GC stimulated by LH (hCG), this treatment resulted in disruption of actin containing stress fibers and formation of large number of cellular projection (Amsterdam/Rotmensch, 1987; Ben-Ze'ev/Amsterdam, 1989). Such behavior of GC is highly reminiscent to the redistribution of F-actin in cumulus cells at the onset of LH induced cumulus expansion. This causes extensive ruffling of cytoplasmic membranes, followed by the formation of the anastomosing network of cellular projections maintaining the cell-to cell contacts in an expansion undergoing cumulus oophorus (Šutovský et al, 1993). The disruption of microfilament cytoskeleton by dihydro-cytochalasin B inhibits cumulus expansion (Wert/Larsen, 1989). F-actin seems to participate in endocytotic removal of cumulus cell GJs after preovulatory LH peak (Larsen et al, 1979). Thus, microfilament directed GJ endocytosis is necessary for cumulus expansion. Our recent experiments revealed that cytochalasin-treatment of LH stimulated bovine OCCs does not terminate the cumulus cell-GJs redistribution, but prevents membrane ruffling and formation of cellular processes by CC. This inhibits their elongation and polarization (Šutovský et al, 1994). MF also seems to participate in the control of GC steroidogenesis since disruption of MF by cytochalasin promotes progesterone secretion by GC in absence of gonadotropin (Ben-Ze'ev/Amsterdam, 1989).

Besides of cytoskeletal function, involvement in intracellular signalling has been ascribed to actin microfilaments. Indeed, F-actin transmits the signals from ECM, when coupled with integrins, the embrane receptors of ECM glycoporteins (Luna/Hitt, 1992). This function of actin deserves particular interest because of spectacular temporal and spatial coincidence. This occurs between the redistribution of F-actin and overexpression of ECM glycoproteins in LH-stimulated bovine and murine OCCs (Šutovský et al, 1993, and unpublished data). Concomitantly with the secretion of ECM proteins, the receptors for laminin (integrin subunit $\alpha 6$) and fibronectin (integrin subunit $\beta 1$) (Figure 4) are found in the cytoplasmic membranes of bovine CGC. Moreover, the cytochalasin-treatment of LH stimulated bovine or murine OCCs suppresses the expression of ECM glycoproteins and disarranges the distribution of integrins (Šutovský et al; unpublished data). Thus, the linkage of ECM with cytoskeleton may stabilize cumulus ECM and provides very effective tool for signal transduction from cumulus cells to ECM and vice versa.

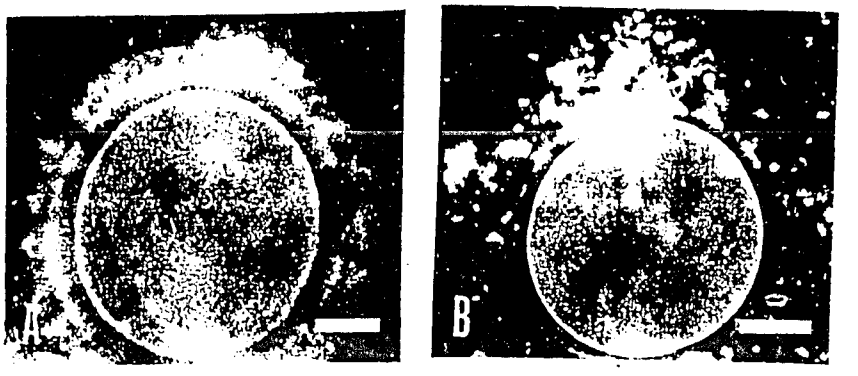

Figure 3: Microfilament assembly is an initial event throughout LH induced expansion of bovine cumulus oophorus. The labelling of filaments actin with rhodamine-conjugated phalloidin shows regular distribution of microfilaments in an unstimulated bovine OCC (A).
B) Following 6h of culture in presence of LH, the microfilaments are assembled into large bundles. Both bars = 25 μm.

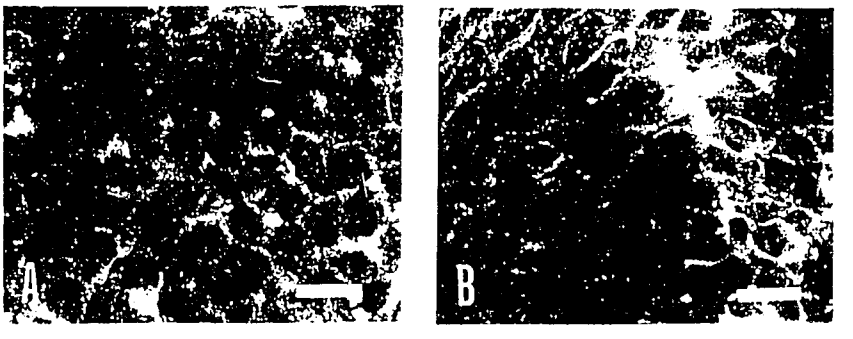

Figure 4: Expression of integrin subunit β1, occurring both laminin and fibronectin receptor, by bovine cumulus granulosa cells before LH stimulus (A) and after 24 h of culture in LH containing medium (B). The receptor was visualized by indirect immunofluorescence labelling with anti-β1 rat monoclonal antibody and FITC-conjugated anti-rat IgG. Both bars = 10 μm.

114

ECM potentiates the differentiation of cultured GC (Furman et al, 1985). Although LH receptors in GC are colocalized with cellular projections particularly rich in microfilaments (Amsterdam/Rotmensch, 1987). There is no direct association between MF and LH receptor. However, the occupation of LH receptor activates protein-kinase C (Davis et al, 1986), engaged in the assembly of MF (Phatak et al, 1988). Actin assembly is an initial step in transmission of signal from LH receptor. The association of actin with nuclear skeleton and RNA polymerase II may also suggest that actin could be involved in regulation of transcription of specific genes (Scheer et al, 1984).

C. Other cytoskeletal elements/final differentiation of cumulus granuloosa

Microtubules and intermediate filaments participate in elongation and polarization of cumulus cells during the expansion (Allworth/Albertini, 1993; Šutovský et al, 1993). In contrast to actin, gonadotropin stimulation seems to have no effect on the synthesis of tubulin, vimentin and cytokeratin by cultured GC (Amsterdam/Rotmensch, 1987). Similarly, the changes in distribution of these cytoskeletal elements during cumulus expansion are less dramatic than those occuring in F-actin. Association of microtubules with Golgi and RER, observed in expanding bovine cumulus cell (Šutovský et al, 1994) and in cultured human granulosa cells (Amsterdam et al, 1989), indicates that the MTs may monitor the reorganization of cellular organelles during GC differnetiation and cumulus expansion.

.. accumulation of lipid granules and their interaction with IFs are typical features of steroidogenic cells, possibly involving IF-directed cytoplasmic transport of steroid precursor lipid, cholesterol (Almshbobi et al, 1993). Since the MT-stabilizing compounds (taxol) reduce progesterone production by granulosa cells, the crucial role in the transport of lipids is ascribed to MTs (Carnegie et al, 1987). The lipid droplets are exclusively associated with IF (Almahbobi et al, 1993; Šutovsky et al, 1994). This discrepancy may be explained by the fact that the networks of IF and MT are closely associated and functionally linked (Skalli/Goldman, 1991).

D. Composition/organization of cumulus extracellular matrix

The main component of cumulus ECM, synthesized upon LH stimulus is hyaluronic acid (HA). This hydrophillic glycosaminoglycan forms hydrated gels that generate high osmotic pressure necessary for the spatial segregation of cumulus cells and volumetric expansion of cumulus oophorus (Dekel et al, 1979; Eppig, 1979). The enlargement of CO is contributed by the synthesis of other glycosaminoglycans and proteoglycans (Ball et al, 1982; Yanagishita/Hascall, 1987). Concomitantly with HA secretion, several new proteins appear in cumulus ECM (VIrji et al, 1990; Dandekar et al, 1992).

The ECM glycoproteins laminin, type IV collagen and fibronectin have been identified in bovine and murine cumulus ECM, predominantly localized at the surface of CGC (Šutovský et al, manuscripts in preparation). These proteins contain both domains binding to integrin membrane receptors and those displaying high affinity to HA and other ECM components (Buck/Horwitz, 1987). Such an arrangement suggests that these proteins insure the anchorage of cumulus ECM at the cytoplasmic membranes of CGC. Moreover, the link between integrins and F-actin may provide a pathway for the regulation of ECM assembly by the cytoskeleton of cumulus cells. This fits together with the hypothesis emphasizing the role of F-actin in mediation of LH stimulus. Accordingly, the treatment of LH stimulated bovine and murine OCCs with microfilament disruptor cytochalasin B decreases the expression of above listed glycoproteins and inhibits cumulus expansion (Šutovský et al, in preparation).

115

Once assembled in the extracellular spaces, cumulus ECM needs to be protected against the eventual degradation by follicular and later oviductal environment. The retention of cumulus ECM is probably insured by the presence of ECM stabilizing factor(s) in the follicular fluid (Camaioni et al, 1993). One of the most serious candidates is inter-α-trypsin inhibitor (IαI), an inhibitor of endogenous proteinases (Chen et al, 1992), isolated from mouse folliculat fluid and from fetal bovine serum, which is an essential component of culture media for in vitro maturation of mammalian OCCs.

E. Cumulus ECM/fertilization/oocyte development

The cumulus oophorus exerts a positive effect on the developmental potency of mammalian oocytes (Ball et al, 1983; Pavlok/McLaren, 1972; Staigmiller/Moor, 1984). The mechanisms of such action are unknown. Some of these effects have been ascribed to cumulus ECM. The involvement of ECM in controlling the access of sperm to the oocyte has been proposed (Cherr et al, 1990). The acrosome reaction is improved by the presence of cumulus ECM (Tesařík 1985). Moreover, the fertilization of human oocytes can be blocked by antibodies developed against a cell free preparation of human cumulus ECM (Tesařík 1989). The sperm cytoplasmic membrane contains integrin ligands (Blobel et al, 1992). It would appear that cumulus ECM facilitates sperm trapping by an ovulated OCC and/or sperm penetration through the expanded cumulus.

The glycoproteins of cumulus ECM, generated throughout the period of cumulus expansion may also influence the preimplantation stage of embryogenesis. Murine oocytes and blastocysts selectively sequestrate fibronectin (Kapur/Johnson, 1986). The addition of soluble fibronectin into culture medium significantly increases the cleavage rate of two-cell bovine embryos (Larson et al, 1992).

The growth factors (GF), present in ovarian follicles of mammals, stimulate both differentiation of granulosa cells (cumulus expansion) and oocyte maturation (Downs et al, 1988; Singh et al, 1993). Among others, insulin-like GF (IGF), epidermal GF (EGF) abd fibroblast GF (FGF) are synthesized and secreted by granulosa cells of different species (Geitshovel et al, 1989; Neufeld et al, 1987; Roy/Greenwald, 1990). The GF-binding proteins bind to laminin, type III and IV collagen and fibronectin (Jones et al, 1993). Since these ECM glycoproteins are overexpressed during cumulus expansion and associated with CGC surface (Šutovský et al, in preparation), the cumulus ECM may bind GF and thus increase and/or maintain their concentration around the preovulatory and ovulated oocyte. Besides the effect on the progression of oocyte meiotic maturation, the expand cumulus provides an essential support for the ovulated oocyte and may be an important source of metabolities utilized by the oocyte during further embryonic development.

Acknowledgements

Special thanks are due to Dr. J.E. Flechon for his stimulating discussion and critical remarks. The preliminary results presented in this manuscript have been achieved with the support of A.I.D. grant number 12.061E and grant Z 503 from Czech Ministry of Economics. Many thanks are due to our colleagues J. Kalous, J.E. Fléchon, E. Nagyová and A. Pavlok for permitting us the publication of preliminary results.

References

Allworth AE, Albertini DF (1993) Meiotic maturation in cultured bovine oocytes is accompanied by remodelling of the cumulus cell cytoskeleton. *Dev Biol* **158**:101-112

Almahbobi G, Williams LJ, Han XG, Hall PF (1993) Binding of lipid droplet and mitochondria to intermediate filaments in rat Leydig cells. *J Reprod Fert* **98**:209-217

Amsterdam A, Rotmensch S (1987) Structure-function relationship during granulosa cell differnetiation. *Endocrin Rev* **8**:309-337

Amsterdam A, Rotmensch S, Ben-Ze'ev A (1989) Coordinated regulation of morphologic and biochemical differentiation in a steroidogenic cell: The granulosa cell model. *Trends Biochem Sci* **14**:377-382

Ball GD, Bellin ME, First NL (1982) Glycosaminoglycans in bovine cumulus-oocyte complexes: Morphology and Chemistry. *Mol Cell Endocrin* **28**:113-122

Ball GD, Leibfried ML, Lenz RW, Ax RL, Bavister BD, First NL (1983) Factors affecting successful in vitro fertilization of bovine follicular oocytes. *Biol Reprod* **28**:717-725

Barron DJ, Valdimarsson G, Paul DL, Kidder GM (1989) Connexin32, a gap junction protein is a persistent oogenetic product through preimplantation development of the mouse. *Dev Genet* **10**:318-323

Ben-Ze'ev A, Amsterdam A (1989) Regulation of cytoskeletal protein organization and expression in human granulosa cells in response to gonadotropin treatment. *Endrocrinology* **124**:1033-1041

Blobel CP, Wolfsberg TG, Turck CW, Myles DG, Primakoff P, White JM (1992) A potential fusion peptide and an integrin ligand domain in a protein active in sperm-egg fusion. *Nature* **356**:248-252

Buccione R, Vanderhydnden BC, Caron PJ, Eppig JJ (1990) FSH-induced expansion of the mouse cumulus oophorus in vitro is dependent upon a specific factor(s) secreted by the oocyte. *Dev Biol* **138**:26-32

Buck CA, Horwitz AF (1987) Cell surface receptors for extracellular matrix molecules. *Ann Rev Cell Biol* **3**:179-205

Byskov AG (1974) Does the rete ovarii act as a trigger for the onset of meiosis? *Nature* **252**:396

Camaioni A, Hascall VC, Yanagishita M, Salustri A (1993) Effect of exogenous hyaluronic acid and serum on matrix organization and stability in the mouse cumulus cell-oocyte complex. *J Biol Chem* **268**:20473-20481

Carnegie JA, Dardick I, Tsang BK (1987) Microtubules and gonadotropic regulation of granulosa cell steroidogenesis. *Endocrinology* **120**:819-828

Chen L, Mao SJT, Larsen WJ (1992) Identification of a factor in fetal bovine serum that stabilizes the cumulus extracellular matrix. *J Biol Chem* **267**:12380-12386

Chen L, Wert SE, Hendrix M, Russel PT, Cannon M, Larsen WJ (1990) Hyaluronic acid synthesis and gap junction endocytosis are necessary for normal expansion of the cumulus mass. *Mol Reprod Dev* **26**:236-247

Cherr GN, Yudin A, Katz DF (1990) Organization of the hamster cumulus extracellular matrix: A hyaluronate-glycoprotein gel which modulates sperm access to the oocyte. *Develop Growth Differ* **32**:353-365

Dandekar P, Aggeler J, Talbot P (1992) Structure, distribution and composition of the extracellular matrix of human oocytes and cumulus masses. *Human Reprod* **7**:391-398

Davis JS, Weaklanf LL, West LA, Farese RV (1986) Luteinizing hormone stimulates the formation of inositol triphosphate and cyclic AMP in rat granulosa cells. Evidence for phospholipase C generated second messengers in the action of luteinizing hormone. *Biochem J* **238**:567-604

Dekel N, Hillensjo Y, Kraicer PF (1979) Maturation effects of gonadotropins on the cumulus-oocyte complex of the rat. *Biol Reprod* **20**:191-197

Dekel N (1988) Regulation of oocyte maturation by cell to cell communication. In: Cell to cell communication in endocrinology. Serono symposia publication, Raven Press, 1988, **49**:181-194

Downs SM, Daniel SAJ, Eppig JJ (1988) Induction of maturation in cumulus enclosed mouse oocytes by follicle stimulating hormone and epidermal growth factor: evidence for a positive stimulus of somatic cell origin. *J Exp Zool* **245**:86-96

Eppig JJ (1979) FSH stimulates hyaluronic acid synthesis by oocyte-cumulus cell complex from mouse preovulatory follicles. *Nature* **281**:483-484

Funkenstein B, Waterman MR, Simpson ER (1984) Induction of synthesis of cholesterol side chain cleavage cytochrome ^P-450 and adrenodoxin by follicle-stimulating hormone 8-bromo-cyclic AMP, and low density lipoprotein in cultured bovine granulosa cells. *J Biol Chem* **259**:8572-8577

Furman A, Rotmensch S, Kohen F, Mashiach S, Amsterdam A (1985) Regulation of rat granulosa cell differntiation by extracellular matrix produced by bovine corneal endothelial cells. *Endocrinology* **118**:1878-1886

Geitshovel F, Moretti-Rojas I, Asch RH, Rojas FJ (1989) Expression of insulin-like growth factor-II (IGF-II) messenger ribonucleic acid (mRNA), but not IGF-I mRNA, in human preovulatory cells. *Human Reprod* **4**:899-902

Gilula NB, Epstein ML, Beers WH (1978) Cell-to-cell communication and ovulation. *J Cell Biol* **78**:58-75

Haghighat N, van Winkle LJ (1990) Developmental change in follicular cell-enhanced amino acid uptake into mouse oocytes that depends on intact gap junctions and transport system gly. *J Exp Zool* **253**:71-82

Jones JI, Gockerman A, Busby WH Jr, Camacho-Hubner C, Clemmons DR (1993) Extracellular matrix contains insulin-like growth factor binding protein-5: Potentiation of the effect of IGF-I. *J Cell Biol* **121**:679-687

Kapur RP, Johnson LV (1986) Selective sequestration of an oviductal fluid glycoprotein i the periviteline space of mouse oocytes and embryos. *J Exp Zool* **238**:249-260

Larsen WJ, Tung HN, Murray SA, Swenson CA (1979) Evidence for the participation of actin microfilaments and bristle coats in the internalization of gap junction membrane. *J Cell Biol* **83**:576-587

Larsen WJ, Wert SE, Brunner GD (1987) Diffrential modulation of rat follicle cell gap junction populations at ovulation. *Dev Biol* **122**:61-71

Larson RC, Ignotz GG, Currie WB (1992) Effect of fibronectin in early embryo development in cows. *J Reprod Fert* **96**:289-297

Luna EJ, Hi Al (1992) Cytoskeleton-plasma membrane interactions. *Science* **258**:955-964

Maro B, Johnson MH, Pickering S, Flash G (1984) Changes in actin distribution uring fertilization of the mouse egg. *J Embryol Exp Morphol* **81**:211-237

Moriya S, Tanaka T, Okada Y, Kikucho T, Fujimoto S, Ichinone K (1988) Influence of the oocyte upon proliferation, differentiation and steroidogenesis of cultured granulosa cells. In: "Preservation of tubo-ovarian function in gynecologic benign and malignant diseases", Serono Symp Publ, Vol 48, Raven Press, New York, pp 146-161

Motlík J, Fulka J, Fléchon JE (1986) Changes in intercellular coupling between pig oocytes and cumulus cells during final maturation in vivo and in vitro. *J Reprod Fert* **76**:31-37

Musil LS, Cunningham BA, Edelamn GM, Goodenough DA (1990) Differential phosphorylation of the gap junction protein connexin43 in junctional communication-competent and deficient cell lines. *J Cell Biol* **111**:2077-2088

Nekola MV, Nalbandov (1971) Morphological changes of rat follicular cells as influenced by oocyte. *Biol Reprod* **4**:154-160

Neufeld G, Ferrara N, Schveigerer LI, Mitchell R, GOspodarowicz D (1987) Bovine granulosa cells produce basic fibroblast growth factor. *Endocrinology* **121**:597-603

Paton AC, Collins WP (1992) Differentiation processes of granulosa cells. *Oxford Rev Reprod Biol* **14**:168-223

Pavlok A, Mc Laren A (1972) The role of cumulus cells and the zona pellucida in the fertilization of mouse eggs in vitro. *J Reprod Fert* **29**:91-97

Phatak PD, Packman CH, Lichtman MA (1988) Protein kinase C modulates actin conformation in human T lympnocytes. *J Immunol* **141**:2929-2938

Procházka R, Nagyová E, Rimkevičová Z, Nagai T, Kikuchi K, Motlík J (1991) Lack of effect of oocyetctomy on expansion of the porcine cumulus. *J Reprod Fert* **93**:569-576

Rigby BW, Workman J, McLean M, Hanzely L, Lewitz-Rigby F (1986) Morphometric analysis of in vivo development of porcine ovarian granulosa cells in preovulatory antral follicle. *Cytobios* **45**:17-24

Risek B, Guthrie S, Kumar N, Gilula NB (1990) Modulation of gap junction transcript and protein expression during pregnancy in the rat. *J Cell Biol* **110**:269-282

Rotmensch S, Dor J, Furnam A, Rudak E, Mashiach S, Amsterdam A (1986) Ultrastructural characterization of human granulosa cells in stimulated cycles: Correlation with oocyte fertilizability. *Fertil Steril* **45**:671-679

Roy SK, Greenwald GS (1990) Immunohistochemical localization of epidermal growth factor-like activity in the hamster ovary with a polyclonal antibody. *Endocrinology* **126**:1309-1317

Salustri A, Yanagishita M, Hascall VC (1990) Mouse oocytes regulate hyaluronic acid synthesis and mucification by FSH-stimulated cumulus cells. *Dev Biol* **138**:26-32

Salustri A, Yanagishita M, Underhill CB, Laurent TC, Hascall VC (1992) Localization and synthesis of hyaluronic acid in the cumulus cells and mural granulosa cells of the preovulatory follicle. *Dev Biol* **151**:541-551

Scheer U, Hinssen H, Franke W, Jockysch B (1984) Micro-injection of actin-binding proteins and actin antibodies demonstrated involvement of nuclear actin in transcription of lampbruch chromosomes. *Cell* **39**:111-222

Sirard [illegible]) Granulosa cells inhibit the resumption of meiosis in bovine oocytes in vitro. *Biol Reprod* **43**:777-783

Skalli O, Goldman RD (1991) Recent insights into the assembly, dynamics, and function of intermediate filament networks. *Cell Motil Cytoskelet* **19**:67-79

Staigmiller RB, Moor RM (1984) Effect of follicle cells on the maturation and developmental competence of ovine oocytes matured outside the follicle. *Gamete Res* **9**:221-229

Šutovský P, Fléchon JE, Pavlok A (1994a) Microfilaments, microtubules and intermediate filaments fulfil differential roles in gonadotropin-induced expansion of bovine cumulus oophorus. *Reprod Nutr Develop* Submitted

Šutovský P, Fléchon JE, Fléchon B, Motlík J, Peynot N, Chesné P, Heyman Y (1993) Dynamic changes of gap junctions and cytoskeleton during in vitro culture of cattle oocyte cumulus complexes. *Biol Reprod* **49**:1277-1287

Tesařík J (1985) Comparison of acrosome reaction-inducing activities of human cumulus oophorus, follicular fluid and ionophore A23187 in human sperm populations of proven fertilizing ability in vitro. *J Reprod Fert* **74**:383-388

Tesařík J (1989) Immunoinhibition of human fertilization in vitro by the antibodies to the cumulus oophorus intercellular matrix. *J Reprod Fert* **87**:193-198

Thibault C, Szollosi D, Gerard M (1987) Mammalian oocyte maturation. *Reprod Nutr Develop* **27**:865-896

Toole BP, Goldberg RL, Chi-Rosso G, Underhill CB, Orkin RW (1984) Hyaluronate-cell interactions. In: The role of extracellular matrix in development. RL Trelstad (Ed), pp 43-66, Alan Liss, New York

Valdimarsson G, De Sousa PA, Kidder GM (1993) Coexpression of gap junction proteins in the cumulus-oocyte complex. *Mol Reprod Dev* **36**:7-15

Vanderhyden BC, Caron PJ, Buccione R, Epigg JJ (1990) Developmental pattern of the secretion of cumulus expansion-enabling factor by mouse oocytes and the role of oocytes in promoting granulosa cell differentiation. *Dev Biol* **140**:307-317

Vanderhymden BC (1993) Species differences in the regulation of cumulus expansion by an oocyte-secreted factor(s). *J Reprod Fertil* **98**:219-227

Virji N, Philips DM, Dumbar BS (1990) Identification extracellular matrix proteins in the rat cumulus oophorus. *Mol Reprod Dev* **25**:339-344

Wert SE, Larsen WJ (1989) Meiotic resumption and gap junction modulation in the cultured rat cumulus-oocyte complexes. *Gamete Res* **22**:143-162

Yanagishita M, Hascall VC (1987) Proteoglycan metabolism by rat ovarian granulosa cell *in vitro*. In: Biology of extracellular matrix: A series Biology of proteoglycans. Wright TN & Mecham RP (Eds), Academic Press, Orlando, USA

Reprod Nutr Dev (1994) 34, 415-425
© Elsevier/INRA

Original article

Microfilaments, microtubules and intermediate filaments fulfil differential roles during gonadotropin-induced expansion of bovine cumulus oophorus

P Šutovský [1#], JE Fléchon [2*], A Pavlok [1]

[1] *Institute of Animal Physiology and Genetics, Czech Academy of Sciences, 27721 Liběchov, Czech Republic;*
[2] *INRA, Laboratoire de Biologie Cellulaire et Moléculaire, 78350 Jouy-en-Josas, France*

(Received 12 April 1994; accepted 4 July 1994)

Summary — The relationship between cytoskeleton and morphology of cumulus granulosa cells in expanding bovine oocyte–cumulus complexes (OCCs) cultured *in vitro* has been investigated by the means of indirect immunofluorescence and transmission electron microscopy. The round-shaped cells in unstimulated control OCCs displayed a homogeneous distribution of cytoskeletal networks and cytoplasmic organelles. Luteinizing hormone (LH) stimulation caused the redistribution of microfilaments (MFs), accelerated the development of Golgi apparatus, and led to the generation of lipid droplets in cumulus cells. These changes culminated in the elongation and polarization of cumulus cells and in the extension of the cytoplasmic networks of microtubules (MTs) and intermediate filaments (IFs) into the newly formed cytoplasmic projections. The culture of OCCs in the presence of microfilament disruptor cytochalasin B prevented cumulus expansion, formation of cellular projections and cell elongation and suppressed the development of the Golgi apparatus. On the contrary, cytochalasin had no effect on the abundance and distribution of lipid droplets and on the integrity of IFs and MTs. The present data support the hypothesis that the response of cumulus granulosa cells to LH is partially mediated by F-actin.

cumulus expansion / oocyte maturation / cytoskeleton / F-actin / tubulin / vimentin

Résumé — Les microfilaments, les microtubules et les filaments intermédiaires jouent des rôles différents pendant l'expansion du cumulus oophorus bovin induit par les gonadotropines. *Les rapports entre le cytosquelette et la morphologie des cellules de la granulosa dans les complexes ovocytes cumulus (OCCs) bovins cultivés* in vitro *ont été analysés à l'aide des techniques d'immunofluorescence et de microscopie électronique à transmission. Dans les OCCs témoins non*

* Correspondence and reprints.
# Present address: University of Wisconsin, Department of Zoology, 1117, West Johnson Street, Madison, WI 53706, USA

120

expansés, les cellules arrondies montrent une distribution homogène du cytosquelette et des organites cellulaires. La stimulation par l'hormone lutéinisante (LH) provoque la redistribution des microfilaments (MFs), le développement de l'appareil de Golgi et le dépôt de gouttelettes lipidiques dans les cellules du cumulus. Ces modifications aboutissent à l'élongation et à la polarisation des cellules et à l'extension des réseaux de microtubules (MTs) et de filaments intermédiaires (IFs) dans les nouvelles projections cytoplasmiques. La culture d'OCCs, en présence de cytochalasine B qui bloque la polymérisation des microfilaments, empêche l'expansion du cumulus, la formation de projections cytoplasmiques et l'élongation cellulaire et inhibe le développement de l'appareil de Golgi. Au contraire, la cytochalasine n'a pas d'effet sur l'accumulation et la distribution de gouttelettes lipidiques ni sur l'intégrité des IFs et des MTs. Les résultats obtenus sont en faveur d'une transmission partielle par l'actine F de la réponse à la LH des cellules du cumulus oophorus.

expansion du cumulus / maturation ovocytaire / cytosquelette / actine F / tubuline / vimentine

INTRODUCTION

The expansion of cumulus oophorus seems to be a necessary preliminary step for the release of matured mammalian oocytes from ovarian follicles (Dekel *et al*, 1979). Until now, cumulus expansion has been considered as a consequence of the increased synthesis and deposition of hyaluronic acid-rich extracellular matrix by the innermost population of granulosa cells, termed cumulus cells. This has been supposed to cause the volumetric enlargement of cumulus oophorus, the spatial isolation of cells from one another, and the interruption of transport pathway between oocytes and somatic follicle cells (Eppig, 1980; Larsen *et al*, 1986). Consequently, meiotic resumption has been explained by the cessation of the uptake of granulosa cell-generated inhibitory molecules into the oocyte, due to the down-regulation of cumulus cell gap junctions (Larsen *et al*, 1987).

In contrast with these findings, the recent studies of Allworth and Albertini (1993) and Šutovský *et al* (1993) demonstrated that the LH-induced expansion of bovine cumulus oophorus involved dramatic cytoskeletal rearrangement, gradually affecting all the cytoskeletal components of cumulus cells including microfilaments (MFs), intermediate filaments (IFs) and microtubules (MTs). Moreover, the preovulatory rearrangement of gap junctions seems to have no effect on the efficiency of gap junctional communication between the cells of the expanded cumulus oophorus (Šutovský *et al*, 1993). The involvement of the cytoskeleton in cumulus expansion is supported by the finding that the microfilament disruptor dihydrocytochalasin B or its analogues cytochalasin B, cytochalasin D, inhibit cumulus expansion (Wert and Larsen, 1989). These facts may be related to the hypothesis that the effect of LH on granulosa cells *in vitro* is partially mediated by F-actin (Ben Ze'ev and Amsterdam, 1989).

The present work is aimed at deducing the relationship between the reorganization of the cytoskeleton and the process of cumulus cell differentiation throughout the period of cumulus expansion *in vitro*. The present data provide evidence that individual cytoskeletal components play differential roles during cumulus expansion and support the idea that F-actin is involved in the transduction of LH-induced signals inside cumulus cells.

MATERIALS AND METHODS

Isolation and in vitro *culture of bovine oocyte–cumulus complexes*

Bovine ovaries were collected at a local slaughterhouse and used for isolation of oocyte–cumu-

12

lus complexes (OCCs) from large antral follicles 2–8 mm in diameter. Part of OCCs were cultured for up to 24 h in modified M199 culture medium (Pavlok *et al*, 1992), supplemented with 10% fetal calf serum (Flow Laboratories) ± 0.4 mg/ml LH. The other part of OCCs was cultured in the above culture medium with addition of 5–20 mg/ml of cytochalasin B. The culture was carried out at 39°C in a humid atmosphere enriched by 5% CO_2. Freshly isolated OCCs and OCCs withdrawn from culture at intervals of 3 h were processed for immunofluorescence or electron microscopy.

We will term the cells from freshly isolated OCCs at time 0 (t0) unstimulated cumulus cells. The results were the same with OCCs cultured without LH (data not shown).

Immunofluorescence

The OCCs were fixed for 20 min in 2.5% paraformaldehyde dissolved in washing medium (phosphate-buffered saline, ph 7.3), treated for 1 h with a solution of 50 mM ammonium chloride to eliminate free aldehydic groups, rinsed and conserved in washing medium containing 0.05% sodium azide and 1 mM phenylmethylsulfonyl fluoride. A 2-step indirect immunocytochemical procedure including saponin permeabilization was applied as described previously (Šutovský *et al*, 1993). To visualize the Golgi apparatus, we used the anti-Golgi CTR433 mouse monoclonal antibody recognizing a Triton X-100 extractable antigen of the medium compartment in the Golgi (Jasmin *et al*, 1989). This antibody, kindly provided by M Bornens (CNRS, Gif-sur-Yvette, France), was diluted to 1:5. MTs were visualized by TU 01 mouse monoclonal antibody (Viklický *et al*, 1982), diluted 1:20. This was kindly provided by V Viklický (Institute of Molecular Genetics, Praha, Czech Republic). This antibody recognizes bovine α-tubulin (Dráber *et al*, 1986). An anti-vimentin mouse monoclonal antibody (Sigma, Saint Louis, MO; diluted 1:200), given as highly specific for bovine cells, was used for the visualization of IFs. Negative controls were obtained by the omission of all the first antibodies. The microfilaments were labelled by rhodamine-conjugated phalloidin (Molecular Probes, Eugene, OR). The oocyte nuclear maturation was assessed by staining cumulus-free oocytes with Hoechst 33258 (5 μg/ml). The OCCs were examined and photographed with a fluorescence microscope (Polyvar-Reichert Jung or Orthoplan-Leitz).

Electron microscopy

The OCCs were fixed for 1 h in a mixture composed of 0.6% paraformaldehyde and 2.5% glutaraldehyde in PBS, postfixed in 1% osmium tetroxide, dehydrated by ethanol, perfused and embedded in Epon 812 (Serva, Heidelberg, Germany). Epon blocks with the samples were cut with the ultramicrotome Reichert-Jung Ultracut E, contrasted by uranyl acetate and lead citrate and observed with a Jeol 1200 EX electron microscope.

RESULTS

Effect of LH stimulus and cytochalasin B on the morphology of bovine cumulus granulosa cells

The round-shaped cumulus cells in the unstimulated (t0) OCCs displayed a homogeneous constitution of the cytoplasm, containing large mitochondria, rough endoplasmic reticulum (RER) and rare lipid droplets (fig 1A, B). Numerous small microvilli were found at the surface of these cells (fig 1A). A 24-h culture in the presence of LH induced the expansion of cumulus oophorus and the extension of intercellular spaces. The cells acquired an elongated shape, characterized by the polarization of cytoplasm and the formation of a large radially oriented cellular projections (fig 1C). These projections contained mainly bundles of IFs and MTs (fig 1D), but the opposite cytoplasmic pole was generally occupied by large clusters of lipid droplets, a well-developed Golgi apparatus and abundant RER profiles (fig 1E, 4C). This development of the Golgi apparatus has also been demonstrated by immunofluorescent labelling with the CTR433 antibody. In con-

122

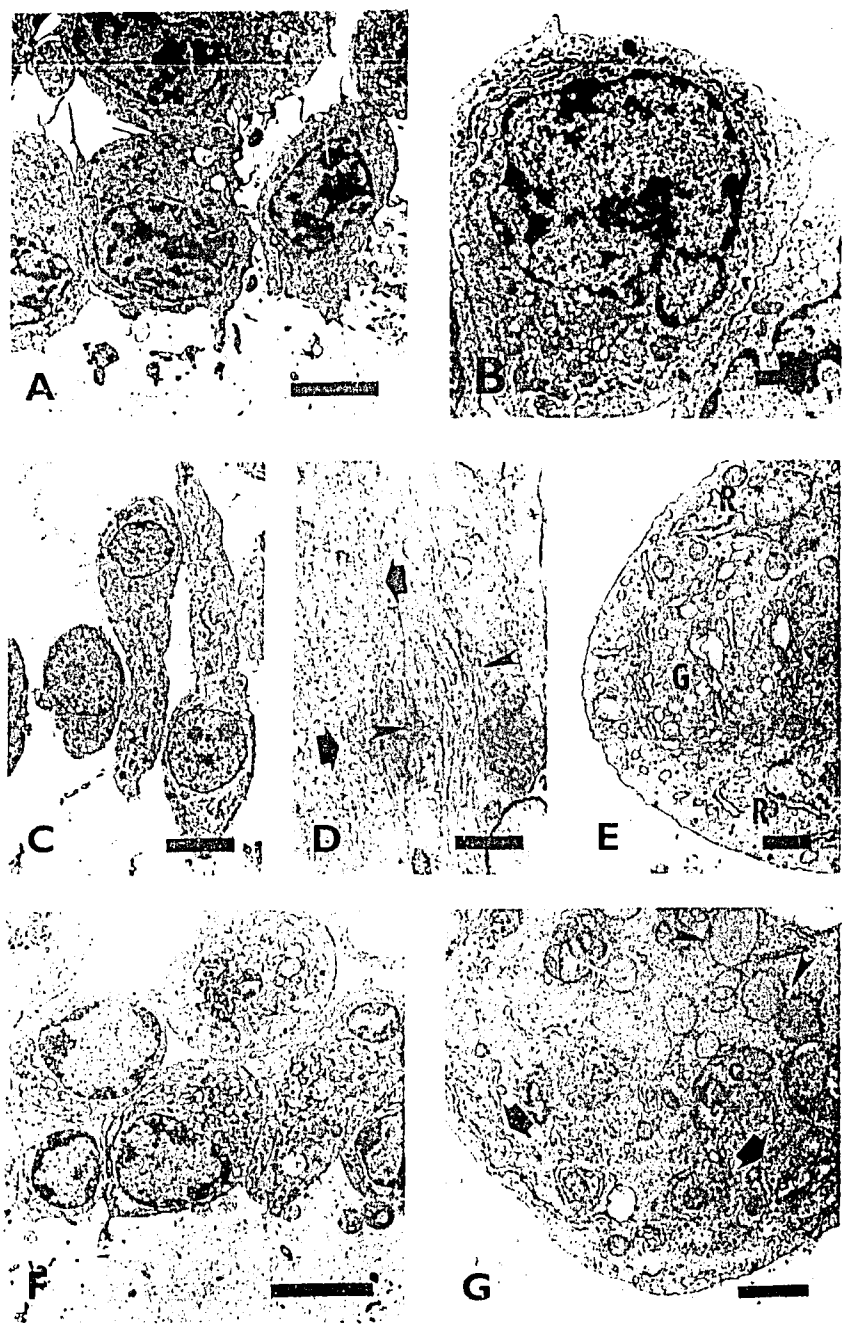
A
B
C
D
E
R
G
R
F
G

trast with the diffuse or dispersed Golgi complex in unstimulated cumulus cells (fig 2A) or cells cultured in the presence of cytochalasin B (fig 2C), the cells in expanded cumuli contained strongly labelled perinuclear caps of Golgi apparatus (fig 2B). The OCCs cultured for 24 h in LH-containing medium with 20 μg/ml of cytochalasin B failed to expand and their cells retained a round shape and were devoid of microvilli and large projections (fig 1F). Randomly distributed rough endoplasmic reticulum poorly developed Golgi and numerous lipid droplets were regularly observed in the cytoplasm of these cumulus cells (fig 1G).

Distribution of actin microfilaments

Rhodamine-phalloidin staining demonstrated a regular distribution of F-actin at the cell periphery of unstimulated cumulus cells (fig 3A, B). Following 6 h of culture, a time point coinciding with oocyte germinal vesicle breakdown, MF assembly occurred in the cytoplasm (fig 3C). This caused extensive ruffling all along the plasma membranes and subsequent formation of large cellular projections (fig 3F). After 24 h of culture, the MFs were assembled in individual foci, coinciding with cytoplasmic projections (fig 3D). The addition of 5 μg/ml cytochalasinB to gonadotropin-supplemented medium was sufficient to block F-actin assembly in the OCCs cultured for 6–9 h. However, doses as high as 20 μg/ml of cytochalasin B were necessary to block cumulus expansion for 24 h. This treatment caused the emergence of large actin bundles in the cytoplasm of cumulus cells (fig 3E).

Microtubules and intermediate filaments

Immunofluorescence revealed regular networks of MTs and IFs in the cytoplasm of unstimulated cumulus cells (figs 4A, 5A). Following culture in the presence of LH, the organization of MTs and IFs reflected the alterations of cellular morphology. The IFs and MTs extended into the radial projections of cumulus cells within the expanded cumulus (figs 4B, 5B). As was the case before stimulation, neither MTs nor IFs of corona radiata cells could be detected in the zona spanning projections (fig 4C). At the ultrastructural level, the MTs were also associated with the stacks of the Golgi apparatus (fig 4D). The clusters of lipid droplets, appearing as a consequence of LH stimulus, were regularly embedded in large bundles of IFs (fig 5C).

The IFs were often closely associated with these droplets (fig 5D) and with the nuclear envelope (fig 5E). The treatment with cytochalasin D did not induce aggre-

Fig 1. Effect of cytochalasin B on the expansion of cumulus oophorus and the elongation and polarization of cumulus granulosa cells. **(A)** Cells in unstimulated OCCs (*t0*) are round and possess numerous small microvilli. Corona cells show frequent transzonal processes, bar = 5 μm. **(B)** The cytoplasm of such cells contains numerous mitochondria, RER and Golgi, bar = 1 μm. **(C)** The cells in an expanded OCC, cultured for 24 h in the presence of LH, form large radially oriented cytoplasmic projections, bar = 5 μm. **(D)** These projections are mainly occupied by longitudinally arranged microtubules (arrows) and intermediate filaments (arrowheads), bar = 200 nm. **(E)** The perinuclear region of an elongated cumulus cell is occupied by a well-developed Golgi apparatus (G) and RER (R), bar = 1 μm. **(F)** The cells in an OCC cultured for 24 h in LH-supplemented medium with 20 μg/ml of cytochalasin B are tightly packed and lack the microvilli and cytoplasmic projections, bar = 5 μm. **(G)** Treatment with cytochalasin B did not affect the accumulation of lipid droplets (arrowheads) and randomized the distribution of RER (arrows) in the cytoplasm. The Golgi apparatus is not developed, bar = 1 μm. In micrographs **A**, **C** and **F**, the zona pellucida is located at the bottom of the micrograph.

124

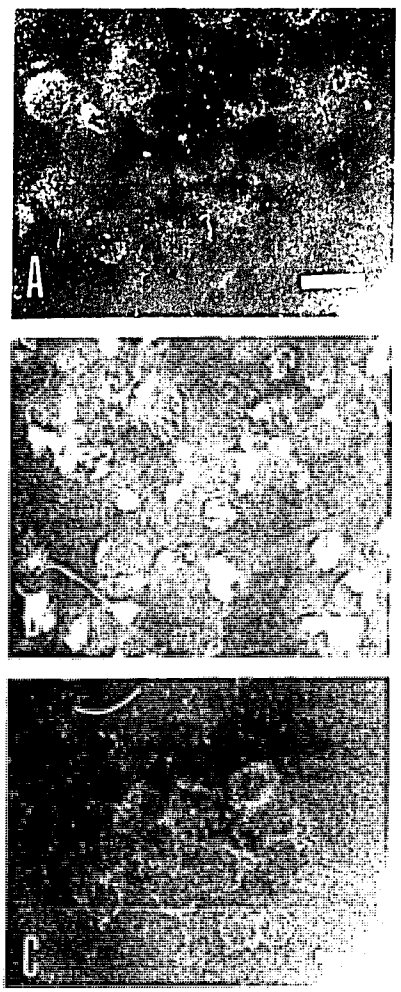

Fig 2. Distribution of the Golgi apparatus in bovine cumulus cells, demonstrated with CTR 433-antibody. **(A)** Diffuse labelling of the Golgi apparatus in unstimulated OCC (t0). **(B)** Well-developed Golgi stacks are assembled in one pole of cumulus cell after 24 h of culture. **(C)** The addition of cytochalasin B to LH-supplemented medium prevents the development and polarization of the Golgi apparatus, bar = 10 μm for each micrograph.

gates of MTs, or IFs as for MFs, and did not affect their association with organelles.

DISCUSSION

Cumulus expansion is the final step in the differentiation of cumulus granulosa cells (Paton and Collins, 1992), including the acceleration of extracellular matrix synthesis, cytoskeletal rearrangement, redistribution of gap junctions and volumetric enlargement of the cumulus oophorus. These changes result in the polarization and elongation of cumulus cells, allowing them to maintain intercellular communications inside the expanded cumulus oophorus (Allworth and Albertini, 1993; Šutovský *et al*, 1993).

Recently, we showed that the alterations in cumulus cell morphology and cumulus expansion are preceded by an extensive rearrangement of MFs in their cytoplasm, suggesting an important, if not crucial role of F-actin in the control of cumulus expansion (Šutovský *et al*, 1993). Whereas previous studies proposed that MFs could promote cumulus expansion by directing the endocytotic removal of cumulus cell gap junctions (Wert and Larsen, 1989; Chen *et al*, 1990), our recent results indicate that MFs are not directly associated with these junctions (Šutovský *et al*, 1993) and that cytochalasin treatment prevents cumulus expansion by suppressing membrane ruffling and subsequent polarization and elongation of cumulus cells (this study). The above data corroborate the studies on cultured granulosa cells, showing that gonadotropin-stimulation disrupts F-actin cytoskeleton, decreases the expression of actin and α-actinin and elicits important alterations of cellular morphology and function (Ben Ze'ev and Amsterdam, 1989). On the contrary, we have not observed a direct effect of LH on IFs and MTs before cell elongation. Similarly, the gonadotropin stimulation of cultured granulosa cells does not affect the

125

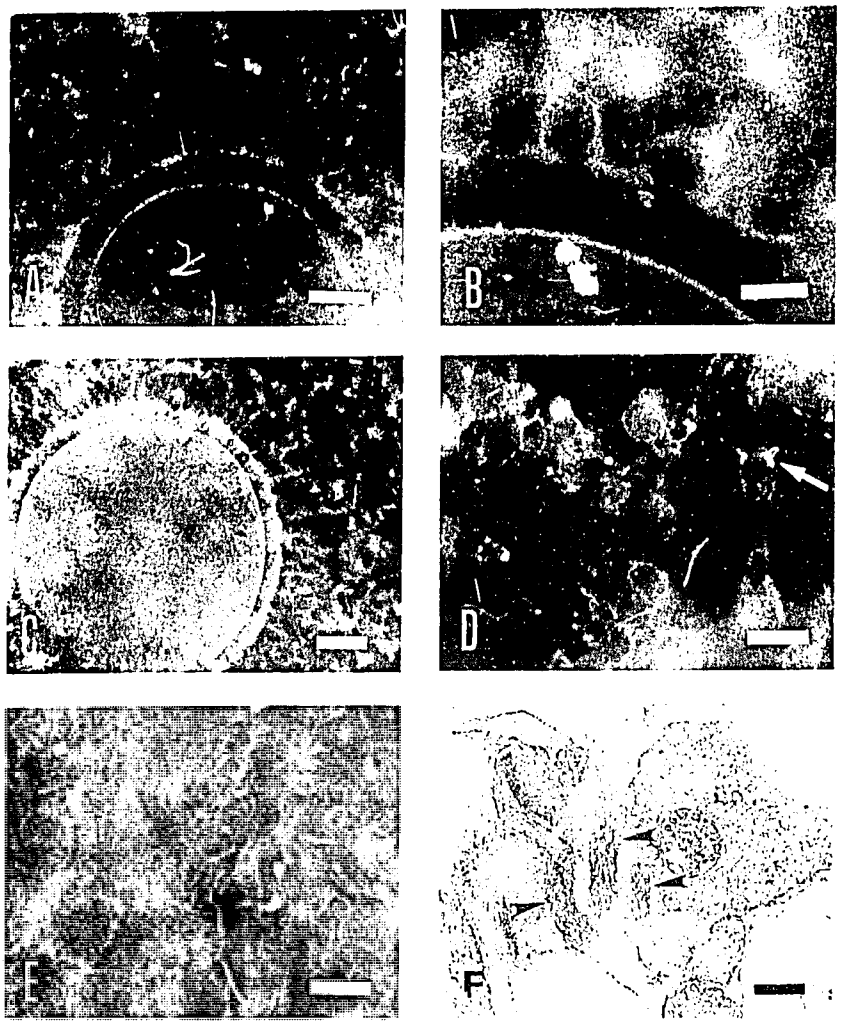

Fig 3. Dynamics of microfilaments during LH-induced cumulus expansion, demonstrated by rhodamine–phalloidin staining (A–E) and electron microscopy (F). **(A)** Regular distribution of F-actin in unstimulated OCC (t0), bar = 20 μm. **(B)** Detail of an unstimulated OCC, showing uniform distribution of F-ac[illegible] along the plasma membranes of cumulus cells. F-actin is also visible in zona-spanning projections of corona cells, bar = 10 μm. **(C)** Massive redistribution of F-actin occurs in cumulus cells within first 6 h culture in the presence of LH, bar = 20 μm. **(D)** After 24 h of culture, the MFs are assembled in individual foci (arrow) at the foot of the cytoplasmic projections, bar = 20 μm. **(E)** Cytochalasin B treatment causes dispersion of MFs and formation of stress fibre-like bundles in cumulus cell cytoplasm, bar = 10 μm. **(F)** Membrane ruffles in an OCC cultured for 6 h are loaded by large bundles of MFs (arrowheads), bar = 200 nm.

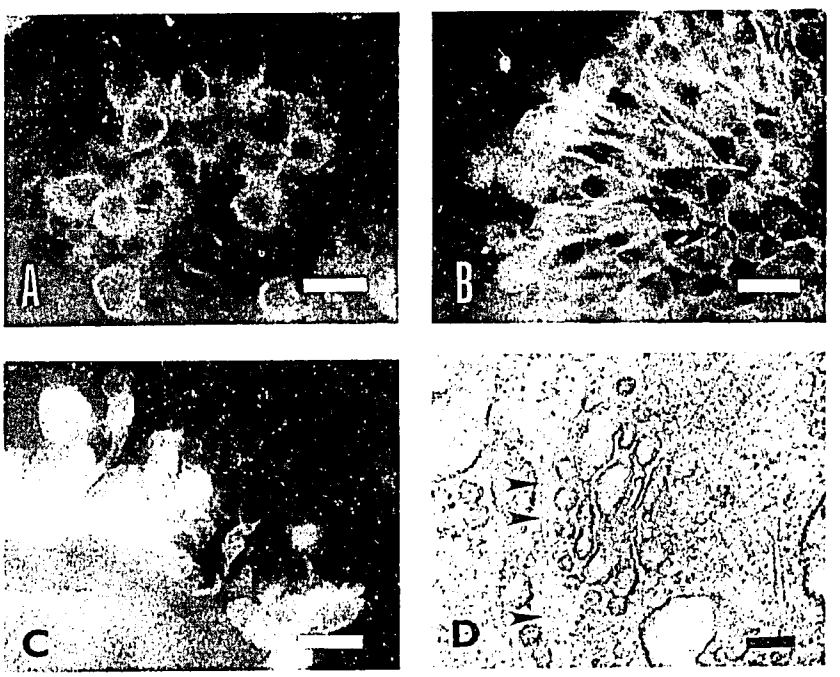

Fig 4. Immunofluorescent and ultrastructural localization of microtubules in bovine OCCs. The MTs form perinuclear networks in both unstimulated **(A)** and expanded **(B)** complexes. In **B**, the long cytoplasmic projections also contain MTs. **(C)** No positivity to tubulin could be seen inside zona pellucida and periviteline space before (not shown) or after expansion. **(D)** At the ultrastructural level, the MTs (arrowheads) are frequently associated with the Golgi apparatus, bar = 20 μm for micrographs **A–C** and 100 nm for **D**.

expression of tubulin, vimentin and cytokeratin (Ben Ze'ev and Amsterdam, 1987). As well as cAMP-dependent protein kinase (PK-A), the LH receptor activates the phospholipase C-dependent regulatory pathway (PK-C), which induces the assembly of F-actin (Davis *et al*, 1986; Phatak *et al*, 1988). Moreover, LH-receptor distribution coincides with actin-loaded compartments of cytoplasmic membranes in granulosa cells (Amsterdam and Rotmensch, 1987). Altogether, these data strongly suggest that F-actin mediates the response of cumulus cells to gonadotropins, influences the acquisition of final phenotype by these cells, and regulates cumulus expansion.

The generation of lipid droplets associated with IFs is a typical feature of steroidogenic cells, such as Leydig cells (Almahbodi *et al*, 1993) and granulosa cells (Silberzahn *et al*, 1985). Their accumulation in granulosa cells reflects the increased turnover of precursor lipid cholesterol during the LH-induced conversion from estrogen

127

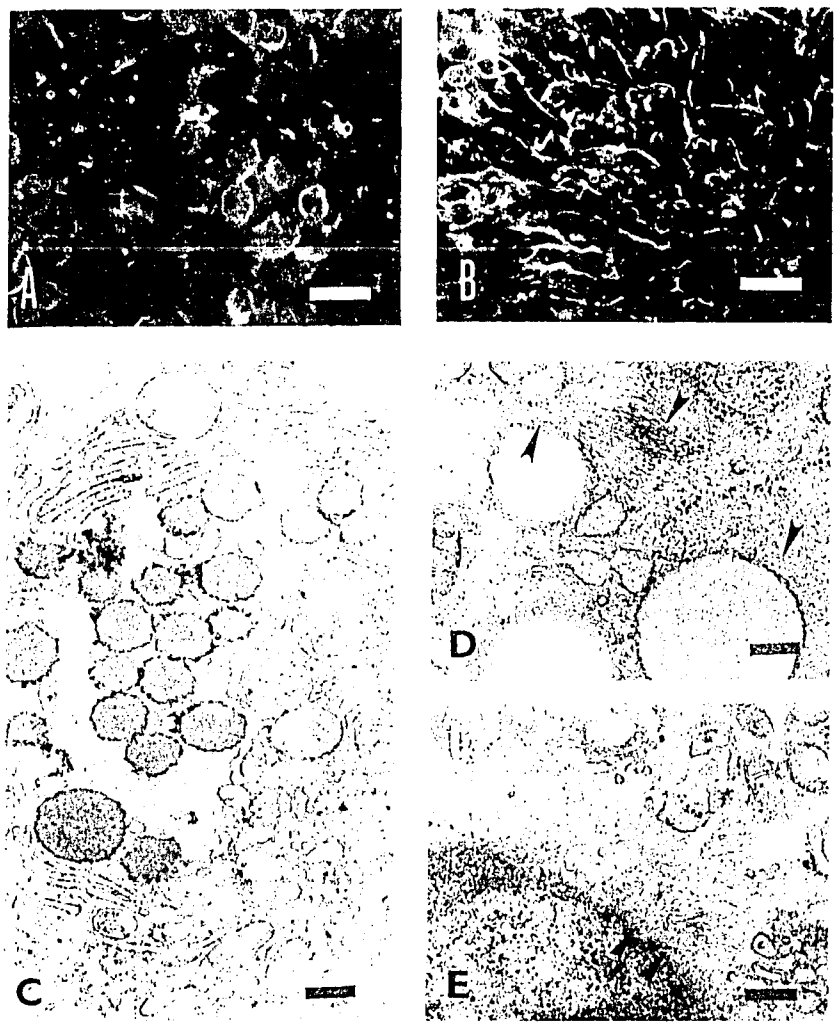

Fig 5. The distribution of IFs parallels that of MTs in cumulus cells of unstimulated (I0) **(A)** and matured OCCs **(B)**, bar = 20 μm for **A** and 30 μm for **B**. **(C)** Large clusters of lipid droplets are surrounded by bundles of IFs in cumulus cells of an OCC cultured for 24 h in LH-containing medium, bar = 500 nm. **(D)** In such cells, the IFs (arrowheads) are closely associated with lipid droplets, bar = 200 nm. **(E)** Sagittal section of the cell nucleus in an expanded OCC. Note apparent binding of IFs to the nuclear envelope (arrowheads), bar = 200 nm.

128

synthesis towards the secretion of progesterone (Collins *et al*, 1991). Intracellular transport of cholesterol was found to be vimentin dependent (Sarria *et al*, 1992). Experiments with microtubule stabilizing compounds such as taxol and colchicine (Carnegie *et al*, 1987) indicated that MTs control the cytoplasmic transport of lipid droplets. However, our study and others (Almahbodi and Hall, 1990) demonstrated that lipid droplets are exclusively associated with IFs. This discrepancy may be explained by the fact that the cytoplasmic networks of MTs and IFs are functionally linked and the disruption of MTs also damages the IF network (Skalli and Goldman, 1991). As well as IFs, the MFs also seem to participate in the regulation of granulosa cell steroidogenesis. Indeed, it was shown that cytochalasin treatment does not affect the generation of lipid droplets in LH-stimulated granulosa cells, but induces the secretion of progesterone by unstimulated ones (Ben Ze'ev and Amsterdam, 1987).

It is of general acceptance that MTs are involved in the polarization of Golgi apparatus and the control of cytoplasmic transport of Golgi vesicles (Vale, 1987). Since the close localization of Golgi with MTs has been described in bovine cumulus cells (this study) and in cultured human granulosa cells (Amsterdam *et al*, 1989), it seems likely that MTs determine the arrangement of cytoplasmic organelles and direct their reorganization in LH-stimulated granulosa cells.

We report here that gonadotropin stimulation promotes the development of Golgi and RER in cumulus cells. The functional significance of this event should be considered with regard to other events occurring at the time of cumulus expansion. In recent studies we showed that cumulus expansion in cattle is accompanied by the increased secretion of extracellular matrix glycoproteins laminin, type IV collagen and fibronectin, and by the anchorage of extracellular matrix at cytoplasmic membranes of cumulus cells (Šutovský *et al*, manuscript in preparation) The enzymatic machinery involved in the posttranslational modification and trafficking of glycoproteins has been localized in the RER and Golgi (Hirschberg and Snider, 1987; Hong and Tang, 1993). Thus, the polarization and increased size of the components of RER and Golgi apparatus in cumulus cells may be a prerequisite for the acceleration of glycoprotein secretion.

Taken together with the data discussed above, the present results suggest that individual cytoskeletal components fulfil spatially and temporally diversified functions throughout the gonadotropin-induced cumulus expansion in cattle. Although IFs and MTs participate in the determination of cell shape and in cytoplasmic movements of several organelles, F-actin seem to fulfil a crucial role in transduction of LH signals and in the control of the final differentiation of cumulus granulosa cells.

ACKNOWLEDGMENTS

The authors wish to thank M Bornens and V Viklický for their generous gift of antibodies. The technical assistance of S Delassale, J Degrolard and V Pech are gratefully acknowledged. The work was partially supported by AID grant number 12 061E and grant Z-503 from Czech Ministry of Economics. The stay of P Šutovský at INRA Jouy-en-Josas was supported by scholarship from the CIES Paris, France.

REFERENCES

Allworth AE, Albertini DF (1993) Meiotic maturation in cultured bovine oocytes is accompanied by remodelling of the cumulus cell cytoskeleton. *Dev Biol* 158, 101-112

Almahbodi G, Hall PF (1990) The role of intermediate filaments of adrenal steroidogenesis. *J Cell Sci* 97, 679-687

Almahbodi G, Williams LJ, Han XG, Hall PF (1993) Binding of lipid droplet and mitochondria to intermediate

129

filaments in rat Leydig cells. *J Reprod Fert* 98, 209-217

Amsterdam A, Rotmensch S (1987) Structure–function relationship during granulosa cell differentiation. *Endocrin Rev* 8, 309-337

Amsterdam A, Rotmensch S, Ben Ze'ev A (1989) Coordinated regulation of morphological and biochemical differentiation in a steroidogenic cell: the granulosa cell model. *Trends Biochem Sci* 14, 377-382

Ben Ze'ev A, Amsterdam A (1987) *In vitro* regulation of granulosa cell differentiation. *J Biol Chem* 262, 5366-5376

Ben Ze'ev A, Amsterdam A (1989) Regulation of cytoskeletal protein organization and expression in human granulosa cells in response to gonadotropin regutreatment. *Endocrinology* 124, 1033-1041

Carnegie JA, Dardick I, Tsang BK (1987) Microtubules and gonadotropic regulation of granulosa cell steroidogenesis. *Endocrinology* 120, 819-828

Chen L, Wert SE, Hendrix M, Russel PT, Cannon M, Larsen WJ (1990) Hyaluronic acid synthesis and gap junction endocytosis are necessary for normal expansion of the cumulus mass. *Mol Reprod Dev* 26, 236-247

Collins W, Jurkovic D, Bourne T, Kurjak A, Campbell S (1991) Ovarian morphology, endocrine function and intra-follicular blood flow during the periovulatory period. *Human Rep* 6, 319-324

Davis JS, Weakland LL, West LA, Farese RV (1986) Luteinizing hormone stimulates the formation of inositol triphosphate and cyclic AMP in rat granulosa cells. Evidence for phospholipase-C-generated second messengers in the action of luteinizing hormone. *Biochem J* 238, 567-604

Dekel N, Hillensjo Y, Kraicer PF (1979) Maturation effects of gonadotropins on the cumulus–oocyte complex of the rat. *Biol Reprod* 20, 191-197

Dráber P, Dráberova E, Zicconi D, Sellitto C, Viklický V, Cappuccinelli P (1986) Heterogeneity of microtubules recognized by monoclonal antibodies to alpha tubulin. *Eur J Cell Biol* 41, 82-88

Eppig JJ (1980) Regulation of cumulus oophorus expansion by gonadotropins *in vivo* and *in vitro*. *Biol Reprod* 23, 545-552

Hirschberg CB, Snider MD (1987) Topography of glycosylation in the rough endoplasmic reticulum and Golgi apparatus. *Ann Rev Biochem* 46, 631-664

Hong W, Tang BL (1993) Protein trafficking along the exocytotic pathway. *Bioassays* 15, 231-238

Jasmin BJ, Cartaud J, Bornens M, Changeux JP (1989) Golgi apparatus in chick skeletal muscle: changes in its distribution during end plate development and after denervation. *Proc Natl Acad Sci USA* 86, 7218-7222

Larsen WJ, Wert SE, Brunner GD (1986) A dramatic loss of cumulus cell gap junctions is correlated with germinal vesicle breakdown in rat oocytes. *Dev Biol* 113, 517-521

Larsen WJ, Wert SE, Brunner GD (1987) Differential modulation of rat follicle cell gap junction populations at ovulation. *Dev Biol* 122, 61-71

Paton AC, Collins WP (1992) Differentiation processes of granulosa cells. *Oxford Rev Reprod Biol* 14, 168-223

Pavlok A, Lucas-Hahn A, Niemann H (1992) Fertilization and developmental competence of bovine oocytes derived from different categories of antral follicles. *Mol Reprod Dev* 31, 63-67

Phatak PD, Packman CH, Lichtman MA (1988) Protein kinase C modulates actin conformation in human T-lymphocytes. *J Immunol* 141, 2929-2938

Sarna AJ, Panini SR, Evans M (1992) A functional role for vimentin intermediate filaments in the metabolism of lipoprotein-derived cholesterol in human SW-13 cells. *J Biol Chem* 27, 19455-19463

Silberzahn P, Almahdobi G, Dehennin L, Meroune A (1985) Estrogen metabolites in equine ovarian follicles: a chromatographic-mass spectrometric determination in relation to follicular ultrastructure and progestin content. *J Steroid Biochem* 22, 501-505

Skalli O, Goldman RD (1991) Recent insights into the assembly, dynamics, and function of intermediate filament networks. *Cell Motil Cytoskelet* 19, 67-79

Šutovský P, Fléchon JE, Fléchon B, Motlík J, Peynot N, Chesné P, Heyman Y (1993) Dynamic changes of gap junctions and cytoskeleton during *in vitro* culture of cattle oocyte cumulus complexes. *Biol Reprod* 49, 1277-1287

Vale RD (1987) Intracellular transport using microtubule-based motors. *Ann Rev Cell Biol* 3, 373-378

Viklický V, Dráber P, Hasek J, Bartek J (1982) Production and characterization of monoclonal antitubulin antibody. *Cell Biol Int Rep* 6, 725-730

Wert SE, Larsen WJ (1989) Meiotic resumption and gap junction modulation in the cultured rat cumulus–oocyte complexes. *Gamete Res* 22, 143-162

130

MOLECULAR REPRODUCTION AND DEVELOPMENT 37:210–215 (1994)

Chromatin Condensation and Histone H1 Kinase Activity During Growth and Maturation of Rabbit Oocytes

LADISLAVA JELÍNKOVÁ,[1] MICHAL KUBELKA,[1,2] JAN MOTLÍK,[1] AND PIERRE GUERRIER[2]
[1]*Department of Genetics, Institute of Animal Physiology and Genetics, Czech Academy of Sciences, Liběchov, Czech Republic; and* [2]*Laboratoire de Biologie Moléculaire et Cellulaire, Ecole Normale Supérieure de Lyon, Lyon, France*

ABSTRACT Fully grown rabbit oocytes, isolated from preovulatory follicles, exhibit highly condensed bivalents within an intact germinal vesicle while a very low level of histone H1 kinase activity could be detected in their extracts. Chromatin condensation started in growing oocytes isolated from antral follicles presenting a diameter of 0.5 mm. This event was accompanied by a transient rise in histone H1 kinase activity which culminated in large antral follicles measuring 0.75 to 1 mm in diameter.

However, the extent of histone H1 kinase activity observed in these growing oocytes remained far less important than that recorded in extracts prepared from in vitro cultured metaphase I and metaphase II oocytes. Moreover, this activity was insufficient to induce germinal vesicle breakdown which will only occur with an increasing efficiency, following in vitro culture of medium, large, and fully grown antral follicles. © 1994 Wiley-Liss, Inc.

Key Words: Meiosis, Cell Cycle, Phosphorylation, $p34^{cdc2}$

INTRODUCTION

During their growth phase, mammalian oocytes are blocked in the diplotene/dictyate stage of the first meiotic prophase and present decondensed chromosomes, distributed in the oocyte nucleus (Thibault et al., 1987; Szöllösi et al., 1991). An intensive synthesis of ribosomal RNA (rRNA) and heterogenous RNA (hnRNA) characterizes this stage (Crozet et al., 1981, 1986; Šutovský et al., 1993). Concomitantly with achievement of their full size, the oocyte nucleoli become compact (Chouinard, 1971) and rRNA synthesis stops (Crozet et al., 1981, 1986; Šutovský et al., 1993). However, chromosomes remain decondensed and are not visible at the light microscope level. The hnRNA synthesis continues in fully grown (FG) oocytes up to their resumption of meiosis (Rodman and Bachvarova, 1976).

Chromatin condensation occurs in FG oocytes in response to the preovulatory surge of gonadotropin hormones (Thibault et al., 1987; Eppig, 1991) and the subsequent activation of M-phase promoting factor (MPF) in oocyte cytoplasm (Nurse et al., 1990; Pines and Hunter, 1990). In the active form, this factor possesses histone H1 kinase activity, which is generally used as biochemical assay for revealing MPF activity (Arion et al., 1988; Dunphy et al., 1988; Labbé et al., 1988a,b). The condensation of chromatin into chromosomes during M-phase is accompanied by a specific phosphorylation of histones H1 and H3, suggesting that condensation is, at least partially, induced by these histone posttranslational modifications (Gurley et al., 1978; Hohmann et al., 1976; Matsumoto et al., 1980; Newport and Spann, 1987).

In contrast to all mammalian species so far studied, FG rabbit oocytes possess an intact germinal vesicle (GV) filled with highly condensed bivalents (Motlík et al., 1989) and the process of chromatin condensation occurs during the growth phase of oocyte development (Šutovský et al., 1993).

In this study, the process of chromatin condensation was followed in rabbit oocytes isolated from early antral follicles and their meiotic competence was tested concomitantly. Changes of histone H1 kinase activity in growing, FG, and maturing oocytes were compared.

MATERIALS AND METHODS

Isolation of Oocytes

Oocytes of various size categories were obtained from adult hormonally stimulated rabbit females. At 17th, 18th, and 19th day of pseudopregnancy, induced by 150 IU hCG (Praedyn, Spofa Czechoslovakia), the females were injected twice daily with 5.7 IU of FSH (Folicotropin, Spofa Czechoslovakia). One day later, the rabbits were killed and ovaries removed aseptically. Fully grown oocytes were isolated after rupturing follicles measuring 1.5–2 mm in diameter in Krebs-Ringer bicarbonate buffer supplemented with 10% fetal calf serum (FCS). After cutting off the cortical part of the ovaries, antral follicles were isolated and separated according to their diameter into the following categories: small antral follicles (S), 0.25 mm in diameter; middle antral follicles (M), 0.5 mm in diameter; large antral follicles (L), 0.75–1 mm in diameter; and preovulatory follicles (P), 1.5–2 mm in diameter. Oocyte cumulus complexes (OCC) were collected from each follicular

Received April 27, 1993; accepted July 8, 1993.
Address reprint requests to L. Jelínková, Institute of Animal Physiology and Genetics, Czech Academy of Sciences, 277 21 Liběchov, Czech Republic.

© 1994 WILEY-LISS, INC.

131

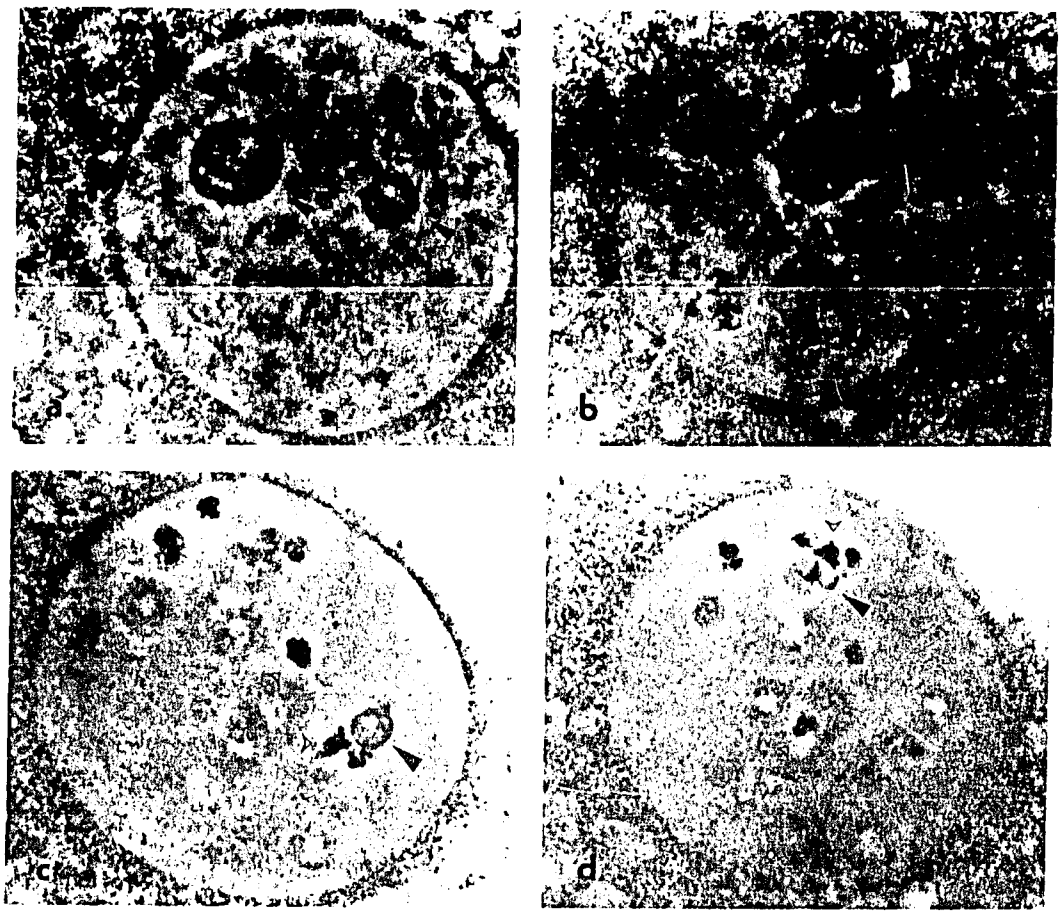

Fig. 1. The process of chromatin condensation during the growth phase of rabbit oocytes. Photomicrographs of GVs of rabbit oocytes isolated from antral follicles, mounted on slides, fixed, stained with orcein, and photographed under the phase contrast. Filled arrowheads, nucleoli; open arrowheads, condensed chromatin. a: S category. b: M category. Clumps of condensed chromatin began to form around nucleolus and in nucleoplasm. c: L category. The vacuolated nucleolus and chromatin in advanced stages of condensation. d: P category. Highly condensed chromosomes around the compact nucleolus and in nucleoplasm.

category under the dissecting microscope. Immediately after isolation, control oocytes were denuded of cumulus cells and the diameter of oocytes without zona pellucida was measured using an ocular micrometer. Oocytes were then mounted on slides, fixed in acetic acid-alcohol (1:3 v/v) for 24 hr, and stained with 1% orcein. The morphology of GV was evaluated under phase-contrast microscopy.

Condensed chromosomes in GVs of fully grown oocytes were detected using Hoechst staining. Oocytes were incubated for 5–10 min in culture medium containing 5 μl of stock solution (10 mg of Hoechst No. 33342/ml DMSO) in 1 ml, mounted on slides, and evaluated.

Cultivation and Evaluation of Oocytes

For determination of meiotic competence, the growing oocytes, isolated from each follicular category and fully grown (FG) oocytes, were cultured for 6 or 20 hr in vitro. The culture medium (280 mOsmol, pH 7.4) contained 86.5 ml isotonic TC 199 medium (USOL Praha, Czechoslovakia), 3.5 ml 7% $NaHCO_3$ + 0.002% phenol red, 10 ml 5.5% (w/v) glucose solution, 9 mg sodium pyruvate, 3 mg penicillin (Spofa, Czechoslovakia), 5 mg Streptomycin sulfate, and 1 IU FSH/ml (Folicotropin, Spofa).

Oocytes were cultured in 500 μl of medium on watch glass under paraffin oil, at 38°C in an atmosphere containing 5% CO_2.

132

Fig. 2. Highly condensed chromatin in the intact GV of FG oocyte, immediately after isolation from preovulatory follicle. Hoechst staining. Arrowhead, germinal vesicle.

At the end of culture, cumulus cells were removed by hyaluronidase (Sevac, Czechoslovakia) treatment (247 TRU/ml) for 10 min and by repeated pipetting with a narrow bore micropipette. Denuded oocytes were fixed and examined as previously described.

Histone H1 Kinase Assay

To measure histone H1 kinase activity in growing oocytes, we used oocytes from M (oocyte diameter 100–120 μm) and L (oocyte diameter 120–135 μm) categories. FG oocytes cultured for 0, 4, and 6 hr were used as a control. The oocytes were freed of cumulus cells, washed several times in PBS, and transferred into the homogenization buffer (Meijer and Pondaven, 1988). After one round of freezing and thawing, the oocytes were mechanically homogenized and centrifuged for 10 min at 10,000*g*, at 4°C. Supernatants were used as "crude extracts" for further procedures. Twenty FG oocytes were used for each extract, while the number of growing M and L oocytes was calculated to reach the same volume of cytoplasm. H1 kinase activity was tested using a modification of the procedure described previously by Meijer and Pondaven (1988). The reaction mixture contained 5 μl sample, 0.2 mg/ml histone H1 (Boehringer), 1 μM PKI-synthetic peptide (Sigma Chemical Co., St. Louis, MO), and 2 μCi of γ-^{32}P-ATP (3,000 Ci/mM, Amersham, PB 10168) in 30 μl of kinase buffer (66 mM Na-glycerolphosphate, pH 7.4, 15 mM p-nitrophenylphosphate, 5 mM EGTA, 15 mM $MgCl_2$, and 1 mM dithiothreitol). The final concentration of ATP in the reaction mixture was adjusted with non-radioactive ATP to 0.1 mM. The mixtures were incubated for 15 min at 30°C and the reaction stopped by addition of 1/2 vol of 3× concentrated electrophoresis sample buffer. Then, samples were boiled for 5 min, loaded on 10% SDS polyacrylamide gels (Laemmli, 1970). Dried gels were subjected to autoradiography.

RESULTS

Morphology of Growing Rabbit Oocytes

Diameter of the oocytes released from S follicles was about 95 μm (95 ± 16.2 μm), which represents 68% of the FG oocyte diameter. The germinal vesicle (GV) of oocytes possessed 2–3 vacuolated nucleoli. No signs of chromatin condensation were visible using phase contrast, after orcein staining (Fig. 1a).

M follicles contained oocytes which measured 120 μm (122 ± 10.8 μm) in diameter (87% of the FG oocyte diameter). In their GV, vacuolated nucleoli were visible as well as several clumps of condensed chromatin, appearing in the nucleoplasm and around the nucleoli (Fig. 1b).

L follicles contained oocytes of nearly full size (135 ± 5.1 μm). GV of these oocytes possessed condensed chromatin. Individual bivalents were visible around the nucleolus and in the nucleoplasm. In contrast to other species, bivalents and vacuolated nucleoli were thus simultaneously present in the GV of rabbit oocytes at this stage (Fig. 1c).

FG rabbit oocytes (140 ± 13.4 μm in diameter) possessed highly condensed bivalents in the GV, some of them being attached to the compact nucleolus (Fig. 1d, 2).

Meiotic Competence

Oocytes isolated from S follicles were not meiotically competent. Even after 20 hr of in vitro culture they remained in the GV stage (Table 1). After 20 hr of culture, 32% of the oocytes from M follicles had underwent GVBD, although 11% of them did not overpass late diakinesis (LD); 7.8% of these oocytes reached the MII stage. In the remaining 70%, the progress in chromatin condensation occurred within an intact GV. A substantial rise in meiotic competence was observed in oocytes recovered from L follicles: 73% and 94% of these oocytes underwent GVBD, after 6 and 20 hr of culture, respectively. After 20 hr of culture, 25% of these oocytes extruded their first polar body. The capability of FG oocytes for GVBD was about 91% and 64% formed the first polar body.

Histone H1 Kinase Activity

In FG oocytes, H1 kinase activity raised from a very low level found in preovulatory (P) oocytes (0 hr of culture), through substantially increased levels in oocytes undergoing GVBD (4 hr) up to maximum levels recorded in metaphase I (6 hr) or metaphase II (20 hr) (Fig. 3, lanes 3–6). Interestingly, compared with P oocytes (0 hr), an increased H1 kinase activity was observed in growing M oocytes. This transient rise in phosphorylating activity reached maximum in L oocytes. However, its extent was clearly lower than that observed in metaphase oocytes (Fig. 3, lanes 1–2). Such an increased H1 kinase activity as observed in growing oocytes was highly reproducible and occurred concomitantly with the appearance chromosome condensation.

TABLE 1. Meiotic Competence of Oocytes, Isolated From Follicles of Different Diameters

Type of follicle[a]	Time of culture (hr)	Number of oocytes	Nuclear stages[b]				
			GV	LD	M I	M II	%GVBD
P	6	79	6	32	27	12	92%
L		19	5	10	2	2	73%
M		43	29	14			32%
S		44	44				0%
P	20	79	9	14	5	51	87%
L		32	2	19	2	8	94%
M		64	50	7	2	5	21%
S		54	51	3			6%

[a]P, preovulatory follicles (1.5–2 mm in diameter); L, large antral follicles (0.75–1 mm in diameter); M, medium antral follicles (0.5 mm in diameter); and S, small antral follicles (0.25 mm in diameter).
[b]GV, germinal vesicle; LD, late diakinesis; M I, metaphase I; and M II, metaphase II.

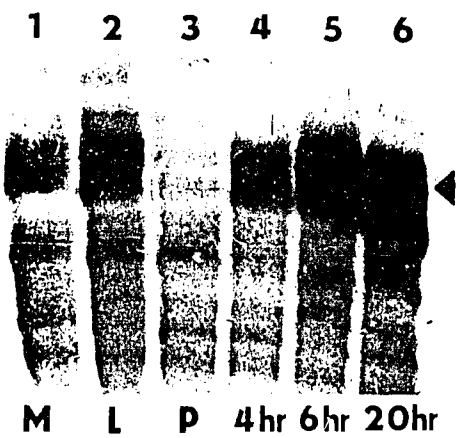

Fig. 3. The activation of histone H1 kinase activity during growth and maturation of rabbit oocytes. Arrowhead, stripe of histone H1. Lane 1: M category oocytes, in comparison with P category (lane 3), the increase of the activity of H1 kinase is evident. Lane 2: L category oocytes. The transient rise of histone H1 activity reached the maximum. Lane 3: P category oocytes immediately after isolation. Lane 4: After 4 hr of culture. Lane 5: After 6 hr of culture. Metaphase I stage. Lane 6: After 20 hr of culture. Metaphase II stage.

DISCUSSION

Meiotic Competence

It has been demonstrated for several rodent species that meiotic competence appeared coincidentally with antrum formation (Erickson and Sorensen, 1974; Sorensen and Wassarman, 1976). At this time, oocytes concomitantly attain their definitive size (Chouinard, 1971; Schultz and Wassarman, 1977). A different situation prevails in pigs and cows where the follicular antrum is already fully differentiated in follicles measuring about 0.5 mm in diameter, while the oocyte diameter is still only three quarters of its final size. These oocytes have a very limited ability to initiate nuclear maturation in vitro (Motlík et al., 1984; Crozet et al., 1986). In the rabbit, as in pig and cattle oocytes, the rate of oocyte meiotic competence increases with the diameter of antral follicle. The follicular antrum is fully developed in follicles of 0.15–0.2 mm in diameter according to Smith et al. (1978). Nicosia et al. (1975) describe well defined antrum in follicles >0.45 mm, and oocytes of 92 μm in diameter are considered as fully grown. Similarly, Bonhoff and Adams (1985) reported maximal diameter of 86.6 ± 12 μm in rabbit oocytes isolated from follicles measuring 0.63 ± 0.22 mm in diameter. In contrast, we report in the present study that early antral follicles (0.25 mm in diameter) already contained growing oocytes of about 95 μm in diameter. Fully grown oocytes (140 μm) were only found in antral follicles of 1 mm and more in diameter.

In agreement with the previous results (Smith et al., 1978), we found that oocytes from S follicle category did not resume meiosis in culture. The evidence for meiosis resumption, that we observed in three oocytes, were probably caused by a beginning of follicle atresia (Eppig, 1981; Byskov, 1978).

In comparison with the 47–74% values, reported by Smith et al. (1978), we found that only 32% of oocytes from the M follicular category resumed meiosis in the present study. This discrepancy may be partly dependent on the presence of nutritional factors and hormones in the culture medium (Smith et al., 1973; Bonhoff and Adams, 1985). Moreover, the ability to complete the MI to MII transition coincides with the achievement of oocyte full size and the process of nucleolar compaction (Motlík et al., 1984). In our results, M category oocytes achieved 87% of their definite size and presented vacuolated, synthetically active nucleoli in the GV. After 20 hr of culture, nucleolar morphology has not changed, while chromatin condensation has already occurred within their GV. The increase in histone H1 kinase activity, accompanying chromatin condensation, did not affect the integrity of the nuclear membrane in 70% of M oocytes. In addition to phosphorylation, the nuclear envelope breakdown requires a stochiometrically binding factor (Newport and Spann, 1987), which, probably, is not present in sufficient quantity in the M category oocytes which may also require other regulatory factors. The small number of

134

oocytes (7.8%) reaching MII was probably due to some heterogeneity of oocyte population isolated from this follicle category. Bonhoff and Adams (1985) observed that 29.6% of rabbit oocytes underwent GVBD in intact follicles in the ovary and the 2.8% of oocytes attained the MII stage. This heterogeneity might by partly excluded, using animals hormonally stimulated after pseudopregnancy.

In L oocyte category the transient rise of histone H1 kinase activity reached maximum. The percentage of GVBD after 20 hr of culture was comparable with FG oocytes, but only 25% L oocytes achieved MII stage. It is possible, that the late synthesis of hnRNA occurring in L oocyte category is necessary for extruding of the first polar body (Rodman and Bachvarova, 1976; Motlík et al., 1984).

Chromatin Condensation and Histone H1 Kinase Activity

The resumption of meiosis in oocytes is accompanied by several morphological changes such as nuclear membrane breakdown, condensation of chromosomes, lamina depolymerization, and rearrangement of microtubule arrays (Masui, 1985; Moor, 1988, Guerrier et al., 1990). However, the activity leading to nuclear membrane breakdown can be experimentally separated from that inducing chromatin condensation (Newport and Spann, 1987; Kubelka et al., 1988; Vigers and Lohka, 1992).

Rabbit oocytes seem to be a very good model for studying chromatin condensation. Indeed, in contrast to other species, their fully grown oocytes already possess highly condensed chromosomes in an intact germinal vesicle before the preovulatory LH surge has occurred (Motlík et al., 1989; Šutovský et al., 1993). We correlated this chromatin condensing activity, found in growing rabbit oocytes, with MPF activity. The histone H1 kinase activity assay, generally supposed to be a biochemical proof of the presence of MPF, was recently used to follow its progress of maturation in the oocytes of several mammalian species, such as mouse (Rime and Ozon, 1990), pig (Naito and Toyoda, 1991), and cattle (Kalous et al., 1993). In this study, we have shown that histone H1 kinase activity increased in growing rabbit oocytes. This increase did not reach the level characteristic for metaphase oocytes and was only transient, falling down to low levels in FG germinal vesicle arrested oocytes.

Our results clearly reveal that chromatin condensation in growing rabbit oocytes is accompanied by a transient increase in histone H1 kinase activity, the level of which remaining, however, insufficient for inducing germinal vesicle breakdown and microtubule rearrangements. These events, which are initiated later during oocyte maturation, are accompanied by a higher rise in H1 kinase activity, which reaches its maximum in metaphase.

ACKNOWLEDGMENTS

We thank Ms Lenka Vyšohlídová for preparing photographs and Ms Zelenková for excellent technical assistance. Michal Kubelka was supported by Postdoctoral grant 053224K from MRT, France. This work was partially supported by U.S. A.I.D. grant 12.061 E. and by grants from INSERM (910708), and Association pour la Recherche sur le Cancer (6145), to Pierre Guerrier.

REFERENCES

Arion D, Meijer L, Brizuela L, Beach D (1988): cdc2 is a component of the M-phase specific histone H1 kinase: Evidence for identity with MPF. Cell 55:371–378.

Bonhoff AJ, Adams CE (1985): Relationships of hormonally induced developmental changes in preovulatory follicles of the rabbit. Lab Animals 19:27–31.

Byskov AG (1978): Follicular atresia. In Jones RE (ed): "The Vertebrate Ovary." New York: Plenum Press, pp 533–562.

Chouinard LA (1971): A light- and electron microscope study of the nucleolus during growth of the oocyte in the prepuberal mouse. J Cell Sci 9:637–663.

Crozet N, Motlík J, Szöllosi D (1981): Nucleolar fine structure and RNA synthesis in porcine oocytes during the early stages of antrum formation. Biol Cell 41:35–42.

Crozet N, Kaňka J, Motlík J, Fulka J (1986): Nucleolar fine structure and RNA synthesis in bovine oocytes from antral follicles. Gamete Res 14:65–73.

Dunphy WG, Brizuela L, Beach D, Newport JW (1988): The *Xenopus* cdc2 protein is a component of MPF, a cytoplasmic regulator of mitosis. Cell 54:423–431.

Eppig JJ (1991): Maintenance of meiotic arrest and the induction of oocyte maturation in mouse oocyte-granulosa cell complexes developed in vitro from preantral follicles. Biol Reprod 45:824–830.

Erickson GF, Sorensen RA (1974): In vitro maturation of mouse oocytes isolated from late, middle, and pre-antral Graafian follicles. J Exp Zool 190:123–127.

Guerrier P, Colas P, Neant I (1990): Meiosis reinitiation as a model for the study of cell division and cell differentiation. Int J Dev Biol 34:93–109.

Gurley RL, D'Anna JA, Barham SS, Deaven LL, Tobey RA (1978): Histone phosphorylation and chromatin structure during mitosis in Chinese hamster cells. Eur J Biochem 84:1–15.

Hohmann P, Tobey R, Gurley L (1976): Phosphorylation of distinct regions of H1 histone. J Biol Chem 251:3685–3692.

Jacobs T (1992): Control of the cell cycle. Dev Biol 153:1–15.

Kalous J, Kubelka M, Rimkevičová Z, Guerrier P, Motlík J (1993): Okadaic acid accelerates germinal vesicle breakdown (GVBD) and overcomes cycloheximide and 6-dimethylaminopurine block in cattle and pig oocytes. Dev Biol 157:448–454.

Kubelka M, Motlík J, Fulka JJr, Procházka R, Rimkevičová Z, Fulka J (1988): Time sequence of germinal vesicle breakdown in pig oocytes after cycloheximide and p-aminobenzamidine block. Gamete Res 19:423–431.

Labbé JC, Picard A, Karsenti E, Dorée M (1988a): An M-phase specific protein kinase of *Xenopus* oocytes: Partial purification and possible mechanism of its periodic activation. Dev Biol 127:157–169.

Labbé JC, Lee MG, Nurse P, Picard A, Dorée M (1988b): Activation at M-phase of a protein kinase encoded by a starfish homologue of the cell cycle control gene cdc2+. Nature 335:251–254.

Laemmli, UK (1970): Cleavage of structure proteins during the assembly of the head of bacteriophage T4. Nature 227:680–685.

Masui Y (1985): Problems of oocyte maturation and the control of chromosome cycles. Dev Growth Diff 27:295–309.

Matsumoto Y, Yasuda H, Mita S, Marunouchi T, Yamada M (1980): Evidence for the involvement of H1 histone phosphorylation in chromosome condensation. Nature 284:181–183.

Meijer L, Pondaven P (1988): Cyclic activation of histone H1 kinase during sea urchin egg mitotic divisions. Exp Cell Res 174:116–129.

135

Moor RM (1988): Regulation of the meiotic cycle in oocytes of domestic mammals. Ann N Y Acad Sci 541:248–258.

Motlík J, Crozet N, Fulka J (1984): Meiotic competence in vitro of pig oocytes isolated from early antral follicles. J Reprod Fertil 72:323–328.

Motlík J, Fulka J Jr, Procházka R, Rimkevičová Z, Kubelka M, Fulka J (1989): RNA and protein synthesis requirements for the resumption of meiosis in rabbit oocytes: The role of cumulus cells. Reprod Nutr Dev 29:601–609.

Naito K, Toyoda Y (1991): Fluctuation of histone H1 kinase activity during meiotic maturation in porcine oocytes. J Reprod Fertil 93: 467–473.

Newport J, Spann T (1987): Disassembly of the nucleus in mitotic extracts: Membrane vesicularization, lamina disassembly, and chromosome condensation are independent processes. Cell 48:219–230.

Nicosia CV, Evangelista I, Batta SK (1975): Rabbit ovarian follicles. I. Isolation technique and characterization at different stages of development. Biol Reprod 13:423–447.

Nurse P (1990): Universal control mechanism regulating onset of M-phase. Nature 344:503–508.

Pines J, Hunter T (1990): $p34^{cdc2}$: The S and M kinase? New Biol 2:389–401.

Rime H, Ozon R (1990): Protein phosphatases are involved in the in vivo activation of histone H1 kinase in mouse oocyte. Dev Biol 141:115–122.

Rodman TC, Bachvarova R (1976): RNA synthesis in preovulatory mouse oocytes. J Cell Biol 70:251–257.

Schultz RM, Wassarman PM (1977): Biochemical studies of mammalian oogenesis: Protein synthesis during oocyte growth and meiotic maturation in the mouse. J Cell Sci 24:167–194.

Smith DM, Tyler JPP, Erickson GF (1978): Effects of medium composition and progesterone on maturation in vitro of rabbit oocytes from Graafian follicles of different sizes. J Reprod Fertil 54:393–400.

Sorensen RA, Wassarma: PM (1976): Relationship between growth and meiotic maturation of the mouse oocyte. Dev Biol 50:531–536.

Šutovský P, Jelínková L, Antalíková L, Motlík J (1993): Ultrastructural cytochemistry of the nucleus and nucleolus in growing rabbit oocytes. Biol Cell 77:173–180.

Szöllösi MS, Debey P, Szöllösi D, Rime H, Vautier D (1991): Chromatin behaviour under influence of puromycin and 6-DMAP at different stages of mouse oocyte maturation. Chromosoma 100:339–354.

Thibault C, Szöllösi D, Gérard M (1987): Mammalian oocyte maturation. Reprod Nutr Dev 27:865–896.

Vigers GPA, Lohka MJ (1992): Regulation of nuclear envelope precursor functions during cell division. J Cell Sci 102:273–284.

136

4205

Molecular Human Reproduction vol.1, Human Reproduction vol.10 no.9 pp. 0000–0000, 1995

Composition of the human zona pellucida and modifications following fertilization

Jiri Moos[1,2,4], Daniel Faundes[3], Gregory S.Kopf[2] and Richard M.Schultz[1,5]

[1]Department of Biology, and [2]Division of Reproductive Biology, Department of Obstetrics and Gynecology, University of Pennsylvania, Philadelphia, PA 19104, USA and [3]Department of Obstetrics and Gynecology, State University of Campinas, Campinos, Sao Paulo, Brazil

[4]Current address: Institute of Molecular Genetics, Czech Academy of Sciences, Videnska 1083, 142 20 Praha 4, The Czech Republic

[5]To whom correspondence should be addressed

The composition of individual human zonae pellucidae and modifications to this extracellular coat both before and after fertilization were analysed using a rapid, sensitive, non-radioactive biotinylation- or lectin-based detection system; these assays use commercially available reagents and can be performed on fragments of individual zonae pellucidae. The zona pellucida from unfertilized eggs is composed of three glycoprotein species designated as huZP1, huZP2 and huZP3. Under non-reducing conditions, the molecular weights of these proteins are ~150 kDa, ~100 kDa, and ~55–65 kDa respectively. Following fertilization, huZP1 was not detected under either non-reducing or reducing conditions. In contrast, after fertilization huZP2 was detected under non-reducing conditions, but not under reducing conditions. The ability to detect pre- and post-fertilization changes in a single human zona pellucida is discussed in relation to its value in assessing deficiencies in clinical and laboratory protocols used for in-vitro fertilization.

Key words: fertilization/human/in-vitro fertilization/zona pellucida

Introduction

All mammalian eggs are surrounded by the zona pellucida, an extracellular coat that is synthesized by the oocyte (reviewed in Wassarman, 1988). The zona pellucida is the site of the initial interaction of the spermatozoon with the oocyte. These interactions include the species-specific binding of spermatozoa and the induction of the acrosome reaction; both of these events are prerequisites for successful in-vivo fertilization. Analysis of the zona pellucida composition from several different species indicates that it is composed of three or four glycoproteins; this is consistent with results of cDNA cloning of the zona pellucida genes (Epifano and Dean, 1994).

The best characterized zona pellucida is that of the mouse oocyte with respect to both its glycoprotein composition and the biological function of its individual components (Wassarman, 1988, 1990). The mouse zona pellucida is composed of three sulphated glycoproteins called ZP1, ZP2 and ZP3, present in molar ratios of about 1:10:10. ZP1 is a homodimer (M_r = 200 000) connected by intermolecular disulphide bonds. ZP2 (M_r = 120 000) forms a heterodimer with ZP3 (M_r = 83 000). This heterodimer forms long filaments with a repeating structure. ZP1 provides the structural integrity of the zona pellucida by cross-linking these ZP2/ZP3 heterodimers within the filaments.

Although all mouse zona pellucida proteins have a structural function, only ZP2 and ZP3 have been shown to possess biological functions. Acrosome-intact spermatozoa bind to ZP3 via an O-linked carbohydrate moiety (Florman and Wassarman, 1985). Following sperm binding, ZP3 induces the acrosome reaction of those bound spermatozoa (Bleil and Wassarman, 1983). The acrosome-reacted spermatozoon, which can no longer interact with ZP3, is then postulated to bind to ZP2 (Bleil *et al.*, 1988) and this interaction is thought to be required for maintaining the association of the spermatozoon with the zona pellucida as it progresses through the zona pellucida. Cortical granule exocytosis following fertilization is the likely cause for modifications of the zona pellucida that constitute a block to polyspermy. ZP3 is converted to a form called $ZP3_f$, which no longer binds acrosome-intact spermatozoa and no longer induces the acrosome reaction (Bleil and Wassarman, 1983). The modification responsible for the loss of both of these biological activities is thought to be due to the release of a CG-derived glycosidase (Miller *et al.*, 1993), since O-linked carbohydrates are implicated in ZP3 interaction with spermatozoa and there is no apparent change in the electrophoretic mobility of $ZP3_f$ (Bleil and Wassarman, 1980; 1983). ZP2 is converted to a form called $ZP2_f$ that no longer interacts with acrosome-reacted spermatozoa (Bleil and Wassarman, 1986). $ZP2_f$ arises by a proteolytic cleavage that is mediated by a CG-derived protease (Moller and Wassarman, 1989) and is detected by a shift in electrophoretic mobility (from M_r = 120 000 to M_r = 90 000) under reducing conditions (Bleil *et al.*, 1981). These zona pellucida modifications constitute the zona pellucida block to polyspermy. It should be noted that there is an apparent conservation of both the protein composition and biological function of the individual zona pellucida components in the zona pellucida of other species

© Oxford University Press

137

such as the hamster and pig (Moller *et al.*, 1990; Bagavant *et al.*, 1993; Yurewicz *et al.*, 1993).

In contrast to these aforementioned species, we know of only two reports regarding the composition of the human zona pellucida prior to and following fertilization (Shabanowitz and O'Rand, 1988; Shabanowitz, 1990). In these reports, although two components of M_r = 90 000–110 000 and M_r = 57 000–73 000 were detected and on the basis of their molecular weight could correspond to the mouse ZP2 and ZP3 respectively, a zona pellucida component corresponding to the mouse ZP1 dimer of M_r = 200 000 was not detected. The identity of these human zona pellucida components in one of these reports was based on detection following radio-iodination of solubilized zona pellucida (Shabanowitz and O'Rand, 1988). We have observed, however, that the mouse ZP1 dimer is frequently not detected following radio-iodination (Kurasawa *et al.*, 1989). Since there are three genes for the human zona pellucida (Epifano and Dean, 1994; Harris *et al.*, 1994) that correspond to the mouse ZP1–3, it seems likely that the inability to detect a human ZP1 dimer is due to the method used for detection rather than a basic difference in the composition of the mouse and human zona pellucida.

We report here, using a biotinylation- and lectin-based assay for zona pellucida proteins, one-dimensional sodium dodecyl sulphate polyacrylamide gel electrophoresis (SDS-PAGE) under both reducing and non-reducing conditions, and two-dimensional reduction gel electrophoresis, that the human zona pellucida from unfertilized oocytes is composed of three protein species that we call huZP1–3. Under non-reducing conditions the molecular weights of huZP1–3 are ~150 kDa, ~100 kDa, and ~55–65 kDa respectively. Following fertilization, huZP1 is not detected under either non-reducing or reducing conditions. In contrast following fertilization, huZP2 is detected under non-reducing conditions, but not under reducing conditions.

Materials and methods

Collection of human unfertilized and fertilized oocytes

All oocytes were obtained from women (aged 25–34 years) who were patients in the in-vitro fertilization (IVF) programme administered by the Department of Obstetrics and Gynecology at the State University of Campinas, Brazil. All couples involved in the IVF programme had signed an informed consent document, authorizing the use of non-transferred unfertilized and fertilized oocytes for the isolation and characterization of the zona pellucida.

Follicular development was induced using the long-acting gonadotrophin-releasing hormone (GnRH) analogue treatment (Caspi *et al.*, 1989). Briefly, s.c. administration of the GnRH analogue leuprolide acetate was initiated on day 21 of the cycle at a dose of 1 mg per day until bleeding occurred. From this day, the dose was reduced to 0.5 mg per day and coupled with the i.m. administration of 300 IU of human menopausal gonadotrophin (HMG) per day for 2–4 days, depending on the patient's response in previous cycles. Thereafter, the dose of HMG was reduced to 150 IU per day until the mean follicular diameter was 20 mm. Oocyte maturation was induced by the i.m. administration of 10 000 IU of human chorionic gonadotrophin (HCG) and oocyte retrieval was performed ~36 h later under general anaesthesia.

The retrieved oocytes were individually and mechanically denuded of cumulus cells, washed in Ham's F10 medium containing 2.5 mM calcium lactate and 25 mM $NaHCO_3$, and then cultured in Ham's F10 containing 30% fetal umbilical cord serum, 75 mg/l of both penicillin (125 625 IU/l) and streptomycin for 4 h at 37°C in a humidified atmosphere containing 5% CO_2 prior to insemination in this medium. Cord serum was filter sterilized and heat treated for 1 h at 56°C.

IVF was conducted using 100 000 capacitated spermatozoa prepared as previously described (Berger *et al.*, 1985). Sperm capacitation was carried out in Ham's F10 medium containing 30% fetal umbilical cord serum, 75 mg/l of both penicillin (125 625 IU/l) and streptomycin. The first observation for signs of fertilization was made 12 h following co-incubation of the spermatozoa and oocytes. Subsequent observations were made every 12 h. In most cases the zona pellucida was isolated 48–72 h after oocyte retrieval, the interval depending on how long the embryos were cultured prior to selection and transfer. Oocytes possessing the second polar body or displaying the presence of two pronuclei were considered to be fertilized. In other instances, the zona pellucida was obtained from fertilized oocytes that developed but arrested at the 2–4-cell stage.

A maximum of five morphologically normal embryos were transferred per cycle. Of those embryos not transferred and that normally would have been destroyed, only those with clear signs of fertilization, e.g. pronucleus formation, or those that cleaved to the 2-cell stage were considered fertilized and used for zona pellucida isolation and analysis. Following insemination, if the oocytes did not possess a second polar body or pronucleus, they were deemed unfertilized and were not transferred. These unfertilized oocytes were used for zona pellucida isolation and analysis.

Zona pellucida isolation, biotinylation and solubilization

Intact, single zona pellucida were isolated and washed as previously described (Kurasawa *et al.*, 1989). Each zona pellucida was placed in an individual microcentrifuge tube containing phosphate-buffered saline (PBS) and then shipped to University of Pennsylvania, USA, for zona pellucida analysis. Single zonae pellucidae were biotinylated using the water soluble sulphosuccinimidyl-6(biotinamido) hexanoate (NHS-LC-Biotin, Pierce, IL, USA) as previously described for mouse zonae pellucidae (Moos *et al.*, 1994). Both biotinylated and non-labelled zonae pellucidae, which were used in the lectin-based assay (see below), were solubilized by boiling in SDS sample buffer and material from an individual zona pellucida was loaded per lane and analysed by SDS-PAGE (Laemmli, 1970). In some experiments, single zonae pellucidae were solubilized under non-reducing conditions, half of the resulting volume was transferred to another tube and further boiled in the presence of 5% 2-mercaptoethanol.

Detection of zona pellucida proteins following electrophoresis

SDS-PAGE was performed in 9% slab gels according to the method of Laemmli (1970). In two-dimensional SDS-PAGE, the first dimension was run in the absence of reducing agents. Following electrophoresis, strips of the gel containing glycoproteins from an individual zona pellucida were cut from the slab, boiled in SDS sample buffer with 5% 2-mercaptoethanol, and then subjected to SDS-PAGE in the second dimension. Following electrophoresis in the second dimension, proteins were electrophoretically transferred onto an Immobilon P membrane (Millipore Corp; Bedford, MA, USA) and the biotinylated proteins detected as previously described (Moos *et al.*, 1994). When non-labelled zonae pellucidae were analysed, membranes with the electro-transferred zona pellucida glycoproteins were incubated with 1 μg/ml of the N-acetylglucosamine specific biotinylated wheat germ

138

agglutinin (WGA; Boehringer Mannheim, IN, USA) in 20 mM Tris-HCl, pH 7.5, containing 150 mM NaCl, 0.05% Tween 20, 1 mM $MgCl_2$, 1 mM $MnCl_2$, and 1 mM $CaCl_2$ for 1 h, and the bound lectins were then detected using Vectastain ABC kit (Vector Laboratories, CA, USA) according to the manufacturer's instructions. The bound avidin–peroxidase was detected using an Amersham ECL (Amersham, Arlington Heights, IL, USA) detection kit.

Results

One-dimensional gel electrophoretic analysis of human zona pellucida

Biotinylation of a single intact human zona pellucida from an unfertilized oocyte, followed by solubilization and analysis of one half of the sample each under non-reducing and reducing conditions is shown in Figure 1A. Under non-reducing conditions, the huZP2 had an apparent M_r = 100 000, whereas ZP3 was resolved as multiple species of M_r = 62 000–65 000 (ZP3a) and M_r = 55 000–60 000 (huZP3b) (lane 1); a minor band of M_r = 110 000 was also observed. Under reducing conditions, two major protein species of M_r = 110 000 and 60 000–75 000 were observed (lane 2). These will be referred to as huZP2 and huZP3 respectively, based on the nomenclature and the size of the huZP2 and huZP3 components of the mouse zona pellucida. It should be noted that in several instances, huZP3a and huZP3b could be distinguished under reducing conditions. These results using biotinylation are similar to those reported by Shabanowitz and O'Rand (1988) using radio-iodination in that both huZP2 and huZP3 were detected and had similar molecular weights, and that huZP1 was not detected. The inability to detect huZP1 by biotinylation was not surprising, since this method does not detect mouse ZP1 (Moos *et al.*, 1994).

Since the human zona pellucida binds a variety of lectins, including wheat germ agglutinin (WGA; Maymon *et al.*, 1994), we elected to use WGA as a probe to detect components of the human zona pellucida following electrophoresis. As shown in Figure 1B following gel electrophoresis under non-reducing conditions, ovulated, unfertilized oocytes possessed huZP1, huZP2, and huZP3a/3b of M_r = 150 000, 110 000, 62 000–65 000/55 000–60 000 respectively (lane 1). Under reducing conditions, only huZP2 and huZP3a/3b were detected (lane 3), and huZP3a/3b showed the same retardation in electrophoretic mobility observed following biotinylation and electrophoresis under reducing conditions (Figure 1A, lane 2). Following fertilization, huZP2 and huZP3a/3b were detected under non-reducing conditions (lane 2), whereas under reducing conditions, only huZP3a and huZP3b were observed (lane 4).

Two-dimensional reduction gel electrophoretic analysis of human zona pellucida

Since the detection as well as the electrophoretic mobility of the human zona pellucida components depended upon the state of disulphide reduction, we analysed the zona pellucida from both unfertilized and fertilized oocytes by two-dimensional reduction gel electrophoresis (Figure 2). Four components were detected in the zona pellucida from unfertilized oocytes, and their electrophoretic mobilities were con-

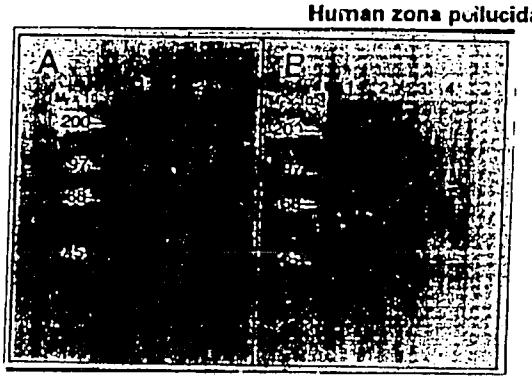

Figure 1. Chemiluminescent detection of human zona pellucida proteins following one-dimensional gel electrophoresis.
(A) Biotinylation method in which a single human zona pellucida from an unfertilized egg was biotinylated and solubilized. The sample was then divided in half and subjected to electrophoresis under non-reducing (lane 1) or reducing (lane 2) conditions.
(B) Wheat germ agglutinin (WGA)-based assay in which a single human zona pellucida from unfertilized eggs (lane 1 and 3) and fertilized eggs (lanes 2 and 4) was subjected to electrophoresis under non-reducing conditions (lanes 1 and 2) or reducing conditions (lanes 3 and 4). In these experiments ~15–20 zonae pellucidae were analysed. Representative examples are shown.

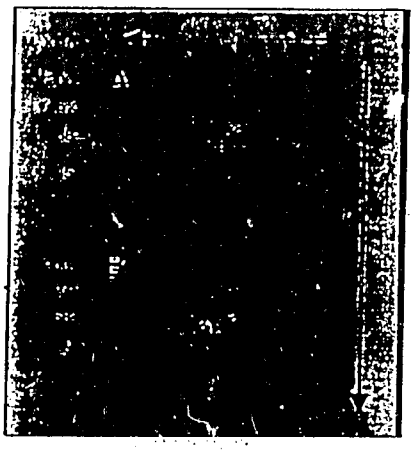

Figure 2. Chemiluminescent detection of human zona pellucida following two-dimensional reduction gel electrophoresis using WGA. (A) A single human zona pellucida isolated from an unfertilized egg. (B) A single human zona pellucida isolated from a fertilized egg. The numbers (1, 2, 3a, and 3b) refer to huZP1, huZP2, huZP3a, and huZP3b respectively. In these experiments at least two zonae pellucidae were analysed for each group. For technical reasons the electrophoretic mobilities of the zona pellucida proteins in the second dimension are slightly retarded with respect to those of the molecular weight standards, since the zona pellucida glycoproteins are applied to the second dimension within the polyacrylamide gel, whereas the standards are in solution. The assignment of the zona pellucida glycoproteins is based on their position following electrophoresis in the first dimension (non-reducing).

-739-

sistent with the presence of a huZP1 dimer that contains intermolecular disulphide bonds, huZP2, and huZP3a/3b (Figure 2A). In contrast, only two species that corresponded to huZP3a and huZP3b were detected in the zona pellucida from fertilized oocytes (Figure 2B).

Discussion

The detection of a species in the human zona pellucida with the electrophoretic properties that correspond to mouse ZP1 using a lectin-based assay is consistent with presence of a gene in the human that is homologous to mouse *ZP1*. In addition, the presence of huZP2 and huZP3, whose electrophoretic properties are similar to those of mouse ZP2 and ZP3, suggests that the protein composition of the human zona pellucida is similar to that of the mouse, and this is also consistent with the presence of two genes in the human that are homologous to mouse *ZP2* and *ZP3* (Epifano and Dean, 1994). Following fertilization, huZP1 is not detected. This contrasts with the mouse, in which mouse ZP1 is present and is apparently unaltered following fertilization (Bleil *et al.*, 1981). Since our assay for human zona pellucida detection is lectin-based, and cortical granule-derived glycosidases are likely to be released following fertilization (Miller *et al.*, 1993), huZP1 may be present but its carbohydrate moiety(ies) modifies such that it is no longer recognized by WGA. Alternatively, cortical granule-derived proteases may degrade huZP1 to forms that are not detectable.

Based on the electrophoretic mobility under reducing conditions, the species that we call huZP2 appears to correspond to the protein that Shabanowitz and O'Rand call ZP1 (Shabanowitz and O'Rand, 1988). Following fertilization, huZP2 is apparently proteolysed such that it is not detected under reducing conditions (Figures 1B, lane 4, and 2B). A similar loss of human ZP2 following fertilization was also reported by Shabanowitz and O'Rand (1988). In the mouse, fertilization results in a proteolytic cleavage of ZP2 in which the two resulting fragments are held together by an intramolecular disulphide bond. Thus, ZP2 is detected under both non-reducing and reducing conditions, although there are differences in the electrophoretic mobility that reflect the proteolysed and non-proteolysed forms. In the human, huZP2 is detected in fertilized oocytes only under non-reducing conditions (Figure 1B, lane 3). Thus, fertilization of both the mouse and human oocytes results in the proteolysis of the huZP2 counterparts that are held together by intramolecular disulphide bonds, but in the human this proteolysis may be more extensive. This might account for our inability to detect these fragments as they could have run off from the gel and/or because the fragments do not contain sufficient amounts of carbohydrates to be detected by WGA. It is possible that glycosidases released following fertilization hydrolyze sugars recognized by WGA and thus huZP1 is not detected

Both the biotinylation- and lectin-based assays detect two forms of huZP3, i.e. huZP3a and huZP3b, and fertilization apparently does not result in either a shift in electrophoretic mobility or the amount of either protein. This situation is similar to that in the mouse in which there is no apparent change in either the amount or electrophoretic mobility of ZP3 following fertilization (Bleil *et al.*, 1981). Shabanowitz and O'Rand (1988) also reported that following fertilization there are neither changes in the electophoretic mobility nor the amount of species that they term ZP2 and ZP3. Thus, we would suggest that the proteins that we call huZP3a and huZP3b probably correspond to those that Shabanowitz and O'Rand (1988) term ZP2 and ZP3 respectively.

DNA sequence analysis indicates that there is a substantial degree of conservation of the proteins that comprise the zona pellucida in mouse, hamster, and human. Nevertheless, there do appear to be significant differences in the glycosylation of these polypeptides, since the lectin-based assay that we use for human zona pellucida using WGA does not detect zona pellucida proteins in either the mouse or the monkey (J.Moos, G.S.Kopf and R.M.Schultz, unpublished observations). Assuming that the conservation in DNA sequence of the different zona pellucida proteins in different species reflects conservation of biological function of that protein, a variability in glycosylation of ZP3 probably reflects the basis for the species-specific interaction of spermatozoa with the zona pellucida.

The results presented here may also have clinical relevance. The lectin-based assay is rapid and sensitive; it requires only a portion of an intact human zona pellucida (J.Moos, G.S.Kopf and R.M.Schultz, unpublished observations). Again, if the biological functions of the zona pellucida proteins of mouse and human are conserved, the proteolysis of huZP2 that follows fertilization may be indicative of zona pellucida modifications that could lead to a zona pellucida block to polyspermy. Thus, this assay for huZP2 conversion could provide a sensitive and rapid retrospective analysis for the molecular basis for failed fertilization in IVF programmes. A high incidence of human zonae pellucidae containing proteolysed ZP2 may indicate ovulation protocols or culture conditions that lead to a precocious loss of cortical granules. It should be noted that in the mouse, oocyte maturation is accompanied by the limited release of cortical granules (Ducibella *et al.*, 1990a) that, in the absence of the follicular milieu (*in vivo*) or media containing serum, follicular fluid, or fetuin (*in vitro*) (Ducibella *et al.*, 1990a; Schroeder *et al.*, 1990; Kalab *et al.*, 1993), leads to modifications of the zona pellucida that constitute the zona pellucida block to polyspermy (Ducibella *et al.*, 1990a). Such events could lead to metaphase II-arrested oocytes of reduced fertilizability. If a similar situation exists in the human, the knowledge gleaned from analysing the human zona pellucida following unsuccessful IVF could indicate deficiencies in the culture conditions used for the maturation of oocytes that have not reached metaphase II (Ducibella *et al.*, 1990b). Alternatively, such analyses may point to deficiencies in the ovulation induction protocols that give rise to aged metaphase II-arrested oocytes that have undergone cortical granule exocytosis and the fertilization-induced modifications of the zona pellucida.

Acknowledgements

J.Moos was supported by a grant from the Agency for International Development (12.061E). D.Faundes was supported in part by a re-entry grant from the Rockefeller Foundation (RF 89033).

140

References

Bagavant, H., Yurewicz, E.C., Sacco, A.G., Talwar, G.P. and Gupta, S.K. (1993) Block in porcine gamete interaction by polyclonal antibodies to a pig ZP3 β-fragment having partial sequence homology to human ZP3. *J. Reprod. Immunol.*, 25, 277–283.

Berger, T., Marrs, R.P. and Moyer, D.L. (1985) Comparison of techniques for selection for motile spermatozoa. *Fertil. Steril.*, 43, 268–273.

Bleil, J.D. and Wassarman, P.M. (1980) Mammalian sperm–egg interaction: identification of a glycoprotein in mouse egg zonae pellucidae possessing receptor activity for sperm. *Cell*, 20, 873–882.

Bleil, J.D. and Wassarman, P.M. (1983) Sperm–egg interactions in the mouse: sequence of events and induction of the acrosome reaction by a zona pellucida glycoprotein. *Dev. Biol.*, 95, 317–324.

Bleil, J.D. and Wassarman, P.M. (1986) Autoradiographic visualization of the mouse egg's sperm receptor bound to sperm. *J. Cell Biol.*, 102, 1363–1371.

Bleil, J.D., Beall, C.F. and Wassarman, P.M. (1981) Mammalian sperm–egg interaction: fertilization of mouse eggs triggers modification of the major zona pellucida glycoprotein, ZP2. *Dev. Biol.*, 86, 89–97.

Bleil, J.D., Greve, J.M. and Wassarman, P.M. (1988) Identification of a secondary sperm receptor in the mouse egg zona pellucida: role in maintenance of binding of acrosome-reacted sperm to eggs. *Dev. Biol.*, 128, 376–385.

Caspi, E., Ron-El, R., Golan, A., Nachum, H., Herman, A., Soffer, V. and Weinraub, Z. (1989) Results of in vitro fertilization and embryo transfer by combined long-acting gonadotrophin-releasing hormone analog D-Trp-6-luteinizing hormone-releasing hormone and gonadotrophins. *Fertil. Steril.*, 51, 95–99.

Ducibella, T., Kurasawa, S., Rangarajan, S., Kopf, G.S. and Schultz, R.M. (1990a) Changes in distribution of mouse egg cortical granules during meiotic maturation and correlation with an egg-induced modification of the zona pellucida. *Dev. Biol.*, 137, 46–55.

Ducibella, T., Kopf, G.S. and Schultz, R.M. (1990b) Use of serum and timing of insemination for IVF. *J. IVF Embryo Transfer*, 7, 121–123.

Epifano, O. and Dean, J. (1994) Biology and structure of the zona pellucida: a target for immunocontraception. *Reprod. Fertil. Dev.*, 6, 319–330.

Florman, H.M. and Wassarman, P.M. (1985) O-linked oligosaccharides of mouse egg ZP3 account for its sperm receptor activity. *Cell*, 41, 313–324.

Harris J.D., Hibler, D.W., Fontenot, G.K., Hsu, K.T., Yurewicz, E.C. and Sacco, A.G. (1994) Cloning and characterization of zona pellucida genes and cDNAs from a variety of mammalian species: the ZPA, ZPB and ZPC gene families. *DNA Sequence*, 4, 361–393.

Kalab, P., Schultz, R.M. and Kopf, G.S. (1993) Modifications of the mouse zona pellucida during oocyte maturation: Inhibitory effects of follicular fluid, fetuin, and α_2HS-glycoprotein. *Biol. Reprod.*, 49, 561–567.

Kurasawa, S., Schultz, R.M. and Kopf, G.S. (1989) Egg-induced modifications of the zona pellucida of mouse eggs: effects of microinjected inositol 1,4,5-trisphosphate. *Dev. Biol.*, 13 , 295–304.

Laemmli, U.K. (1970) Cleavage of structural proteins during the assembly of the head of bacteriophage T4. *Nature*, 227, 680–685.

Maymon, B.B., Maymon, R., Ben-Nun, I., Gheller, Y., Shalgi, R. and Skutelsky, E. (1994) Distribution of carbohydrates in the zona pellucida of human oocytes. *J. Reprod. Fertil.*, 102, 81–86.

Miller, D.J., Gong, X., Decker, G. and Shur, B.D. (1993) Egg cortical granule N-acetylglucosaminidase is required for the mouse zona block to polyspermy. *J. Cell Biol.*, 123, 1431–1440.

Moller, C.C. and Wassarman, P.M. (1989) Characterization of a proteinase that cleaves zona pellucida glycoprotein ZP2 following activation of mouse eggs. *Dev. Biol.*, 132,103–112.

Moller, C.C., Bleil, J.D., Kinloch, R.A. and Wassarman, P.M. (1990) Structural and functional relationships between mouse and hamster zona pellucida glycoproteins. *Dev. Biol.*, 137, 276–286.

Moos, J., Kalab, P., Kopf, G.S. and Schultz, R.M. (1994) A rapid, non-radioactive, and quantitative method to analyze zona pellucida modifications in single mouse eggs. *Mol. Reprod. Dev.*, 38, 91–93.

Schroeder, A.C., Schultz, R.M., Kopf, G.S., Taylor, F.R., Becker, R. and Eppig, J.J. (1990) Fetuin inhibits zona pellucida hardening and conversion of ZP2 to ZP2$_f$ during spontaneous mouse oocyte maturation *in vitro* in the absence of serum. *Biol. Reprod.*, 43, 891–897.

Shabanowitz, R.B. (1990) Mouse antibodies to human zona pellucida: evidence that human ZP3 is strongly immunogenic and contains two distinct isomer chains. *Biol. Reprod.*, 43, 260–270.

Shabanowitz, R.B. and O'Rand, M.G. (1988) Characterization of the human zona pellucida from fertilized and unfertilized eggs. *J. Reprod. Fertil.*, 82, 151–161.

Wassarman, P.M. (1988) Zona pellucida glycoproteins. *Ann. Rev. Biochem.*, 57, 414–442.

Wassarman, P.M. (1990) Profile of a mammalian sperm receptor. *Development*, 108,1–17.

Yurewicz, E.C., Hibler, D., Fontenot, G.K., Sacco, A.G. and Harris, J. (1993) Nucleotide sequence of cDNA encoding ZP3 α, a sperm-binding glycoprotein from zona pellucida of pig oocyte. *Biochim. Biophys. Acta*, 1174, 211–214.

Received on April 24, 1995; accepted on June 10, 1995

141

BIOLOGY OF REPRODUCTION 53, 692–699 (1995)

Potential Role of Mitogen-Activated Protein Kinase in Pronuclear Envelope Assembly and Disassembly Following Fertilization of Mouse Eggs[1]

Jiri Moos,[3] Pablo E. Visconti,[4] Grace D. Moore,[4] Richard M. Schultz,[3] and Gregory S. Kopf[2,4]

Department of Biology[3] and Division of Reproductive Biology[4]
Department of Obstetrics and Gynecology, University of Pennsylvania, Philadelphia, Pennsylvania

ABSTRACT

Changes in the activities of the $p34^{cdc2}$/cyclin B complex and mitogen-activated protein (MAP) kinase were analyzed after insemination of mouse eggs in vitro. Whereas histone H1 kinase activity ($p34^{cdc2}$/cyclin B) fell to negligible levels by 90 min postinsemination, a decrease to negligible levels of myelin basic protein kinase activity (i.e., MAP kinase) was not observed until about 7 h postinsemination. The decrease in MAP kinase activity appeared to be linked to the prior decline in $p34^{cdc2}$/cyclin B kinase activity, since inhibiting the fertilization-induced destruction of cyclin B by treating eggs with the microtubule inhibitor nocodazole prevented the decrease in each of these protein kinases; an intact spindle is required for cyclin destruction. Moreover, experimental elevation of MAP kinase activity by okadaic acid treatment under conditions that maintain negligible levels of $p34^{cdc2}$/cyclin B kinase activity suggested that MAP kinase could be involved in pronuclear envelope dynamics. Specifically, preventing the fertilization-induced decrease in MAP kinase activity was correlated with inhibiting pronucleus formation, and elevating MAP kinase activity subsequent to pronucleus formation resulted in precocious pronuclear envelope breakdown prior to entry into M phase.

INTRODUCTION

The interaction and fusion of the plasma membranes of the mammalian sperm and metaphase II-arrested egg ultimately gives rise to a series of cellular responses in the egg that is required for the exit from metaphase II and the initiation of embryonic development. These responses occur in a temporal fashion and include a transient rise in intracellular calcium concentration [1], which leads to cortical granule exocytosis and subsequent zona pellucida (ZP) modifications, resumption of meiosis (and the cell cycle), recruitment of maternal mRNAs [2], pronucleus (PN) formation and initiation of DNA synthesis, and cleavage. The process by which the second meiotic cell cycle is completed and the mitotic cell cycle is initiated after fertilization is poorly understood at the molecular level.

In contrast to somatic cells, which immediately enter interphase after mitosis, oocytes of many species, including the mouse, arrest at metaphase II after resumption of meiosis. This arrest is due to at least two factors—M-phase promoting factor (MPF) and cytostatic factor (CSF) [3]. MPF is a complex of cyclin B1/B2 and the $p34^{cdc2}$ protein kinase and displays a cyclic activity that peaks at metaphase [4]. The MPF-associated protein kinase activity is also referred to as histone H1 kinase, since this enzyme displays a pronounced activity towards this substrate [5]. CSF is postulated to maintain elevated levels of MPF activity [6] and hence may be responsible for metaphase II arrest [7]; this point, however, is controversial [8]. Although the exact composition of CSF is unknown, c-*mos* is likely to be a component [7, 9].

The fertilization-induced rise in intracellular calcium leads to the destruction of the cyclin component of MPF [10, 11]. Cyclin destruction results in a loss of the histone H1 kinase activity of MPF that, in turn, leads to an exit from M phase. Although fertilization is also accompanied by a loss of CSF activity [12], the loss of MPF activity as assessed by cyclin destruction precedes the loss of CSF activity as assessed by c-*mos* destruction [13].

Mitogen-activated protein kinase (MAP kinase) represents an additional protein kinase that appears to be involved in signaling pathways regulating the cell cycle (for review see [14]). MAP kinases represent a family of protein kinases of M_r 40 000 to M_r 46 000 that are activated after the phosphorylation of nearby threonine and tyrosine residues by MAP kinase [14, 15]. Inactivation of MAP kinase is essentially complete after the dephosphorylation of either of these residues.

MAP kinase is inactivated after ethanol activation of mouse eggs, and this inactivation follows the decrease in $p34^{cdc2}$/cyclin B kinase activity [16]. It should be noted that the decrease in MAP kinase correlates temporally with the formation of a PN. In this report, we explore the possibility that the decrease in $p34^{cdc2}$/cyclin B kinase activity following fertilization is requisite for the decrease in MAP kinase activity and that activated MAP kinase is incompatible with the presence of a nuclear envelope. We demonstrate that nocodazole treatment, which inhibits the fertilization-induced decrease in $p34^{cdc2}$/cyclin B kinase activity by preventing cyclin destruction [17], prevents the decrease in

Accepted May 1, 1995.
Received February 21, 1995.
[1]This research was supported by grants from the NIH (HD 22732 to G.S.K. and R.M.S., HD 06274 to G.S.K., and HD 22681 to R.M.S.) J.M. was supported by the Agency for International Development (12 061E). G.D.M. and P.E.V. were supported by the Rockefeller Foundation.
[2]Correspondence. Gregory S. Kopf, Division of Reproductive Biology, Department of Obstetrics and Gynecology, Room 313, John Morgan Building, School of Medicine, University of Pennsylvania, Philadelphia, PA 19104-6080. FAX (215) 349-5118

142

MAP kinase activity that normally occurs after fertilization. We also show that treatment of fertilized eggs containing a PN with okadaic acid (OA) under conditions that maintain low levels of $p34^{cdc2}$/cyclin B kinase activity results in both the activation of MAP kinase activity and precocious pronuclear envelope breakdown.

MATERIALS AND METHODS

Collection of Mouse Eggs and One-Cell Embryos

Ovulated metaphase II-arrested eggs were isolated from superovulated 6-wk-old CF-1 (Harlan Sprague Dawley, Indianapolis, IN) female mice. For all experiments, the isolated and washed metaphase II-arrested eggs from the different animals were pooled before use in the appropriate assays. Eggs were obtained by injection of 5 U eCG (Calbiochem, La Jolla, CA), followed by an injection of 5 U hCG (Sigma Chemical Co., St. Louis, MO) 48 h later. The intact cumulus-oocyte complexes were recovered 13–16 h after hCG injection. Cumulus cells were dispersed in 0.05% hyaluronidase-supplemented bicarbonate-free minimal essential medium (Earle's salts; Sigma) containing 100 μg/ml pyruvate and 3 mg/ml polyvinylpyrrolidone and buffered with 25 mM HEPES (Sigma), pH 7.2. Eggs were washed in the same medium without hyaluronidase and transferred into Whitten's medium [18] containing 15 mg/ml BSA for in vitro fertilization (IVF) as previously described [19]. Eggs in Whitten's medium were mixed with epididymal and capacitated spermatozoa in the same medium to a final concentration of 2500 spermatozoa/μl for IVF. In some experiments, the ZP was removed by treatment with acidic Tyrode's solution [20] prior to IVF. Treatment of eggs and embryos with nocodazole was carried out as reported [17].

Histone H1 Kinase Assay

Three eggs were transferred in 1.5 μl of the appropriate culture medium into 3.5 μl of a solution containing 10 μg/ml leupeptin, 10 μg/ml aprotinin, 10 mM *p*-nitrophenyl phosphate, 20 mM β-glycerophosphate, 0.1 mM sodium orthovanadate, and 5 mM EGTA. The eggs were immediately frozen on dry ice and stored at −80°C until the assay was performed. Concentrated (double-strength) histone H1 kinase buffer (24 mM *p*-nitrophenyl phosphate, 90 mM β-glycerophosphate, 24 mM $MgCl_2$, 24 mM EGTA, 0.2 mM EDTA, 4.6 mM sodium orthovanadate, 4 mM NaF, 1.6 mM dithiothreitol, 60 μg/ml leupeptin, 60 μg/ml aprotinin, 2 mg/ml of polyvinyl alcohol, 2 mg/ml histone [III-S, Sigma Chemical Company, St. Louis, MO], 2.2 μM protein kinase A inhibitor peptide [Sigma], 0.6 mM ATP, 40 mM 3-(n-morpholino)propanesulfonic acid) [MOPS], pH 7.2) was aliquoted and frozen at −80°C. Immediately before the assay, [^{32}P-γ]ATP (3000 Ci/mmol; Amersham Corp. Arlington Heights, IL) was added to the double-strength histone H1 kinase buffer to a final concentration of 500 μCi/ml. Five microliters of this solution was then mixed with 5 μl of the egg extract. The samples were incubated for 30 min at 30°C, the reaction was stopped by the addition of SDS-sample buffer [21], and the samples were boiled for 3 min. After SDS-PAGE (10% gel), the gel was stained with Coomassie R-250 dye, destained, and dried. After autoradiography, the histone bands were cut from the gel, and the radioactivity was quantified by liquid scintillation counting. The assay was linear for up to 1 h, and the extract from only 3 eggs was required (Fig. 1, A and B). In some experiments, a peptide substrate based on the $p34^{cdc2}$/cyclin B complex phosphorylation site in histone H1 (PKTPKKAKK [the threonine phosphorylation site is underlined]; catalog #12127, Upstate Biotechnology, Inc., Lake Placid, NY) was used instead of histone H1. The method for quantifying the amount of phosphorylation of this peptide was essentially the same as that described below for myelin basic protein (MBP) kinase activity.

MBP Kinase Assay

Eggs and embryos were aliquoted and processed, and the reaction was run as described for the histone H1 kinase assay. Concentrated (double-strength) MBP kinase buffer contained 40 mM β-glycerophosphate, 2 mM dithiothreitol, 0.2 mM sodium orthovanadate, 4 mM EGTA, 40 mM $MgCl_2$, 10 μg/ml leupeptin, 10 μg/ml aprotinin, 0.6 mM ATP, and 1 mM myelin basic protein-derived peptide substrate (A*PRTT*GGRR [the threonine phosphorylation site is underlined, and the italicized sequence corresponds to amino acids 95–98 of MBP; the rest of the sequence does not correspond to that of MBP]; catalog #12125, Upstate Biotechnology, Inc.), and 40 mM HEPES, pH 7.4. The samples were incubated for 30 min at 30°C, and the reaction was then stopped by addition of 15 μl of 20% trichloroacetic acid (TCA). BSA (5 μl of a 10-mg/ml solution) was added, protein was precipitated for 10 min on ice, and the sample then centrifuged at 10 000 × *g* for 6 min. Aliquots of the supernatant (15 μl) were spotted onto 2 × 2-cm squares of phosphocellulose P81 paper (Whatman, Clifton, NJ) and immediately immersed in about 500 ml of 0.75 mM phosphoric acid for at least 5 min. The P81 paper squares were then washed 5 times (5 min per wash) with 0.75 mM phosphoric acid and then immediately subjected to liquid scintillation counting. The assay was linear for up to 1 h, and the extract from only 3 eggs was required (Fig. 1C).

Electrophoresis and Immunoblotting

SDS-PAGE was performed on 10% slab gels according to the method of Laemmli [21]. Proteins were electrophoretically transferred to Immobilon P (Millipore Corp., Bedford, MA) and immunostained as previously described [22] by use of the Amersham ECL Western blotting detection system according the manufacturer's instructions. Monoclonal and polyclonal antibodies against p42 and p44 MAP kinase (po-

143

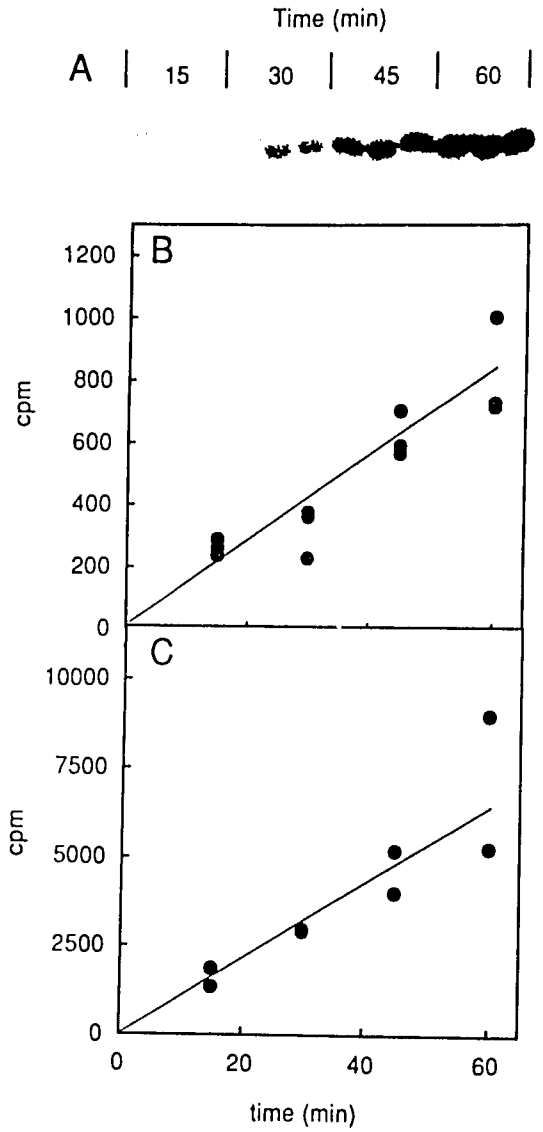

FIG. 1. Relationship between product formation and time with respect to histone H1 kinase and MBP kinase activities. Assays for histone H1 kinase and MBP kinase were performed as described under *Materials and Methods*. A) Autoradiogram of radiolabeled histone H1 phosphorylated by extracts of metaphase II-arrested eggs for times indicated. Assay was run in triplicate as shown. B) Graphic representation of data shown in A. C) Time course of phosphorylation of MBP peptide in which assay was performed in duplicate.

lyclonal, catalog #06182; monoclonal, catalog #05157), cyclin B1 (monoclonal, catalog #05158), and cdc2 (polyclonal, catalog #06194) were purchased from Upstate Biotechnology, Inc. Forty eggs or embryos were loaded per lane. The ZP2 to $ZP2_f$ conversion was monitored as previously described [23] with use of a rabbit polyclonal antiserum made against purified mouse ZP2; this antiserum recognizes both ZP2 and $ZP2_f$.

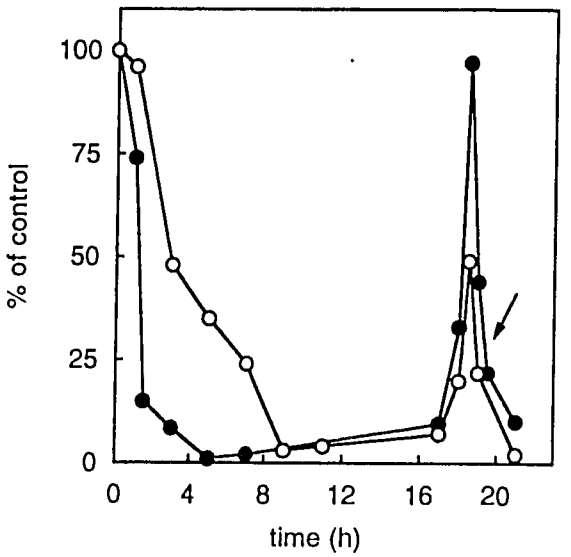

FIG. 2. Time courses of histone H1 and MBP kinase activities during first cell cycle. After insemination in vitro, histone H1 kinase (solid circles) and MBP kinase (open circles) activities were assayed at times indicated. Data are expressed relative to respective mean for histone H1 kinase activity or MBP kinase activity present in metaphase II-arrested eggs; this value was set at 100%. Time course was performed 3 times. For each time point in each experiment, at least two replicates were assayed. Arrow indicates time of cell division. Average SEM of mean value for all experiments was approximately 10%.

RESULTS

Temporal Changes in Histone H1 and MBP Kinase Activities Following Fertilization

Fertilization of ZP-intact eggs resulted in a decrease in both histone H1 and MBP kinase activities (Fig. 2), although the decrease in histone H1 kinase preceded the decrease in MBP kinase. Whereas histone H1 kinase was virtually undetectable by 3 h after insemination, 50% of the MBP kinase activity was still present and could be detected for up to 7 h after insemination. This decrease in MBP kinase activity correlated with both the change in electrophoretic mobility of MAP kinase to the inactive, dephosphorylated form (Fig. 3) and the appearance of a PN, which formed 5–7 h after insemination. Each of these activities showed a transient increase starting around 17 h after insemination (Fig. 2), and this corresponded with entry into M phase, which normally occurs between 18–20 h after insemination. It was observed that relative to the amount of activity for each enzyme in metaphase II-arrested eggs, the increase in MBP kinase ac-

144

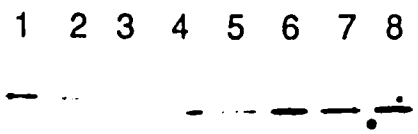

FIG. 3. Immunoblots of MAP kinase at different times after insemination. Metaphase II-arrested eggs were fertilized in vitro, eggs/embryos were withdrawn at various times after insemination, and extracts were prepared and analyzed by immunoblotting with anti-MAP kinase antibody with 30 eggs/embryos used per lane. Lane 1, MAP kinase in MII-arrested eggs; lanes 2–8, blots at 5, 7, 9, 11, 17, 19, and 21 h postinsemination, respectively. At 21 h, the embryos had cleaved to 2-cell stage (lane 8). Transition of phosphorylated, slower migrating form of MAP kinase towards its dephosphorylated, faster migrating form was observed to occur by 7 h postinsemination (lane 3). Experiment was conducted twice, with similar results.

tivity (20–30%) was always significantly less than the increase in histone H1 kinase activity (50–100%). Results of immunodepletion experiments using antibodies to $p34^{cdc2}$ and cyclin B1 indicated that the increase in MBP kinase activity was due to the ability of $p34^{cdc2}$/cyclin B kinase to phosphorylate the peptide substrate used to measure MBP kinase activity (data not shown). Consistent with the conclusion that MAP kinase activity did not increase during this time was the observation that MAP kinase remained dephosphorylated during this time (Fig. 3, lanes 6–8).

Effects of Nocodazole on the Fertilization-Induced Changes in $p34^{cdc2}$/Cyclin B and MAP Kinase Activities and Modification of the ZP

An intact spindle appears to be required for cyclin B destruction, since nocodazole-induced disruption of the spindle inhibits cyclin B degradation in metaphase II-arrested eggs [17]. If the decrease in $p34^{cdc2}$/cyclin B kinase activity is requisite for the decrease in MAP kinase activity, nocodazole treatment of metaphase II-arrested eggs should inhibit the fertilization-induced decreases in both $p34^{cdc2}$/cyclin B kinase and MAP kinase activities.

As anticipated, culture of metaphase II-arrested eggs in nocodazole resulted in an increase in histone H1 kinase activity (since cyclin B synthesis continues but degradation is inhibited), and insemination of eggs in the presence of nocodazole resulted in an inhibition of the fertilization-induced decrease in histone H1 kinase activity (Fig. 4A), as well as PN formation (data not shown). In contrast, addition of nocodazole 4 h after insemination, a time at which histone H1 kinase activity had already decreased (Fig. 2), neither elevated histone H1 kinase activity (Fig. 4A) nor inhibited PN formation (data not shown). It should be noted that laser-scanning confocal microscopy of metaphase II-arrested eggs cultured in the absence of nocodazole and stained with anti-tubulin antibodies revealed the presence of an intact spindle, whereas unfertilized eggs treated with nocodazole did not have a spindle (data not shown). It

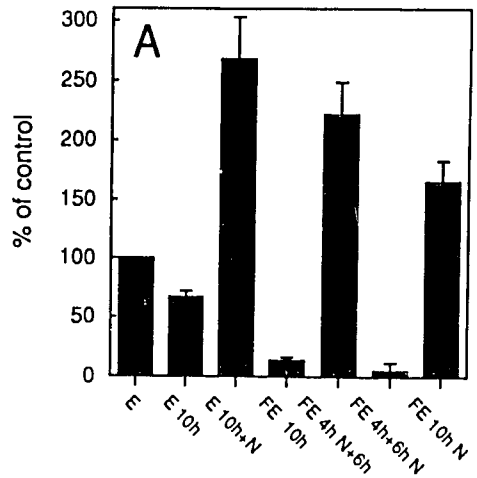

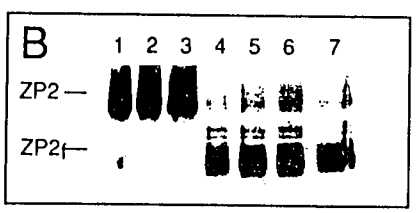

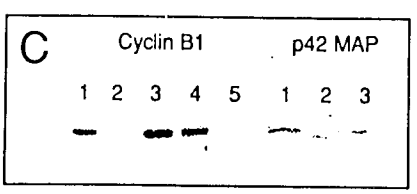

FIG. 4. Effect of nocodazole on histone H1 kinase activity, cyclin B1 accumulation, MAP kinase phosphorylation, and ZP2 to $ZP2_f$ conversion. A) Histone H1 kinase activity in ovulated eggs (E) or in in vitro-fertilized eggs (FE) was analyzed after 10 h of incubation in absence or presence of 10 μM nocodazole (N). In some experiments, unfertilized eggs (E 10 h) or inseminated eggs were incubated for 4 h in presence (FE 4h N + 6h) or absence (FE 4h + 6h N) of nocodazole, transferred to fresh medium with (FE 4h + 6h N) or without (FE 4h N + 6h) nocodazole, and then incubated for additional 6 h. Some eggs (E 10 h + N) or inseminated eggs (FE 10h + N) were continuously incubated in the presence of nocodazole for 10 h. Experiment was performed twice, and for each sample in each experiment, assay was performed in quadruplicate. Data are expressed as mean ± SEM. B) Effect of nocodazole treatment on fertilization-induced ZP2 to $ZP2_f$ conversion. Shown are immunoblots probed with polyclonal antiserum to ZP2 for presence of ZP2 (upper band) or its proteolyzed form $ZP2_f$ (lower band). Lanes 1–7 correspond to bars in A labeled E, E 10h, etc., respectively. Experiment was performed three times, with similar results; representative example shown. C) Immunoblots probed for either cyclin B1 or MAP kinase. Cyclin B1: lanes 1–3, conditions used for first three bars in A, i.e., E, E 10h, and E 10h + N, respectively; lane 4, extracts prepared from inseminated eggs continuously cultured in the presence of nocodazole for 10 h (FE 10h N); lane 5, fertilized eggs collected 10 h after insemination (FE 10h). p42 MAP: lane 1, MAP kinase in eggs fertilized in presence of nocodazole; lanes 2 and 3, conditions used in A for FE 4h + 6h N and FE 4h N + 6h. Only embryos used in lane 2 showed developed pronuclei. Experiment was performed three times, with similar results; representative example shown. Apparent lack of correlation between drop in histone H1 kinase activity in eggs incubated for 10 h (A) and dramatic decrease in immunoreactive cyclin B1 (C) appears because A represents average of several experiments, whereas only results of one experiment are shown in C.

1
145

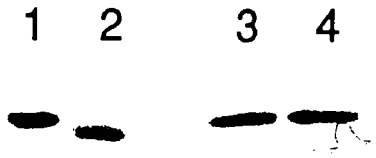

FIG. 5. Immunoblot of MAP kinase from inseminated eggs treated with OA. Lane 1, extracts prepared from metaphase II-arrested eggs; lane 2, extracts prepared from fertilized eggs 8 h postinsemination; lane 3, extracts prepared from eggs to which OA was added 5 h postinsemination and then cultured for additional 7 h; lane 4, extracts prepared from eggs to which OA was added 8 h postinsemination and then cultured for additional 4 h. At 5 h postinsemination, eggs had emitted 2nd polar body but did not contain visible PN. At 8 h postinsemination 80% of eggs contained visible PN. Experiment was performed twice, with similar results.

should also be noted that the effect of nocodazole (Fig. 4, panel A, FE 4h N + 6 h) was reversible, since removal of nocodazole by extensive washing resulted in resumption of normal development as assessed by a decrease in histone H1 kinase activity, dephosphorylation of MAP kinase, and PN formation (data not shown).

The effect of nocodazole to block the reduction in histone H1 kinase activity in fertilized eggs was apparently due to inhibition of cyclin B destruction (Fig. 4C, lanes 4 and 5). It should be noted that consistent with the changes in histone H1 kinase in metaphase II-arrested eggs cultured in either the absence or presence of nocodazole were parallel changes in the amount of cyclin B1 (Fig. 4C, lanes 1–3); this is similar to that observed by Kubiak et al. [17].

It is possible that the nocodazole-treated and inseminated eggs that did not display the decrease in histone H1 kinase activity were, in fact, not fertilized. To exclude this

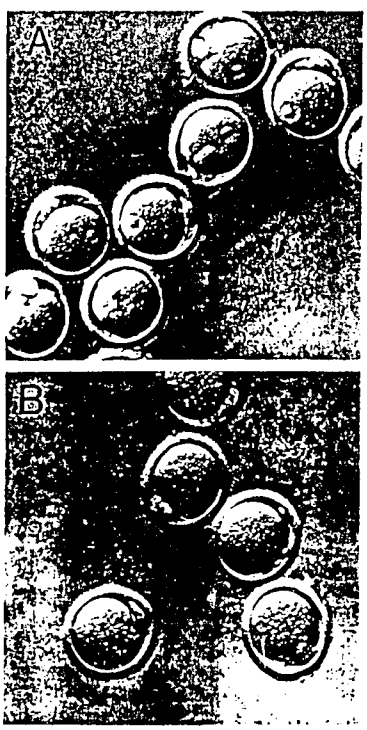

FIG. 6. Photomicrographs of (A) fertilized eggs cultured for 12 h or (B) fertilized eggs cultured for 8 h, at which time OA was added and eggs were cultured additional 4 h. When OA was added at 8 h postinsemination, all eggs had PN.

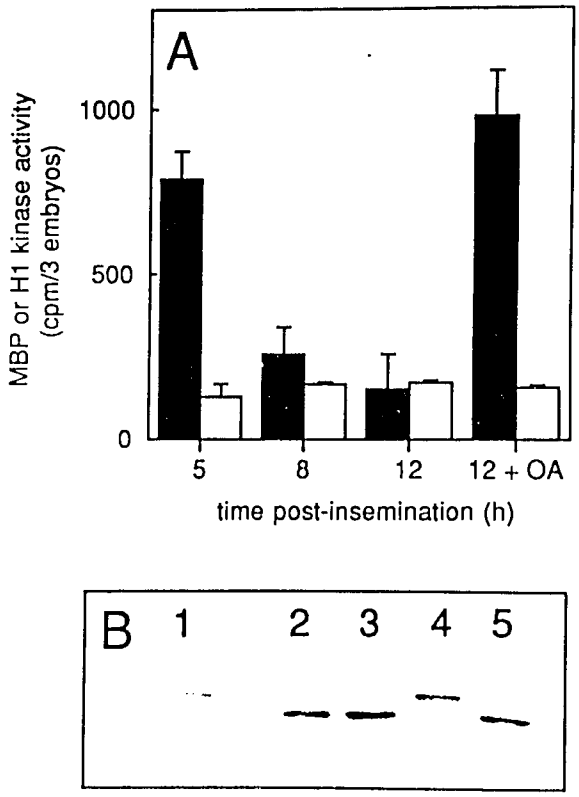

FIG. 7. Effect of OA on histone H1 kinase activity, MBP kinase activity, and phosphorylation state of MAP kinase. A) Fertilized eggs were assayed for either MBP kinase activity (solid bars) or histone H1 kinase activity (open bars) at times after insemination indicated. In one sample, OA was added 8 h after insemination and eggs were cultured additional 4 h (12 + OA). In each experiment cycloheximide was added (final concentration of 10 μg/ml) 5 h postinsemination. Experiment was performed three times, and for each experiment assay was performed in duplicate. Data are expressed as mean ± SEM. B) Immunoblot of extracts probed for MAP kinase. Lane 1, extracts prepared from fertilized eggs 5 h postinsemination; lane 2, extracts prepared from fertilized eggs cultured 8 h postinsemination; lane 3, extracts prepared from fertilized eggs cultured 12 h postinsemination; lane 4, extracts prepared from fertilized eggs cultured for 8 h, at which time OA was added and eggs were cultured additional 4 h. In each case, cycloheximide was added 5 h postinsemination. Lane 5, fertilized eggs cultured for 12 h postinsemination in absence of cycloheximide. Eggs used for lanes 2, 3, and 5 developed pronuclei. Experiment was conducted three times, with similar results; representative experiment shown.

146

possibility, we examined the effect of nocodazole treatment of inseminated eggs on the conversion of the ZP glycoprotein ZP2 to its postfertilization form $ZP2_f$. This modification is due to proteolysis and can be detected as an electrophoretic mobility shift under reducing conditions [24]. Nocodazole treatment of inseminated eggs did not inhibit the sperm-induced ZP2 to $ZP2_f$ conversion (Fig. 4B), which occurs as a consequence of cortical granule exocytosis that normally accompanies fertilization. This demonstrates that nocodazole most likely did not inhibit fertilization.

Nocodazole also blocked the fertilization-induced dephosphorylation of MAP kinase (Fig. 4C). Continuous culture of inseminated eggs for 10 h in nocodazole prevented the electrophoretic shift in MAP kinase that indicates MAP kinase inactivation (Fig. 4C, lane 1). Culture of inseminated eggs for 4 h in the absence of nocodazole, a time during which histone H1 kinase activity had decreased but MAP kinase remained phosphorylated (see Fig. 3), followed by incubation in nocodazole for 6 h resulted in the electrophoretic shift in MAP kinase (Fig. 4C, lane 2) and PN formation (data not shown). In contrast, culture of inseminated eggs for 4 h in the presence of nocodazole prior to transfer to nocodazole-free medium for 6 h inhibited both the shift in electrophoretic mobility of MAP kinase (Fig. 4C, lane 3) and PN formation (data not shown).

Effect of OA on MAP Kinase Activity and Pronuclear Envelope Assembly and Breakdown

Treatment of fertilized eggs that contain pronuclei with the protein phosphatase inhibitor OA results in precocious pronuclear envelope breakdown, i.e., pronuclear envelope breakdown prior to M phase [25]. It seemed unlikely that reactivation of histone H1 kinase, which is low at this time (Fig. 2), by OA was responsible for OA-induced pronuclear envelope breakdown, since OA inhibits protein synthesis [25] and this would prevent the accumulation of cyclin B that is required for activation of cdc2. Thus, it seems likely that another protein kinase was implicated in OA-induced pronuclear envelope breakdown. We examined whether MAP kinase was a candidate since a decrease in MAP kinase activity correlates with nuclear envelope formation (Fig. 3), and we reasoned that high levels of MAP kinase activity were perhaps incompatible with the presence of a nuclear envelope.

As demonstrated above, fertilized eggs containing a PN have a MAP kinase that exhibits an increased electrophoretic mobility relative to unfertilized eggs (Fig. 5, lanes 1 and 2). Addition of OA 5 h after insemination, a time when a PN was not present, followed by culture for an additional 3 h, at which time pronuclei were present in control inseminated eggs, inhibited MAP kinase dephosphorylation (Fig. 5, lane 3) and PN formation (data not shown). Addition of OA 8 h after insemination, when a PN is present and MAP kinase is dephosphorylated, followed by culture for an additional 4 h resulted in the rephosphorylation of MAP kinase (Fig. 5, lane 4) and pronuclear envelope breakdown (Fig. 6). Consistent with this latter result was the observation that OA treatment of eggs containing a PN resulted in an increase in MBP kinase activity, rephosphorylation of MAP kinase, and pronuclear envelope breakdown, and that this increase occurred in the absence of a reactivation of histone H1 kinase activity (Fig. 7A). To ensure that reactivation of $p34^{cdc2}$ could not occur during OA treatment, the fertilized eggs were also cultured in the presence of cycloheximide, which would prevent the accumulation of cyclin B and the subsequent activation of $p34^{cdc2}$.

The fertilization-induced dephosphorylation of MAP kinase occurred in the presence (Fig. 7B, lanes 1–3) or the absence of cycloheximide (Fig. 7B, lane 5); cycloheximide does not inhibit PN formation [26]. Moreover, in the presence of cycloheximide, OA induced a decrease in the electrophoretic mobility of MAP kinase (Fig. 7B, lane 4), and this was consistent with the increase in MBP kinase activity. Taken together, results of these experiments suggest a role for MAP kinase in pronuclear envelope assembly and disassembly.

DISCUSSION

We report that inhibition of the fertilization-induced decrease in $p34^{cdc2}$/cyclin B kinase activity is correlated with inhibition of the decline in MAP kinase activity. We also observe that maintaining an elevated level of MAP kinase activity is incompatible with the presence of a nuclear envelope; i.e., maintaining an elevated level of MAP kinase activity inhibits PN formation, and activating MAP kinase subsequent to PN formation results in precocious pronuclear envelope breakdown. This suggests that MAP kinase may play a role in nuclear envelope dynamics.

In an attempt to dissociate the decrease in MAP kinase activity from that of $p34^{cdc2}$/cyclin B kinase activity, we treated both metaphase II-arrested eggs and inseminated eggs with nocodazole. Treatment of metaphase II-arrested eggs with nocodazole resulted in an increase in histone H1 kinase activity, and this increase in activity appeared to be due to an accumulation of cyclin B1 protein. This observation is consistent with the continuous synthesis of cyclin B and the requirement for an intact spindle for cyclin B degradation [17]. As anticipated, insemination of nocodazole-treated eggs prevented the decrease in $p34^{cdc2}$/cyclin B activity but also the decrease in MAP kinase activity as assessed by its inability to be dephosphorylated. This inability to dissociate the decrease in MAP kinase from that of $p34^{cdc2}$/cyclin kinase suggests that the decrease in MAP kinase activity is contingent upon the decrease in $p34^{cdc2}$/cyclin kinase; the mechanism by which changes in these two enzyme activities are linked is unclear. It should be noted, however, that some events of egg activation (cell

147

cycle resumption, cortical granule exocytosis, mobilization of maternal mRNA) can be uncoupled from one another. For example, we show here that although nocodazole treatment of inseminated eggs blocks cell cycle resumption, cortical granule exocytosis still occurs, as determined by the ZP2 conversion. The dissociation of these two events of egg activation is consistent with our previous reports [26–28].

The most intriguing result in the present report is the observation that inhibiting the fertilization-induced decrease in MAP kinase activity by OA treatment is correlated with inhibiting PN formation, and that inducing an increase in MAP kinase activity by OA treatment following PN formation results in precocious pronuclear envelope breakdown, i.e., pronuclear envelope breakdown prior to M phase. It must be stressed that these changes in MAP kinase activity and nuclear envelope behavior occur at a time when $p34^{cdc2}$/cyclin kinase activity is low and experimentally maintained at a low level by inclusion of cycloheximide, which would prevent cyclin accumulation. Thus, elevated levels of MAP kinase activity appear to be incompatible with the existence of a nuclear envelope; i.e., high levels prevent the formation of a nuclear envelope, and induction of MAP kinase activity results in pronuclear envelope breakdown. Consistent with this conclusion is the observation that, although progression from metaphase I to metaphase II during oocyte maturation in *Xenopus* [29] and mouse [30] is accompanied by a transient decrease in histone H1 kinase activity, MAP kinase activity remains constant and elevated, and no nuclear envelope formation and breakdown occurs during the metaphase I/II transition. Similarly, treatment of mouse oocytes with OA results in an increase in MAP kinase activity and germinal vesicle breakdown in the apparent absence of an increase in histone H1 kinase activity prior to germinal vesicle breakdown [31, 32].

The experimental unmasking of this potential function of MAP kinase to initiate pronuclear envelope breakdown may reflect the fact that MAP kinase and $p34^{cdc2}$/cyclin B kinase share common substrates that are ultimately linked to nuclear envelope assembly/disassembly; e.g., both can phosphorylate nuclear lamins [33]. Nuclear envelope dynamics in the mouse appear to be under the regulation of $p34^{cdc2}$/cyclin B kinase. For example, during oocyte maturation, the increase in $p34^{cdc2}$/cyclin B kinase occurs prior to germinal vesicle breakdown, and the increase in MAP kinase occurs subsequently [16, 30]. Moreover, there is an increase in $p34^{cdc2}$/cyclin B kinase activity only during M phase of the first cell cycle. Nevertheless, it should be noted that an increase in MAP kinase activity precedes germinal vesicle breakdown during *Spisula* oocyte maturation induced by fertilization and that this increase occurs while $p34^{cdc2}$ is still phosphorylated on tyrosine and is presumably inactive [34]. Thus, in this species, MAP kinase may be the primary regulator of nuclear envelope assembly/disassembly.

REFERENCES

1. Miyazaki S, Shirakawa H, Nakada K, Honda Y. Essential role of the inositol 1,4,5-trisphosphate receptor/Ca^{2+} release channel in Ca^{2+} waves and Ca^{2+} oscillations at fertilization of mammalian eggs. Dev Biol 1993; 158:62–78.
2. Cascio SM, Wassarman PM. Program of early development in the mammalian: post-transcriptional control of a class of proteins synthesized by mouse oocytes and early embryos. Dev Biol 1982; 89:397–408.
3. Masui Y, Markert CL. Cytoplasmic control of nuclear behavior during meiotic maturation of frog oocytes. J Exp Zool 1971; 177:129–145.
4. Gautier J, Minshull J, Lohka M, Glotzer M, Hunt T, Maller JL. Cyclin is a component of maturation-promoting factor from Xenopus. Cell 1990; 60:87–494.
5. Gautier J, Norbury C, Lohka M, Nurse P, Maller JL. Purified maturation-promoting factor contains the product of a Xenopus homolog of the fission yeast cell cycle control gene cdc2+. Cell 1988; 54:433–439.
6. Masui Y. The role of cytostatic factor (CSF) in control of oocyte cell cycles—a summary of 20 years of study. Dev Growth & Differ 1991; 33:543–551.
7. Sagata N, Watanabe N, Vande Woude GF, Ikawa Y. The c-*mos* proto-oncogene product is a cytostatic factor responsible for meiotic arrest in vertebrate eggs. Nature 1989; 342:512–518.
8. Nebreda AR, Hunt T. The c-*mos* proto-oncogene protein kinase turns on and maintains the activity of MAP kinase, but not MPF, in cell-free extracts of Xenopus oocytes and eggs. EMBO J 1993; 12:1979–1986.
9. Haccard O, Sarcevic B, Lewellyn A, Hartley R, Roy L, Izumi T, Erikson E, Maller JL. Induction of metaphase arrest in cleaving Xenopus embryos by MAP kinase. Science 1993; 262:1262–1265.
10. Murray AW. Creative blocks: cell-cycle checkpoints and feedback controls. Nature 1993; 359:599–604.
11. Lorca T, Cruzalegui FH, Fesquet D, Cavadore J-C, Mery J, Means A, Dorée M. Calmodulin-dependent protein kinase II mediates inactivation of MPF and CSF upon fertilization of Xenopus eggs. Nature 1993; 366:270–273.
12. Gerhart J, Wu M, Kirschner M. Cell cycle dynamics of an M-phase specific cytoplasmic factor in Xenopus laevis oocytes and eggs. J Cell Biol 1984; 98:1247–1255.
13. Watanabe N, Hunt T, Ikawa Y, Sagata N. Independent inactivation of MPF and cytostatic factor (Mos) upon fertilization of Xenopus eggs. Nature 1991; 352:247–248.
14. Nishida E, Gotoh Y. The MAP kinase cascade is essential for diverse signal transduction pathways. TIBS 1993; 18:128–131.
15. Pelech SL, Sanghera JS. Mitogen-activated protein kinases: versatile transducers for cell signaling. TIBS 1992; 17:233–238.
16. Verlhac M-H, Kubiak JZ, Clarke HJ, Maro BH. Microtubule and chromatin behavior follow MAP kinase activity but not MPF activity during meiosis in mouse oocytes. Development 1994; 120:1017–1025.
17. Kubiak JZ, Weber M, de Pennart H, Winston NJ, Maro B. The metaphase II arrest in mouse oocytes is controlled through microtubule-dependent destruction of cyclin B in the presence of CSF. EMBO J 1993; 12:3773–3778.
18. Whitten WK. Nutrient requirements for the culture of preimplantation embryos in vitro. Adv Biosci 1971; 6:129–139.
19. Moore GD, Ayabe T, Visconti PE, Schultz RM, Kopf GS. Roles of heterotrimeric and monomeric G proteins in sperm-induced activation of mouse eggs. Development 1994; 120:3313–3323.
20. Hogan B, Kostantini F, Lacy E. Manipulating the Mouse Embryo, 1st ed. Cold Spring Harbor, NY: Cold Spring Harbor Laboratory Press, 1986; p. 276.
21. Laemmli UK. Cleavage of structural proteins during the assembly of the head of bacteriophage T4. Nature 1970; 227:680–685.
22. Towbin H, Staehelin T, Gordon J. Electrophoretic transfer of proteins from polyacrylamide gels to nitrocellulose sheets: procedure and some application. Proc Natl Acad Sci USA 1979; 76:4350–4354.
23. Moos J, Kalab P, Kopf GS, Schultz RM. A rapid, non-radioactive, and quantitative method to analyze zona pellucida modifications in single mouse eggs. Mol Reprod Dev 1994; 38:91–93.
24. Wassarman PM. Zona pellucida glycoproteins. Annu Rev Biochem 1988; 57:415–442.
25. Schwartz DA, Schultz RM. Stimulatory effect of okadaic acid, an inhibitor of protein phosphatases, on nuclear envelope breakdown and protein phosphorylation in mouse oocyte and one-cell embryos. Dev Biol 1991; 145:119–127.
26. Moore GD, Kopf GS, Schultz RM. Complete mouse egg activation in the absence of sperm by stimulation of an exogenous G protein-coupled receptor. Dev Biol 1993; 159:669–678.
27. Kurasawa S, Schultz RM, Kopf GS. Egg-induced modifications of the zona pellucida of mouse eggs: effects of microinjected inositol 1,4,5-trisphosphate. Dev Biol 1989; 133:295–304.
28. Williams CJ, Schultz RM, Kopf GS. Role of G proteins in mouse egg activation: stimulatory

148

effects of acetylcholine on the ZP2 to $ZP2_f$ conversion and pronuclear formation in eggs expressing a functional m1 muscarinic receptor. Dev Biol 1992; 151:288–296.
29. Ferrell JE, Wu M, Gerhart JC, Martin GS. Cell cycle tyrosine phosphorylation of p34 cdc2 and microtubule associated protein kinase homolog in Xenopus oocytes and eggs. Mol Cell Biol 1991; 11:1965–1971.
30. Verlhac M-H, de Pennart H, Maro B, Corb MH, Clarke HJ. MAP kinase becomes stably activated at metaphase and is associated with microtubule-organizing center during meiotic maturation of mouse oocytes. Dev Biol 1993; 158:330–340.
31. Gavin AC, Cavadore JC, Schorderet-Slatkine S. Histone H1 kinase activity, germinal vesicle breakdown and M phase entry in mouse oocytes. J Cell Sci 1994; 107:275–283.
32. Chesnel F, Eppig JJ. Induction of precocious germinal vesicle breakdown (GVB) by GVB-incompetent mouse oocytes: possible role of MAP kinases rather than p34cdc2 kinase. Biol Reprod 1995; 52:895–902.
33. Peter M, Sanghera JS, Pelech SL, Nigg EA. Mitogen-activated protein kinases phosphorylate nuclear lamins and display sequence specificity overlapping that of mitotic protein kinase $p34^{cdc2}$. Eur J Biochem 1992; 205:287–294.
34. Shibuya EK, Bolton TG, Cobb MH, Ruderman JV. Activation of p42 MAP kinase and the release of oocytes from cell cycle arrest. EMBO J 1992; 11:3963–3975.

149

MOLECULAR REPRODUCTION AND DEVELOPMENT 41:521–529 (1995)

F-Actin Is Involved in Control of Bovine Cumulus Expansion

PETER ŠUTOVSKÝ,[1,2] JACQUES E. FLÉCHON,[2] AND ANTONÍN PAVLOK[1]
[1]*Institute of Animal Physiology and Genetics, LIBĚCHOV, Czech Republic;* [2]*INRA, Laboratoire de Biologie Cellulaire et Moléculaire, Jouy-En-Josas, France*

ABSTRACT Previously, we showed that the gonadotropin-induced expansion of bovine cumulus oophorus occurs concomitantly with the rearrangement of microfilaments (MFs) inside cumulus cell cytoplasm (Šutovský et al., 1993: Biol Reprod 49:1277–1287; Šutovský et al., 1994: Reprod Nutr Dev 34:415–425) and that cumulus expansion in cattle is accompanied by the increased expression of extracellular matrix (ECM) glycoproteins laminin and type IV collagen as well as of their actin-linked membrane receptors, integrin subunits α-6 and β-1 (Šutovský and Motlík, 1994). The present study was undertaken to determine the spatial and temporal relationship between cytoskeletal rearrangement and ECM synthesis during cumulus expansion. Using electron microscopy and confocal (LSCM) and conventional fluorescence microscopy, we compared the expression of the above integrins and ECM proteins and the rearrangement of cytoskeleton in the gonadotropin-stimulated bovine oocyte cumulus complexes (OCCs) with those exposed to gonadotropin stimulation and to ECM synthesis inhibitor 6-diazo-5-oxo-L-norleucin (DON), or MF-disorganizing drug cytochalasin B (CB). In control OCCs, the 24-hr culture in the presence of follicle stimulating hormone/luteinizing hormone (FSH/LH) caused the expansion of cumuli oophori and an extensive rearrangement of MFs in the cytoplasm of cumulus cells. Concomitantly, we observed an increased deposition of laminin and type IV collagen in the intercellular spaces among cumulus cells. The redistribution of microtubules (MTs), intermediate filaments (IFs), and integrin chains α-6 and β-1 also occurred at this time. The addition of 20 μg/ml of CB prevented cumulus expansion and accumulation of laminin and type IV collagen in the OCCs. Moreover, cytochalasin treatment blocked the redistribution of MTs and IFs, and caused the disorganization of MFs and dispersion of integrins in cumulus cells. In contrast, the distribution of integrins and cytoskeletal elements was not affected when we blocked cumulus expansion and ECM protein accumulation by DON. These data suggest that F-actin acts upstream of ECM synthesis in the cascade of events leading to the expansion of bovine cumulus oophorus. © 1995 Wiley-Liss, Inc.

Key Words: Cumulus expansion, Actin, Cytoskeleton, Extracellular matrix, Integrin

© 1995 WILEY-LISS, INC.

INTRODUCTION

Gonadotropin-induced cumulus expansion, a process necessary for the release of matured mammalian oocyte into the oviduct, is believed to arise from the increased deposition of cumulus extracellular matrix (ECM) enriched by hyaluronic acid (HA; Dekel et al., 1979; Eppig, 1979; Salustri et al., 1992). Although cumulus expansion in mice requires an oocyte-secreted expansion enabling factor (Buccione et al., 1990; Salustri et al., 1990), this is not necessary for cumulus expansion in pig and cattle (Procházka et al., 1991; Motlík et al., unpublished data). The assembly of cumulus ECM depends upon stabilizing factor(s) present in follicular fluid and also found in fetal bovine serum, an essential component of media used for in vitro culture of mammalian oocyte cumulus complexes (OCCs; Camaioni et al., 1993; Chen et al., 1992). In line with these data, it was shown that cumulus expansion can be blocked by 6-diazo-5-oxo-L-norleucin (DON), a compound preventing the synthesis of proteoglycan and glycoprotein precursor N-acetyl-glucosamine (Chen et al., 1990). Interestingly, the same inhibitory effect can be achieved using the actin depolymerizing drug cytochalasin B (CB; Šutovský et al., 1994), or its analogs dihydrocytochalasin B (Wert and Larsen, 1989) and cytochalasin D (CD; De Smedt and Szöllosi, 1991). CB treatment also enhances the process of granulosa cell differentiation in vitro (Ben-Ze'ev and Amsterdam, 1987).

Our recent studies reveal that cumulus expansion in cattle parallels the redistribution of individual cytoskeletal components in cumulus cells, starting by massive assembly of actin microfilaments (MF; Šutovský et al., 1993, 1994). Furthermore, the secretion of ECM glycoproteins (laminin, type IV collagen, and fibronectin) occurs during cumulus expansion in cattle and mice and is accompanied by the expression of their membrane receptors, integrins α-6 and β-1 (Šutovský and Motlík, 1994). Since these integrins are linked with the microfilament cytoskeleton (Luna and

Received November 21, 1994; accepted January 27, 1995.
Address reprint requests to Peter Šutovský, Department of Zoology, University of Wisconsin, 1117 West Johnson Street, Madison, WI 53706.

150

Hytt, 1992), it is possible that this link mediates the anchorage of HA-rich cumulus ECM to the plasma membrane of cumulus cells. Moreover, the above observations raise the question whether the interaction between cumulus ECM and the cytoskeleton of cumulus cells could be a pathway regulating cumulus expansion in response to gonadotropins.

In the present study, we compare the effect of DON and CB on the accumulation of ECM glycoproteins, rearrangement of cytoskeletal elements, and redistribution of integrins during in vitro expansion of bovine OCCs. Our results show that CB causes the internalization of integrin subunits α-6 and β-1, inhibition of cytoskeletal rearrangement in cumulus cell cytoplasm, and block of the accumulation of laminin and type IV collagen in cumulus ECM. Similar to CB, the inhibition of ECM synthesis by DON enhances the expression of laminin and type IV collagen by cumulus cells. However, this treatment does not affect cytoskeleton and integrin rearrangement. Thus, it seems likely that F-actin regulates cumulus expansion upstream of the secretion of cumulus ECM and this regulatory pathway may involve the control of ECM assembly by integrin membrane receptors.

MATERIALS AND METHODS

Collection and Culture of Bovine OCCs

Bovine ovaries were collected at the slaughterhouse and immediately transported to the laboratory. The ovaries were briefly washed with 70% ethyl alcohol followed by double washing with phosphate-buffered saline (PBS). The large follicles and corpora lutea were removed and the ovaries were cut open at the margo mesoovaricus. Each ovary was then put into 90 mm Petri dishes and sliced by surgical knives mounted in parallel. The sedimented OCCs with tissue fragments and some follicular fluid were redistributed into a 90 mm Petri dish. The compact OCCs with at least five layers of cumulus cells were collected from the bottom of the dishes and cultured for 24 hr in M199 culture medium, supplemented with 10% fetal calf serum (FCS; Flow Laboratories, McLean, VA), 1 μg/ml of estradiol, and 10 μg/ml of follicle stimulating hormone-luteinizing hormone (FSH-LH; Stimufol, Rhone-Merieux, Lyon, France). The culture was maintained at 39°C in humid atmosphere of 5% CO_2 in air. In order to block ECM synthesis and cumulus expansion, one group of OCCs was cultured for 24 hr in the above medium (further referred to as complete medium) supplemented with 20 μg/ml of DON (Sigma, St. Louis, MO). Alternatively, the OCCs were cultured for 24 hr in the presence of 20 μg/ml of CB (Serva Heidelberg, Germany) causing the block of cumulus expansion. In a control experiment, the same inhibitory effect of cumulus expansion and ECM synthesis was achieved using 10 μg/ml of cytochalasin D (data not shown). To evaluate the reversibility of CB treatment, a group of control OCCs was withdrawn from CB containing culture medium after 24 hr of culture, washed, and cultured for up to 24 hr in complete medium. Following the culture, the OCCs from individual control and experimental groups were examined with a stereomicroscope in order to determine the degree of cumulus expansion according to the subjective scoring method described by Vanderhyden et al. (1990). Thus, only the OCCs with all layers of cumulus cells expanded were referred to as expanded complexes. At least 20 representative OCCs from every culture group were processed for immunofluorescence or electron microscopy. In parallel, uncultured 0-hr controls were fixed. The present results summarize the data from five experiments including 0-hr and 24-hr control and the treatments with DON and CB at the concentrations defined above.

Immunofluorescence

The OCCs were processed using a protocol described previously (Šutovský et al., 1993). Briefly, they were fixed for 20 min in 2.5% paraformaldehyde in PBS (pH 7.3), incubated for 1 hr in 50 mM ammonium chloride to remove remaining free aldehydic groups, washed, and conserved in 0.1 M PBS with 0.05% sodium azide and 1 mM PMSF (Serva Heidelberg). The following antibodies were used to trace the distribution of integrins, ECM proteins, and cytoskeleton: anti-α-6 (VLA-6 integrin subunit) rat monoclonal antibody (Sonnenberg et al., 1988; diluted 1/20) from Central Laboratory of Blood Transfusion of the Netherlands Red Cross, Amsterdam; anti-β-1 (VLA-1 integrin subunit) mouse monoclonal antibody (Yllane and Virtanen, 1989; diluted 1/2) from University of Helsinki, Finland; anti-laminin (Demarchez et al., 1987; Duband and Thiery, 1987; diluted 1/150), and anti-type IV collagen (Duband and Thiery, 1987; diluted 1/100) rabbit polyclonal antibodies (Institut Pasteur, Lyon, France). Microtubules (MTs) were labelled by the anti-α-tubulin TU01 (Viklický et al., 1982; diluted 1/40) mouse monoclonal from Institute of Molecular Genetics, Prague, Czech Republic; intermediate filaments (IFs) were labelled by anti-vimentin (Virtanen et al., 1988; diluted 1/2) mouse monoclonal antibody from University of Helsinki, Finland; MFs were labelled by rhodamine-conjugated phalloidin (Molecular Probes, Eugene, OR). Secondary antibodies were FITC-conjugated anti-mouse IgG and anti-rabbit IgG (both from USOL Praha; diluted 1/40) and FITC-conjugated anti-rat IgG (Biosys, Compiegne, France; diluted 1/400). All antibodies used in this study were previously shown to display specific reactions with the antigens in bovine cumuli oophori (Šutovský et al., 1993, 1994; Šutovský and Motlík, 1994). Nonspecific reactions were prevented by incubation in 0.1 M PBS, containing 2% of bovine serum albumin (BSA; Sigma), 0.05% sodium azide, and 0.05% saponin (Sigma). Then the OCCs were incubated for 1 hr with primary antibody diluted in the same solution as used for preincubation, thoroughly washed in 0.1 M PBS with 0.2% BSA, 0.05% sodium azide, and 0.05% saponin, treated with secondary antibody, washed, and mounted on slides in a mixture of Mowiol V 4-88 (Hoechst, Frankfurt, Germany) and n-propyl-gallate

15

(Sigma). An average number of 20 OCCs was processed with each antibody and at each time point in individual culture and control groups. The OCCs were examined and photographed with Polyvar (Reichert Jung) and Leitz Axiophot (Leica) fluorescence microscopes (ECM and cytoskeletal proteins) or Zeiss confocal microscope (integrin chains α-6 and β-1). In both cases, the images were recorded on Ilford 400 Delta black and white film. The negatives were scanned by a Nikon Coolscan image scanner, recorded by a Macintosh Quadra 840AV computer, and the figure plates were created using Adobe Photoshop3 software (Adobe Systems Inc., Mountain View, CA).

Electron Microscopy

The OCCs were fixed for 1 hr at 4°C in a mix of 2.5% glutaraldehyde and 0.6% paraformaldehyde in cacodylate buffer (pH 7.4), washed, postfixed for 1 h in 1% osmium tetroxide, washed in distilled water, postfixed for 30 min in 1% tannic acid, dehydrated in ascending ethanol series, and embedded in Epon 812. The ultrathin sections were obtained using a Reichert Jung Ultracut E microtome, placed on the formvar-coated copper grids, contrasted with uranyl acetate and lead citrate, and observed with a Jeol 1200 EX electron microscope.

RESULTS

Both CB and DON Treatments Suppress Accumulation of Laminin and Type IV Collagen in the OCCs

Dot-like patterns of immunofluorescence labelling of laminin and type IV collagen demonstrated the low amounts of these proteins in the unstimulated OCCs (Fig. 1A,A′). A 24-hr culture in the presence of gonadotropins caused full expansion of cumuli oophori in 100% of cultured OCCs and significantly increased the secretion of laminin and type IV collagen, visible as large deposits at the surfaces of cumulus cells (Fig. 1B,B′). Both 24-hr cultures in gonadotropin-supplemented medium with addition of 20 μg/ml of DON (Fig. 1C,C′) or 20 μg/ml of CB (Fig. 1D,D′) prevented cumulus expansion and decreased the assembly of laminin and type IV collagen in the extracellular spaces. The labelling patterns of laminin and type IV collagen in CB or DON-treated OCC resembled those observed in unstimulated controls (Fig. 1A,A′).

CB Treatment Randomizes the Distribution of F-Actin and Prevents the Redistribution of MTs and IFs

MFs were regularly dispersed throughout the cortical cytoplasm of cumulus cells in the unstimulated OCCs (Fig. 2A). A 24-hr culture in gonadotropin-supplemented medium induced the assembly of F-actin and formation of long MF bundles (Fig. 2B). Most prominently, the bundling of actin MFs occurred in the cytoplasmic projections of cumulus cells. The assembly of actin MFs, reminiscent to the one observed in fully expanded OCCs, and the formation of cytoplasmic projections were observed in the OCCs cultured in DON-supplemented medium (Fig. 2C). In the OCCs cultured for 24 hr in the presence of CB, the MFs were aggregated in large clumps or bundles, randomly distributed throughout the cytoplasm of cumulus cells, and no projections were seen (Fig. 2D). Following the removal of OCCs from CB-supplemented culture medium and further culture in the presence of gonadotropins alone, the MF cytoskeleton of cumulus cells was restored to a pattern similar to unstimulated OCCs. However, neither cumulus expansion nor elongation of cumulus cells occurred, even if the culture was prolonged up to 24 hr after cytochalasin removal (not shown).

The MTs and IFs formed regular cytoplasmic networks in the round-shaped cells of the unstimulated OCCs (Fig. 2A′,A″). Following cumulus expansion, the cytoskeletal networks protruded into newly formed cytoplasmic projections (Fig. 2B′,B″). Similar to gonadotropin-stimulated OCCs (24 hr), the cells in the OCCs treated with DON possessed large projections loaded with MTs and IFs (Fig. 2C′,C″). Despite the high concentration of gonadotropins in culture medium, the cells in CB-treated OCCs remained round and did not form the projections and membrane ruffles. The distribution of MTs and IFs (Fig. 2D′,D″) remained similar to that of controls (0 h).

CB Treatment Causes the Internalization of Integrin Subunits α-6 and β-1

Using laser scanning confocal microscopy (LSCM), the immunofluorescence labelling of integrin subunits α-6 and β-1 was localized to the surface of cumulus cells in both unstimulated (Fig. 3A,A′) and expanded (24 h) OCCs (Fig. 3B,B′). A slight increase in labelling intensity was recorded in the expanded ones. The treatment with DON had no effect on integrin distribution (Fig. 3C,C′) and resulted in labelling patterns similar to those observed in fully expanded cumuli. On the contrary, the arrangement of both integrin subunits was dramatically disturbed by cytochalasin treatment, causing their internalization and spreading throughout the cytoplasm of cumulus cells (Fig. 3D,D′).

CB but not DON Treatment Prevents the Elongation and Polarization of Cumulus Cells

Unstimulated bovine OCCs contained tightly packed round cells with numerous small microvilli (Fig. 4A). Twenty-four hours of culture in the presence of gonadotropins resulted in a complete expansion of cumuli oophori including the innermost layers of cumulus cells. This was characterized by the extension of extracellular spaces, elongation of cumulus cells, and polarized distribution of their cytoplasmic organelles. Large cytoplasmic projections oriented towards the oocyte were the most prominent feature of these cells (Fig. 4B). Inhibition of ECM synthesis by DON prevented the extension of intercellular spaces among cumulus cells, but had no effect on their polarization and elongation: after 24 hr of culture in DON-supplemented

152

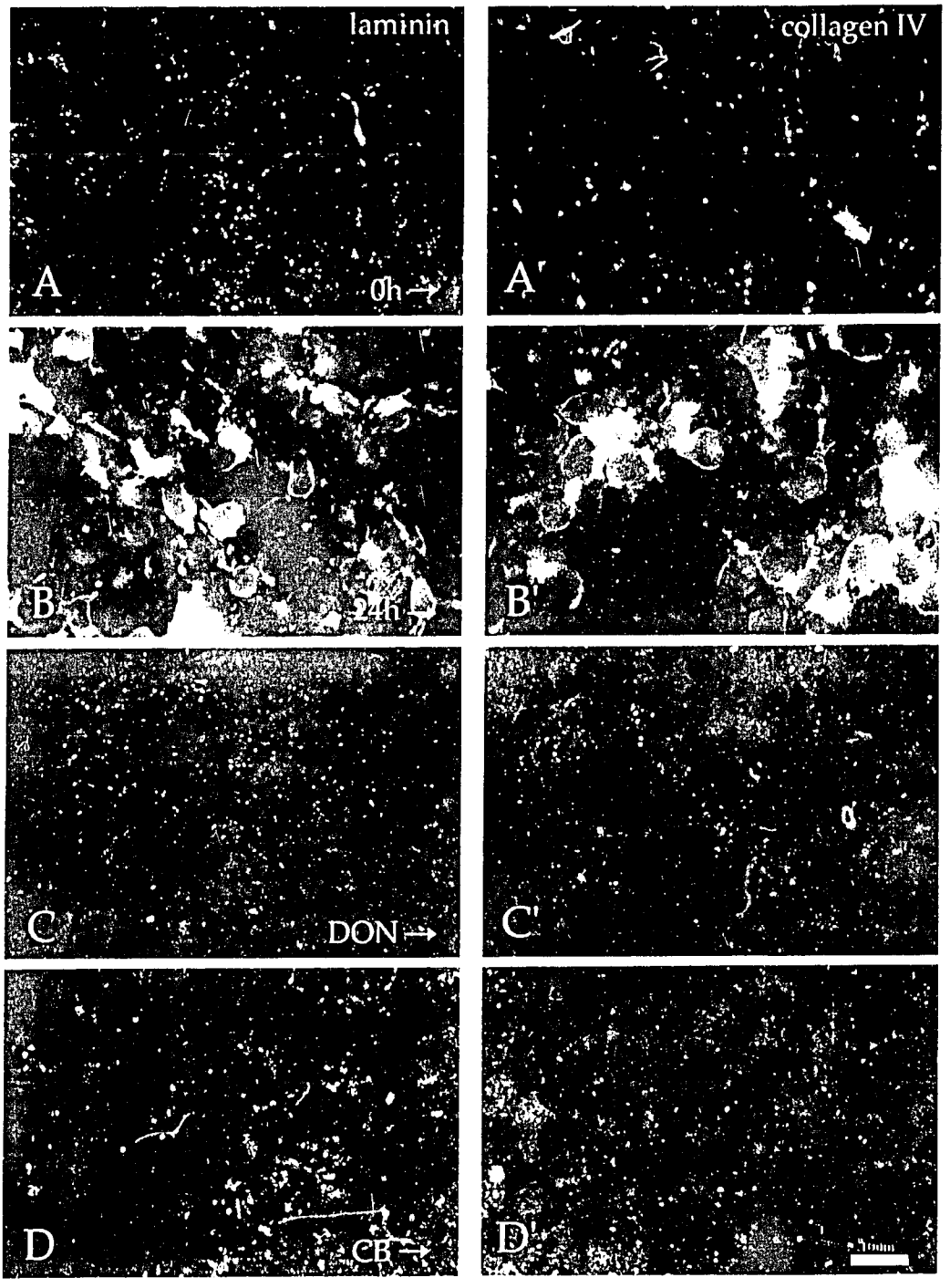

Fig. 1. Increased expression of laminin and type IV collagen in bovine cumulus cells by gonadotropin stimulation is repressed in the presence of DON or CB. The OCC's were processed for immunofluorescence with anti laminin (A-D) or anti-type IV collagen (A'-D') antibody either uncultured (A,A') or after 24 hr of culture in gonadotropin-supplemented (complete) medium (B,B') and after 24 hr of culture in complete medium supplemented by DON (C,C') or CB (D,D'). Images were taken by conventional fluorescence microscope. Bar 10 µm.

153

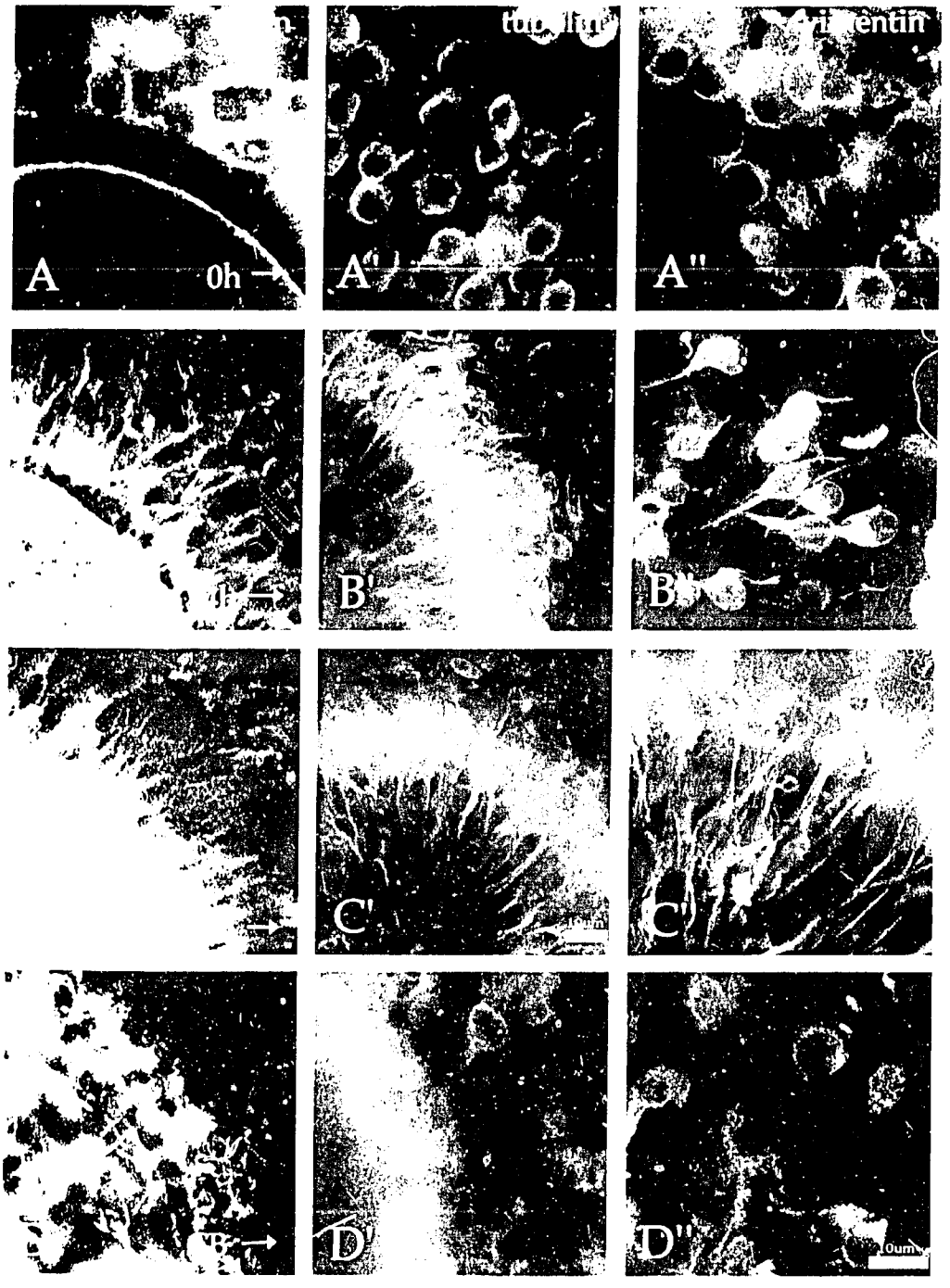

Fig. 2. Distribution of MFs (A-D, actin), MTs (A'-D', tubulin), and IFs (A''-D'', vimentin) in the cells of bovine OCCs cultured for 0 hr (A,A''), for 24 hr in complete medium with gonadotropins only (B-B''), for 24 hr in complete medium supplemented by DON (C'-C''), or for 24 hr in complete medium dotted by CB (D-D''). DON-treated cells display similar cytoskeletal arrangement and shape to the cells in expanded OCCs, whereas CB treatment resulted in the block of cytoskeletal reorganization and cell elongation. Images were recorded by conventional fluorescence microscope and digitalized. Both bars = 10 μm.

154

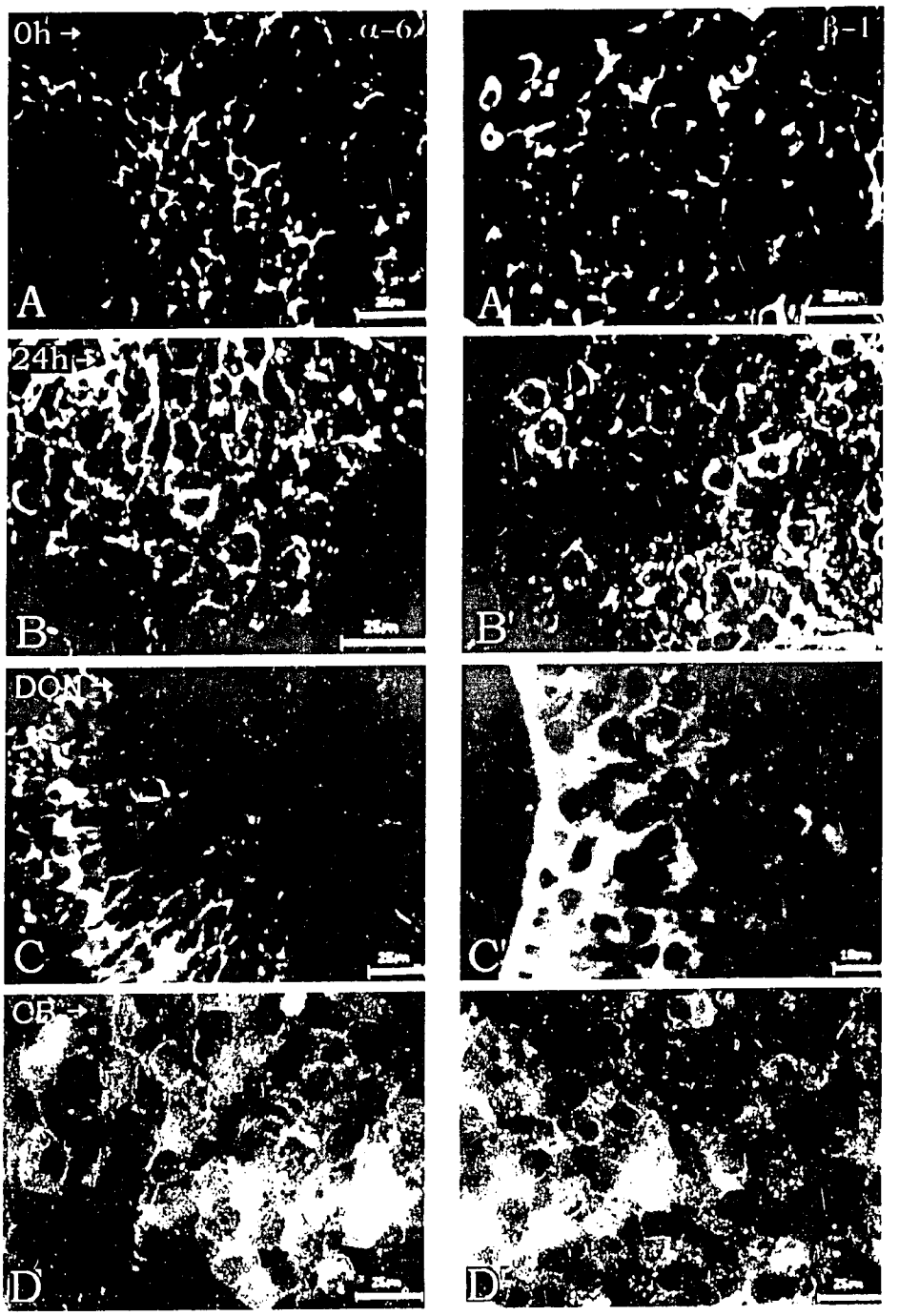

Fig. 3. CB causes the internalization of integrin chains α-6 (A-D) and β-1 (A'-D') in the cells of gonadotropin-stimulated bovine OCC's. The integrins are predominantly localized to the plasma membrane of cumulus cells in both unstimulated (0 hr; A,A') and expanded (24 hr; B,B') complexes. Although similar integrin distribution occurs in DON-treated complexes (C,C'), both integrin chains are scattered throughout the cytoplasm of cumulus cells in the OCC's cultured in the presence of CB (D,D'). Images show one focus plane section of cumulus oophorus as recorded by confocal microscope. Bars = 25 μm, except C' = 10 μm.

155

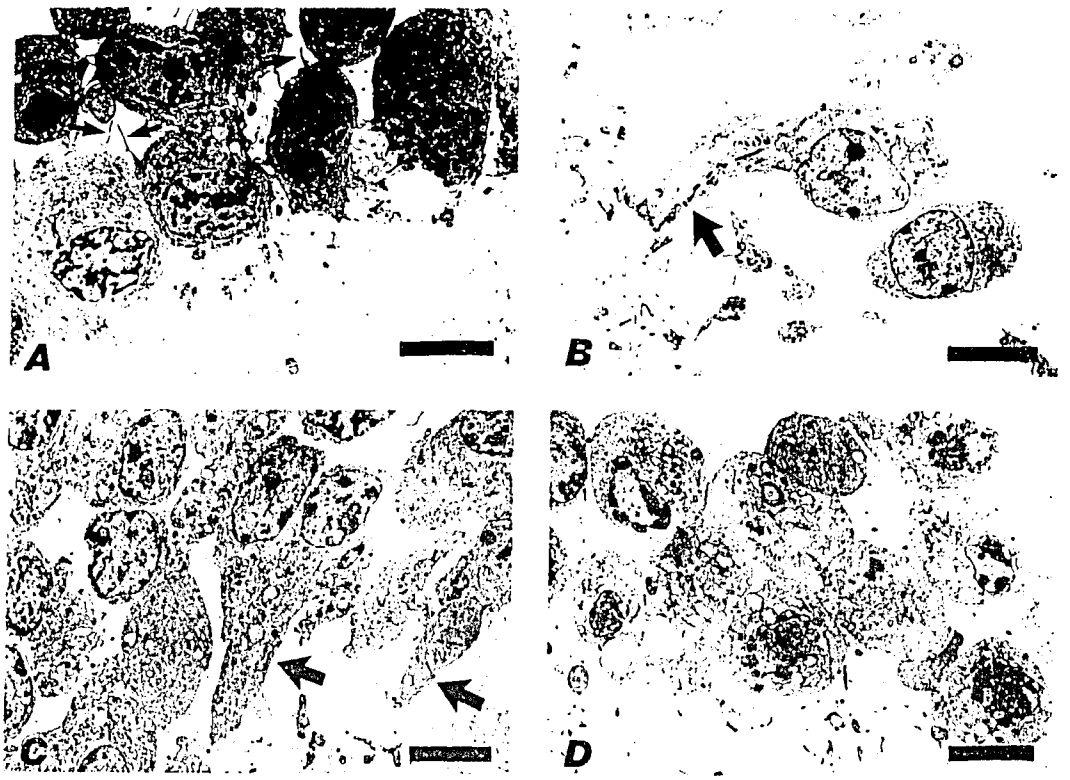

Fig. 4. Electron micrographs showing the degree of cumulus expansion and the morphology of cumulus cells in the OCCs processed for electron microscopy after different culture intervals and treatments. Whereas the round-shaped cells in an unstimulated OCC (A) display numerous microvilli (arrows), the large, foot-like projections (arrow) are seen after cumulus expansion (B). This kind of cytoplasmic projection (arrows) was also found in DON-treated cumuli, where the cells remained tightly packed (C). CB treatment inhibited both the extension of intercellular spaces and the formation of cytoplasmic projections. Moreover, the round-shaped cells in these OCCs are completely devoid of microvilli (D). All bars = 5 μm.

medium with gonadotropins, the cells remained tightly packed but displayed a morphology similar to that found in fully expanded control complexes (Fig. 4C). In the presence of 20 μg/ml of CB, the cumulus cells also remained tightly packed and retained their round shape (Fig. 4D). Neither large cytoplasmic projections nor surface microvilli were found in these cumulus cells (Fig. 4D).

DISCUSSION

The present study is aimed to determine the spatial and temporal relationship between cytoskeletal rearrangement and ECM assembly in gonadotropin-stimulated bovine cumulus oophorus cells.

The timing of the events giving rise to cumulus expansion revealed that this process is initiated by the rearrangement of MFs in the cumulus cell cytoplasm, preceding the acceleration of ECM synthesis, redistribution of MTs and IFs, and the modification of the gap junctional pathway between cumulus cells and oocyte (Šutovský et al., 1993, 1994). To distinguish these particular processes, we blocked cumulus expansion by preventing actin polymerization (CB or CD), or by suppressing the synthesis of cumulus ECM (DON). In agreement with our expectation, the addition of DON into gonadotropin-supplemented culture medium suppressed the increased expression of laminin and type IV collagen, presumably by blocking the synthesis of N-acetyl-glucosamine (Chen et al., 1990). However, this treatment had no effect on the process of cumulus cell morphological differentiation. Thus, regardless of the block of cumulus expansion, the cells in the DON-treated OCCs acquired the elongated shape and displayed typical features of cells in fully expanded cumuli oophori (Albertini and Rider, 1994; Allworth and Albertini, 1993; Šutovský et al., 1993, 1994). Disruption of MF by cytochalasins, previously shown to block cytoskeletal rearrangement during cumulus cell differentiation in bovine (Šutovský et al., 1994), rat (Wert and Larsen, 1989; Chen et al., 1990), and sheep (De Smedt

156

and Szöllösi, 1991), also prevented the accumulation of laminin and type IV collagen at the surface of cumulus cells and caused the internalization of integrin subunits α-6 and β-1. Since the link between MFs and integrins is now well established (reviewed in Luna and Hytt, 1992; Juliano and Haskill, 1993), we can speculate that the MF-directed assembly of integrins at the plasma membrane of cumulus cells is a prerequisite for the binding of the components of cumulus ECM to plasma membrane. Whereas Chen et al. (1992) proved that the retention of ECM in cumulus oophorus depends upon the intrinsic factor crosslinking its components, the necessity of an additional mechanism involved in control of cumulus ECM assembly has been suggested by Camaioni et al. (1993). Perhaps, one way for cumulus ECM stabilization may involve the MF-controlled integrin turnover and/or topology at the plasma membrane of cumulus cells. In line with this theory, Schwartz and Ingber (1994) proposed that mechanical forces (i.e., cytoskeleton) may regulate the change of integrin clustering or conformation and thus activate intracellular signalling pathways.

The present data indicate that cumulus expansion shares common features with the process of cell adhesion to the ECM. Cell adhesion is achieved by the assembly of MFs and integrins at focal adhesion sites, and is directed by specific tyrosine kinase $pp125^{FAK}$ (Burridge et al., 1992; Lipfert et al., 1992). Similarly, cumulus expansion is preceded by the assembly of MFs and paralleled by the redistribution of integrins and changes in cell shape as documented by Albertini and Rider (1994), Allworth and Albertini (1993), and Šutovský et al. (1993, 1994). Thus, it would not be surprising to detect some specific components of focal adhesion in mammalian cumuli oophori undergoing expansion.

The cellular differentiation (as studied in vitro) seems to be regulated by the adhesion on ECM. However, the interaction between cytoskeleton and ECM is reciprocal and cumulus expansion provides an excellent opportunity to follow the reverse sequence of events: the assembly of MFs, similar to the formation of stress fibers at the focal adhesion site, occurs before and probably is required for ECM synthesis and/or assembly during cumulus expansion. According to this view, cumulus ECM seems to be assembled as a consequence of cytoskeletal reorganization and could play roles other than the one required for cumulus cell differentiation and ovulation. The establishment of an integrin link between cumulus cell cytoplasm and ECM may in turn favor the acquisition of the final morphology by cumulus cells.

Taken together, the present study provides the support for the existence of two distinct steps necessary for cumulus expansion: actin-driven cytoskeletal rearrangement and assembly of cumulus ECM. Whereas our and others' previous studies (reviewed in Šutovský and Motlík, 1994) suggest the cooperation of the cytoskeleton and ECM during cumulus expansion, we report here that these two steps can be separated and that cytoskeletal rearrangement is probably placed upstream of ECM synthesis in the cascade of events leading to cumulus expansion. The redistribution of cytoskeleton is not affected by the presence of ECM synthesis inhibitor DON, but no ECM assembly occurs when the MFs are disrupted by CB. Thus, the present data provide further evidence for the role of the MF cytoskeleton in mediation of the response induced by gonadotropins in granulosa cells (Amsterdam and Rotmensch, 1987).

ACKNOWLEDGMENTS

We gratefully acknowledge the technical assistance of Mrs. Jiřinka Zelenková and Mr. Václav Pech, the assistance of Dr. Petr Dvořák with confocal microscopy, and the provision of light microscopic facility by Dr. Leopold Veselský. Special thanks are addressed to professor Gerald Schatten and Dr. Jan Motlík for stimulating discussion and reading the manuscript. This research was supported in part by grant 12.061E, Office of the Science Advisor, U.S. Agency for International Development, Washington, D.C. (P.S.); grant Z-503, Czech Ministry of Economics, Prague, Czech Republic (A.P.); and by grants from the NIH (P.S., Gerald Schatten), USDA (Gerald Schatten), and the Centre International des Etudiants et Stagiaires, Paris, France (P.S.)

REFERENCES

Albertini DF, Rider V (1994): Patterns of intercellular connectivity in the mammalian cumulus-oocyte complex. Microsc Res Tech 27:125–133.

Allworth AE, Albertini DF (1993): Meiotic maturation in cultured bovine oocytes is accompanied by remodelling of the cumulus cell cytoskeleton. Dev Biol 158:101–112.

Amsterdam A, Rotmensch S (1987): Structure-function relationship during granulosa cell differentiation. Endocr Rev 8:309–337.

Ben-Ze'ev A, Amsterdam A (1987): In vitro regulation of granulosa cell differentiation. J Biol Chem 262:5366–5376.

Buccione R, Vanderhyden BC, Caron PJ, Eppig JJ (1990): FSH-induced expansion of the mouse cumulus oophorus in vitro is dependent upon a specific factor(s) secreted by the oocyte. Dev Biol 138:26–32.

Burridge K, Turner CE, Romer LH (1992): Tyrosine phosphorylation of paxillin and $pp125^{FAK}$ accompanies cell adhesion to extracellular matrix: A role in cytoskeletal assembly. J Cell Biol 119:893–903.

Camaioni A, Hascall VC, Yanagishita M, Salustri A (1993): Effect of exogenous hyaluronic acid and serum on matrix organization and stability in the mouse cumulus cell-oocyte complex. J Biol Chem 268:20473–20481.

Chen L, Wert SE, Hendrix M, Russel PT, Cannon M, Larsen WJ (1990): Hyaluronic acid synthesis and gap junction endocytosis are necessary for normal expansion of the cumulus mass. Mol Reprod Dev 26:236–247.

Chen L, Mao SJT, Larsen WJ (1992): Identification of a factor in fetal bovine serum that stabilizes the cumulus extracellular matrix. J Biol Chem 267:12380–12386.

Dekel N, Hillensjo Y, Kraicer PF (1979): Maturation effects of gonadotropins on the cumulus-oocyte complex of the rat. Biol Reprod 20:191–197.

Demarchez M, Hartmann DJ, Herbage D, Ville G, Prunieras M (1987): Wound-healing of human skin transplanted onto the nude mouse. 2. An immunohistological and ultrastructural study of the epidermal basement membrane zone reconstruction and connective tissue reorganization. Dev Biol 121:119–129.

De Smedt V, Szollosi D (1991): Cytochalasin D induces meiotic resumption in follicular sheep oocytes. Mol Reprod Dev 29:163–171.

157

Duband JL, Thiery JP (1987): Distribution of laminin and collagen during avian neural crest development. Development 101:461–478.

Eppig JJ (1979): FSH stimulates hyaluronic acid synthesis by oocyte-cumulus cell complex from mouse preovulatory follicles. Nature 281:483–484.

Juliano RL, Haskill S (1993): Signal transduction from extracellular matrix. J Cell Biol 120:577–585.

Lipfert L, Haimovich B, Schaller MD, Cobb BS, Parsons JT, Brugge JS (1992): Integrin-dependent phosphorylation and activation of the protein tyrosine kinase pp125^{FAK} in platelets. J Cell Biol 119:905–912.

Luna EJ, Hitt AL (1992): Cytoskeleton-plasma membrane interactions. Science 258:955–964.

Prochazka R, Nagyova E, Rimkevicova Z, Nagai T, Kikuchi K, Motlik J (1991): Lack of effect of oocytectomy on expansion of the porcine cumulus. J Reprod Fertil 93:569–576.

Salustri A, Yanagishita M, Hascall VC (1990): Mouse oocytes regulate hyaluronic acid synthesis and mucification by FSH-stimulated cumulus cells. Dev Biol 138:26–32.

Salustri A, Yanagishita M, Underhill CB, Laurent TC, Hascall VC (1992): Localization and synthesis of hyaluronic acid in the cumulus cells and mural granulosa cells of the preovulatory follicle. Dev Biol 151:541–551.

Schwartz MA, Ingber DE (1994): Integrating with integrins. Mol Biol Cell 5:389–393.

Sonnenberg A, Modderman PW, Hogervorst F (1988): Laminin receptor on platelets is the integrin VLA-6. Nature 336:487–489.

Šutovsky P, Motlik J (1994): Cumulus expansion in mammals. An interplay between cumulus granulosa cell cytoskeleton, extracellular matrix and oocyte secretion. ARTA J 604:2–4.

Šutovsky P, Flechon JE, Flechon B, Motlik J, Peynot N, Chesne P, Heyman Y (1993): Dynamic changes of gap junctions and cytoskeleton during in vitro culture of cattle oocyte-cumulus complexes. Biol Reprod 49:1277–1287.

Šutovsky P, Flechon JE, Pavlok A (1994): Microfilaments, microtubules and intermediate filaments fulfil differential roles in gonadotropin induced expansion of bovine cumulus oophorus. Reprod Nutr Dev 34:415–425.

Vanderhyden BC, Caron PJ, Buccione R, Eppig JJ (1990): Developmental pattern of the secretion of cumulus-expansion enabling factor by mouse oocytes and the role of oocytes in promoting granulosa cell differentiation. Dev Biol 140:307–317.

Vikhrky V, Draber P, Hašek J, Bartek J (1982): Production and characterization of monoclonal antitubulin antibody. Cell Biol Int Rep 6:725–730.

Virtanen I, Narvanen O, Lehto VP (1988): Differential immunoreactivity and Ca^{2+}-dependent degradation of vimentin in human fibroblast and fibrosarcoma cells. Int J Cancer 42:256–260.

Wert SE, Larsen WJ (1988): Meiotic resumption and gap junction modulation in the cultured rat cumulus-oocyte complexes. Gamete Res 22:143–162.

Yllane J, Virtanen I (1989): The Mr 140 000 fibronectin receptor complex in normal and virus-transformed human fibroblasts and in fibrosarcoma cells: Identical localization and function. Int J Cancer 43:1126–1136.